



Identifying targets for potentiators in *S. aureus* using chemical genetic approaches

Citation

Rajagopal, Mithila. 2016. Identifying targets for potentiators in *S. aureus* using chemical genetic approaches. Doctoral dissertation, Harvard University, Graduate School of Arts & Sciences.

Permanent link

<http://nrs.harvard.edu/urn-3:HUL.InstRepos:33840649>

Terms of Use

This article was downloaded from Harvard University's DASH repository, and is made available under the terms and conditions applicable to Other Posted Material, as set forth at <http://nrs.harvard.edu/urn-3:HUL.InstRepos:dash.current.terms-of-use#LAA>

Share Your Story

The Harvard community has made this article openly available.
Please share how this access benefits you. [Submit a story](#).

[Accessibility](#)

Identifying targets for potentiators in *S. aureus* using chemical genetic approaches

A dissertation presented

by

Mithila Rajagopal

to

The Department of Chemistry and Chemical Biology

in partial fulfillment of the requirements

for the degree of

Doctor of Philosophy

in the subject of

Chemistry

Harvard University

Cambridge, Massachusetts

June 2016

© 2016 Mithila Rajagopal

All Rights Reserved

Identifying targets for potentiators in *S. aureus* using chemical genetic approaches**Abstract**

Staphylococcus aureus is a highly feared Gram-positive pathogen. The rise in antibiotic resistance has made *S. aureus* infections intractable. To find new ways to treat *S. aureus* infections, it is important to understand how this organism protects itself from antibiotics. We probed *S. aureus* transposon libraries with different classes of antibiotics and used Tn-Seq to identify intrinsic resistance factors that are important in withstanding antibiotics. We identified and validated the importance of a number of previously known intrinsic resistance factors such as *mprF*, *fmtA* and the *graRS/vraFG* multi-component sensing system, as well as a number of novel factors whose involvement in antibiotic resistance has not been previously appreciated. In the course of this work, we realized that Tn-Seq data could be mined to predict antibiotic mechanism of action. We used a machine learning approach to predict that a class of anti-MRSA antibiotics that were thought to cause membrane damage actually bind to lipid II and inhibit cell wall synthesis. This predicted mechanism was validated. Finally, we report the identification of a class of disubstituted urea compounds against which the inactivation of *mprF* is protective. As the inactivation of *mprF* usually sensitizes to most antibiotics, these compounds might belong to a new class of inhibitors that could be used as tool compounds to further probe *S. aureus* cell biology. We have developed a strategy that could be useful in identifying the targets of such compounds. The results described here have opened several interesting avenues for a more in-depth understanding of *S. aureus* biology and antibiotic resistance.

Acknowledgements

I am very thankful to my advisors Dr. Daniel Kahne, and especially Dr. Suzanne Walker. She has been patient, encouraging and enthusiastic throughout my Ph.D. and I have been fortunate to have been able to learn from her for all these years. I am also thankful to all the members of both the Kahne and Walker labs, especially Marina and Wonsik, with whom I worked most closely. I hope I will be lifelong friends with the many of my labmates, as I treasure their influences in my life both scientific and otherwise. I feel very lucky to be supported in chasing whatever dreams I have by wonderful friends. It was reassuring to know that they always had my back. Finally, I would definitely not be here without my family. Their unconditional support, love, and their faith in me, even when I don't have faith in myself, is what enables me to accomplish anything at all. I owe my success to them: to their unwavering energy, enthusiasm and interest in the goals I pursue, their constant belief in me, and their inspiring trailblazing. For these and so many other reasons, I would not know what to do without them.

Table of Contents

Chapter 1: Envelope Structures of Gram-positive Bacteria	1
1.1 Introduction	1
1.2 Cell membrane.....	2
1.3 Peptidoglycan	6
1.3.1 Peptidoglycan structure	7
1.3.2 Peptidoglycan biosynthesis	9
1.3.3 Tailoring modifications of peptidoglycan	15
1.4 Teichoic acids	17
1.4.1 Wall teichoic acid structure	18
1.4.2 Wall teichoic acid biosynthesis	19
1.4.3 Lipoteichoic acid structure	21
1.4.4 Lipoteichoic acid synthesis	22
1.4.5 Tailoring modifications of teichoic acids.....	25
1.4.6 Roles of teichoic acids and their tailoring modifications in cell physiology and immune evasion	27
1.5 Capsular polysaccharides	31
1.5.1 Structural diversity of capsular polysaccharides	32
1.5.2 Capsular polysaccharides, host immunity and vaccine development	33
1.6 Exopolysaccharides and biofilm formation	34
1.7 Antibiotics targeting the cell envelope	35

1.8 The quest for novel antibiotic targets	39
--------------------------------------------------	----

Chapter 2: Validation of Tn-Seq approach to identify intrinsic resistance

factors	41
2.1 Why is understanding factors that contribute to antibiotic resistance important ...	41
2.2 Transposon libraries and their use in identifying intrinsic resistance factors	43
2.3 Experimental approach and data analysis	47
2.4 Intrinsic factors that increase or decrease susceptibility to antibiotics.....	53
2.5 Intrinsic factors that impact multiple classes of antibiotics	63
2.6 GraRS/VraFG is the single most important multi-component sensing system across tested antibiotics	64
2.7 Contribution of intrinsic resistance factors to antibiotic resistance can vary across strains.....	69
2.8 Conclusions	70
2.9 Methods	71

Chapter 3: Genes that contribute to bacterial fitness in the presence of

peptidoglycan biosynthesis inhibitors	76
3.1 Rationale for expanding the set of Tn-Seq derived fitness profiles	76
3.2 Peptidoglycan biosynthetic inhibitors tested.....	77
3.3 Identifying a core set of genes relevant under cell wall perturbation.....	79
3.4 Previously characterized genes relevant under cell wall perturbation.....	84

3.5 Three previously uncharacterized genes important under cell wall stress	86
3.6 Machine learning approach to suggest potential pathways genes of unknown function could be involved in	93
3.7 Discussion on parameters to consider for library treatment	96
3.8 Conclusions	100
3.9 Methods	100
Chapter 4: Predicting the mechanism of action of antibiotics	106
4.1 The use of fitness profiles to cluster antibiotics by mechanism of action	106
4.2 An expanded set of antibiotics were tested in Tn-Seq	107
4.3 Hierarchical clustering of antibiotic fitness profiles	111
4.4 K-nearest neighbors algorithm to classify antibiotics by mechanism of action ...	113
4.5 Predicting the mechanism of action of an unknown compound	120
4.6 General discussions on approaches to optimize Tn-Seq based data analysis...	121
4.7 Methods	129
Chapter 5: Compounds against which inactivation of <i>mprF</i> is protective	131
5.1 Summary	131
5.2 Targeting intrinsic resistance factors	131
5.3 High-throughput screening for β -lactam potentiators	134
5.4 Characterization of lead compounds MR100 and MR101	141
5.5 Inactivation of <i>mprF</i> is strongly protective against MR100/MR101	148

5.6 Identifying other compounds that are also protected by the inactivation of <i>mprF</i>	153
5.7 Strategy for target identification	155
5.7.1 Identifying genes that are synthetically lethal with <i>mprF</i>	157
5.7.2 Raising resistant mutants to MR101	161
5.8 Conclusions and future directions	164
5.9 Methods	166
Appendices	174
Appendix 1: MATLAB code for analyzing high-throughput screening data.....	174
Appendix 2: Hits identified in high-throughput screening for β -lactam potentiators	180
Appendix 3: Dual dose response assays	186
Appendix 4: HPLC and NMR analyses.....	189
Appendix 5: Results from transposon-based experiments on MR100/MR101	191
Appendix 6: Transmission electron microscopy images of <i>ugtP-mprF</i> and <i>ItaA-mprF</i> double inactivation mutants	195
Appendix 7: Strains and primers used in this work.....	198
References Cited	202

List of Figures

Figure 1.1: The Gram-positive cell envelope	5-6
Figure 1.2: PG structure, and common variations	8
Figure 1.3: Synthesis of PG and antibiotics that target PG synthesis	10-11
Figure 1.4: WTA structure and common variations	18
Figure 1.5: TA biosynthesis and modification pathways	24-25
Figure 2.1: Schematics of two methods of sample preparation of pooled transposon libraries for Illumina sequencing	44-46
Figure 2.2: Transposon library 2 is constructed with six different transposon constructs	48
Figure 2.3: Intrinsic resistance factors that contribute to antibiotic resistance can be identified by Tn-Seq.....	50-51
Figure 2.4: Inactivation of the oxidative phosphorylation pathway confers resistance to gentamicin	56-57
Figure 2.5: Tn-Seq results were validated by testing transposon inactivation mutant fitness in spot dilution assays	61-62
Figure 2.6: Tn-Seq results were validated by testing the fitness of deletion mutants in Newman in spot dilution assays	67-68
Figure 3.1: Tn:: <i>SAOUHSC_02149</i> is sensitive to cell envelope antibiotics vancomycin and daptomycin	87

Figure 3.2: Tn:: <i>SAOUHSC_01025</i> and tn:: <i>SAOUHSC_01050</i> are particularly sensitive to antibiotics that damage the cell envelope	90-91
Figure 3.3: Tn:: <i>SAOUHSC_01025</i> and tn:: <i>SAOUHSC_01050</i> show no increase in sensitivity to triton X-100 induced lysis	92
Figure 3.4: <i>SAOUHSC_01025</i> and <i>SAOUHSC_01050</i> are important for cell envelope integrity	94-95
Figure 3.5: Tn:: <i>SAOUHSC_01025</i> and tn:: <i>SAOUHSC_01050</i> showed increased hemolysis	96
Figure 4.1: Hierarchical clustering showed that antibiotics of similar mechanisms of action have similar fitness profiles and cluster together	112
Figure 4.2: A schematic description of the K-nearest neighbors algorithm to predict antibiotic mechanism of action.....	114-115
Figure 4.3: WAP1 inhibits processing of lipid II by PBP2	121
Figure 4.4: Pooling together reads from inactivation and outward facing promoter constructs can improve significance of hits identified	125-126
Figure 4.5: Compiling reads from all constructs resulted in lower p-values and more genes that meet the significance cut-off	128-129
Figure 5.1: Examples of compounds that potentiate the activity of β -lactams	134
Figure 5.2: Compounds were classified into three categories	138-139
Figure 5.3: Number of compounds and hits identified in each category	140-141
Figure 5.4: MR100 is a potent β -lactam potentiator for numerous strains	144-145

Figure 5.5: Characterization of MR101.....	147
Figure 5.6: Inactivation of <i>mprF</i> has a fitness advantage in the presence of MR100 and MR101	151-152
Figure 5.7: Structures of the three lethal compounds whose bioactivity is suppressed by <i>mprF</i> inactivation (BSIM compounds)	154
Figure 5.8: Strategy to identify resistant mutants to BSIM compounds that are not <i>mprF</i> nulls.....	156
Figure 5.9: LTA synthesis genes are synthetically lethal with <i>mprF</i>	158
Figure 5.10: Validation of synthetic lethality of <i>ItaA</i> and <i>ugtP</i> with <i>mprF</i>	160
Figure 5.11: Tn:: <i>948</i> is more sensitive to MR101 than tn:: <i>ugtP</i>	162
Figure 5.12: A larger increase in MIC of MR101 was observed in HG003 tn:: <i>948</i>	163
Figure A4.1: HPLC showed that MR100 had contaminants	189
Figure A4.2: H1-NMR of MR101	190
Figure A5.1: Inactivation insertion mutants of <i>mprF</i> raised to MR100	194
Figure A6.1: Transmission electron microscopy images of <i>ugtPmprF</i> and <i>ItaAmprF</i> double inactivation mutants	195-197

List of Tables

Table 2.1: 80 unique genes were identified as important for fitness by treatment of pooled transposon libraries with six antibiotics	54
Table 3.1: Peptidoglycan biosynthetic inhibitors that were tested in Tn-Seq.....	78
Table 3.2: Genes that are relevant under cell wall perturbation	82-83
Table 4.1: Antibiotics tested in Tn-Seq cover a variety of chemical classes and targeted pathways	109
Table 4.2: Machine learning can predict the class of an unknown antibiotic	117-118
Table 5.1: Predicted outcomes for small molecules screened	135
Table A2.1: High-throughput screening hits identified in the strong category.....	180
Table A2.2: High-throughput screening hits identified in the medium category....	181-183
Table A2.3: High-throughput screening hits identified as potentially causing growth defects, prioritized by percent survival in the presence of β -lactam	184-185
Table A5.1: Hits that are >5x enriched under MR100 or MR101 and that were significant in at least one condition	191
Table A5.2: Hits that are >5x depleted under MR100 or MR101 and that were significant in at least one condition	192-193
Table A7.1: Table of strains used in this work.....	198
Table A7.2: Table of primers used in this work	201

Abbreviations

PG	Peptidoglycan
TAs	Teichoic acid
WTA	Wall teichoic acid
LTA	Lipoteichoic acid
GlcNAc	N-acetylglucosamine
MurNAc	N-acetylmuramic acid
GalNAc	N-acetylgalactosamine
Und-P	Undecaprenyl phosphate
DAG	Diacylglycerol
CPS	Capsular polysaccharides
WT	Wildtype
MIC	Minimum inhibitory concentration
MSC	Minimum sensitizing concentration
BSIM	Bioactivity suppressed by inactivation of <i>mprF</i>

Chapter 1: Envelope structures of Gram-positive bacteria

A version of this chapter has been published [1].

1.1 Introduction

The cell envelope is one of the most important parts of the bacterial cell and the target of numerous antibiotics. Many of the proteins involved in cell envelope biosynthesis or its modification contribute to antibiotic resistance. In order to study resistance to these antibiotics, an understanding of the cell envelope structure, its biosynthesis and its modification is crucial.

The cell envelope is a complex, dynamic, multilayered structure that serves to protect bacteria from their unpredictable and often hostile surroundings. The cell envelopes of most bacteria fall into one of two major groups. Gram-negative bacteria have an inner, cytoplasmic membrane surrounded by a thin layer of peptidoglycan (PG) and an outer membrane containing lipopolysaccharide. The outer membrane functions as a permeability barrier to control the influx and egress of ions, nutrients and environmental toxins, and it also contributes to osmoprotection. Gram-positive bacteria lack a protective outer membrane but the PG layers are many times thicker than those in Gram-negative organisms [2, 3]. Embedded in the inner membrane and attached to the PG layers are long anionic polymers called teichoic acids (TAs), which play multiple roles in cell envelope physiology as well as pathogenesis [4-6]. Membrane-embedded and wall-associated proteins serve as environmental sensors, regulate passage of nutrients and ions across the cytoplasmic membrane, facilitate efflux of toxins and other molecules, modulate surface adhesion, and participate in enzymatic synthesis, degradation, and remodeling of the cell envelope during growth and division, and in

response to environmental stress [7-11]. Other important cell envelope components in Gram-positive organisms include capsular polysaccharides (CPS), which are covalently attached to PG, and extracellular polysaccharides, which form an amorphous outer layer [12, 13] (Fig. 1.1).

The importance of the cell envelope for bacterial survival makes it a target for antibiotics, and several classes of clinically used antibiotics inhibit biosynthesis of PG, resulting in osmotic rupture. Other antibiotics damage the membrane barrier [14]. Because resistance to clinically used antibiotics has become widespread, there is a push to better understand cell envelope biogenesis and regulation, and to identify new cell envelope targets that can be exploited in the development of next generation antibiotics. In this chapter, we will focus on important cell envelope components of Gram-positive pathogens using *Staphylococcus aureus* as a focal point, except where other Gram-positive pathogens are better studied. Attention will also be given to the non-pathogenic *Bacillus subtilis* because its genetic tractability and other biological characteristics have led to its adoption as the principal Gram-positive model organism.

1.2 Cell membrane

Gram-positive organisms are surrounded by bilayer membranes that can vary substantially in composition but typically include large amounts of phosphatidylglycerol and cardiolipin. In *Bacillus* species, phosphatidylethanolamine is abundant as well [15-17]. Many Gram-positive species express at least one type of aminoacylatedphosphatidylglycerol [18, 19]. For example, in *S. aureus*, lysyl-phosphatidylglycerol is found in significant amounts, particularly during logarithmic growth [20]. This phospholipid is synthesized by a polytopic membrane protein, MprF,

which catalyzes the transfer of lysine from lysyl-tRNA to phosphatidylglycerol on the inner leaflet of the membrane and then translocates this species to the outer leaflet of the membrane [20, 21]. Lysyl-phosphatidylglycerol reduces susceptibility to antimicrobial peptides produced during host infection [22] and also provides protection against aminoglycosides, bacitracin, daptomycin, and some β -lactams [23, 24]. Daptomycin-resistant *S. aureus* clinical isolates frequently contain mutations that increase MprF expression or translocase activity [25-28]. Other species of Gram-positives have MprF homologs that have been implicated in similar functions [29]. It is thought that the positive charges of lysyl-phosphatidylglycerol serve to repel positively charged antibiotics or antibiotic-metal complexes [23, 29].

The composition of both the head groups and the fatty acyl chains in membrane phospholipids can change rapidly in response to environmental conditions, such as low pH, osmotic stress, or temperature extremes [30]. For example, branched chain fatty acid content in membranes can vary substantially depending on growth conditions. Membrane lipid composition affects membrane viscosity, which modulates membrane permeability and can influence both solute transport and protein interactions. Membrane lipid homeostasis is thus a crucial process and interfering with it can compromise viability [30, 31].

In addition to the lipid components, the cell membrane contains the lipid anchor component of lipoteichoic acid (LTA), and includes numerous transmembrane and lipoproteins with functions in cell envelope synthesis, transport of cell envelope precursors and nutrients, and export of toxic compounds (Fig. 1.1). Among these transmembrane proteins are the sensory components of several two-component

sensing systems that regulate the cell's response to external stimuli, including cell density and presence of damaging toxins. For instance, the amount of lysyl-phosphatidylglycerol in *S. aureus* is regulated by a complex of proteins that includes a two-component signaling system, GraRS, and a two-component ABC-transporter-like system, VraFG. This complex, which senses and responds to a variety of stimuli, including the presence of antimicrobial peptides, also regulates D-alanylation of TAs [32-35]. Modulating the negative charge density of the cell envelope through lysinylation of phosphatidylglycerol and D-alanylation of TAs decreases susceptibility of *S. aureus* to antimicrobial peptides produced during host infection and increases resistance to cationic antibiotics administered to treat infection [4, 29, 36, 37].

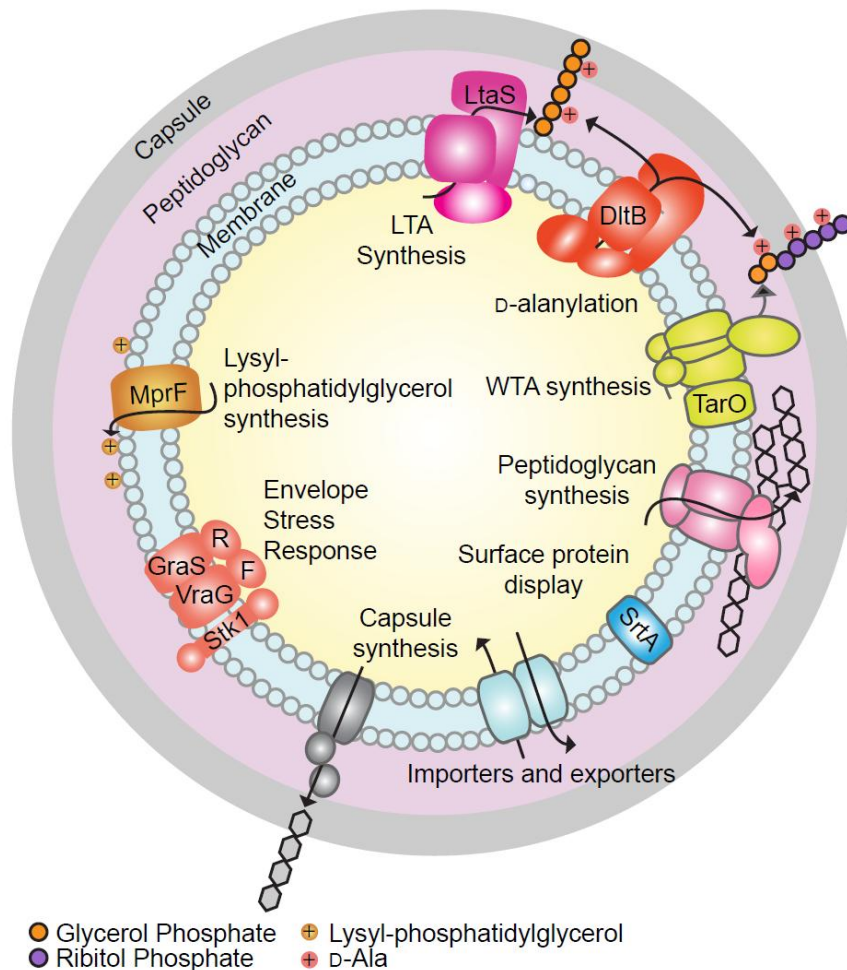


Figure 1.1: The Gram-positive cell envelope. The complex Gram-positive cell envelope is the first line of defense for the organism. Here, the *S. aureus* envelope is shown as an example. Major pathways involved in the synthesis of the cell envelope include capsule, PG and TA synthesis. TAs can be modified by D-alanylation. D-alanylation and lysyl-phosphatidylglycerol synthesis are known factors for antibiotic resistance. Envelope stress response regulators modulate the organism's response to toxic molecules or conditions that perturb the cell envelope. Importers and exporters, ubiquitously present among bacteria, serve the necessary role of channeling in nutrients and pumping out toxic molecules. Finally, surface protein display systems function to

(Continued) tether proteins to the cell membrane or cell wall, which perform important roles in adhesion and interaction with the environment.

1.3 Peptidoglycan

Gram-positive bacteria are surrounded by many layers of peptidoglycan (PG), which form a protective shell that is 30-100 nm thick [2]. The PG layers are covalently modified with carbohydrate polymers including wall teichoic acids (WTAs) or functionally related anionic glycopolymers as well as CPS. The PG layers also scaffold numerous proteins, some of which are bound non-covalently through interactions with PG-binding modules such as LysM domains [7] while others are covalently attached by sortases [38] (Schneewind and Missiakas 2012). Some wall-associated proteins play important roles in cell envelope remodeling during growth and division, whereas others scavenge nutrients and metals from the environment or serve as adhesins that promote surface binding and colonization [9]. PG has numerous important functions but perhaps the most important is that it stabilizes the cell membrane, enabling it to withstand high internal osmotic pressures. This function is critical for cell survival because the turgor pressure pushing against the cell membrane can reach 20 atmospheres in some Gram-positive bacteria [39, 40]. Since PG is essential for viability and the biosynthetic pathway is highly conserved in Gram-positive and Gram-negative organisms, PG biosynthesis is a target for many clinically used antibiotics, including β -lactams, which are the most successful class of antibiotics in history, and vancomycin, which is still widely used to treat serious Gram-positive infections, including methicillin-resistant *Staphylococcus aureus* (MRSA) infections.

1.3.1 Peptidoglycan structure

PG is composed of linear chains of repeating disaccharide units cross-linked via peptide side chains (Fig. 1.2). The disaccharide subunit is completely conserved and consists of *N*-acetylglucosamine (GlcNAc) coupled through a β -1,4-linkage to *N*-acetylmuramic acid (MurNAc) [41]. The average chain length of the glycan strands can vary considerably across species. In *S. aureus*, the glycan strands are relatively short, averaging 6-18 disaccharide units [42, 43] while in *B. subtilis*, the glycan chains are much longer. Early measurements of *B. subtilis* glycan strands indicated an average chain length of 54-96 disaccharide units, but more recent experiments using atomic force microscopy to probe size exclusion-purified glycan strands have suggested that glycan chains can reach 5000 disaccharide units in length [43, 44]. The longer glycan chains found in *B. subtilis* may be a result of the cylindrical shape, which results in a substantially greater stress imparted on the cylindrical walls compared with the poles [44].

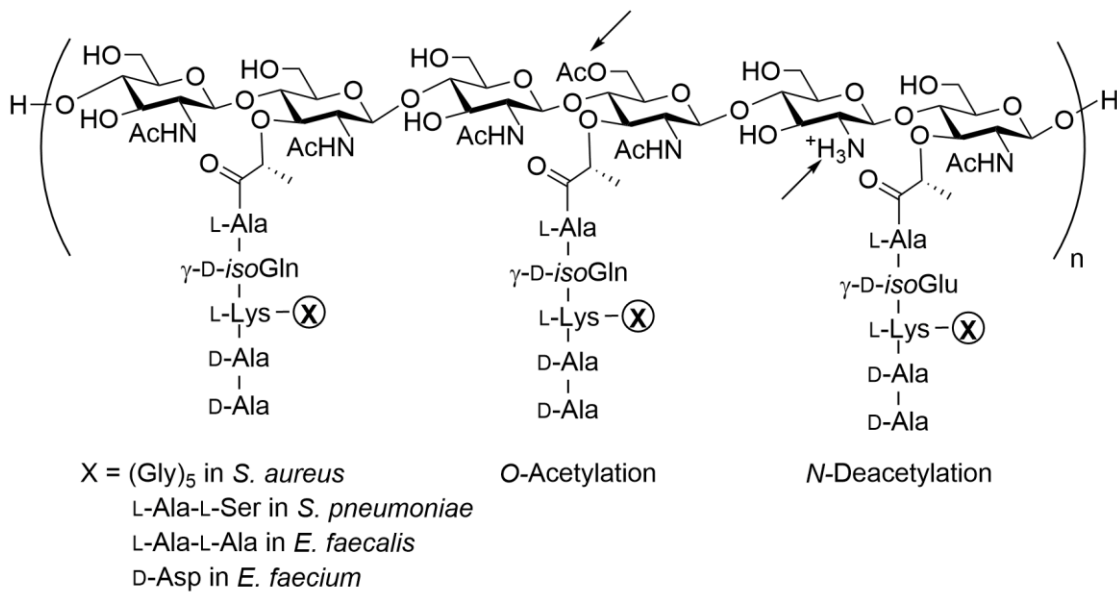


Figure 1.2. PG structure, and common variations. PG consists of chains of alternating GlcNAc and MurNAc residues. The MurNAc residues are functionalized with pentapeptide units which are cross-linked via the substituents on L-Lys to generate the mature PG. The linear glycan chain is highly conserved across both Gram-positives and Gram-negatives. The stem pentapeptide is well conserved across Gram-positives, aside from *B. subtilis* which contains *meso*-diaminopimelic acid instead of L-Lysine at position 3 of the stem pentapeptide. There is considerable variation in the substituents on the L-Lys across Gram-positive species as indicated. PG can be modified by *O*-acetylation of MurNAc or *N*-deacetylation of GlcNAc moieties in response to challenge from antimicrobials such as lysozyme.

MurNAc, a sugar unique to bacteria, contains a C3 lactate group. In nascent (uncrosslinked) PG of Gram-positive organisms, this group is bonded to the N-terminus of a linear peptide consisting of five amino acids. The first, L-alanine, is typically

followed by D-isoglutamine, and the terminal dipeptide is D-Ala-D-Ala. Position 3 of the pentapeptide chain is either L-lysine or *meso*-diaminopimelic acid (*m*-DAP), with the former being found in *S. aureus*, *Streptococcus pneumoniae*, *Enterococcus faecalis*, and *Enterococcus faecium*, and the latter being found in *B. subtilis* [41]. The ϵ -amino group of L-Lys is typically coupled to one or more additional amino acids. In *S. aureus*, for example, L-lysine is coupled to pentaglycine, although serine can also be incorporated in some strains [41, 45]. *S. pneumoniae* and *E. faecalis* contain dipeptide substituents consisting of L-Ala-L-Ser or L-Ala-L-Ala, respectively [41, 46, 47]. *S. pneumoniae* PG is unusual in that it can be a mixture of either dipeptide-substituted or un-substituted stem peptides [47, 48]. *E. faecium* contains a D-aspartate substituent [3, 49]. Canonical glycan strand crosslinking occurs via formation of an amide bond between the side chain or branching peptide on amino acid 3 of one stem peptide and the backbone carbonyl of amino acid 4 on another stem peptide, with the loss of the terminal D-ala [41]. Crosslinks can also form to the carbonyl of amino acid 3 in some species of Gram-positive organisms [41, 50-52].

1.3.2 Peptidoglycan biosynthesis

PG biosynthesis takes place in distinct stages, the first of which involves assembly of a UDP-MurNAc pentapeptide in the cytoplasm. This stage is followed by coupling of the phospho-MurNAc pentapeptide to the undecaprenyl phosphate (Und-P) "carrier lipid" embedded in the membrane to form a lipid-linked monosaccharide known as Lipid I, which is glycosylated to form the disaccharide Lipid II. Additional amino acids, if any, are appended to the pentapeptide chain at this point and then Lipid II is translocated

across the membrane. In the final stage of PG biosynthesis, Lipid II is polymerized and the resulting glycan strands are cross-linked to give mature PG. The lipid carrier released during glycan chain polymerization is recycled back into the cell to continue synthesis. Most of the enzymatic steps for the majority of the biosynthetic pathway are well-conserved across both Gram-negative and Gram-positive bacteria (Fig. 1.3).

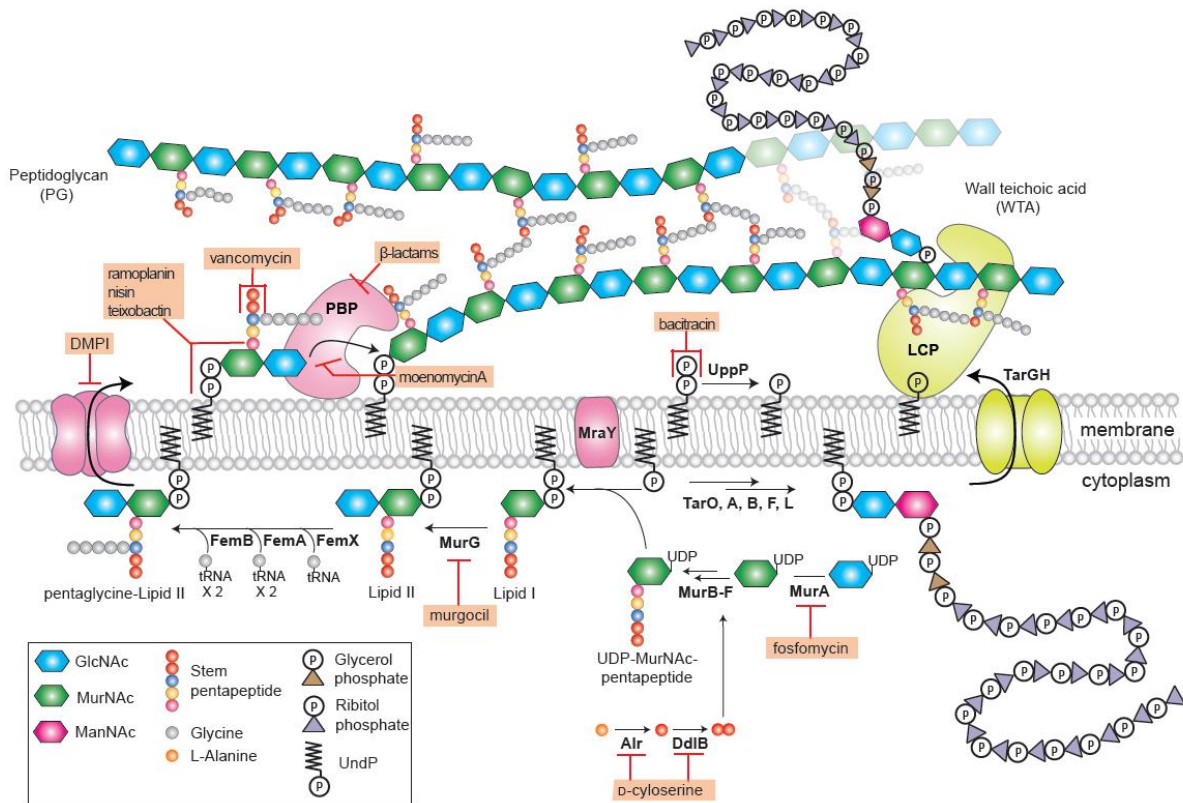


Figure 1.3: Synthesis of PG and antibiotics that target PG synthesis. The enzymatic steps for PG synthesis are well conserved across species. Here, the biosynthesis of *S. aureus* PG is shown as an example. The synthesis begins with the assembly of the GlcNAc-MurNAc-pentapeptide and its attachment to carrier lipid Und-P in the cell membrane. After this point, the L-Lysine at position 3 is substituted with additional amino acids and then flipped to the outside of the cell where it is cross-linked by PBPs. The same lipid carrier is also utilized for WTA (shown here) and capsule

(Continued) synthesis. The synthesis of PG is crucial to the cell and over time, several antibiotics have been discovered that target various steps in PG biosynthesis.

Assembly of Lipid II:

The first committed step in PG synthesis involves the MurA-catalyzed transfer of enolpyruvate from phosphoenolpyruvate to the C3 hydroxyl of UDP-GlcNAc [53]. Some low GC Gram-positive organisms, including *S. aureus*, *S. pneumoniae* and *B. subtilis* contain two *murA* alleles, which are differently regulated [54-56]. The secondary *murA* allele may allow for increased flux into the PG biosynthetic pathway in response to cell wall stress [54]. MurB reduces the C3 enolate to the lactate, resulting in formation of UDP-MurNAc [57]. The pentapeptide chain is then coupled in a stepwise manner, with MurC, MurD, MurE adding L-alanine, D-glutamic acid and L-lysine (or *m*-DAP), respectively. Using D-Ala produced from L-Ala by D-alanine racemase (Alr), D-Ala-D-Ala ligase (Ddl) makes the dipeptide, which is then added to the UDP-MurNAc-tripeptide by MurF. Since peptide bond formation is thermodynamically unfavorable, the ligases use ATP to activate the amino acids and provide a driving force for coupling [58-60].

The next stage of PG synthesis begins with the transfer of phospho-MurNAc pentapeptide to a lipid carrier in the bacterial membrane, typically Und-P, although *Mycobacterium smegmatis* uses decaprenylphosphate [61]. This step is catalyzed by MraY [62-64] and produces the first lipid-linked intermediate, Lipid I. Finally, MurG catalyzes the addition of GlcNAc to give Lipid II [65-67]. Amidation of the α -carboxylate of *iso*-glutamic acid at position 2 of the peptide chain, which is observed in many organisms [3], most likely occurs intracellularly after lipid-linked PG precursors are

formed. The enzymes involved in this modification were recently identified in *S. aureus* as MurT and GatD [68, 69].

When a peptide branch is present, the required amino acids are usually added to the completed Lipid II moiety. One exception is *Lactobacillus viridescens* where the first amino acid of the L-Ala-L-Ser bridge is added to the UDP-N-acetylmuramylpentapeptide [70]. In *S. aureus*, the pentaglycine is assembled by FemX, FemA and FemB, which sequentially add one, two and two glycines, respectively. These enzymes utilize glycyl-tRNA donors [71-74]. Serines rather than glycines are incorporated in a similar manner in other staphylococcal strains [75, 76]. This incorporation of serine contributes to resistance to lysostaphin, a glycyglycine endopeptidase [75]. The corresponding enzymes in *E. faecalis* and *S. pneumoniae* have also been identified [77, 78]. It is interesting that the Mur ligases use ATP-activated amino acids directly, but the enzymes that assemble the branching peptides use charged tRNAs. When tRNAs were found to be the aminoacyl donors for PG precursors in the 1960s, it caused some excitement because tRNAs were previously known only for their involvement in protein synthesis [79]. It is now known that phospholipids as well as PG precursors are aminoacylated by acyl-tRNAs (see above).

The final step in the cytoplasmic phase of PG synthesis involves the translocation of Lipid II across the membrane. Although it was initially thought that FtsW, a SEDS family protein, was the Lipid II flippase due to FRET-based assays in liposomes [80], MurJ, a MVF family protein, was later nominated as the Lipid II flippase in an elegant bioinformatic approach [81]. Convincing *in vivo* evidence then showed that MurJ is indeed the Lipid II flippase in a number of organisms [81-83]. Surprisingly, MurJ

homologs in *B. subtilis* were not found to be essential, and this caused some concern in the attribution of MurJ as the Lipid II flippase in Gram-positive organisms. However, it was subsequently shown that in *B. subtilis*, there is also a secondary Lipid II flippase, Amj, in addition to but unrelated to MurJ, that enables survival when MurJ (YtgP) is deleted [84]. It is not sufficiently clear why *B. subtilis* has two lipid II flippases, but it is suggested that expression of Amj is stimulated as an alternate pathway to flip Lipid II when MurJ, the primary flippase, is inhibited [84]

Glycan polymerization and cross-linking:

Once Lipid II is on the outside of the cell, it is polymerized and crosslinked. Glycan polymerization is accomplished by peptidoglycan glycosyltransferases (PGTs; also known as synthetic transglycosylases), while crosslinking is accomplished by transpeptidases. These activities are often found as domains in a single protein, but monofunctional variants of both enzyme classes exist. The nomenclature of PG biosynthetic enzymes is somewhat confusing as many are designated as penicillin-binding proteins, which highlights the fact that they covalently bind β -lactams [85], but obscures their catalytic function, which vary. There are two main categories of PBPs - high molecular mass PBPs that contain a second domain and low-molecular mass PBPs. The high molecular mass PBPs are further divided into Class A and Class B PBPs, with the Class A PBPs distinguished by the presence of an N-terminal PGT domain and the Class B PBPs distinguished by the presence of an N-terminal domain of unknown function. The penicillin-binding domains found in both Class A and Class B PBPs function as transpeptidase domains, serving to crosslink glycan strands. The low

molecular mass PBPs, sometimes called Class C PBPs, typically function as D,D-carboxypeptidases, serving to hydrolyze the terminal D-alanine of the stem peptide [86-88]. Some organisms including *S. aureus* contain low molecular mass PBPs that function as transpeptidases, rather than carboxypeptidases. Methicillin-sensitive *S. aureus* (MSSA) strains contain four PBPs. PBP1 and PBP3 are Class B PBPs [89, 90], PBP2 is a Class A PBP [91], and PBP4 is a low molecular weight PBP that acts as a transpeptidase to form additional crosslinks in PG [92-94]. MRSA strains contain an additional PBP, PBP2A, that is highly resistant to β -lactams. PBP2A serves to crosslink PG when the other PBPs have been inactivated by β -lactams [95, 96]. In addition to these enzymes, *S. aureus* also contains two monofunctional transglycosylases, SgtA and MGT [97-99]. Under optimal laboratory growth conditions, only PBP1 and PBP2 are essential for viability [90, 100, 101]. It is typical for bacteria to contain multiple PBPs and PGTs, with some essential and others important for survival under stressful conditions. In part, this redundancy reflects the central importance of PG for viability. Rod-shaped organisms such as *B. subtilis* typically have more PBPs than cocci such as *S. aureus* [102]. In *B. subtilis*, PG synthesis occurs both at the septum during cell division and along the cylindrical walls during cell elongation, and there is considerable evidence that different biosynthetic machines are involved in these different modes of PG synthesis [102-105]. Deconvoluting the cellular functions of PBPs and other cell wall biosynthetic enzymes has been a major challenge due to redundancy and possible interdependency [101, 106].

Recycling of carrier lipid:

The Und-P carrier lipid is present in limited amounts in bacterial membranes. In addition to serving as a carrier lipid for PG synthesis, Und-P is a carrier for WTA precursors as well as CPS precursors. To ensure an ongoing supply of all these cell wall precursors, the carrier lipid must be rapidly recycled. Hence, once Lipid II has reacted to form the glycan strands of PG, the undecaprenyl pyrophosphate released is converted to Und-P by UppP and other phosphatases [107-109], and Und-P is flipped back inside the cell by an unknown mechanism to enable another round of precursor synthesis.

1.3.3 Tailoring modifications of peptidoglycan

Tailoring modifications of PG subunits modulate the properties of the cell envelope and may protect bacteria from antimicrobial peptides and proteins (Fig. 1.2). There are a number of tailoring modifications found in Gram-positive bacteria. These include *N*-deacetylation, the removal of C2-acetyl groups from GlcNAc and/or MurNAc sugars, and *O*-acetylation of the MurNAc C6 hydroxyl [110, 111].

N-deacetylation has been shown to protect bacteria from lysozyme, a host muramidase that can cleave the glycosidic bond between GlcNAc and MurNAc residues [112]. Some Gram-positive organisms including *S. pneumoniae*, *Bacillus anthracis*, *B. subtilis* and other *Bacillus* species are naturally lysozyme resistant and contain a high proportion of *N*-deacetylated sugars in their cell wall [113-115]. In *S. pneumoniae*, approximately 80% of the glucosamine residues and 10% of the muramic acid residues are *N*-deacetylated [114]. This is comparable to the 88% and 34%, respectively,

observed in *B. anthracis* [115]. The enzyme responsible for GlcNAc deacetylation, PgdA, was first identified in *S. pneumoniae* [114]. PdaA, a MurNAc deacetylase [116], as well as a second MurNAc deacetylase, PdaC, which also has chitin deacetylase activity [117], has been identified in *B. subtilis*. The *pgdA* mutant in *S. pneumoniae* was shown to have attenuated virulence [114] and the *pdaA* mutant in *B. subtilis* is unable to germinate [118], indicating the possibility of other roles of *N*-deacetylation.

O-acetylation of the MurNAc moiety has been observed in several Gram-positive and Gram-negative species in variable amounts. In some strains of *S. aureus*, for example, 60% of MurNAc residues are *O*-acetylated [119]. *O*-acetylation has been shown to be important for lysozyme resistance and the gene responsible was identified as *oatA* in *S. aureus* [120]. Homologs of *OatA* have also been identified in other Gram-positive organisms, including *S. pneumoniae* [121] and *E. faecalis* [122]. Interestingly, while most Gram-positive organisms use *OatA* homologs for *O*-acetylation, Gram-negative organisms use proteins of a different family called Pat. *B. anthracis* produces both kinds of acetyltransferases, and the Pat transferases have been implicated in acetylation of secondary cell wall polysaccharide [123, 124]. In addition to resistance to lysozyme, *O*-acetylation has been shown to play a role in β -lactam resistance in *S. pneumoniae* and *Listeria monocytogenes* [121, 125], and in pathogenesis and immune evasion in *S. aureus* [126, 127]. *O*-acetylation is critical for infection by *L. monocytogenes*, and is reported to decrease cytokine production during early stages of infection of mice [125]. GlcNAc residues in PG can also be *O*-acetylated but this is more unusual. In *Lactobacillus plantarum*, GlcNAc *O*-acetylation plays a role in inhibiting *L. plantarum*'s major autolysin [128].

In addition to these modifications, PG can be modified at the MurNAc C6 position with different glycopolymers including TAs, teichuronic acids and CPS. Proteins are also covalently attached to the pentaglycine branch of stem peptides of PG by sortases [38]. In *S. aureus*, sortase-mediated protein attachment is thought to occur on the outside of the cell before Lipid II is polymerized [129, 130].

1.4 Teichoic Acids

The cell envelopes of Gram-positive bacteria are rich in teichoic acids (TAs). There are two major classes of TAs: lipoteichoic acids (LTAs), which are anchored to a lipid embedded in the cell membrane, and wall teichoic acids (WTAs), which are covalently attached to PG. LTAs are believed to be present in all Gram-positive bacteria with the exception of some *Micrococcus* strains [131]; WTAs are found in many, including *B. subtilis*, *S. aureus*, *Staphylococcus epidermidis*, *S. pneumoniae* and enterococcal species. In organisms where canonical WTAs are not found, other anionic glycopolymers are attached to PG, and may play analogous roles [132]. Under phosphate-limiting conditions, some *B. subtilis* strains produce teichuronic acids instead of WTAs [133-135]. It is estimated that WTAs and other polyanionic polymers comprise up to 60% of the cell wall mass [136]. Along with LTAs, these polymers play central roles in numerous cellular processes. Some of these functions are covered in detail below.

1.4.1 Wall teichoic acid structure

WTAs typically consist of a disaccharide linkage unit that is connected at the reducing end to PG via a phosphodiester linkage and at the non-reducing end to a main chain polymer. The structure of the main chain can vary considerably across species but always contains phosphodiester linkages that impart anionic charges to the cell wall (Fig 1.4). In *S. aureus* and *B. subtilis* WTA main chains are composed of glycerol-phosphate or ribitol-phosphate repeats. The WTA main chains are coupled through a disaccharide linkage unit to PG [4, 132, 137, 138].

Strain	WTA structure	Reference
<i>S. aureus</i> <i>B. subtilis</i> W23	$-\text{GlcNAc}-\text{ManNAc}-\left(\text{GroP}\right)_{1-3}-\left(\text{RboP}\right)_n-$	Brown et al. 2010 Brown et al. 2013
<i>B. subtilis</i> 168	$-\text{GlcNAc}-\text{ManNAc}-\left(\text{GroP}\right)_n-$	Pereria and Brown, 2009
<i>S. pneumoniae</i>	$\left(2\text{-acetamido-4-amino-2,4,6-trideoxyGal}-\text{Gluc}-\text{RboP}-\text{GalNAc}-\text{GalNAc}-\text{choline-P}-\text{choline-P}\right)_n-$	Denapite et al. 2012
<i>E. faecalis</i> 12030	$\left(\text{Gal}-\text{GalNAc}-\text{GlcNAc}-\overset{\text{Gluc}}{\text{Gal}}-\text{RboP}\right)_n-$	Theilacker et al. 2012
<i>E. faecium</i> U0317	$\left(\text{GalNAc}-\text{GalNAc}-\text{GroP}\right)_n-$	Bychowska et al. 2012

Figure 1.4. WTA structure, and common variations. WTAs are anionic polymers with a sugar-phosphate backbone attached to the C6 position of MurNAc in PG. The structure of WTAs is highly variable across Gram-positive species. WTA polymer structures for specific strains are indicated here with the following abbreviations: Glycerol-phosphate (GroP), Ribitol Phosphate (RboP), *N*-acetylmannosamine (ManNAc), Galactose (Gal), Glucose (Gluc), *N*-acetylgalactosamine (GalNAc), *N*-acetylglucosamine (GlcNAc), phosphorylcholine (choline-P).

In *S. pneumoniae*, the main chain repeat is composed of 2-acetamido-4-amino-2,4,6-trideoxygalactose, glucose, ribitol-phosphate and two GalNAc moieties, each decorated with phosphorylcholine. The incorporation of phosphorylcholine in WTAs is extremely rare and appears to be exclusive to *S. pneumoniae* [139, 140]. In *E. faecalis* 12030, the repeating unit contains D-glucose, D-galactose, 2-acetamido-2-deoxy-D-galactose, 2-acetamido-2-deoxy-D-glucose and ribitol-phosphate [141]. In *E. faecium* U0317, the WTA polymer is simpler, consisting of repeating units of two residues of 2-acetamido-2-deoxy-D-galactose and glycerol-phosphate [142].

1.4.2 Wall teichoic acid biosynthesis

The biosynthetic pathways for WTA assembly in *B. subtilis* and *S. aureus* have been well established [143-146] (Fig. 1.5). The assembly begins in a similar manner to PG assembly. Briefly, phosphoGlcNAc is transferred from UDP-GlcNAc to the Und-P lipid carrier by the initiating enzyme called TagO in *B. subtilis* and TarO in *S. aureus* [147], and then this "starter unit" is further elaborated by a series of intracellular enzymes to assemble the full polymeric precursor. TarA adds the next sugar, a ManNAc from UDP-ManNAc to the starter unit [148, 149], after which TarB adds a glycerolphosphate moiety from CDP-glycerol to this disaccharide lipid [148, 150]. While the structures of the main chains made in *B. subtilis* and *S. aureus* are similar, particularly in WTAs from *B. subtilis* W23 and *S. aureus*, there are substantial differences in the biosynthetic pathways that were not evident from bioinformatic analysis [143, 144, 151, 152]. Whereas in *B. subtilis* 168, TagF adds glycerol-phosphate units to make the full polymer [151], in *B. subtilis* W23, which makes ribitol-phosphate

WTAs, the polymer is primed and polymerized with only ribitol-phosphates by TarK and TarL respectively, and in *S. aureus*, TarF adds a glycerol phosphate unit, but TarL then adds ribitol-phosphate units to make the full polymer [143, 144, 152]. It is not yet possible to predict the enzymatic functions of putative teichoic acid primases and polymerases accurately. Once the full chain is polymerized inside the cell, it is flipped by a two-component ABC transporter, TarGH, to the outer surface of the bacterial membrane and ligated to the PG [153]. The exact mechanism by which this transport takes place is not yet known. The pathway in *S. pneumoniae* and other species has not been as well elucidated and most of the enzymes, apart from those responsible for choline uptake, have been deduced by bioinformatic analysis and remain to be experimentally validated [139].

Unlike PG, WTAs are not essential for survival of *S. aureus in vitro* as the first two genes in the pathway can be deleted. However, the subsequent genes in the pathway were identified as essential [154, 155]. This apparent paradox was resolved by studies showing that the downstream genes in the WTA pathway can be deleted as long as one of the first two genes has been disrupted [156]. This finding implied that the essentiality of the downstream genes was conditional on flux into the pathway, and it was suggested that lethality due to a late block in WTA biosynthesis could arise from accumulation of a toxic metabolite or from sequestration of the Und-P carrier lipid in WTA intermediates, which would lead to inhibition of PG biosynthesis [157]. It was recently shown that inhibiting a late step in WTA biosynthesis results in rapid depletion of the PG precursor Lipid II, consistent with lethality arising from inhibition of PG biosynthesis [93]. Other cell envelope polymers such as CPS are synthesized on the

Und-P carrier lipid, and the biosynthetic pathways for some of these also contain a mix of non-essential early genes and conditionally essential late genes [158]. Conditional essentiality of the late genes depends on whether intermediates can be metabolized through an alternative pathway to release the carrier lipid.

The final step of the WTA pathway involves the ligation of WTAs onto PG. The LytR-CpsA-Psr protein family was recently shown to be involved in this process [159-161]. *B. subtilis*, *S. aureus*, and *S. pneumoniae* strains have three LytR-CpsA-PsR homologs. In the case of *S. aureus*, one of these homologs, LcpC, has been shown to be involved in ligation of CPS to PG [162]. The other two appear to be involved in ligation of WTAs to PG [163], but their cellular functions had not been clearly delineated. Recent studies in the Kahne and Walker lab have shown that while LcpA and LcpB are able to ligate WTA onto PG in a reconstituted *in vitro* assay, LcpA is the primary WTA ligase *in vivo* [164].

1.4.3 Lipoteichoic acid structure

In most organisms, LTAs are synthesized by completely different biosynthetic pathways from WTAs, except in the case of *S. pneumoniae* where the repeating units are structurally identical and are thought to be assembled using the same enzymes [139, 140]. The most common LTA structure comprises a polyglycerol-phosphate chain anchored to a glycolipid in the membrane. This type of LTA is found in *S. aureus*, *B. subtilis*, and *L. monocytogenes*. In other species of Gram-positive organisms, LTAs contain additional sugar moieties connecting the glycolipid anchor to the polyglycerol-phosphate polymer. The glycolipid anchor is usually diacylglycerol with two glucose

moieties (Glc₂DAG), as in *S. aureus* and *B. subtilis*, but it can also contain more than two glucose residues (*Clostridium difficile*) as well as other sugar moieties such as galactose (in *L. monocytogenes*) or GlcNAc (in *Clostridium innocuum*) [5, 165].

1.4.4 Lipoteichoic acid synthesis

LTA synthesis begins in the cytoplasm with the assembly of the glycolipid anchor (Fig. 1.5). In *S. aureus* and *B. subtilis*, YpfP (also called UgtP) is responsible for attaching both glucose units to diacylglycerol (DAG) to give the glycolipid anchor, Glc₂DAG [166, 167], which is then flipped across the membrane by LtaA [168]. LtaS then builds the polymer chain by transferring glycerol-phosphate from phosphatidylglycerol to Glc₂DAG [169]. Deleting *ypfP* or *ltaA* does not abolish the synthesis of LTA, but results in polymers with altered structure. Evidently, LTA can be synthesized on DAG, as well as Glc₂DAG [168]. LtaS is a polytopic membrane protein with an extracellular domain. The crystal structure of the extracellular domain of LtaS (eLtaS) bound to glycerol-phosphate has been reported and suggests a possible covalent mechanism for LtaS in which an active site threonine reacts with phosphatidylglycerol to form a covalent glycerol-phospho-threonine intermediate. This intermediate is resolved by reaction with the hydroxyl group of the growing LTA chain [170, 171]. Some organisms such as *L. monocytogenes*, contain a two-enzyme pathway to make LTA main chains [172]. One enzyme, LtaP, functions as a primase to add one unit of glycerol-phosphate to the glycolipid anchor. In the case of *L. monocytogenes*, this glycolipid anchor is Gal-Glc-DAG. A polymerase, LtaS, then extends the chain. LtaP is not essential for LTA synthesis; however LTAs from a *ltaP* null mutant are longer than

those from the wild type strain [172], as in a *ltaA* or *ypfP* deletion in *S. aureus*. The mechanistic basis for length differences between "primed" and "unprimed" glycolipid anchors is not understood. A recent crystal structure of LtaS from *L. monocytogenes* reveals a glycerol-phosphate binding site that may accommodate part of the growing LTA chain [173]. While glycerol-phosphate polymerization activity has not been reconstituted for any LtaS, perhaps because some of the transmembrane helices form part of the active site for polymerization, eLtaS from *S. aureus* was shown to be sufficient for cleavage of the phosphodiester bond in phosphatidylglycerol [174]. The diacylglycerol product released in the LtaS reaction with phosphatidylglycerol is recycled back into the cell and the protein responsible for recycling has been identified as diacylglycerol kinase DgkB [175].

While *S. aureus* contains only one LtaS and *L. monocytogenes* has LtaP and LtaS, *B. subtilis*, has four LtaS homologs [169, 171]. It has been reported that while three of these homologs - LtaS, YqgS, and YfnI - have LtaS-like activity, one of them, YvgJ, functions as a primase [176]. Unlike in *L. monocytogenes*, the *B. subtilis* primase is not required for normal LTA synthesis, suggesting that the LtaS enzymes are capable of initiating synthesis of LTA polymers efficiently. YfnI has been shown to make LTA polymers that are substantially longer than those produced by LtaS or YqgS [176]. The observation that *yfnI* expression is regulated by the alternative sigma factor SigM, which responds to stress conditions [177], suggests that certain stresses call for the production of elongated polymers in *B. subtilis* [176]. Phenotypically, *ltaS* mutants show increased cell elongation and chain length, reduced cell diameter, cell bending, lysis and abnormally thick septa, whereas single deletions of the other three homologs do not

have any obvious defects. The *ltaS-yqgS* double mutant has sporulation defects; all other double mutant combinations with *ltaS* can sporulate. These results implicate LtaS and YqgS in sporulation. The quadruple mutant is viable, although it has a more severe phenotype than the single *ltaS* mutant [171]. Deletion of *ltaS* in *S. aureus* has also been accomplished, but viable mutants have suppressors that enable growth through a mechanism that involves increased levels of cyclic-di-AMP, which may regulate cell membrane functions [178, 179]. Even with the suppressor, these mutants have severe cell division defects [169, 179, 180]. Hence, LTAs are critical even for *in vitro* growth of many Gram-positive organisms.

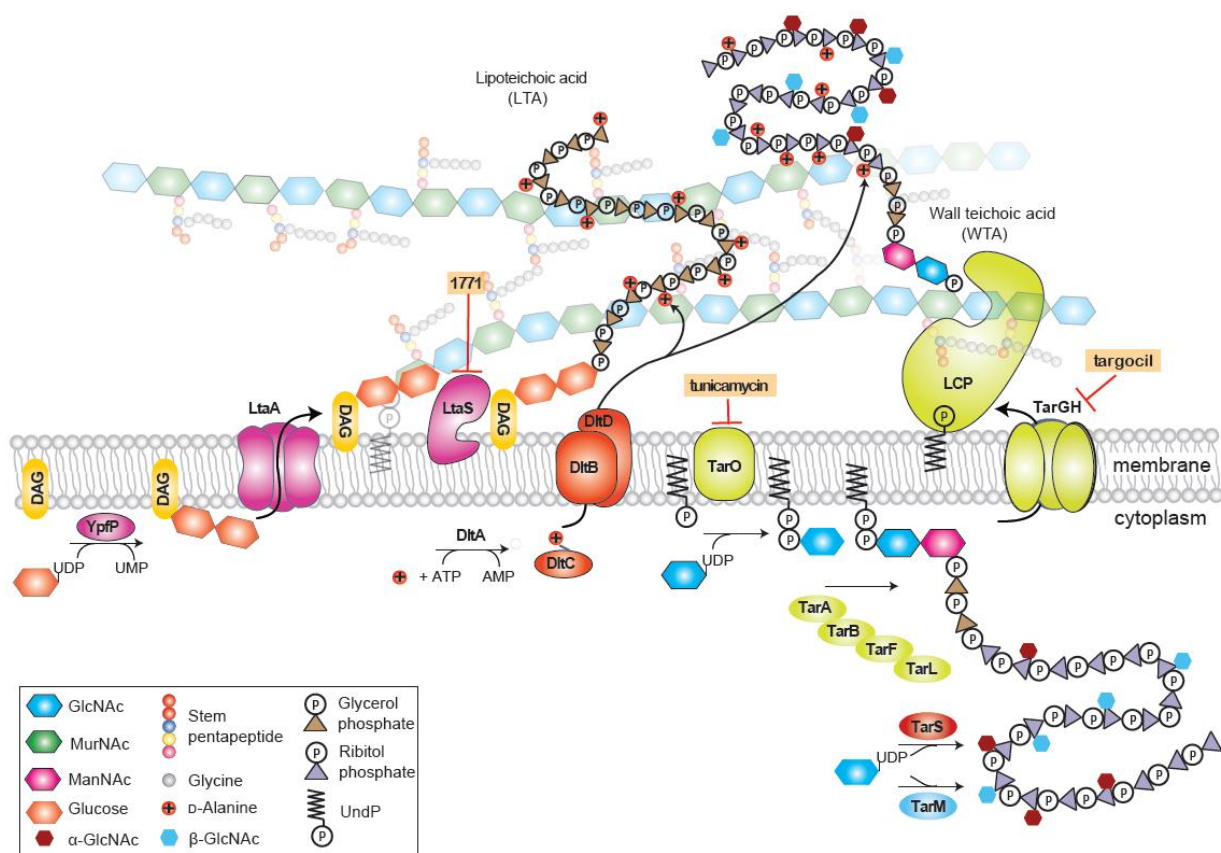


Figure 1.5: TA biosynthesis and modification pathways. LTA and WTA biosynthetic pathways in *S. aureus* are shown here. Although both are anionic sugar-phosphate

(Continued) backbones, they are assembled differently by separate biosynthetic pathways in *S. aureus*. TAs are further modified with D-alanine residues by the *dlt* pathway and with α - or β - GlcNAC residues installed by glycosyltransferases TarM and TarS, respectively. TAs perform several functions for the cell including playing roles in biofilm formation, adhesion, phage attachment, virulence and antibiotic resistance, most notably resistance to β -lactams. D-alanylation has been shown to play an important role in these functions as well. Specifically, the absence of D-alanine modifications sensitizes to cationic antimicrobial peptides, including host defensins. The only known roles for α - and β - GlcNAC modifications are in phage attachment, and for β -GlcNAcs, in β -lactam resistance. Due to its roles in adhesion, virulence and antibiotic resistance, attempts are being made to target TA biosynthesis and modification pathways. The known compounds targeting these pathways are shown here.

1.4.5 Tailoring modifications of teichoic acids

Both LTAs and WTAs are often modified with D-alanine esters to modulate the charges of the cell envelope. They can also be modified with sugar moieties. These tailoring modifications have been implicated in numerous functions in cell physiology and infection.

D-alanylation: The ribitol (in WTA) or glycerol (as in *S. aureus* LTA) groups in TAs are frequently decorated with D-alanine moieties, which introduce positive charges to neutralize the negatively charged phosphates in the polymer backbone. On ribitol groups, D-alanylation occurs at the C2 position [132]. D-alanine moieties are added by four proteins, DltABCD, encoded by the *dlt* operon (Fig. 1.5). DltA activates D-alanine as

the AMP ester and then transfers it to the sulfhydryl group on the phosphopantetheinyl arm of the carrier protein DltC [181-184]. DltA is similar to carrier protein ligases found in non-ribosomal peptide synthetases [4, 5, 185]. The next steps are not understood. DltB is a polytopic membrane protein belonging to the mBOAT family (for membrane-bound O-acetyl transferases), which is ubiquitous in all kingdoms of life [186]. DltD contains a single membrane spanning helix and an extracellular domain with predicted esterase/thioesterase activity [4, 187]. It has been proposed that DltC transfers D-alanine to Und-P to form an acyl-phosphate intermediate, which is then transferred through the membrane by DltB to modify LTAs with the assistance of DltD [183, 187]. There is no evidence for the proposed acyl-phosphate intermediate and the reaction to form it from the thioester is thermodynamically unfavorable, although it may conceivably be coupled to hydrolysis of the pyrophosphate released during D-alanine activation by DltA. Pulse-chase experiments have suggested that D-alanines installed on LTAs are subsequently transferred to WTAs [188, 189], but the mechanistic details of the transfer are unclear. In particular, it is not known whether an enzyme is involved in the process.

Glycosylation: The majority of ribitol phosphate groups in WTAs in *S. aureus* are glycosylated with GlcNAc on the ribitol C4 position [4]. Similarly, LTAs can also be glycosylated with GlcNAc or α -galactose in *B. subtilis* [5]. In *S. pneumoniae*, LTA can be glycosylated with GalNAc [190]. In staphylococci, it has been shown that D-alanylation and glycosylation compete for the same position on LTAs. Approximately 70% of the glycerol-phosphates carry D-alanines while 15% carry GlcNAc moieties [6]. WTA precursors are glycosylated intracellularly and the enzymes responsible for glycosylation have been identified in a number of organisms. In *B. subtilis* 168, TagE

attaches α -glucosyl units to the polyglycerol-phosphate WTA chains [191]; in *B. subtilis* W23, TarQ attaches β -glucosyl units to the polyribitol-phosphate WTA chains [192]. In *S. aureus*, TarM attaches α -GlcNAc residues while TarS attaches β -GlcNAc residues [192-194]. No enzymes responsible for LTA glycosylation, which occurs extracellularly, have yet been identified. It is likely that these enzymes use membrane-anchored sugar substrates that cannot diffuse away from the cell, and therefore do not resemble the nucleotide-diphosphate sugar transferases that glycosylate WTA precursors inside the cell.

1.4.6 Roles of teichoic acids and their tailoring modifications in cell physiology and immune evasion

Roles in cell division and morphology: TAs perform several crucial functions for the cell. In *B. subtilis*, WTAs are required to maintain the rod-shaped morphology [195-197]. In the quadruple mutant lacking all four LtaS homologs, there are severe cell division and septation defects that cause filamenting and clumping of cells and the mutant grows very slowly, indicating that LTAs are required for proper cell division [171]. Disruption of YpfP caused the rod-shaped cells to become bent and distended, and also disrupted the localization of the cytoskeletal protein MreB, important for the rod-shape in *B. subtilis* [198]. Interestingly, YpfP has also been implicated in a metabolic sensing role, localizing to the division site in a nutrient-dependent manner and inhibiting the assembly of FtsZ. It is important that the number of Z-rings to cell length is maintained at a constant ratio so cells do not initiate division before reaching the correct cell mass. Thus, YpfP could play a significant role in cell cycle events [199]. In *S. aureus*, both LTAs and WTAs have been implicated in cell division: mutants defective in either LTA or

WTA biosynthesis have major septal defects, including placing new septa at angles non-orthogonal to previous septa and forming multiple septa almost simultaneously. These mutants are also impaired in separation after division [169, 180, 200]. In *S. aureus*, LTAs are more critical to the cell than WTAs *in vitro* as evidenced by the fact that the *ltaS* deletion strain is viable only in the presence of suppressors [179], whereas *tarO* mutants grow fairly well. WTAs, however, become very important *in vivo* [201-203]. Simultaneous disruption of WTAs and LTAs is lethal in both *S. aureus* and *B. subtilis* [171, 180, 204]. In *S. aureus*, cells lacking both polymers are unable to form the essential division ring (Z-ring) [204]. Interestingly, in the absence of WTAs, D-alanyl modifications on LTAs become essential. Both WTAs and D-alanylation have been implicated in autolysin regulation, and when WTAs and D-alanines are both missing, cells lyse rapidly. The evidence suggests that LTAs and WTAs have overlapping but not fully redundant roles in cell division and autolysin regulation [204].

Roles in ligand binding and scaffolding: TAs have been implicated in binding cations, and this correlates inversely with D-alanylation levels [132, 205]. Cation homeostasis is thus an important function of TAs that can be regulated through D-alanylation. WTAs also serve as phage receptors in *S. aureus* [192, 194, 206, 207]. Phage binding is mediated by the GlcNAc modifications added on to WTAs [192, 194]. A requirement for glucose in TAs for phage adsorption has been shown in *B. subtilis* [168] as well [191, 207]. WTAs have also been implicated in other protein scaffolding roles. For instance, in *S. aureus*, FmtA, a protein that plays a role in methicillin-resistance in MRSA strains, was shown to bind to WTAs [208]. In *S. pneumoniae*, several proteins bind specifically to the choline moieties on TAs. These proteins, which

include the highly studied virulence protein PspA, have been implicated in numerous functions from adhesion to virulence, and cell wall hydrolysis [209-213]. In *L. monocytogenes*, InIB, a protein that promotes entry into mammalian cells is shown to interact with LTAs [214]. The domain necessary for interaction with LTAs in this protein contains GW modules (conserved modules of ~80 amino acids which have the dipeptide Gly-Trp). These modules have also been identified in Ami, a *L. monocytogenes* autolysin and the *S. aureus* autolysin Atl [215]. Autolysins are hydrolases that degrade PG and thus play an essential role in cell division and separation. In *S. aureus*, WTA plays a role in Atl localization. While Atl is usually localized to the cross-wall, it is mislocalized across the cell surface in WTA deficient strains. Mislocalization of autolysins could be one reason WTA-deficient mutants are prone to autolysis [216]. It has been suggested that D-alanylation is also involved in autolysin regulation [217]. Similarly, PBP4 in *S. aureus* is also mislocalized when WTAs are absent [218], indicating a role for WTAs in the localization of PG biosynthetic machinery.

Roles in antibiotic resistance and virulence: In MRSA, the lack of WTAs dramatically reduces the organism's resistance to β -lactams, indicating that WTAs play a major role in methicillin-resistance of *S. aureus* [200]. The influence of WTAs on resistance has been traced specifically to the β -GlcNAc modification on WTAs, which suggests that β -GlcNAcylated WTAs scaffold a factor required for β -lactam resistance [192]. In *S. aureus*, WTAs also provide resistance to antimicrobial fatty acids on the skin during skin colonization [219]. D-alanylation plays an important role in modulating resistance to certain antibiotics. It is very important for repelling cationic antimicrobial

peptides (CAMPs), a crucial part of host immune response [220-222]. This has been observed in several Gram-positive species including *S. aureus* [222], *S. pneumoniae* [223] and *E. faecalis* [224]. An increase in D-alanylation is also observed in mutants resistant to daptomycin, an antibiotic used to treat MRSA [225]. Antimicrobial resistance due to D-alanylation has been attributed to its functions in imparting positive charges to the cell surface and its contributions to changes in the biophysical aspects of the cell envelope [226, 227].

TAs in their D-alanylated form play a major role in biofilm formation, adhesion to the surface of cells and medical devices, colonization of host tissue, and virulence, likely due to surface charge effects [4, 5, 132, 228, 229]. Biofilms, which consist of viable cells held together by an extracellular matrix of DNA and proteins from lysed cells as well as extracellular polysaccharides and other polymers, form on surfaces of medical instruments or in hosts, and enable the organism to evade both natural and synthetic antimicrobials [230-232]. Thus, adhesion and biofilm formation are key tools in a pathogen's arsenal. The role of TAs in adhesion and effective host colonization has been well established in several Gram-positive organisms [224, 233-235]. In *S. aureus*, WTA glycosylation has specifically been implicated in adhesion [236]. For all these reasons, TAs are potent virulence factors and mutants lacking TAs or D-alanylation have highly attenuated virulence [203, 220, 237-240]. As mentioned above, several choline-binding proteins in *S. pneumoniae* have roles in virulence and mutants made to grow independent of choline have highly attenuated virulence [241].

LTAs contribute to the immune response generated during infection by Gram-positive bacteria [242]. Although there was some controversy concerning whether the

immunomodulation arises from LTAs or from lipoproteins that are often copurified [243, 244], evidence suggests that LTAs likely affect the immune system response on their own as well [245-247]. LTAs are reported to stimulate the production of cytokines [248-250] and those from *S. pneumoniae* and *S. aureus* can activate immune cells via toll-like receptor 2, lipopolysaccharide binding protein and CD14 [251, 252]. They also activate the complement system of the immune response [253, 254] and can affect other macrophage parameters, including secretion of tumor necrosis factor α and nitrite [255]. Antibodies have been identified that are directed towards non-D-alanylated LTAs in *E. faecalis* [256]. Due to this ability to modify host immunity, efforts are ongoing to develop LTA-conjugated vaccines against gram-positive bacteria [5]. The choline-binding proteins anchored to TAs in *S. pneumoniae* could be used as vaccine candidates as well [213, 257].

1.5 Capsular Polysaccharides

Capsular polysaccharides (CPS) are highly variable glycopolymers that are anchored to PG [13, 158, 162, 258]. They extend above the cell wall and have been implicated in phage resistance and immune evasion [259, 260]. Although not present in all Gram-positive organisms, encapsulation is observed in most highly-pathogenic strains. Since CPS is best studied in *S. pneumoniae*, we will focus on the structural diversity in CPS in *S. pneumoniae* and their function in immune evasion.

1.5.1 Structural diversity of capsular polysaccharides

A phenomenal 93 different serotypes of pneumococcal capsule have been identified over the years and most of the serotypes can cause infection [13, 261]. Recombinational exchanges at the CPS biosynthetic locus can result in a large amount of variation in capsular type [262]. Disruption and sequence changes in the genes of the CPS cluster occurring naturally can change the CPS serotype from one to another [263-265] contributing to the diversity of pneumococcal capsules. These differences are usually observed in the gene responsible for modifying sugar moieties in CPS with *O*-acetyl groups. In fact, *in vivo* switching from one capsule type to another has been observed [266]. This switch has been attributed to a change in the number of short tandem TA nucleotide repeats in the putative *O*-acetyltransferase gene, which could explain reversible switching between serotypes that might occur *in vivo* [265].

CPS is made of long chains of repeating oligomeric units and the repeating units vary between serotypes. As an example, the repeat unit of *S. pneumoniae* serotype 2 is made of a backbone with glucose-rhamnose-rhamnose-rhamnose unit and a glucose-glucuronic acid side chain [267]. Recently, serotypes of *S. pneumoniae* that have CPS containing two different repeat units have been described [268, 269]. There are multiple different serotypes in *S. aureus* as well. Out of the 11 serotypes described for *S. aureus*, serotypes 5 and 8 are responsible for the majority of human infections [259].

1.5.2 Capsular polysaccharides, host immunity and vaccine development

It has long been known that CPS reduces the ability of bacteriophage to interact with the cell surface [270]. CPS plays a major role in virulence of bacterial pathogens and capsule mutants are avirulent. Capsule has been shown to facilitate abscess formation by activating T-cells in the host immune system [271]. The complement system is important in immune response activation and clearing an infection. Capsule is able to mask the binding of opsonic C3 fragments to the complement receptor, thus decreasing opsonization and phagocytosis by leukocytes [272, 273]. This has also been demonstrated in *E. faecalis*, where capsule masks C3 deposits and LTAs from detection by the host immune system, thereby decreasing tumor necrosis factor α production [274]. In Group B *Streptococcus*, the terminal sialic acid groups on capsules have been shown to interact with Siglecs on human leukocytes. They are suggested to mimic the human cell surface glycans, reducing the activation of innate immune response [275, 276].

Due to the high immunomodulatory ability of CPS, it has been explored for vaccine development. It has been known for a long time that immunization with polyvalent pneumococcal polysaccharide is effective as a vaccine [277, 278]. It was later shown that conjugating the polysaccharides to a carrier protein resulted in a more effective vaccine [279]. Today different variations on pneumococcal vaccines are available, incorporating up to 23 polysaccharide variants (PPSV23), or conjugate vaccines incorporating 7 (PCV7) or 13 (PCV13) CPS serotypes [280-282]. PCV13 is used for immunization of infants <2 years of age and has recently also been approved for immunizing adults 50 years or older in series with PPSV23. PPSV23, however, is not

effective in infant immunization. This is because PPSV23 generates immune responses that are T-cell independent and therefore, poorly supported by the immature immune systems of children <2 years. In contrast, PCV13 generates immune responses that are mediated by T-cell dependent mechanisms effective in infants [281]. Efforts are being made in improving not only the polysaccharide composition of vaccines but also the carrier protein used to conjugate the polysaccharide. The immunogenic properties of the carrier protein could alter the immune response to the vaccine [283, 284]. There is a concern that pneumococcal conjugate vaccines select for non-vaccine serotypes. Pelton *et al.* reported that immunization with PCV7 during 2000-2003 reduced vaccine serotypes from 22% to 2% but increased the incidence of non-vaccine serotypes from 7% to 16% [285]. With over 90 different serotypes of *S. pneumoniae*, this is an important concern, and studies are ongoing to resolve this issue [286, 287].

Capsular conjugate vaccines against serotypes 5 and 8 of *S. aureus* have also been explored [288-290]. However, these vaccines have so far not passed clinical trials [291, 292], and evidence has emerged that this reduced efficacy could be due to interference from natural non-opsonic antibodies to PNAG, the *S. aureus* exopolysaccharide, present in human serum [293].

1.6 Exopolysaccharides and biofilm formation

Apart from these major cell envelope structures, other glycopolymers called exopolysaccharides are secreted by cells as well. These exopolysaccharides are long chains that associate with each other to form the biofilm matrix [231, 294, 295].

Polysaccharide intercellular adhesin (PIA) in *S. epidermidis* is a well-studied component

of biofilms [296, 297]. It is a linear polymer of β -1,6-linked GlcNAc moieties, although some residues can be *N*-deacetylated. PIA/PNAG is suggested to be held to the cell surface by ionic interactions of the positively charged, un-acetylated moieties of the polymer, so *N*-deacetylation is important for surface localization of PIA [298]. PIA is synthesized by the *icaADBC* operon in *S. epidermidis*, and homologs have been identified in other species including *S. aureus* [296, 299-301]. In *S. aureus*, this high molecular mass exopolysaccharide termed PNAG is produced by biofilm forming strains. Due to its role in modulating immune responses, vaccines using conjugated PNAG are also being explored [302]. Its role in biofilm formation has created interest in the study of the role of each enzyme in the *icaADBC* operon and how it is regulated [12, 303] (Arciola *et al.* 2015; O'Gara 2007). There are also *ica*-independent methods for biofilm formation which include roles by TAs and cell-surface associated proteins. The mechanism for biofilm formation in MRSA appears to be *ica*-independent; whereas it is *ica*-dependent in the sensitive strains [303]. Biofilm formation is thus a complex and highly regulated system.

1.7 Antibiotics targeting the cell envelope

Due to the crucial importance of the cell envelope to cell survival, many antibiotics that target cell envelope synthesis have been developed over the years (Fig. 1.3) [14]. There are some antibiotics that target the intracellular steps of PG synthesis, including fosfomycin, which inhibits MurA, the first committed step of PG synthesis [304]. However, the greatest clinical successes have been achieved by those antibiotics that target the extracellular steps of cell wall synthesis. These include the unusual

substrate-binding antibiotics, which form complexes with cell wall precursors instead of the enzymes that process them. Binding to these precursors prevents their use and results in inhibition of cell wall synthesis. Vancomycin, a glycopeptide antibiotic used to treat MRSA, belongs to the substrate-binding class of antibiotics. It binds to the D-Ala-D-Ala motif of the stem peptide in Lipid II and nascent PG, thereby interfering with both Lipid II polymerization to form PG strands and with subsequent crosslinking of the strands [305-308]. Binding to and sequestering Lipid II has been established as the mechanism of action of some other antibiotics including ramoplanin, a cyclic lipoglycopeptide antibiotic [309, 310], nisin and other lantibiotics [311-314], and the recently discovered teixobactin [315]. All these compounds recognize the pyrophosphate-sugar moiety of Lipid II. Plectasin, a fungal defensin, also acts by binding to Lipid II [316]. Human defensins have also been shown to interact with Lipid II [317, 318]. It is interesting that antimicrobial peptides produced by the host as part of the innate immune response use Lipid II binding to counteract bacterial threats. The structural diversity of the compounds that bind Lipid II is truly astonishing and indicates that this cell wall precursor is an exceptional target.

Development of resistance to compounds which bind to essential substrates is particularly slow for several reasons. They typically act on the extracellular surface of the membrane and are not subject to efflux pump-mediated resistance mechanisms. Moreover, because they do not bind to a protein target, a single mutation in the gene encoding the target cannot confer high level resistance [319]. In the case of vancomycin, intermediate resistance can arise through multiple mutations that modify the envelope, but high level resistance only arises due to modification of the structure of

the target substrate [320-322]. The modification, which involves replacing D-Ala-D-Ala with a dipeptide to which vancomycin cannot bind, requires several enzymes as well as a two-component sensing system, and the genes encoding these enzymes are encoded on a cassette that is transferred between organisms [323, 324]. Glycopeptide resistance genes originated in a glycopeptide producer as a means of self-immunity, but have now spread widely, particularly in enterococcal strains [325]. D-Ala-D-Lac, synthesized by the *vanA* cassette, is the most common replacement for D-Ala-D-Ala in vancomycin resistant strains. Vancomycin has a thousand fold lower affinity for D-Ala-D-Lac because a crucial hydrogen bond between the drug and the target can no longer be formed [323, 326, 327]. A change from D-Ala-D-Ala to D-Ala-D-Ser in Lipid II can also cause moderate resistance to vancomycin [328, 329]. Although high level vancomycin resistance is common in enterococci (VRE), it has not yet emerged as a major problem in *S. aureus*, likely due to reduced frequency of transfer of the resistance cassette between enterococci and staphylococci [324, 330]. The several cases where vancomycin-resistant *S. aureus* (VRSA) have been identified have involved co-infection with VRE [331-335]. The barriers that prevent facile transfer of *vanA* resistance into *S. aureus* are not well understood, and there is concern that these barriers may be overcome with continued evolution. While there is interest in substrate binders as a class, none of the ones that recognize the sugar pyrophosphate portion of Lipid II have been developed for clinical use, although ramoplanin is in clinical trials [336]. As with vancomycin, high level resistance to ramoplanin does not develop spontaneously. Moderate ramoplanin resistance develops after multiple passaging and involves cell envelope modifications that may impede access to the Lipid II target on the cell surface [337]. If any Lipid II

binders come to be used clinically, resistance genes from the producing organisms may eventually find their way into relevant pathogens, like in the case of vancomycin.

β -lactams, a remarkably successful class of antibiotics, are also among the extracellular PG synthesis inhibitors. β -lactams are proposed structural mimics of D-Ala-D-Ala and inhibit the transpeptidase activity of PBPs by acylating the active site, preventing the cross-linking of stem peptides [338, 339]. Widespread resistance to β -lactams first emerged in the form of β -lactamases, which degrade β -lactams [340]. Combination antibiotics of β -lactams with β -lactamase inhibitors are used to treat many β -lactam resistant infections. One example is Augmentin, a combination of amoxicillin and clavulanic acid [341-343]. While β -lactamases continue to be a major concern in Gram-negative organisms such as *Klebsiella pneumoniae* and *Pseudomonas aeruginosa* [344, 345], some Gram-positive organisms have acquired a different mechanism of resistance. Methicillin-resistant *S. aureus* (MRSA) expresses a penicillin-binding protein (PBP2A) that has reduced affinity for β -lactams [95, 96, 346]. When native PBPs are inhibited by β -lactams, PBP2A can continue to crosslink PG. Due to the growing concern about the spread of MRSA, a significant amount of time has been invested in designing next generation β -lactams that can target the resistant PBP, including ceftobiprole [347] and ceftaroline [348]. In addition, other classes of antibiotics have been developed to treat MRSA, including daptomycin, tedizolid, linezolid, and the glycopeptide analog oritavancin [349-352].

1.8 The quest for novel antibiotic targets

Resistance to antibiotics of all classes is a serious concern for the future of human health, and efforts should be made to identify novel pathways that can be targeted by new antibiotics or whose inhibition can potentiate the effects of existing antibiotics in resistant strains. Efforts are ongoing to identify and target the multiple other steps involved in the PG biosynthetic pathway. For instance, inhibitors of the Lipid II flippase in *S. aureus*, DMPI and CDFI, have been identified [353]. Targeting pathways that contribute to resistance to current antibiotics is also being explored as a viable option. Apart from the β -lactamases described above, the potential for targeting such auxiliary proteins and pathways is immense, particularly in the case of MRSA, where many cellular factors contribute to β -lactam resistance [354]. For instance, changes to the stem peptide and interpeptide bridge re-sensitize MRSA to β -lactams [45, 72, 76, 355]. This has also been observed in *S. pneumoniae* [356]. In *S. aureus*, inactivation of one of the PBPs involved in cross-linking of stem peptides, PBP4, is shown to play a role in resistance to β -lactams [357]. This has also been shown for the inhibition of PG amidation [68]. Inactivation of *tarO*, encoding the first step in WTA biosynthesis, also sensitizes MRSA to β -lactams [200]. Finally, factors affecting methicillin-resistance also include proteins of hitherto unknown functions. FmtA is an example of one such protein factor [358]. Further understanding of the roles and identification of compounds that target these auxiliary factors could be useful in designing effective combination therapies with β -lactams to treat MRSA.

Since TAs and their modifications perform such important functions in cell survival, virulence, and β -lactam resistance, they are being investigated for their

potential in combination therapies and as anti-virulence targets (Fig. 1.5). Tunicamycin, a well-known natural product inhibitor of the first step for WTA synthesis [359], has been shown to restore β -lactam susceptibility in MRSA [200]. Although tunicamycin is toxic to eukaryotes, potent, non-toxic TarO inhibitors could have great potential [360]. In addition, the conditionally essential nature of the WTA pathway has been exploited in a pathway-specific screen to identify downstream inhibitors with antibiotic activity [361]. Targocil and several other downstream inhibitors of the ABC transporter (TarGH) that exports WTA polymers have been reported [202, 362-364]. An inhibitor of LTA polymerization (compound 1771, [2-oxo-2-(5-phenyl-1,3,4-oxodiazol-2-ylamino-ethyl-2-naphtho[2,1-b]furan-1-ylacetate]) was also described recently [365]. Finally, due to its numerous roles in adhesion, virulence, and biofilm formation, the D-alanylation pathway is a potential candidate for anti-virulence therapy. A compound that inhibits the first enzyme in the pathway has been reported [366], but has not been shown to inhibit D-alanylation in cells. Recently, an inhibitor of DltB, amsacrine, that inhibits D-alanylation in cells, has been discovered [367]. Agents that inhibit biofilm formation and adhesion mediated by other factors are being actively investigated as well [368]. Inhibitors of TAs and their modifications are yet to make it to the clinic [369], although late stage WTA inhibitors have shown some efficacy in combination with β -lactams against MRSA in animal models [202].

Chapter 2: Validation of Tn-Seq approach to identify intrinsic resistance factors

Portions of this chapter have been assembled into a manuscript that has been submitted for publication [370].

2.1 Why is understanding factors that contribute to antibiotic resistance

important

Antibiotics have had a dramatic impact on life expectancy and the safety of medical procedures since they were introduced into the clinic in the early 1930s. The period between the 1950s and 1960s, known as the "Golden Age of Antibiotics", saw the development of numerous antibiotic classes that are still in use today, including tetracyclines, macrolides, aminoglycosides and glycopeptides [371, 372]. With the increased use of antibiotics both clinically and for agricultural purposes, there has been a surge in antibiotic resistance [372, 373]. Depending on the antibiotic, resistance can arise and spread quickly. For example, methicillin, a β -lactam antibiotic, was introduced in 1960 and resistance was identified in 1961 [374-376]. Today, methicillin-resistant *S. aureus* (MRSA) infections account for more than half of all fatalities due to antibiotic resistance in the U.S. [377, 378].

Resistance has been reported to antibiotics of all classes and mechanisms of action. The emergence of resistance is inevitable and must be managed by a number of approaches. In addition to tracking resistance and controlling antibiotic usage, it is necessary to identify new antibiotics to treat resistant infections. Some recent efforts to identify novel antibiotics were highlighted in the previous chapter. However, finding novel targets and chemical scaffolds to target drug-resistant infections has been difficult. Most "new" antibiotics are analogues of existing antibiotics, and some are old

antibiotics that have been repurposed by including compounds that target a resistance mechanism [379]. Augmentin, described in the previous chapter, is an example of the latter therapeutic strategy.

The previous chapter discusses the rise of antibiotic resistance in the context of the cell envelope, one of the major targets of many classes of antibiotics. Two major modes of resistance were discussed: acquired resistance and intrinsic resistance. Acquired resistance results from genetic transfer of antibiotic resistance cassettes from a resistant organism to a sensitive one. This type of resistance is observed in MRSA, with the acquisition of the staphylococcal cassette chromosome *mec* (SCC*mec*), containing *mecA*, which encodes for PBP2A, and in vancomycin-resistant *S. aureus* due to the acquisition of the vancomycin resistance cassette by *S. aureus*, as described in the previous chapter [95, 324, 330]. Intrinsic resistance arises due to factors that contribute to the cellular response to antibiotics. Whereas the sole purpose of acquired resistance factors is to confer resistance to antibiotics, intrinsic resistance factors typically play roles in the normal physiology of an organism in addition to increasing fitness under antibiotic stress. Several examples of intrinsic factors to various cell wall antimicrobials were discussed in the previous chapter. The contribution of intrinsic resistance factors to antibiotic resistance is not unique to *S. aureus*. For instance, the outer-membrane of Gram-negative organisms renders them intrinsically resistant to most antibiotics [380-383].

Understanding intrinsic resistance factors provides insight into the biology of an organism and may lead to the discovery of new therapeutic approaches. For instance, the *fem* factors and *tarO*, described in the previous chapter, are important in *S. aureus*

cell envelope biosynthesis and are targets for β -lactam potentiators [71-73]. Although hitherto relatively unexplored, knowledge of intrinsic resistance factors may also guide the use of appropriate combinations of existing antibiotics to suppress resistance that could arise to each individual antibiotic [379].

2.2 Transposon libraries and their use in identifying intrinsic resistance factors

Transposon libraries have been useful tools in identifying intrinsic resistance factors. Transposons are mobile genetic elements that can be moved into different parts of the genome by an enzyme called a transposase [384]. Since their discovery in the 1950s, these transposable elements have become widely used to make libraries of insertional inactivation mutants [385-388]. Many intrinsic resistance factors in *S. aureus* have been identified by arraying mutants selected on plates and screening them individually for increased susceptibility to a given antibiotic. For example, the gene previously known as *llm* and subsequently identified as *tarO*, was found to confer resistance to β -lactams in MRSA by replica plating a library of transposon mutants on a β -lactam [389]. Several other intrinsic factors that protect MRSA from β -lactams have been identified using the same approach. Similarly, *mprF* was first identified by replica plating a transposon mutant library in a *Staphylococcus xylosus* background on the cationic peptide gallidermin [22].

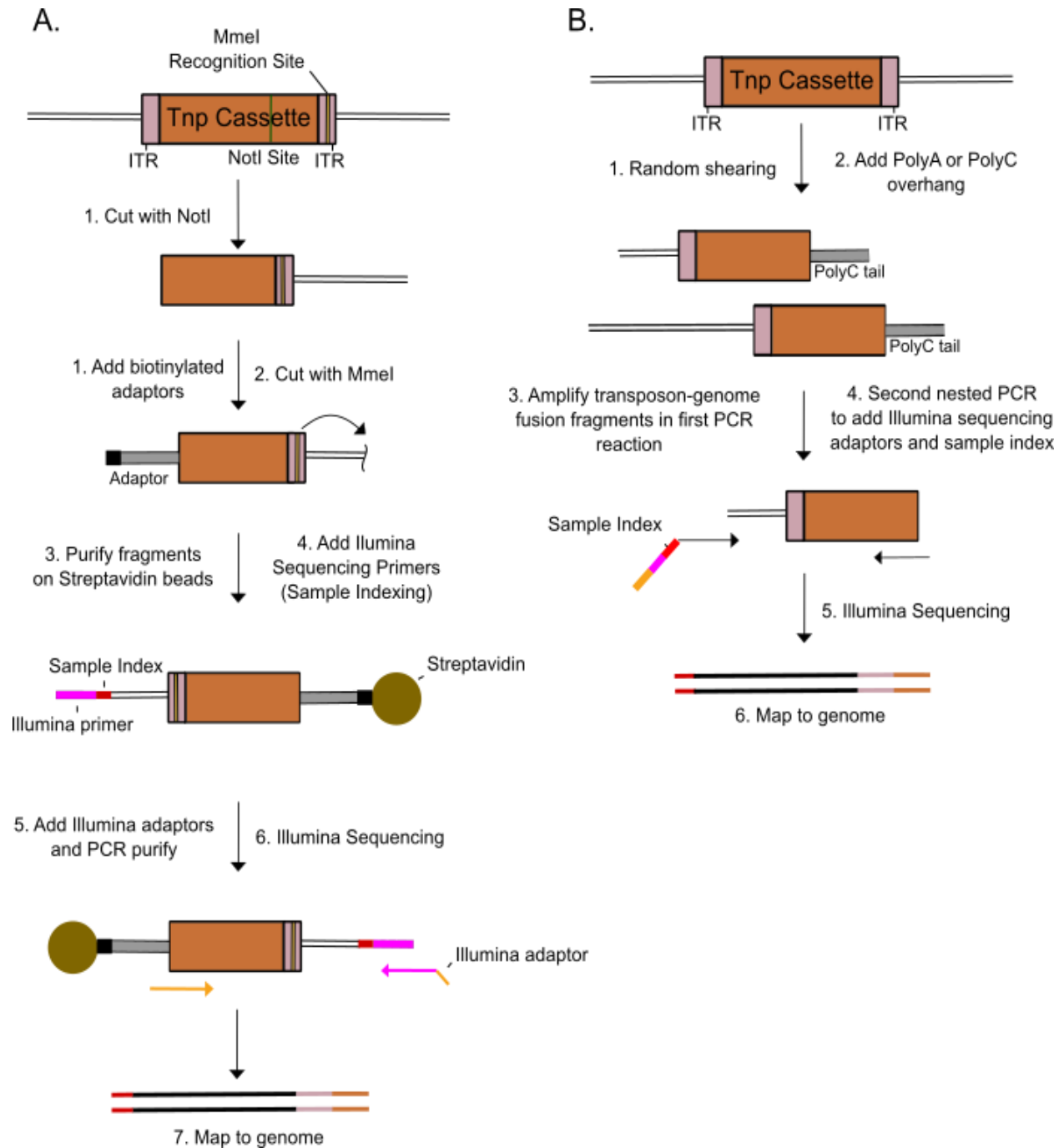
Several recent advances have made the use of insertional mutagenesis highly efficient. The characterization of the *mariner* transposon has allowed the facile creation of high-saturation libraries because the *mariner* transposase does not have extensive sequence recognition requirements: it catalyzes insertion into TA dinucleotides [390,

391]. Next-generation sequencing methods have made it possible to rapidly map the location of all transposon insertions in DNA isolated from pooled mutant libraries, even for mutant libraries containing ~700,000 individual mutants [388, 392]. There are several variants of transposon sequencing including InSeq, Tn-Seq, HTS and TraDIS [388], but all involve sequencing across a transposon-genome junction to identify the location of the transposon insertion. InSeq and Tn-Seq are similar in that the DNA sample preparation for sequencing includes an *MmeI* digestion step [388, 392, 393]; HTS and TraDIS are similar in that DNA samples are prepared using a shearing method (see Fig. 2.1) [201, 388, 394, 395]. In-Seq/Tn-Seq methods produce DNA of a uniform length, which may reduce PCR bias [388]. In any event, the ability to rapidly analyze fitness of all genes in a huge mutant pool upon treatment with an antibiotic allows global identification of intrinsic resistance factors.

Figure 2.1: Schematics of two methods for sample preparation of pooled transposon libraries for Illumina sequencing. The transposon cassette consists of the drug marker and construct specific barcodes (if any), flanked by inverted terminal repeats (ITRs). The transposase recognizes these ITRs and moves the cassette into a location on the genome. (A) In Tn-Seq, the ITR contains an *MmeI* recognition site.

Samples are digested with *NotI* to generate transposon-genome junctions and biotinylated adaptors (shown in grey) are added to facilitate subsequent purification of desired fragments. Then, samples are digested with *MmeI*, which cuts 20bp ahead of its recognition site. This results in biotinylated fragments containing ~16bp of the genome and transposon-genome junction. These fragments are then amplified by PCR to generate the final product. Illumina adaptors are also added at this stage. The amplified product is purified and sequenced by Illumina sequencing. Sequences from each fragment, referred to as reads, are mapped to the genome. Full details of this protocol are described in Santiago *et al.* [392] (B) In the second method, the ITR does not contain an *MmeI* site. The DNA is randomly sheared, resulting in fragments of varying length. PolyA or PolyC tails are added to the fragments. These are then subjected to PCR using a transposon specific primer to amplify transposon-genome junctions. This PCR reaction is used as a template to perform the next nested PCR which further amplifies the transposon-genome junction, and adds Illumina primers, adaptors and the sample index. These are then sequenced by Illumina Sequencing and sequences are mapped to the genome. Full details of this protocol are described in Valentino *et al.* [201]. Sample indexing makes it possible to multiplex several samples together and sequence a pooled library at the same time.

Figure 2.1 (Continued):



The technique of coupling high-throughput sequencing and transposon libraries has been used to identify essential genes in a number of organisms [393, 396, 397]. It has also been used to study the fitness of genes for various pathogens including *Vibrio cholerae* and *P. aeruginosa* in a number of infection models and infection-related ecologies [398-401], and under pressure of antibiotics [402, 403]. In *S. aureus*, in addition to identifying genes essential for *in vitro* growth under ambient, high, and low temperatures [154, 201, 392, 404], and analyzing fitness of genes in infection-related environments [201, 405, 406], this technique has also been used to identify genes that are important under pressure of small molecules [204, 367]. However, a systematic analysis of genes that can confer resistance to multiple classes of antibiotics in *S. aureus* has not yet been reported. We sought to determine whether Tn-Seq can be used to identify intrinsic resistance factors in *S. aureus* for antibiotics of different classes. This work was completed in collaboration with Dr. Marina Santiago, a former graduate student in the Walker Lab and Dr. Melissa Martin from Dr. Michael Gilmore's lab at Massachusetts General Hospital.

2.3 Experimental approach and data analysis

For these experiments, we used two different transposon libraries in the methicillin-sensitive *S. aureus* strain HG003. The first transposon library (Library 1), made by transformation with a temperature sensitive plasmid, contained insertions in 71,000 unique sites [201]. The second library (Library 2) was made using a phage-based transposition approach [392, 407, 408]. The efficiency of the phage-based approach enabled the multiplexing of six different transposon constructs containing

inactivation and outward facing promoter constructs to create a library containing 694,755 unique insertions (Fig. 2.2) [392]. The constructs with outward-facing promoters are useful for determining mechanisms of resistance that involve up-regulation of specific genes [408]. For this initial analysis, however, we wanted to identify effects due to gene inactivation alone, and so the insertions due to only one of the transposon constructs, the inactivation construct, were included in the present analysis, which covered 126,040 unique sites [392].

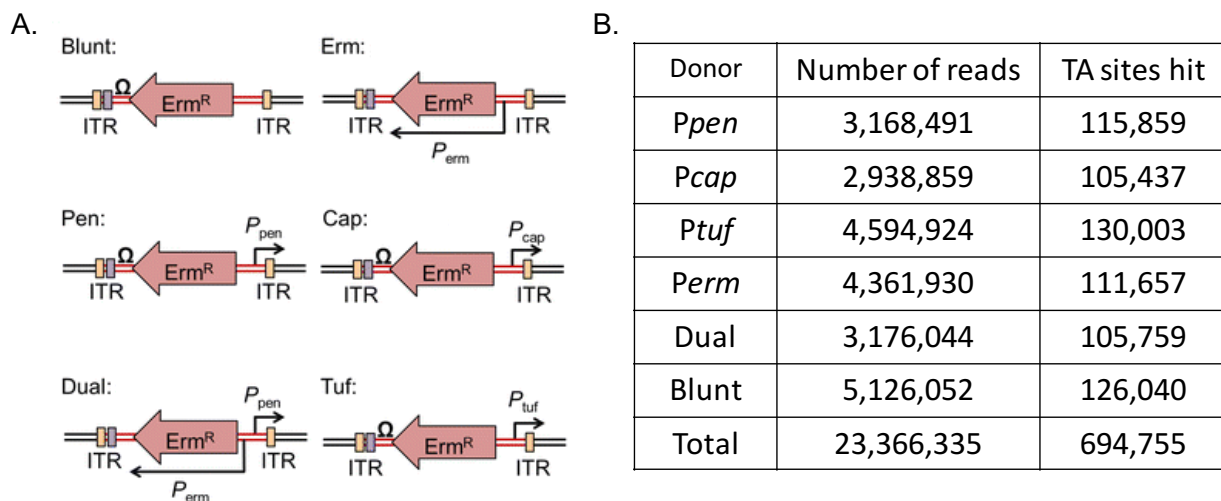


Figure 2.2: Transposon library 2 is constructed with six different transposon constructs. (A) The six different transposon constructs are shown: Blunt constructs are inactivation constructs only and contains no outward facing promoters. Dual contains two promoters oriented in opposite directions suitable for upregulating neighboring genes which are oriented in opposite directions. *Perm*, *Ppen*, *Pcap*, *Ptuf* are outward facing promoters of varying strengths. (B) Number of reads and TA sites hit due to each donor construct from two biological replicates are indicated. The whole library has 694,755 unique mutants, but the inactivation constructs alone covered 126,040 unique sites. Adapted from Santiago *et al.* [392].

DNA from both libraries was prepared for sequencing as described previously [201, 392], using a shearing method for Library 1 and *MmeI* digestion for Library 2 (see Fig. 2.1 and Methods). The two libraries were treated with sub-minimum inhibitory concentrations (sub-MICs) of six antibiotics. There were some differences in sample treatment for the two libraries, and we focused on the factors that were identified under both sets of treatment conditions (see Methods). This makes it unlikely that factors identified are artifacts of methods of library creation or sampling.

We wanted to evaluate the utility of a Tn-Seq approach for identifying intrinsic resistance factors using a relatively small set of antibiotics before expanding our efforts (see the Chapters 3 and 4). Therefore, we focused on six clinically used antibiotics: ciprofloxacin, oxacillin, gentamicin, linezolid, vancomycin and daptomycin. These six antibiotics were chosen for their clinical relevance and selected as representatives of antibiotics that target major pathways: DNA synthesis, protein synthesis, cell wall synthesis, and membrane stability (Fig. 2.3 A-B) [409-415]. For each antibiotic, four DNA samples from different treatment conditions (see Methods) were sequenced.

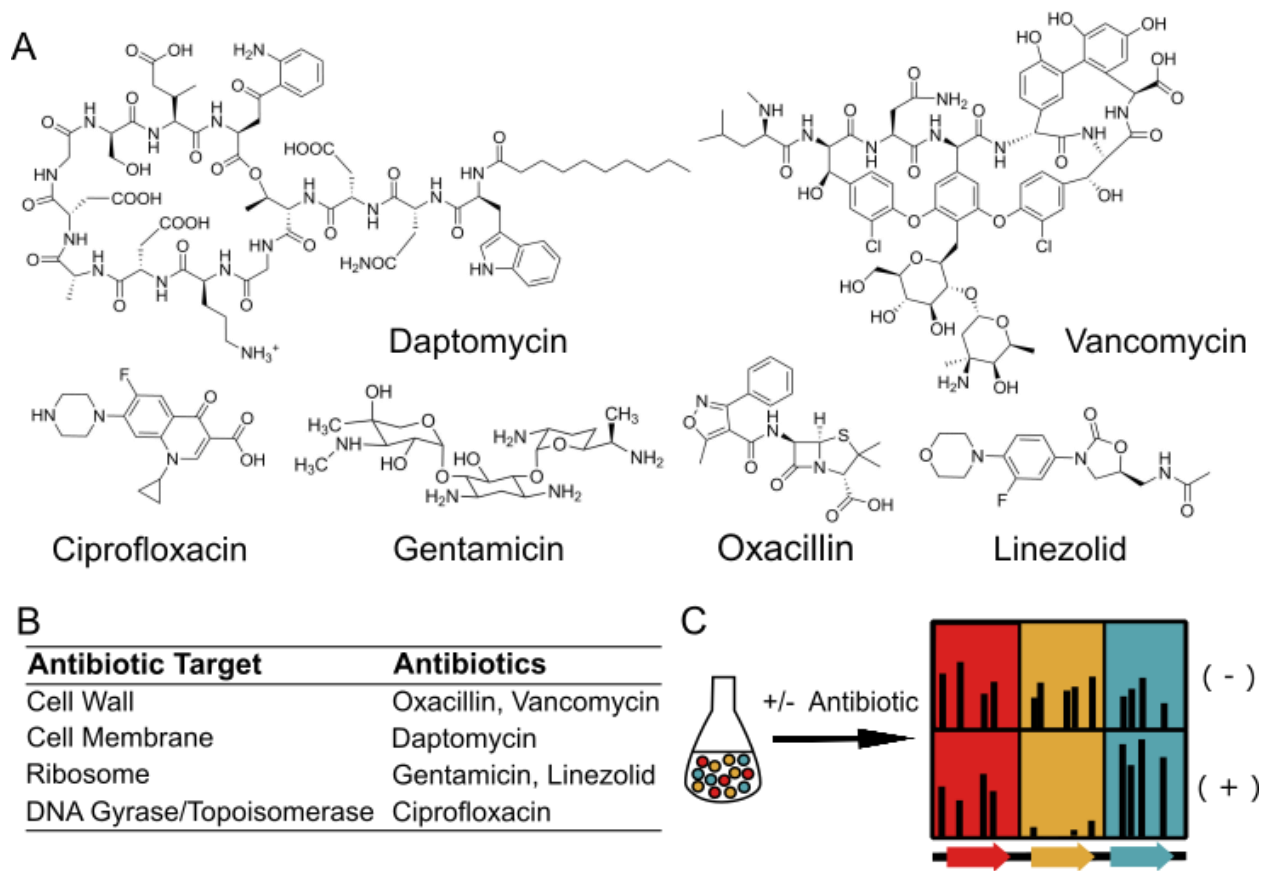


Figure 2.3. Intrinsic resistance factors that contribute to antibiotic resistance can be identified by Tn-Seq. A) The structures of the six different antibiotics used in the Tn-Seq experiments are shown. B) The targets of the six antibiotics are shown. C) A pooled transposon insertion library is grown with or without antibiotic and subjected to Tn-Seq to quantify the number of sequences (reads) that map to each insertion location. The black lines in the three genes depicted represent the number of reads attributed to a particular insertion location. In this example, the red gene has a similar number of reads in the treated and untreated samples. The orange gene has a lower number of reads in the treated sample than in the untreated control. Inactivation of this gene decreases bacterial fitness in the presence of the tested antibiotic. Genes of this type are known as intrinsic resistance factors. Finally, the blue gene has a higher number of

(Continued) reads in the treated sample than in the untreated control. Inactivation of this gene increases bacterial fitness in the presence of the test antibiotic.

The reads obtained for each condition were mapped to the genome using the Galaxy web server, hosted by the Tufts Genomic Core facility [416-418]. This provides the number of reads due to insertions in each site mapping to a gene. The number of reads mapping to a gene in a treated sample can be compared to the number of reads due to insertions in the control condition (Fig. 2.3C). An advantage of this approach is that the genes which when inactivated provide a fitness advantage, as given by an increase in number of reads mapping to the gene in treated condition relative to the untreated control, and genes which when inactivated result in a fitness disadvantage, as given by a decrease in number of reads mapping to the gene in the treated condition relative to the untreated control, can both be identified in a single experiment. This approach is more efficient than individually identifying sensitive mutants by replica plating of individual mutants.

There have been numerous advances in computational methods to analyze the data resulting from next-generation sequencing [204, 392, 393, 396, 419-423]. Here, the fold change in number of reads mapping to a gene in treated condition relative to the untreated control was calculated using the Mann-Whitney U statistical method, as described previously [204] with one additional step: before comparing the number of reads/gene using the Mann-Whitney U test, the experimental condition (antibiotic treatment) was normalized to the untreated control using simulation-based re-sampling to minimize differences between the two conditions [396, 423]. After analyzing all

experiments for both libraries separately, the p-values and depletion/enrichment ratios for each gene under an antibiotic treatment were combined, using Fischer's method for p-values and the geometric mean of fold changes in reads mapping to each gene.

In order to prioritize genes, usually a fixed cut-off is used for either fold change or p-value, or both, depending on the data-set. In examining these data, however, we found that it would not be possible to use fixed cut-offs based on depletion/enrichment ratios to compare the effects of the different antibiotics. Even when used at the same fraction of the MIC, different antibiotics exert different selective pressure on the mutant pool; moreover, very small concentration differences can have large effects on depletion/enrichment ratios (see Chapter 3). Therefore, to enable comparison across different antibiotic treatments we adjusted the cut-off for fold-change in mapped reads/gene for the treated samples relative to the controls so that we obtained approximately the same number of hits for each antibiotic. Only genes with a p-value <0.05 were considered. For the analysis here, we used a sliding cut-off in reads/gene that resulted in a maximum of 20 genes for each antibiotic. Fold change cut-offs ranged from ten-fold (0.1 to 10) for ciprofloxacin to 55-fold for oxacillin. It should be noted that this list of top genes for each antibiotic includes genes with fewer reads mapping to them in the treated sample compared to the control as well as genes with more reads mapping to them. The former represent intrinsic resistance factors because disrupting them results in decreased fitness in the presence of an antibiotic, but the latter are also of interest as they provide information on how antibiotic resistance can arise via gene inactivation.



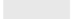
2.4 Intrinsic factors that decrease or increase susceptibility to antibiotics

Of the genes implicated in antibiotic resistance via the analysis described above, 80 were unique (Table 2.1). Whereas the top 20 gene list for most of the six antibiotics included few or no genes with more insertions under the treatment condition than the control, half of the genes in the list for gentamicin belonged in this category.

Table 2.1: 80 unique genes were identified as important for fitness by treatment of pooled transposon libraries with six antibiotics

	Oxa	Cip	Gen	Lin	Van	Dap
Cell Envelope						
SAOUHSC_00646						
SAOUHSC_00703						
SAOUHSC_00952						
SAOUHSC_00998						
SAOUHSC_01359						
SAOUHSC_01361						
SAOUHSC_01423						
SAOUHSC_01462						
SAOUHSC_01739						
SAOUHSC_01759						
SAOUHSC_02305						
SAOUHSC_02423						
SAOUHSC_02571						
SAOUHSC_03049						
DNA/RNA/Protein Synthesis						
SAOUHSC_00803						
SAOUHSC_01095						
SAOUHSC_01099						
SAOUHSC_01352						
SAOUHSC_01620						
SAOUHSC_01688						
Protein Modification/Transport						
SAOUHSC_00877						
SAOUHSC_01162						
SAOUHSC_01747						
SAOUHSC_01778						
Oxidative Phosphorylation/ETS						
SAOUHSC_00878						
SAOUHSC_00982						
SAOUHSC_01001						
SAOUHSC_01002						
SAOUHSC_01040						
SAOUHSC_01772						
SAOUHSC_01776						
SAOUHSC_01852						
SAOUHSC_01915						
SAOUHSC_01960						
SAOUHSC_01962						
SAOUHSC_02340						
SAOUHSC_02345						
Metabolism/Metabolic Transporters						
SAOUHSC_01708						
SAOUHSC_01043						
SAOUHSC_01611						
SAOUHSC_01803						
SAOUHSC_02552						
SAOUHSC_01430						
SAOUHSC_00536						
SAOUHSC_02360						
SAOUHSC_01013						
Transcriptional Regulators						
SAOUHSC_00023						
SAOUHSC_00467						
SAOUHSC_00503						
SAOUHSC_01228						
SAOUHSC_02362						
SAOUHSC_02298						
SAOUHSC_02299						
SAOUHSC_02300						
SAOUHSC_01979						
SAOUHSC_02303						
Multicomponent Sensory System						
SAOUHSC_00665						
SAOUHSC_00666						
SAOUHSC_00667						
SAOUHSC_00668						
SAOUHSC_02098						
SAOUHSC_02099						
SAOUHSC_02100						
SAOUHSC_02261						
SAOUHSC_02262						
SAOUHSC_02265						
SAOUHSC_01419						
Hypothetical						
SAOUHSC_00468						
SAOUHSC_00774						
SAOUHSC_00788						
SAOUHSC_00965						
SAOUHSC_01025						
SAOUHSC_01050						
SAOUHSC_01568						
SAOUHSC_01569						
SAOUHSC_01645						
SAOUHSC_01724						
SAOUHSC_02149						
SAOUHSC_02228						
SAOUHSC_A02189						

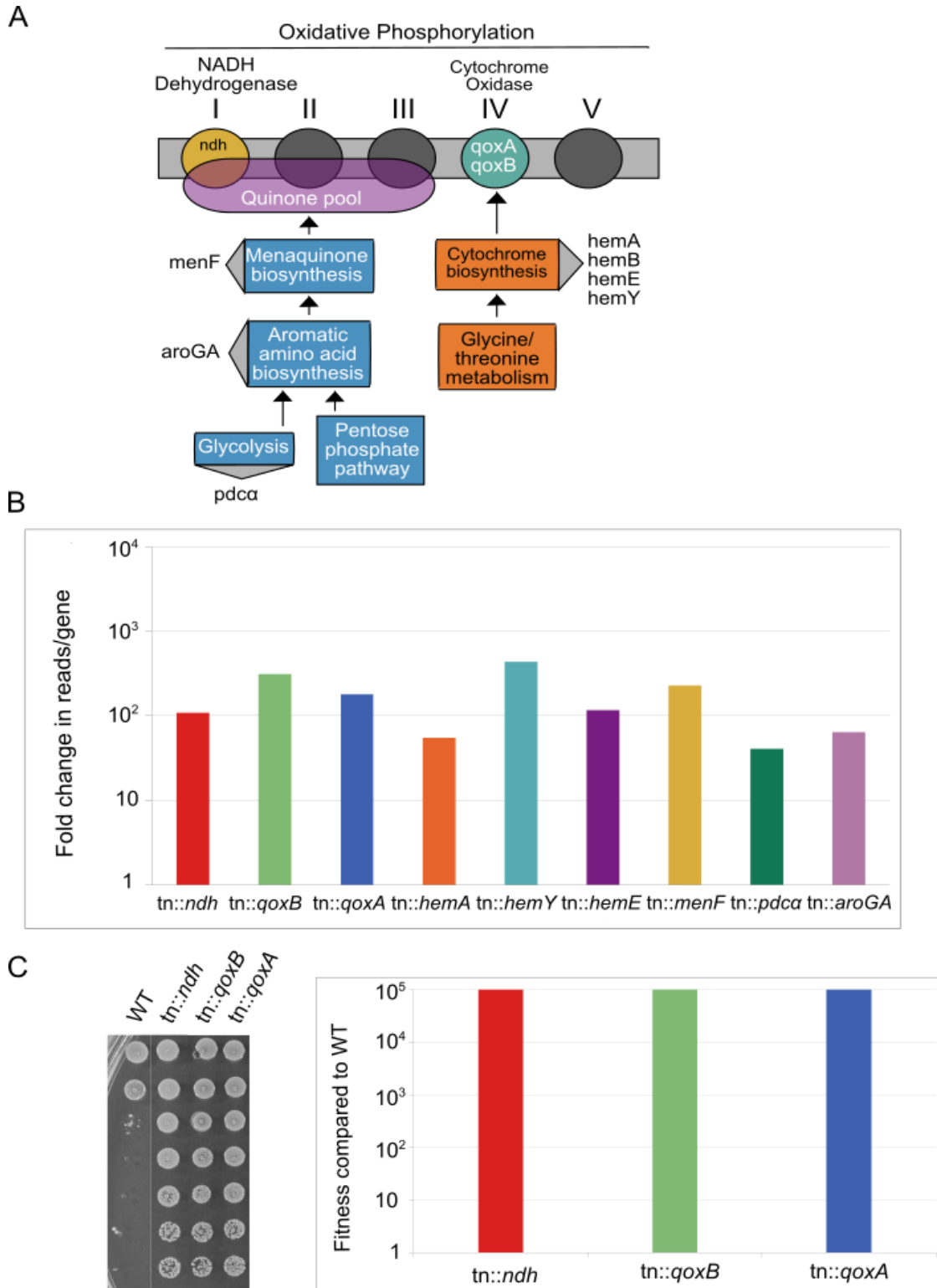
Oxacillin = Oxa
 Ciprofloxacin = Cip
 Gentamicin = Gen
 Linezolid = Lin
 Vancomycin = Van
 Daptomycin = Dap

Significant increase in reads 
 Significant decrease in reads 
 No effect 

All these genes were in the oxidative phosphorylation pathway (Fig. 2.4). It is known that gentamicin and other aminoglycosides rely on the membrane potential to gain entry into cells [424, 425]; disrupting genes in the oxidative phosphorylation pathway therefore limits cellular penetration.

Figure 2.4: Inactivation of the oxidative phosphorylation pathway confers resistance to gentamicin. A) Schematic of the oxidative phosphorylation pathway is depicted here. Reads due to transposon insertions were greatly enriched in the eleven genes named in the figure in samples treated with gentamicin. Inactivation of the oxidative phosphorylation pathway is a known mechanism of resistance to gentamicin, which depends on the membrane potential for cell entry. B) A subset of genes involved in oxidative phosphorylation were tested to determine if inactivation confers resistance to gentamicin. Top panel shows the fold change in reads/gene in the gentamicin-treated sample compared to the control. Bottom panel shows fitness compared to WT of mutant strains in which the indicated genes were inactivated. Spot dilutions of WT and mutant strains were plated on gentamicin and fitness was calculated as the ratio of the highest dilution that allowed growth of WT relative to the mutant (see Methods).

Figure 2.4 (Continued):



Our fitness analysis also identified many other genes previously known to affect antibiotic resistance. For example, *sigB* (SAOUHSC_02298) was among the hits with oxacillin treatment. This gene, and the other components involved in the alternative sigma factor pathway, *rsbV* (SAOUHSC_02300) and *rsbW* (SAOUHSC_02299), were significantly depleted (>100 fold depletion in reads/gene for all three genes) (Table 2.1). It has been shown that over-expressing SigB causes cells to have thicker cell walls, increased transcript levels of penicillin binding proteins, and elevated MICs to β -lactams [426]. Similarly, reads in all three genes of the *vraTSR* operon (SAOUHSC_02100, SAOUHSC_02099, SAOUHSC_02098), which encodes a multi-component sensing system (MCS) that regulates the cell wall stress stimulon [427-430], were substantially depleted in the presence of vancomycin. This MCS regulates expression of the acquired *vanA* gene cassette in vancomycin-resistant *S. aureus* (VRSA) [428], and also of other downstream targets involved in cell wall biosynthesis in other strains [427, 429, 430]. Since its regulon includes cell wall biosynthesis genes, it has also been implicated in β -lactam resistance [427, 429]. Although insertions in these genes are also depleted under oxacillin and gentamicin treatment, they do not meet our cut offs for top 20 most important genes. This suggests that this MCS, while important in other conditions, is uniquely critical for withstanding vancomycin. Reads in *pbp4*, which encodes a penicillin-binding protein involved in secondary crosslinking of peptidoglycan and in β -lactam resistance [93, 357, 431], were also found to be depleted under oxacillin treatment. *NorA*, which encodes an efflux pump that is known to be involved in

ciprofloxacin resistance [432, 433], was identified as an important factor under ciprofloxacin treatment in our analysis as well.

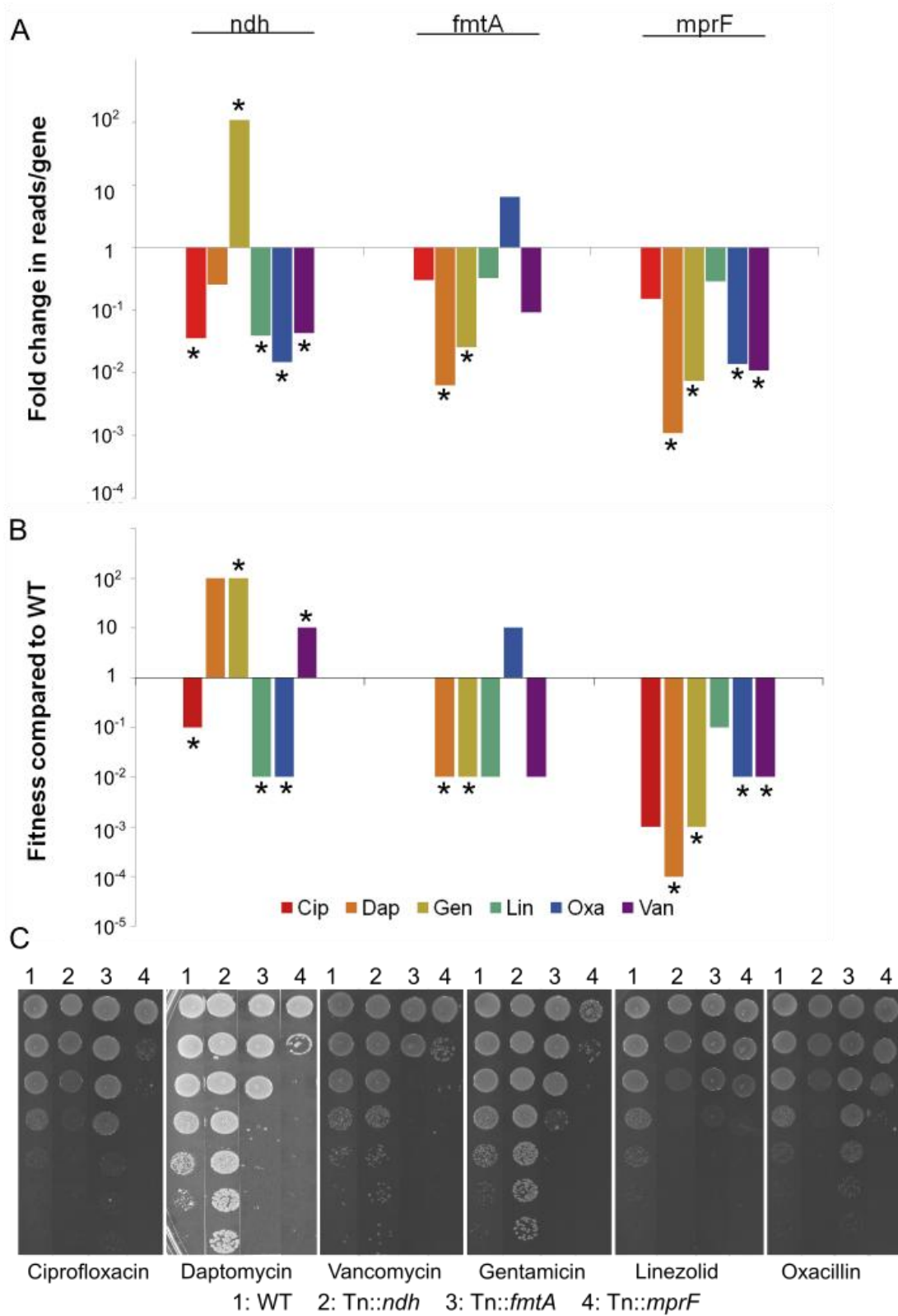
In addition to these and other known intrinsic resistance factors, we have identified 13 hypothetical genes that are important for resistance (Table 2.1). While no inactivated gene was shared between all six antibiotics in the top 20 list, we did identify 21 genes that were hits with more than one antibiotic, and 8 of these were hits with more than two antibiotics. These 8 genes included *mprF* (SAOUHSC_01359), *ndh* (SAOUHSC_00878), *fmtA* (SAOUHSC_00998), components of the *graRS/vraFG* multi-component sensing system (SAOUHSC_00663-668), and two genes of unknown function, SAOUHSC_01025 and SAOUHSC_01050.

Since growing a mutant library in a liquid culture allows competition between mutants to occur, this method selects for those factors that are of particular importance in that treatment condition. Our ability to detect numerous previously identified resistance factors via a fitness profiling approach was encouraging given the substantial differences between testing an antibiotic against a spatially separated single mutant and testing it against a huge pooled mutant collection. To further validate the approach, we tested the fitness of selected mutants against all six antibiotics using a spot dilution assay (Fig 2.5). The spot dilution assay allows the detection of sensitivities of mutants that might otherwise be missed in an end-point MIC assay format. Mutants were chosen based on the genes identified as hits under more than one condition. In general, the agreement between Tn-Seq results and the spot dilution assays was excellent. Given that the spot dilutions do not involve competition between thousands of mutants, were performed at a single concentration (chosen so WT growth is relatively unaffected; see

Methods), and used mutants made in different genetic backgrounds, the high validation rate is remarkable. This suggests that some important intrinsic resistance factors are shared across *S. aureus* strains, both MRSA and MSSA.

Figure 2.5: Tn-Seq results were validated by testing transposon inactivation mutant fitness in spot dilution assays. Tn-Seq results and validation for selected genes are shown. *ndh* encodes an NADH dehydrogenase involved in oxidative phosphorylation; *fmtA* is a cell surface protein of undetermined function; *mprF* synthesizes lysyl-phosphatidylglycerol. Asterisks indicate those conditions under which the pertinent gene was among the top twenty hits for that antibiotic. (A) Bar graph depicting fold change in reads per gene relative to the untreated control for each of the six antibiotics. (B) Bar graph depicting fitness compared to WT of transposon inactivation mutant strains (obtained from Nebraska library) in which the indicated genes are inactivated. Fitness was assessed by spotting ten-fold dilutions of WT and mutant strains on antibiotic plates and comparing the highest dilutions that resulted in growth (see Methods). Because the data is shown on a logarithmic scale, the lack of a bar indicates that no change (fold change = 1) was observed for that mutant under the relevant treatment condition. (C) Spot dilution assay plates are shown for each of the antibiotics tested. Fitness assessed by spot dilution validated the Tn-Seq results for genes which were within the top twenty list of genes, except in one case.

Figure 2.5 (Continued):



2.5 Intrinsic factors that impact multiple classes of antibiotics

Of the eight genes found to impact multiple classes of antibiotics, *ndh* (NADH dehydrogenase) is the only one that when inactivated, promotes resistance to some antibiotics while sensitizing to others. Ndh is a component of the electron transport chain. The electron transport chain creates a membrane potential, which is required for penetration of gentamicin through the cell membrane [434]. We showed here that in addition to conferring resistance to gentamicin when inactivated, *ndh* is an intrinsic factor for oxacillin, linezolid and ciprofloxacin. *Ndh* is in the same pathway as several genes that are commonly found to be inactivated in small colony variants (SCVs), a phenotype correlated with persistent infections that are resistant to β -lactams as well as aminoglycosides [435-438]. β -lactam resistance is attributed to slow growth that occurs when cells switch to anaerobic growth when genes involved in oxidative phosphorylation are inactivated [435, 439]. Our data confirms the importance of the oxidative phosphorylation pathway in antibiotic resistance.

The gene *fmtA* encodes a cell surface protein of uncertain function. It was identified as a factor involved in methicillin resistance, and has since been proposed to act as a carboxypeptidase and a teichoic acid D-ala esterase [208, 358, 440]. We did not find that inactivation of *fmtA* results in increased sensitivity to oxacillin in the Tn-Seq library or in the spot dilution assay. In fact, survival was enhanced in the presence of oxacillin. However, we did observe increased sensitivity to daptomycin and vancomycin. This finding is consistent with an important role for FmtA in withstanding cell envelope stress for at least some classes of antibiotics [441].

MprF catalyzes formation of lysyl-phosphatidylglycerol, a membrane modification that confers protection to cationic antibiotics, which are repelled by the increased cell surface positive charge [20, 23, 28, 442]. MprF is also a known methicillin resistance factor in MRSA strains [24]. In our studies, *mprF* was found to be an intrinsic resistance factor across all the antibiotics tested, although it only makes the top 20 list for four out of six of them (Table 2.1). All four were validated in a spot dilution assay performed on a mutant in a USA300 (MRSA) background (Fig. 2.5B)[443]. Since *mprF* inactivation potently sensitizes to daptomycin, vancomycin, and ciprofloxacin, which are not rich in positive charge, the product of MprF, lysyl-phosphatidylglycerol, likely plays biophysical roles in membrane stability. This has been suggested previously for daptomycin [226, 444].

2.6 GraRS/VraFG is the single most important multi-component sensing system across tested antibiotics

Multi-component sensing systems (MCSs) allow bacteria to sense and respond to their environments. These systems typically include a membrane-anchored extracellular sensory domain fused to an intracellular kinase domain and a separate, cytosolic response regulator but they can also include additional elements. A stimulus sensed by the sensory domain results in a change in phosphorylation of the response regulator, which then modulates the expression of downstream targets [10]. *S. aureus* contains many multi-component sensing systems, and we identified multiple components of three of these systems, *agrABCD*, *vraTSR*, and *graXRS/vraFG*, as top hits under treatment with at least one antibiotic (Table 2.1).

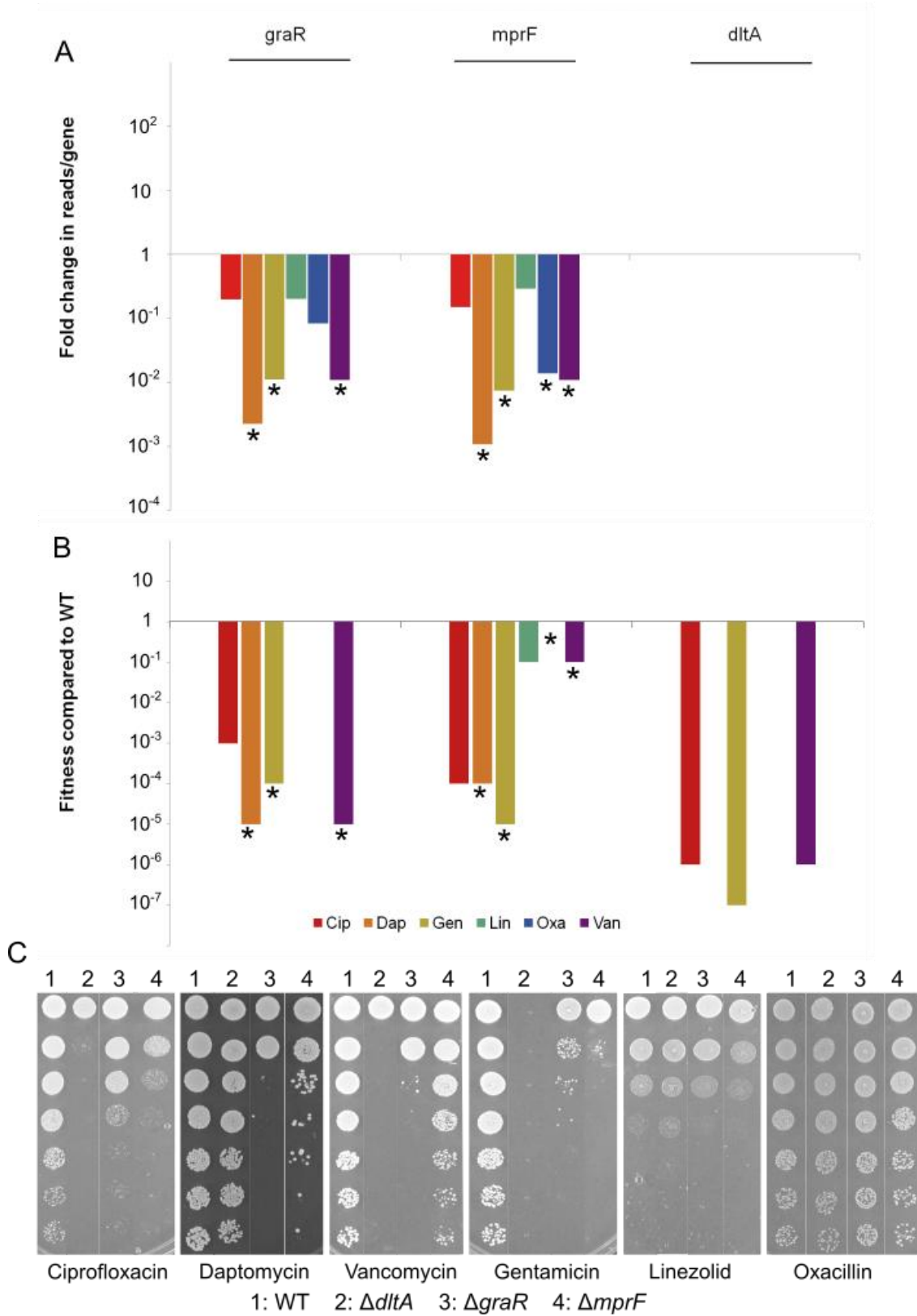
AgrABCD has been implicated in quorum sensing and regulation of virulence factors and autolysin expression [445-449]. Reads mapping to components (*agrABCD*) of this MCS were depleted under oxacillin and daptomycin treatments, suggesting that this MCS could also play a role in the response to these antibiotics, possibly due to its functions in regulating the autolysin *lytM* and the penicillin-binding proteins [447, 450, 451]. While *agrC* was also depleted under these treatments, it did not meet our cut-offs. *AgrB* is a transmembrane protein that is involved in the processing of the *AgrD* propeptide that is the precursor for mature autoinducing peptide [452]. This autoinducing peptide is sensed by the sensory kinase *AgrC* [453]. Although the effects of quorum sensing are multifold and a single connection of this system with antibiotic resistance, if one exists, will be hard to isolate, its role in antibiotic resistance has been previously appreciated [451, 454].

The single most important MCS across all the six antibiotics tested was *graXRS/vraFG*. Four components of this system made our cut-offs under gentamicin, daptomycin, and vancomycin treatment (Table 2.1). Moreover, compared to wildtype, we found the fitness of a Δ *graR* mutant to be reduced by four to five orders of magnitude when plated on these antibiotics (Fig. 2.6B). The mutant was also sensitive to ciprofloxacin, although less so. The regulon of this MCS includes other global regulatory systems such as *agr* and *walkR*, and it has been linked to numerous stress-response and virulence genes [32], but it is most well-known for regulating *mprF* and the *dlt* operon, both of which are involved in modulating cell surface charge. *MprF* attaches lysine to phosphatidylglycerol, as discussed previously, while the *dlt* operon attaches D-alanine to lipo- and wall teichoic acids [132]. As discussed in Chapter 1, the *dlt* pathway

confers protection to cationic antimicrobial peptides, aminoglycosides, and other positively-charged antibiotics [222]. Whereas *mprF* was identified as a top hit under several treatment conditions, transposon insertions in the *dlt* genes were poorly represented in the control libraries because *dlt* mutants have substantial fitness defects and do not compete well with other strains. However, we found the fitness of a *dltA* mutant to be greatly reduced compared to wildtype when plated on three of the six tested antibiotics - vancomycin, ciprofloxacin and gentamicin (Fig. 2.6B).

Figure 2.6: Tn-Seq results were validated by testing the fitness of deletion mutants in Newman in spot dilution assays. Asterisks indicate those conditions under which the pertinent gene was among the top twenty hits for that antibiotic. (A) Bar graph depicting fold change in reads per gene relative to the untreated control for each of the six antibiotics. (B) Bar graph depicting fitness compared to WT of deletion mutants. Fitness was assessed as described previously. Because the data is shown on a logarithmic scale, the lack of a bar indicates that no change (fold change = 1) was observed for that mutant under the relevant treatment condition. (C) Spot dilution assay plates are shown for each of the antibiotics tested. Concentrations for plates were selected as the maximum concentration at which WT is minimally affected, that is, where growth is apparent for at least three or four of the seven dilution factors.

Figure 2.6 (Continued):



Binding of the zwitterionic fluoroquinolones to the cell surface is known to be antagonized by calcium or magnesium ions, and perhaps the presence of D-alanine moieties is similarly antagonistic [455]. The sensitivity of *dltA* mutants to vancomycin has been previously reported and was suggested to be due to increased binding of vancomycin to the cell surface [217]. It was previously shown that the number of positive charges on aminoglycosides correlates with activity against the *dltA* mutant [367], but we did not observe a strong correlation between the number of positive charges and the fitness of the *dltA* mutant across different classes of antibiotics. As D-alanylation plays pleiotropic roles in the cell envelope, the fitness of the *dltA* mutant in the presence of different antibiotics may reflect different roles.

We observed some differences in the sensitization patterns of the *dltA* and *mprF* mutants. The *dltA* mutant was not as sensitive to daptomycin as the *mprF* and *graR* mutants were. Conversely, the *mprF* mutant was not as sensitive to vancomycin as the *dltA* and *graR* mutants were. Our results suggest that the importance of the *graRS/vraFG* MCS can be explained in part by the combined action of these two members of its regulon, *dltA* and *mprF*.

2.7 Contribution of intrinsic resistance factors to antibiotic resistance can vary across *S. aureus* strains

In the spot dilution assay, inactivation of *mprF* resulted in a large increase in sensitivity to oxacillin in the USA300_FPR3757 background, but the inactivation mutant did not show increased sensitivity to oxacillin in the methicillin-sensitive strain Newman

(Fig. 2.5, 2.6). This suggests that the contribution of *mprF* as an intrinsic resistance factor is larger in the USA300_FPR3757 background than in Newman. The initial study, which identified *mprF*'s contribution to β -lactam resistance also reported this difference in strain background. While a dramatic decrease in MIC was observed for MRSA strains COL and KSA8, no decrease in MIC was observed for MSSA strain, RN450 [358]. Strain-specific contributions of another intrinsic resistance factor, *pbp4* (SAOUHSC_00646), have been previously reported. *Pbp4* deletion was shown to sensitize community-acquired MRSA strains, MW2 and USA300, to oxacillin and nafcillin, but the mutant did not show additional sensitivity in HA-MRSA strains N315 and VISA strain, Mu50 [357]. The reason for these differences is not evident. Studies have detailed numerous genetic and gene expression differences between *S. aureus* strains [456-461], suggesting that teasing out the reasons for the relative contribution of intrinsic resistance factors to each strain background will not be simple.

2.8 Conclusions

We have demonstrated that Tn-Seq can be used to rapidly identify intrinsic factors that are impediments to antibiotic activity. Fitness based on Tn-seq profiles correlated well with fitness of individual mutants plated on antibiotics. In addition to several previously characterized factors, we identified several hypothetical genes that are important for antibiotic resistance, indicating that there are still gaps in our knowledge of factors involved in antibiotic resistance. Further investigation into the physiological roles of these hypothetical proteins will be useful in creating a more complete picture of antibiotic resistance in *S. aureus*. The possible differences in

contributions of intrinsic factors in different strain backgrounds is a significant aspect of *S. aureus* to keep in mind. Focusing small molecule targeting efforts on factors that are important for multiple antibiotics across multiple clinically relevant strain backgrounds, like *mprF* and the *dlt* operon, will be of greater clinical use than focusing on those factors which are highly strain-specific, like *pbp4*. The methods described in this study can be rapidly scaled to identify intrinsic resistance factors for any antibiotic, which could be targets for the development of small molecule potentiators, as well as, to identify and prioritize more multi-class intrinsic factors that are particularly important in the *S. aureus* arsenal.

2.9 Methods

Library 1 antibiotic treatment: Library 1 was constructed by transformation of a temperature sensitive plasmid as previously described [201]. Briefly, a 100 μ l aliquot of this initial *S. aureus* HG003 transposon library freezer stock, containing 10^8 cfu, was used to inoculate 100 ml of Mueller Hinton (MH) cation adjusted broth and incubated for 15 h at 37°C with shaking at 200 rpm. A 10 μ l aliquot (10^6 cfu) of this input culture was then inoculated into a final volume of 200 μ l in a 96-well plate broth microdilution format and incubated at 37°C for 8 hours, approximately 5.5 generations (5×10^7 cfu/200 μ l). The 1/2x, 1/4x and 1/8x MIC wells for the library pool were determined based on the MIC of a small mutant pool (consisting of ten innocuous transposon mutants). This small pool was used to determine MICs in order to compensate for potential resistant mutants in the library pool. The chosen wells (1/2x, 1/4x and 1/8x) were then subcultured (3×10^5 cfu) into a second iteration of serial dilutions of antibiotics as

described above and incubated for 15 hours at 37°C, approximately 9 generations (2×10^8 cfu/200 μ l). The 1/2x, 1/4x and 1/8x MIC wells were determined based on the small pool and these wells were transferred to 10 ml of BHI broth, incubated for 4 h at 37°C with shaking at 200 rpm. Biological replicates were conducted for each growth condition. Genomic DNA was harvested using DNeasy Blood and Tissue kit (Qiagen, Valencia, CA) following the manufacturer's instructions.

Library 2 antibiotic treatment: Library 2 was constructed by phage-based transposition of six different transposon constructs as previously described [392]. Tryptic soy broth (TSB) supplemented with 25mg/L Ca²⁺ and 12.5mg/L Mg²⁺ was used for all antibiotics except for oxacillin, which was tested using cation-adjusted MH Broth. For all antibiotics, an untreated control was prepared in the same media as was used for the tested antibiotic. A stock of the complete library was thawed and diluted to an OD₆₀₀ of 0.2 and grown to an OD₆₀₀ of ~0.4 to minimize changes in library composition prior to treatment. The culture was then diluted to 4×10^5 cfu/mL and added to 1mL of media with 2x the desired concentration of the antibiotic, to give a final starting inoculum of 2×10^5 cfu/mL in 2mL culture volumes. Daptomycin and Vancomycin were tested with a final starting inoculum of 10^7 cfu/2mL. Samples were grown at 37°C and harvested when they reached stationary phase. The samples were treated with 2x, 1x, 0.5x and 0.25 x the MIC of the antibiotic. Further details on sample harvesting are discussed in Chapter 3.

Tn-Seq preparation and Illumina sequencing: Library1 was prepared using the shearing method [394]. We treated Library 2 with a panel of antibiotic concentrations, along with an untreated control. Then we identified antibiotic concentrations that caused

the transposon library to reach stationary phase with a few hour delay compared to the untreated control. Library samples treated with these antibiotic concentrations were prepared for sequencing following the protocol described in Santiago *et al.* 2015 [392]. Samples from at least two of the concentrations of Library 2 were sent for sequencing. Illumina sequencing was completed by Harvard Biopolymers Facility or Tufts Genomic DNA Sequencing core facility.

Data analysis: We identified datasets from Library 2 in which reads mapped to approximately 40% of the TA sites hit in the untreated control (with the exception of vancomycin treatment which hit 67% of the TA sites hit in the untreated control). These were processed for further analysis. This percentage decrease was chosen such that we could identify genes with an increase and decrease in number of reads mapping to them. Library 2 contains transposon constructs with outward-facing promoters that can upregulate proximal genes in addition to the traditional construct which can only insert into and inactivate genes. For these experiments, we only considered data from the inactivation constructs. Data was analyzed as described previously with some modifications [392]. Data from biological replicates was combined, and before comparing the number of reads/gene using the Mann-Whitney U test, the experimental data was normalized to the control using simulation-based resampling [396, 423]. Then, data for each antibiotic treatment from each of the Library 1 experiments was combined with the data from the Library 2 experiments using the geometric mean of the ratios and Fisher's method for combining corrected p-values. Top hits were identified by first filtering for genes with a p-value less than 0.05, then by increasing the ratio cut-off by integers until less than or equal to 20 genes were left.

Spot dilution assays: Identified hits *qoxA*, *qoxB*, *ndh* and *fmtA* were validated using transposon mutants from the Nebraska library in background USA300_FPR3757 [443]. Deletion mutants in *dltA*, *mprF* and *graR* were tested in MSSA strain Newman. Agar plates were prepared with TSB supplemented with Ca²⁺ (25mg/L) and Mg²⁺ (12.5mg/L) and a sub-MIC concentration of the 6 antibiotics. Overnight cultures of mutants were diluted 1:100 in fresh TSB and grown to an OD₆₀₀ of 1. They were then diluted serially by 10 fold, spotted on agar plates and incubated at 37°C overnight. The concentration of the antibiotic at which WT was severely inhibited, showing growth in only the highest 1 or 2 dilutions on agar plates under these conditions was determined. This was considered to be the MIC under this condition. The spot dilution assays were then set up using three different antibiotic concentrations. The concentration closest to the MIC at which WT was at most 3 logs more depleted than non-antibiotic control was used to calculate fitness. This concentration was used so that reduced fitness of any mutants could be observed. The exception to this was when the MIC concentration for gentamicin was used to evaluate the resistance of inactivation mutants in the oxidative phosphorylation pathway. Control plates with no antibiotic were set up for all strains assayed and under these conditions, mutants and WT showed equal levels of growth. Fitness was assessed by determining the highest dilution for which growth was observed for a mutant and the WT strain. The highest dilution showing full growth for the mutant was then divided by the highest dilution showing full growth for the WT to calculate its fitness compared to WT. These were plotted on a log scale. Those spots that showed hazy growth indicative of cell lysis, those that showed mixed populations of colonies of different sizes suggesting the possibility of suppressors and reduced fitness

relative to spots with homogenous colonies, and those that had fewer than 10 individual colonies were not regarded as full growth.

Chapter 3: Genes that contribute to bacterial fitness in the presence of peptidoglycan biosynthesis inhibitors.

3.1 Rationale for expanding the set of Tn-Seq derived fitness profiles

We showed in the previous chapter that Tn-Seq is a useful approach to identify important intrinsic resistance factors under antibiotic treatment. The throughput of this technique allows for the simultaneous assessment of the fitness of inactivation mutants of the non-essential genes represented in the transposon library across a large number of antibiotics with relative ease. We will refer to the fitness of all genes under an antibiotic as the fitness profile of the antibiotic, and the fitness of a gene across the antibiotics assayed as the fitness profile of the gene. Knowledge of such fitness profiles of genes and of antibiotics can be useful in a number of ways. Three of these purposes are discussed in this chapter and the next.

First, the fitness profiles of genes generated across multiple antibiotics targeting the same biosynthetic pathway can be used to nominate a collated list of genes that impact the inhibition of this pathway. We chose to focus here on PG biosynthesis inhibitors because PG is the first line of defense for bacteria and its biosynthesis is targeted by multiple antibiotics at various stages of the pathway, resulting in a greater diversity of mechanisms of action that can be assessed. Such a collated list of genes can enable the prioritization of factors that are likely to be important in the cell wall interaction network. Investigating such factors could result in more insight into *S. aureus* physiology. Such factors are also of interest because their inhibition may reduce bacterial fitness under multiple antibiotics.

Fitness profiles of genes across multiple antibiotics will likely be the same for genes which are interacting with each other and are involved in the same system. For instance, we might expect that the components of the *graRS/vraFG* system have the same fitness pattern across a number of antibiotics since they are all involved in the same multi-component sensing system. Therefore, a second possible application for such genome-wide fitness profiles is to identify potential pathways in which a gene of unknown function could be involved by identifying the known genes whose fitness patterns across multiple antibiotics are most similar to that of the gene of interest. We describe here a machine learning approach that we used to nominate potential pathways two genes of unknown function, *SAOUHSC_01025* and *SAOUHSC_01050*, could be associated with. Finally, the fitness profiles for antibiotics can be used to predict the mechanism of action of an unknown antibiotic. This will be discussed in Chapter 4.

The work described in Chapters 3 and 4 was completed in collaboration with Marina Santiago. Dr. Tim Meredith, Dr. Wonsik Lee, Michael George and Truc Do in the Walker lab contributed some of the data sets that were used in this work.

3.2 Peptidoglycan biosynthetic inhibitors tested

In this chapter, we focus on antibiotics that inhibit PG biosynthesis. As an essential first line of bacterial defense, numerous inhibitors for PG biosynthesis have been developed over the years, as described in Chapter 1. The antibiotics used for this analysis have diverse mechanisms of action (Table 3.1). Oxacillin is a β -lactam that inhibit the transpeptidase activity of penicillin-binding proteins (PBPs) [338, 339].

Moenomycin A inhibits the transglycosylase domain of PBP2, interfering with the polymerization of the glycan chain [462, 463]. These are enzymatic inhibitors of PG biosynthesis.

Antibiotic	Chemical Class	Target
Oxacillin	β -lactam	Transpeptidase domain of PBPs
Moenomycin A	Phosphoglycolipid	Transglycosylases
Vancomycin	Glycopeptide	D-ala-D-ala of lipid II
Ramoplanin	Glycopeptide	Pyrophosphate-sugar moiety of lipid II
Lysobactin	Glycopeptide	Pyrophosphate-sugar moiety of lipid II
Bacitracin	Cyclic peptide	Und-PP
Targocil	Triazoloquinazoline	TarGH

Another class of inhibitors is the substrate binding inhibitors, discussed in chapter 1. These include vancomycin, which binds to the D-ala-D-ala subunit of lipid II therefore inhibiting the cross-linking and polymerization of PG [305-308]. Ramoplanin and lysobactin also bind to lipid II and inhibits the transglycosylation reaction. Unlike vancomycin, ramoplanin and lysobactin bind to the sugar-pyrophosphate moiety of lipid II [309, 310, 464-467]. In addition, while vancomycin is bacteriostatic, ramoplanin and lysobactin are both bactericidal and result in rapid lysis [467]. Bacitracin can be regarded as a product binder. It binds to the undecaprenol pyrophosphate released after lipid II polymerization and cross-linking, preventing its recycling and use in future lipid II synthesis [468]. Targocil is unique in its PG biosynthesis inhibition since it is an inhibitor of TarGH, the WTA exporter [361, 362]. Due to inhibition of a conditionally essential step in the WTA pathway, targocil ties up the lipid carrier, preventing its use in PG synthesis, as described in Chapter 1. Experimental evidence for the depletion of lipid II by targocil has been generated recently [93]. In fact, this study showed that while

vancomycin and moenomycin A result in accumulation of lipid II, bacitracin results in a depletion of lipid II levels, consistent with their mechanism of action [93]. The diversity of mechanisms of action of the antibiotics sampled suggests that the genes identified as common hits across all these antibiotics will be important for withstanding pressure that results from PG biosynthesis inhibition in general.

3.3 Identifying a core set of genes relevant under cell wall perturbation

We wanted to identify non-essential genes whose inactivation results in a fitness difference under a majority of the PG biosynthetic inhibitors tested. As the antibiotics have diverse mechanisms of action (Table 3.1), genes which are identified across a majority of these antibiotics will likely play a critical role in the cell wall interactome.

For this approach, we used only data from the blunt inactivation constructs, for all antibiotics under all concentrations tested, which had a minimum of 300,000 reads, and a number of TA sites hit that was at least 40% of the number of TA sites hit in the untreated condition. We determined that these conditions could enable us to identify genes that are relevant to the treatment condition (see Section 3.7). Data sets from two or more concentrations of each of the seven antibiotics were used in this analysis.

We needed a method to compare the multiple concentrations used to treat the cell as well as compare between antibiotics. The method described in Chapter 1, which involved combining fold changes and p-values of each gene under each concentration of antibiotic tested using geometric mean and Fisher method respectively, is useful for identifying the most important factors under each treatment condition. For this analysis, we wanted to take into account genes that were enriched or depleted under all

concentrations of antibiotic tested, to take into account all those genes that are relevant under the tested condition. The fold changes for each gene were modified to account for essentiality (see Methods). The top 75% of those genes with mapped reads that were more than 1.5x enriched or depleted relative to untreated, up to a maximum of 200 genes, were considered for each concentration condition. Next, a list of relevant genes for each antibiotic was generated by compiling a list of the unique genes from each concentration condition. Only the enrichment or depletion status of each gene was considered when comparing between antibiotics or concentrations, and not the actual fold changes.

There are two advantages to using this approach over the geometric mean approach for this analysis. (1) Genes which are not affected under one concentration (<1.5x fold change) but moderately affected in another (>1.5x fold change) are not lost. For example, *SAOUHSC_00620* which encodes the SarA regulator, is within the top twenty enriched genes under moenomycin 0.08µg/mL condition with a fold change in reads of 5.8. While this fold change might not seem impressive, SarA is a known regulator of *AbcA*. *AbcA* overexpression is reported to increase the MIC of moenomycin A by ten-fold and deletion of *sarA* enhances *abcA* expression under starvation conditions [469]. Clearly, *sarA* is a physiologically relevant gene under moenomycin treatment. However, the geometric mean of the fold changes of this gene over the tested concentration range is 1.32, which is indicative of no change. This is because at lower concentrations no change is observed in reads mapping to this mutant. Assaying multiple concentrations was therefore beneficial for this analysis. (2) It accounts for the fact that the enrichment and depletion fold changes cannot be expected to be the same

for factors that are in common across these antibiotics, because of their different mechanisms of action and possibly different effective concentrations. Therefore, a gene which is highly affected under treatment pressure by one antibiotic, and only moderately affected by another could be identified.

To identify a set of genes that are relevant under cell wall perturbation, we searched for those genes that are hits across 5 out of the 7 PG synthesis inhibitors (moenomycin A, vancomycin, ramoplanin, targocil, oxacillin, bacitracin and lysobactin) (Table 3.2). These 57 genes are likely to play important roles in the cell envelope interaction network. Further investigation into the functions of these genes will enable a better understanding of bacterial cell envelope physiology, interactions and regulation.

Table 3.2 (Continued): Genes that are relevant under cell wall perturbation

		Moe	Ram	Van	Oxa	Bac	Lys	Tar
Metabolism								
SAOUHSC_00019	adsS	More	More	More	Not	More	Not	More
SAOUHSC_02354	glyA	More	More	More	Not	More	Not	More
SAOUHSC_02374	abgB	More	More	More	Not	More	Not	More
SAOUHSC_01370	PRAI	More	More	More	Not	More	Not	More
Transcriptional Regulators								
SAOUHSC_02809	gntR	More	More	More	Not	More	Not	More
SAOUHSC_02664	transcriptional regulator	More	More	More	Not	More	Not	More
Multi-component sensing systems								
SAOUHSC_00664	graX	More	More	More	Not	More	Not	More
SAOUHSC_00666	graS	More	More	More	Not	More	Not	More
SAOUHSC_00667	vraF	More	More	More	Not	More	Not	More
SAOUHSC_00668	vraG	More	More	More	Not	More	Not	More
SAOUHSC_01420	arlR	More	More	More	Not	More	Not	More
SAOUHSC_02099	vraS	More	More	More	Not	More	Not	More
SAOUHSC_02100	vraT	More	More	More	Not	More	Not	More
SAOUHSC_02261	agrB	More	More	More	Not	More	Not	More
SAOUHSC_02264	agrD	More	More	More	Not	More	Not	More
Stress responses								
SAOUHSC_00504	mcsB	More	More	More	Not	More	Not	More
SAOUHSC_00480	mazG family	More	More	More	Not	More	Not	More
SAOUHSC_02150	thioredoxin	More	More	More	Not	More	Not	More
SAOUHSC_00938	thioredoxin-like	More	More	More	Not	More	Not	More
SAOUHSC_02369	rpoE	More	More	More	Not	More	Not	More
RNA/Protein Synthesis and modification								
SAOUHSC_00663	rimI	More	More	More	Not	More	Not	More
SAOUHSC_02358	hemK	More	More	More	Not	More	Not	More
SAOUHSC_01269	miaB	More	More	More	Not	More	Not	More
Other								
SAOUHSC_02121	camS	More	More	More	Not	More	Not	More

Moe = Moenomycin; Ram = Ramoplanin
 Van = Vancomycin; Oxa = Oxacillin
 Bac = Bacitracin; Lys = Lysobactin
 Tar = Targocil

More reads in treated sample
 Fewer reads in treated sample
 Not a hit

3.4 Previously characterized genes relevant under cell wall perturbation

We identified several genes whose functions have been previously characterized. As expected, this list included numerous genes with functions in the cell envelope. In this section, we discuss some of these genes. Two of these factors *fmtA* and *mprF* as well as the multi-component sensing systems *graXRS/vraFG*, *vraRST*, and *agrABCD*, components of which were hits in the more stringent criteria used for smaller set of antibiotics, have been previously discussed in detail. The only discrepancy we find is with *fmtA*, which is identified as depleted in the presence of oxacillin under this analysis but was enriched when considering data from the second smaller library, described in chapter 2. This is because the analysis in chapter 2 also included data obtained in the Gilmore lab and these data sets showed reads in *fmtA* to be over 100x increased in the presence of oxacillin, which we did not observe in our data set at any concentration.

The gene *uppP*, also known as *bacA*, is known to be important for resistance to bacitracin [470]. UppP is an undecaprenyl pyrophosphate phosphatase which dephosphorylates the carrier lipid in order to enable its recycling and further use in PG synthesis [109]. Some species of bacteria can have various number of enzymes showing UppP activity and therefore, *uppP* is not essential in these organisms, including *S. aureus* [108]. Although we found both *uppP* and another phosphatase showing uppP activity, *pgpB*, to be upregulated in the presence of bacitracin in our Tn-Seq data, only *uppP* was found to be important across other PG biosynthetic inhibitors, corroborating that it is likely the primary undecaprenyl pyrophosphate phosphatase in *S. aureus*.

Atl is a bifunctional autolysin that has an amidase domain and a glucosaminidase domain [471]. It has been shown that the deletion of *atl* inhibits penicillin-induced lysis [472], which could account for the fitness advantage we observed for the *atl* mutant in the presence of oxacillin in our Tn-Seq assay. We found that Atl is important for fitness of *S. aureus* in the presence of other cell wall antibiotics. *S. aureus* has numerous peptidoglycan hydrolases but only Atl stood out as important under a number of PG biosynthesis inhibitors.

We also identified two genes encoding proteins involved in WTA biosynthesis: *lcpA* and *mnaA*. Recent evidence has shown that LcpA is the primary WTA ligase in *S. aureus*, as discussed in Chapter 1[164]. MnaA is a UDP-GlcNAC-2-epimerase that converts UDP-GlcNAc to UDP-ManNAc and in the absence of *mnaA*, WTA synthesis is abolished [473]. The inactivation of LcpA and of MnaA both have been shown to sensitize MRSA to β -lactams [164, 473]. While reads in *mnaA* and *lcpA* were both depleted under oxacillin treatment in our data set, these genes did not meet our cutoffs because they were not among the top 200 depleted genes. We also find here that WTAs are important for fitness under non- β -lactam PG biosynthesis inhibitors. As expected, we find that reads in *mnaA* are enriched in the presence of targocil. It has been previously shown that the pharmacological inhibition of WTA synthesis rescues from the lethality of targocil [361]. We do not find the enrichment for reads in *lcpA* in the presence of targocil. This is consistent with the role of LcpA in the WTA biosynthesis pathway. Inactivation of LcpA will not have an antagonistic effect on targocil because it is further downstream of the WTA export step that targocil inhibits and therefore, unable to prevent the tying up of the carrier lipid that causes PG biosynthesis inhibition.

3.5 Three previously uncharacterized genes important for under cell wall stress

Hypothetical genes comprised the largest category of the hits identified (19 out of 57 genes). We validated the contribution of three of these genes, *SAOUHSC_02149*, *SAOUHSC_01025* and *SAOUHSC_01050*, to fitness in the presence of various antibiotics.

SAOUHSC_02149 was identified as relevant under all PG biosynthetic inhibitors analyzed except for oxacillin, for which it did not meet our cut-offs. *SAOUHSC_02149* is a small 174 amino acid protein that has one transmembrane helix. The bulk of this protein is extracellular, as predicted by TMHMM server. *SAOUHSC_02149* has a predicted bacterial Pleckstrin homology (PHb) domain, which is known to bind phosphatidylinositol in eukaryotes [474]. However, it has been shown that less than 10% of proteins with this domain bind phosphatidylinositol with high affinity and specificity [475], and *S. aureus* does not produce phosphatidylinositol. It has been suggested for one member of this family, a mammalian inducible tyrosine kinase, that this domain could be acting as putative effector of Ca^{2+} signaling due to its interaction with Calmodulin [476]. This is interesting in the context of daptomycin as daptomycin is known to require Ca^{2+} for bioactivity [477, 478]. However, the other antibiotics *SAOUHSC_02149* is relevant for, like moenomycin and vancomycin, do not require Ca^{2+} for activity, suggesting that this protein plays other roles in *S. aureus*, in addition to roles relating to Ca^{2+} interactions (if any).

We tested the transposon inactivation mutant obtained from the Nebraska library [443] against vancomycin and daptomycin and found it to be sensitive relative to WT in the spot dilution assay described in Chapter 2, as indicated by the Tn-Seq analysis (Fig.

3.1A). Moreover, the up-regulation of *SAOUHSC_02149* promoted resistance to daptomycin, and less dramatically to vancomycin as well (Fig. 3.1B). Its role in resistance to these clinically relevant antibiotics supports the importance of elucidating the function of *SAOUHSC_02149*.

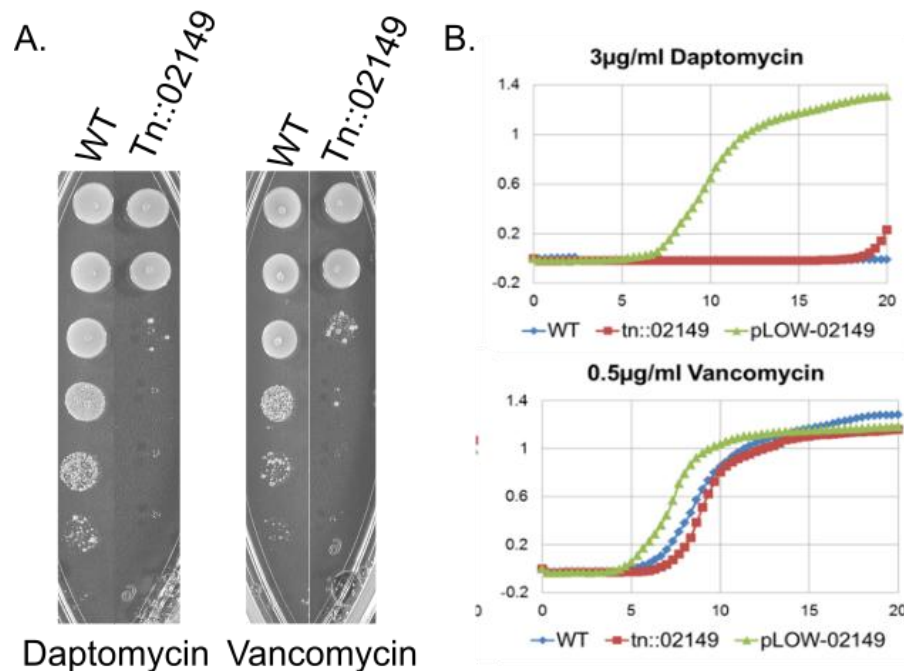


Figure 3.1: Tn::*SAOUHSC_02149* is sensitive to cell envelope antibiotics vancomycin and daptomycin. (A) Spot dilution assays of USA300 JE2 WT and a Nebraska library transposon mutant of *SAOUHSC_02149* (Tn::02149) shows that the mutant is more sensitive than WT to both vancomycin and daptomycin. (B) Growth curves of the inactivation mutant and the complemented strain showed that under daptomycin (top) and vancomycin (bottom), the overexpression of *SAOUHSC_02149* is protective, although the effect is more pronounced for daptomycin.

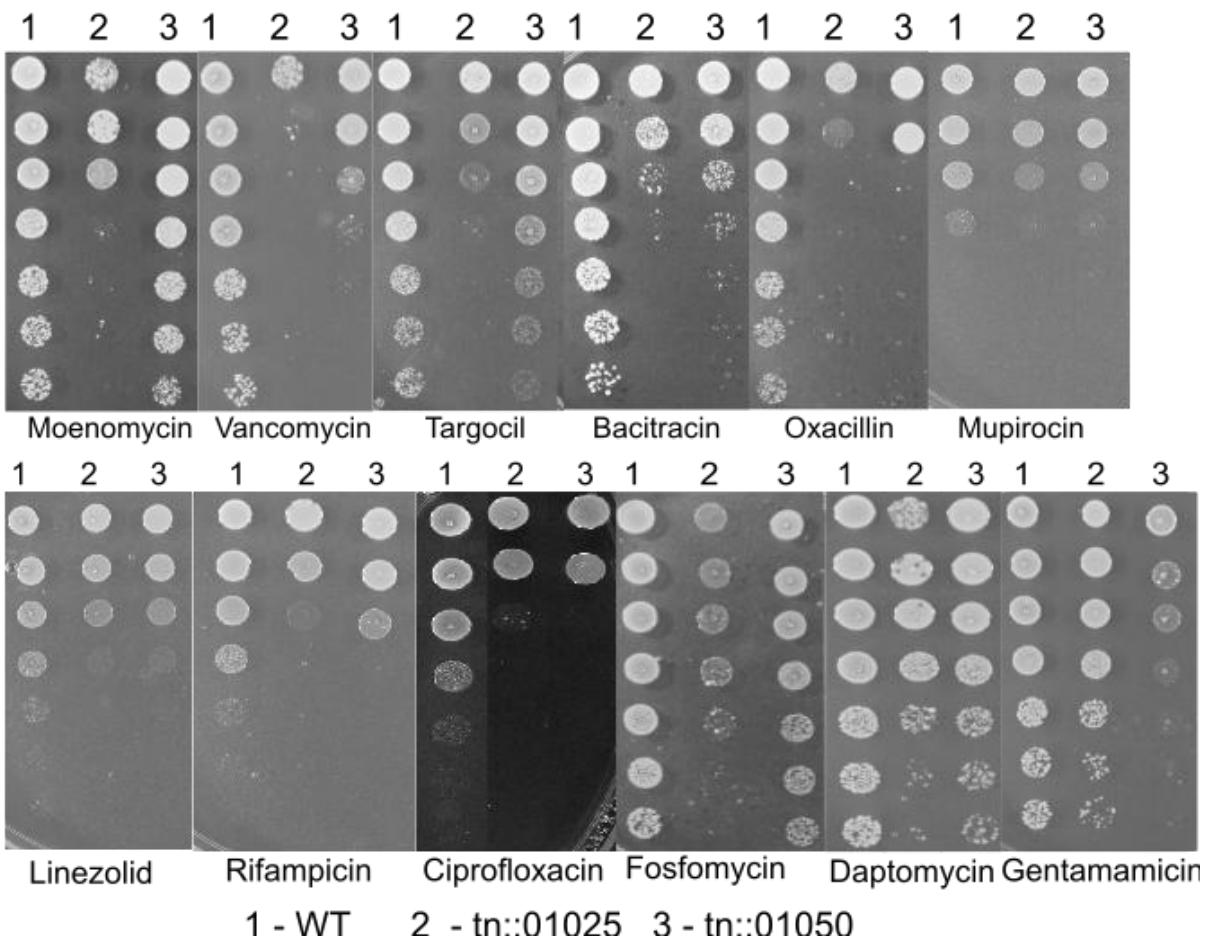
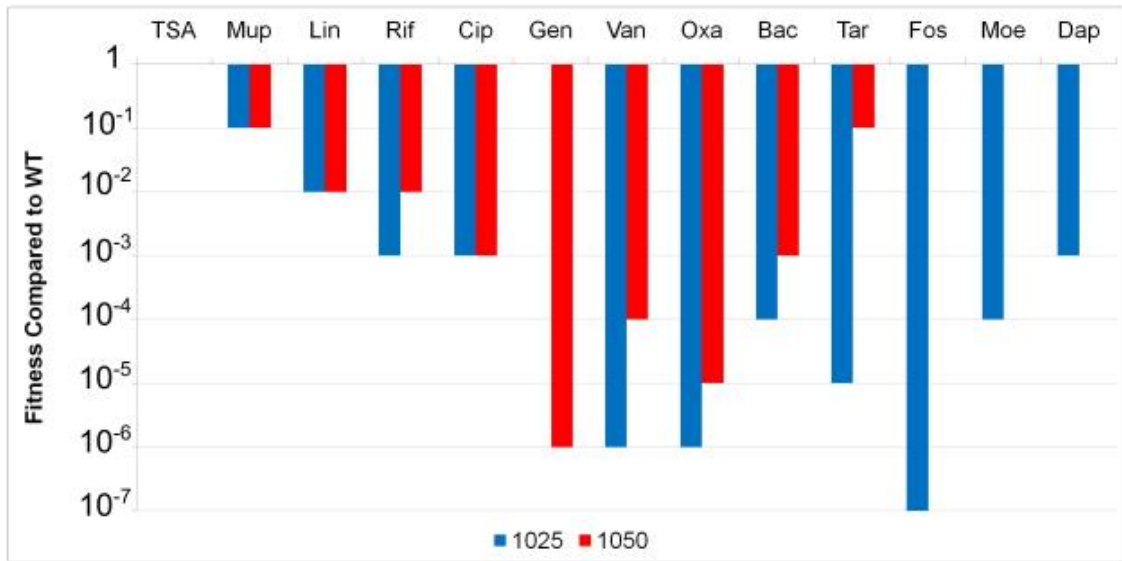
SAOUHSC_01025 is predicted to have six transmembrane helices, a 93 amino acid extracellular domain, and four more transmembrane helices. SAOUHSC_01050 is predicted to have three transmembrane helices and a 191 amino acid extracellular domain. BLAST and PSI-BLAST searches of SAOUHSC_01025 and SAOUHSC_01050 do not reveal high homology to any known genes.

Using our spot dilution approach described in chapter 2, we tested the fitness of mutants with inactivating transposon insertions in *SAOUHSC_01025* (tn::*1025*) and *SAOUHSC_01050* (tn::*1050*) obtained from the Nebraska library [443], against a panel of twelve antibiotics with a range of different targets. We wanted to evaluate the fitness of these mutants under both cell wall and non-cell wall antibiotics in order to determine if these factors are particularly relevant for cell wall antibiotics. We tested oxacillin, vancomycin, moenomycin, targocil, bacitracin, fosfomycin, daptomycin, gentamicin, ciprofloxacin, linezolid, mupirocin and rifampicin (Fig 3.2). We have discussed the mechanisms of action of most of these antibiotics in this and the previous chapter. Mupirocin is an inhibitor of protein translation by targeting isoleucyl-t-RNA synthetase [479] and rifampicin inhibits RNA polymerase, thereby interrupting RNA synthesis [480, 481]. With one exception, both mutants showed moderate and similar reductions in fitness when plated on non-cell wall related antibiotics. The exception was that tn::*1050* was far more sensitive to gentamicin than tn::*1025*, an unusual pattern not observed with any other antibiotic. Against cell wall active antibiotics, both tn::*1025* and tn::*1050* showed greater reductions in fitness compared to WT, with tn::*1025* often found to be more susceptible than tn::*1050*. Moenomycin provides a striking example of this as the fitness of the tn::*1025* mutant decreased by four orders of magnitude while the fitness of

the *tn::1050* mutants did not change. In general, however, both mutants showed reduced fitness compared to the wild type strain. The decreased fitness of both mutants when plated on most cell wall active antibiotics compared with other antibiotics is consistent with an important role in cell envelope integrity.

Figure 3.2: Tn::*SAOUHSC_01025* and tn::*SAOUHSC_01050* are particularly sensitive to antibiotics that damage the cell envelope. The abbreviations used here are mup = mupirocin, lin = linezolid, rif = rifampicin, cip = ciprofloxacin, gen = gentamicin, van = vancomycin, bac = bacitracin, tar = targocil, fos = fosfomycin, moe = moenomycin A, dap = daptomycin. Top panel: A summary of the fitness of these mutants relative to WT was assessed by spot dilution against the above antibiotics. Bottom panel: spot dilution assay plates for these mutants on all antibiotics tested are shown here.

Figure 3.2 (Continued):



We used triton X100-induced autolysis in an initial attempt to evaluate whether *tn::1025* and *tn::1050* mutants had significantly less stable cell envelopes than the WT, but we found no difference in induced lysis rates (Fig. 3.3). In growth curve assays, *tn::1025* and *tn::1050* mutants showed a slightly slower doubling time of 25.37min and 24.39min respectively, compared to the WT doubling time of 22min, which is not indicative of significantly compromised fitness. These factors appear to be more important when there is cell wall stress than in the absence of such stress.

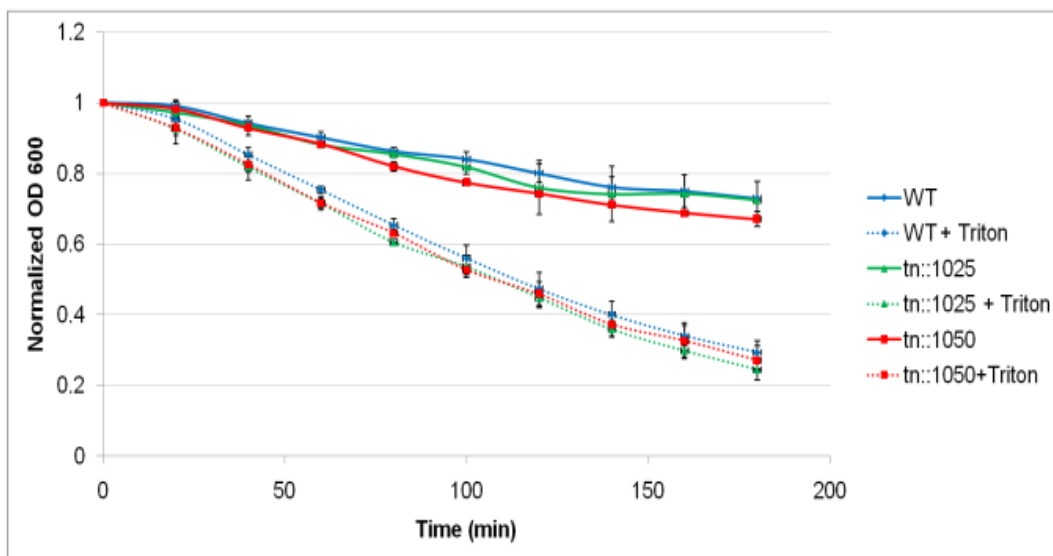


Figure 3.3. *Tn::SAOUHSC_01025* and *tn::SAOUHSC_01050* show no increase in sensitivity to triton X-100 induced lysis. Lysis curves of WT, *tn::1025* and *tn::1050* with or without triton X-100 show that WT and mutants lyse at similar rates. OD600 values were normalized to the initial starting OD of each sample.

3.6 Machine learning approach to suggest potential pathways genes of unknown function could be involved in

We wanted to determine if the fitness profiles of genes across multiple classes of antibiotics can be used to evaluate pathways in which they could be involved. This is based on the hypothesis that genes which have similar phenotypes, that is, similar patterns of sensitization and resistance across various classes of antibiotics will function in closely related pathways. For instance, components of the *graXRS/vraFG* operon can be expected to have highly similar fitness profiles across various antibiotics because they physically interact to respond to stresses (Fig. 3.4 A)

We optimized the K-nearest neighbors algorithm using the sci-kit learn library [482] to identify genes with the most similar fitness profiles (*i.e.*, fitness of a gene across different antibiotic conditions) to *SAOUHSC_01025* and *SAOUHSC_01050* (see Methods). For this approach, we used the data sets discussed in Chapter 2 for the antibiotics oxacillin, daptomycin, vancomycin, gentamicin, linezolid and ciprofloxacin to have representation from inhibitors of diverse mechanisms of action. A "fitness value" was calculated for each gene for each antibiotic, which incorporates the fold changes in reads for the genes, and adjusts the fold changes for genes which have very few reads mapping to them, as these fold changes were considered to be less significant as compared to fold changes that result from a large number of reads mapping to the genes (see Methods). As expected when we used the optimized algorithm to identify the genes with the most similar profiles to either *graX*, *graS*, *vraF*, and *vraG*, we found at least two of the other components of the system were among the five closest genes in the genome.

We then applied the algorithm to identify the five genes with the most similar profiles to *SAOUHSC_01025* and *SAOUHSC_01050*. *SAOUHSC_01025* and *SAOUHSC_01050* were most similar to one another and shared three of four other nearest neighbors, *graS*, *mprF*, and *cvfC* (Fig. 3.4B). In addition, *graR* was identified as similar to *1025* and *vraG* to *1050*. Unlike *mprF*, which is a member of the *graRS/vraFG* sensing system's regulon, *SAOUHSC_01025* and *SAOUHSC_01050* were not shown to be regulated by this system [32]. It is possible that they are involved in responding to the same stresses through an alternate pathway. Nevertheless, the connections identified here strongly suggested that they have functions related to maintaining membrane integrity and withstanding envelope stress, consistent with their roles in cell envelope antibiotic resistance. *CvfC*, one of the genes identified as similar to both *1025* and *1050*, is a known virulence factor, and its inactivation results in reduced hemolysin production in *S. aureus* MSSA strain RN4220 [483, 484].

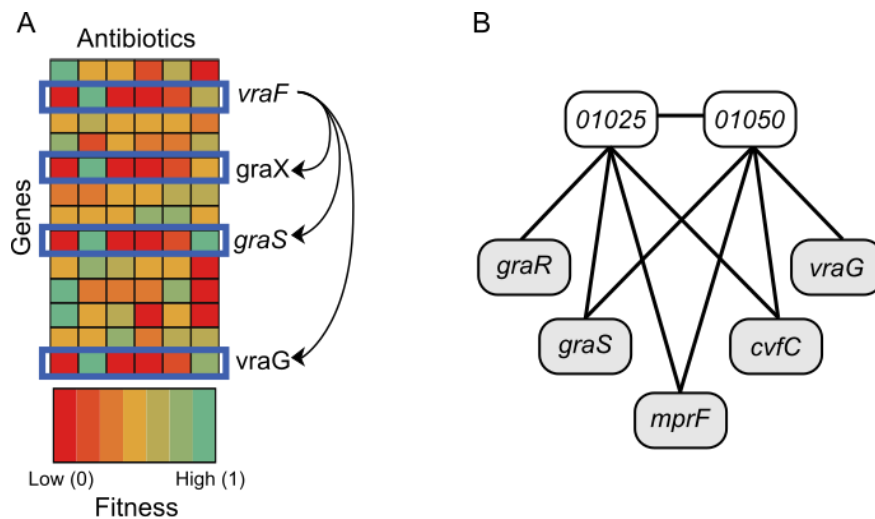


Figure 3.4. SAOUHSC_01025 and SAOUHSC_01050 are important for cell envelope integrity A) Schematic depicting the fitness of a subset of genes upon treatment with different antibiotics. Each column represents an antibiotic and each row

(Continued) represents a gene. Genes having related functions, such as the components of the *graRS/vraFG* MCS, have similar fitness profiles across a panel of antibiotics. Therefore, for any given test gene, it is possible to identify the five genes with the most similar enrichment/depletion patterns, and it is assumed that these genes have functions that are related to the function of the test gene. B) The K-nearest neighbors algorithm predicted that *SAOUHSC_01025* and *SAOUHSC_01050*, which encode polytopic membrane proteins of unknown function, were most similar to one another and also shared three of four other identified neighbors. As these neighbors play an important role in protecting *S. aureus* from certain classes of antibiotics, we predict that *SAOUHSC_01025* and *SAOUHSC_01050* are important for cell envelope integrity.

This connection with *cvfC* prompted us to evaluate the hemolytic phenotypes of *tn::1025* and *tn::1050*. Increased hemolysis as shown by a black clearing on blood agar plates, was observed for these mutants relative to WT (Fig. 3.5), suggesting possible roles in virulence and heme metabolism for these proteins. While the increase in hemolysis is contrary to what was observed for *cvfC* mutants previously, studies on *cvfC* were performed in RN4220 which has a mutated *agr* locus [485]. Since many functions including virulence are regulated by the *agr* operon, and attenuated virulence was observed in a *cvfC* mutant in an RN4220 strain but not in a Newman strain [483], it is possible that background mutations in parent strains account for these differences. Assaying the hemolytic phenotype of inactivation of *cvfC* in the USA300 JE2 strain background will allow us to better evaluate any possible connection with *cvfC*. We can

also determine if *SAOUHSC_01025* and *SAOUHSC_01050* have roles in virulence with *in vivo* studies in infection models. If the roles of these proteins in virulence are validated, it would result in the identification of two new virulence factors in the *S. aureus* arsenal.

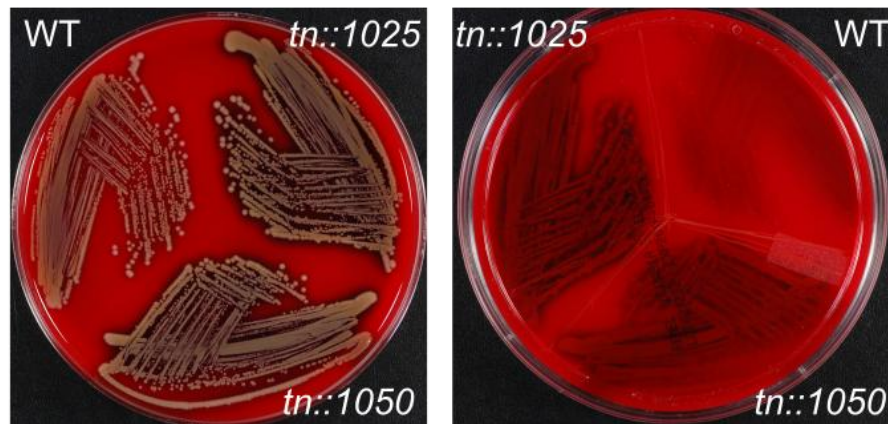


Figure 3.5. Tn::*SAOUHSC_01025* and Tn::*SAOUHSC_01050* showed increased hemolysis. WT, *tn::1025* and *tn::1050* plated on blood agar plates show increased hemolysis by mutant strains relative to WT. Plates were imaged from both the front (left panel) and back (right panel). Hemolysis is visualized as a black clearing on the red agar plates.

3.7 Discussion on parameters to consider for library treatment

There are a number of parameters to consider when treating a transposon library with antibiotics including the concentration of the antibiotic used for treatment, the amount of time a sample is grown for, and the starting inoculum of the library. These are discussed in detail below, and the detailed protocol for transposon library treatment is described in Methods.

Concentration selection:

Determining concentrations with which to treat antibiotics in the library was not a clear-cut task. We wanted to test concentrations at which genes whose inactivation results in fitness advantage and those which result in a disadvantage could both be identified. If the concentration used is too low and does not result in sufficient selective pressure, there will likely be no observable effects on the library. However, a concentration that is too high will deplete most of the mutants in the library as most mutants cannot be expected to result in high-level resistance to the antibiotics.

The percentage of TA sites hit in the treated conditions as compared with the untreated control was used as a marker for the selective pressure of the treatment condition. We found that data sets for treated samples in which the number of TA sites hit was at least 40% of the number of TA sites hit in the untreated control resulted in the identification of genes that have a fitness disadvantage in the presence of the treatment. A majority of the mutants were sensitive in treated data sets in which the number of TA sites hit were less than 40% of the number of TA sites hit in the untreated control, making it difficult to identify those mutants which are particularly relevant for the treatment condition.

We did not observe a strong correlation with the amount of time a treated culture takes to reach an OD600 of 1 and the selective pressure. For example, cultures treated with bacitracin at 8 μ g/ml reached a growth suitable for harvesting at 8hrs and the data set had reads mapping to 88% of the TA sites hit in the untreated control, whereas, for two other antibiotics, fosfomicin at 12.5 μ g/ml and DMPI at 1 μ g/ml which also reached the desired growth level between 8-8.5hrs, the data sets had reads mapping to only

18% and 36% of TA sites hit in the untreated control respectively. It is therefore prudent to test multiple concentrations for each antibiotic. In this study, cultures of the transposon library described in Santiago *et al.* [392] were treated at different fractions of the MIC of the antibiotic, and at least two concentrations of each antibiotic were subjected to Tn-Seq . The two concentrations sequenced were selected as those which resulted in a moderate (1-3 hour growth delay relative to the untreated control) and a severe (>15 hour growth delay). See Methods for full details on the sample harvesting protocol.

Starting inoculum and culture volume:

These two parameters have to be optimized in order to achieve sufficient representation of the library and a significant difference in fold changes of reads for fitness advantaged and disadvantaged mutants from the background. The library we used has ~700,000 mutants, therefore, an inoculum of at least 10^7 cfu is necessary to obtain full representation of the library during experimentation. However, the choice of the inoculum has to be balanced with culture volume and the desired number of generations the sample should undergo prior to harvesting.

For instance, a 50mL culture with 10^7 cfu inoculum will take approximately 11 generations to reach an OD_{600} of 1, however, a 2mL culture with 10^7 cfu inoculum would take only 6 generations to reach an OD_{600} of 1. Antibiotics tested in 2mL culture with 10^7 cfu inoculum resulted in only marginal enrichment and depletion of mutants relative to the untreated control resulting in less robust data sets than those obtained with 50mL culture volumes (Dr. Tim Meredith, personal communication). This is because a mutant that has a 10 min growth delay relative to wild type will be outcompeted by wild type

when they are pooled together. In 6 generations the population of cells will consist of 4 times as many WT cells as mutant cells, whereas in 11 generations, it will consist of 12 times as many WT cells as mutant cells. Therefore, having a larger number of generations will allow mutants that have a fitness advantage to significantly outcompete and stand out from those that have no advantage under the tested condition. Similarly, mutants that result in a fitness disadvantage will be more significantly outcompeted by fitter mutants after a larger number of generations, making it easier to identify these from the pooled library.

However, assaying antibiotics in a 50mL culture volume dramatically reduces the throughput of the approach. In addition, it requires a larger amount of compound than a 2mL culture format, which is a concern if the compound to be tested is not readily available. For these reasons, we reduced the starting inoculum to 4×10^5 cfu's to ascertain 11 generations in a 2mL culture volume for subsequent antibiotic samples. A caveat to keep in mind is that this inoculum does not provide full representation of the transposon library. Therefore, for future Tn-Seq efforts, if a compound does not result in a satisfactory data set with these treatment conditions, 50mL culture format with 10^7 cfu inoculum can be tested. A larger number of generations amplifies the effects of moderately resistant and moderately sensitive mutants and so, if the goal of the experiment is to identify only the most important factors to the treatment condition, then a smaller number of generations might be preferable.

3.8 Conclusions

We were able to successfully use Tn-Seq of multiple antibiotics to identify a core list of genes that are relevant under cell wall stress. Characterizing the functions of these genes may identify processes that are important to maintaining the integrity of the cell wall in the face of external stress. The proteins encoded by these genes could make valuable potential targets for potentiators to multiple antibiotics targeting peptidoglycan. Such broad-spectrum potentiators could be of great clinical value as they can be used in combinations with a number of antibiotics. We also identified numerous hitherto uncharacterized genes that are particularly relevant under cell wall perturbation, emphasizing that our knowledge of the major players in the cell envelope is incomplete. The preliminary results described here for three of these hypothetical genes.

SAOUHSC_02149, *SAOUHSC_01050*, and *SAOUHSC_01025*, substantiate our claim that these genes are indeed crucial players in the cell envelope, important for resistance to multiple PG biosynthesis inhibitors.

3.8 Methods

MIC determination for Tn-Seq experiments: Glycerol stocks of HG003 $\Delta\Phi11$ strain were made by streaking out the strain onto 8 tryptic soy agar (TSA) plates and grown overnight at 30°C. Colonies were resuspended into 25mL of tryptic soy broth (TSB). Cells were spun down (16,000xg for 3min) and resuspended in enough 12.5% glycerol in TSB to yield 5×10^{10} cfu/mL. These were aliquoted and frozen at -80°C until further use. Thawed glycerol stocks were diluted to a OD₆₀₀ of 0.2-0.3 in 10mL TSB and outgrown at 30°C until the OD₆₀₀ is ~ 0.4. The culture was then diluted to 10^7 cfu/mL

and then diluted 1:25 to 4×10^5 cfu/mL in TSB supplemented with Ca^{2+} (25mg/L) and Mg^{2+} (12.5mg/L). Antibiotics were diluted to 2x the desired concentration and serially diluted by 2x for 9 dilutions in a total volume of 100uL of cation-adjusted TSB. 100uL culture was added to 100uL pre-diluted antibiotics to yield a final starting inoculum of 2×10^5 cfu/mL in 96 well plates. A no-antibiotic control well was included. Plates were incubated at 37°C with shaking and MIC was read after incubation for 18 hours as the concentration at which the blanked OD_{600} of a well is <0.2 .

Sample harvesting for Tn-Seq: The above process was repeated with a few changes. Cation-adjusted TSB was used for all antibiotics except oxacillin and bacitracin which were tested in Muller-Hinton Broth II. Exceptions were vancomycin, moenomycin A, ramoplanin and targocil, for which inoculum used was 10^7 cfu/2mL. A glycerol stock of the aliquoted HG003 transposon library [392] was thawed and used as starter culture. This was processed as described previously to 4×10^5 cfu/mL in media. Antibiotics were generally tested at 2x, 1x, 0.5x and 0.25x of MIC. Antibiotic dilutions were prepared at 2x the desired starting concentration in 1mL of media in 15mL culture tubes. 1mL of diluted culture was added to 1mL pre-diluted antibiotics to yield a final starting inoculum of 2×10^5 cfu/mL. A no-antibiotic control was prepared for each set of samples. Culture tubes were incubated at 37°C with shaking and growth was monitored over time. Untreated cultures under these conditions reached stationery phase between 4.5 and 5 hours. Treated conditions which showed delayed growth relative to untreated control were harvested when they reached stationery phase and cell pellets were frozen at -80°C until samples could be processed for Tn-Seq.

Sample preparation for Tn-Seq and Sequencing: Harvested pellets were processed for Tn-Seq as previously described [392]. Six samples containing different experiment barcodes were pooled together and run using single end, Illumina Hi-Seq with 40% Φ X spike-in. Two sets of six samples can usually be run in one flow cell therefore, for each set of 12 samples at least one untreated control processed at the same time as the remaining samples was included. Sequencing was conducted at either the Tufts Genomics Core or at Biopolymers Facility at Harvard Medical School.

Data analysis: Reads from pooled libraries were first processed through the Galaxy server of the Tufts Genomics Core, as previously described [392, 416-418]. Number of reads in the sample and TA sites hit could be determined at this stage, if needed, by using the python Hit Sites Counter script written by Dr. Marina Santiago. Reads from each treated sample were compared to the reads in untreated control by Mann-Whitney U analysis, after simulation based re-sampling to normalize the two samples as previously described [392, 396]. P-values obtained from Mann-Whitney U analysis were corrected for multiple hypothesis testing by using the Benjamini-Hochberg correction as previously described [392].

Identifying core set of genes common among PG biosynthesis inhibitors: Genes which had a fold change in reads mapping to them of $>1.5x$ or $<0.66x$ in the treated sample relative to untreated were collated for each concentration of an antibiotic. This gene list was compared between the different concentrations of the antibiotic, to create a list of unique genes. Those genes where reads were depleted ($<0.66x$ fold change in reads) in one concentration but enriched ($>1.5x$ fold change in reads) in another concentration were not regarded as hits. If however, a gene was unaffected (fold

change between 1.5x and 0.66x) in one concentration, but affected in another, it was considered a hit. Only the enrichment or depletion status of a gene was considered in comparison and not the actual fold change. Thus a final list of genes with enriched and depleted genes was created for each antibiotic. These were compared across antibiotics to identify those that were in common among different classes of antibiotics. 57 genes were identified to be hits in at least five out of seven PG biosynthesis inhibitors.

Gene function prediction using machine learning: We used the machine learning algorithm, K-nearest nearest neighbors, in an unsupervised manner, to identify other genes with similar resistance and sensitization patterns using the scikit-learn Python library [482]. In order to reduce the proportion of essential genes that are identified as hits, all fold changes were first modified for essentiality. This was done by identifying a minimum number of reads in control and experiment by counting all reads in that condition and dividing by 10,000. All read counts/gene that fell below this value were assigned this minimum value. Therefore, any fold changes that are due to a very low number of read counts in each sample set, for example, a fold change of 3x caused due to 3 reads/gene in one sample and 1 read/gene in the other, will now have a fold change closer to 1x will However, because of the different selective pressures exerted by each antibiotic, we cannot use this modified fold change of reads that map to each gene in the experiment versus the control as the metric for classification. In addition, we wanted to distinguish between the two following conditions: 1) A ratio change of 0.1 due to 100 reads in the control and 10 reads in the experiment and 2) A ratio change of 0.1 due to 1000 reads in the control and 100 reads in the experiment. If both genes are the

same length, option 1 will be much less relevant than option 2 because 100 reads/gene and 10 reads/gene both correspond to a gene with a significant fitness defect while a change from 1000 reads/gene to 100 reads/gene is more likely to be a significant change. Therefore, we converted the ratios into a more appropriate value. This value, representing fitness under the antibiotic treatment is calculated by multiplying the converted ratio above by the number of reads mapping to that gene in the treatment condition, and normalizing to the length of the gene. Then, genes were ordered from smallest to largest “fitness”. To place all the samples on the same scale, the gene with the smallest “fitness” was given a value of 0, and the gene with the highest “fitness” was given a value of 1. All other genes were placed in order between these values, in increments that increase by $1/(\text{total number of genes})$. This final value, which we call the “normalized fitness value”, is the value we use for the machine learning analysis. Finally, essential genes were removed from the dataset, and the K-nearest neighbors algorithm was further optimized by adjusting the Minkowski distance metric to output the genes with the most similar resistance/sensitization pattern to the test gene. We identified the five genes (the five nearest neighbors) having the most similar pattern of “normalized fitness values”.

Spot dilution assays: Spot dilution assays were completed as described in Chapter 2. *SAOUHSC_01025* and *SAOUHSC_01050* were validated using transposon mutants from the Nebraska library in background USA300 JE2 [443].

Triton X-100 induced lysis assay: Lysis assays were performed as previously described [363]. Overnight cultures of WT and mutants were diluted 1:100 in fresh TSB and grown to an OD_{600} of 0.6. The cultures were harvested, washed with cold, sterile

water and re-suspended in 0.05M Tris-HCl, pH 7.2, with or without 0.05% Triton X-100. Samples were incubated at 37°C and OD₆₀₀ was measured every 20min for 3 hours. OD was normalized to the initial measurement for each sample. Error bars were obtained from two separate biological replicates.

Growth curves: Overnight cultures were diluted to OD₆₀₀ 0.01 in 25ml TSB and grown with shaking at 37°C and 43°C until stationary phase. OD₆₀₀ was measured every 20 min for the first 100 min until the cultures reached exponential phase, and every 10 min subsequently. Doubling time was calculated between an OD₆₀₀ of ~ 0.2 and ~1.2.

Hemolysin Assay: Cultures of mutants and wild type were grown to an OD₆₀₀ of 1.0 and then streaked out on Columbia agar plates with 5% sheep blood (purchased from Thermo Scientific) using 1µL inoculation loops. Plates were imaged after overnight incubation at 37°C.

Chapter 4: Predicting the mechanism of action of antibiotics

4.1 The use of fitness profiles to cluster antibiotics by mechanism of action

While certain genes are particularly important for resistance, such as those that are involved in the targeted pathway, other genes might be peripherally involved and therefore moderately important, and still others are unlikely to be involved at all. We would expect that the relevance of different genes under antibiotic treatment would be similar for antibiotics targeting the same pathway. In other words, we hypothesized that the enrichment and depletion patterns of the genes in response to an antibiotic will make a unique fitness profile for that antibiotic and that this fitness profile will likely be shared among antibiotics that target the same enzyme or pathway as they should have similar effects on the fitness of mutants. We see evidence of this from the numerous mutants we find to be similarly affected for vancomycin and ramoplanin.

The relative fitness of transposon mutants under antibiotic pressure as given by the fold change in reads mapping to the gene under treatment condition vs. the untreated control can be used to identify those antibiotics that have the most similar fitness profiles. This has also been shown previously in *Pseudomonas aeruginosa*, where 14 tested antibiotics were compared using hierarchical clustering of the relative fitness generated by Tn-Seq analysis. In this study, they showed that antibiotics of same mechanism of action - aminoglycosides and β -lactams - clustered together [403].

In order for such clustering approaches to be successful, we need to have multiple fitness profiles for different antibiotics, including those profiles that are more similar to each other as well as those which are dissimilar. For this reason, we

expanded the set of Tn-Seq derived fitness profiles for antibiotics to include antibiotics which target a number of different pathways.

4.2 An expanded set of antibiotics were tested in Tn-Seq

We assayed 16 antibiotics in addition to those described in previous chapters (Table 4.1).

Cell envelope antibiotics: In addition to oxacillin, moenomycinA, vancomycin, ramoplanin, lysobactin, bacitracin and targocil, whose mechanisms of action have been discussed in previous chapters, we also included cefaclor, D-cycloserine, fosfomicin, DMPI, CDFI, and WTI-11. Cefaclor is also a β -lactam antibiotic. While oxacillin has not been shown to be selective for any particular PBP, cefaclor has been shown to be selective for PBP3 and under some conditions for PBP2 as well [486, 487]. D-cycloserine interrupts the formation of the D-ala-D-ala subunit of the pentapeptide side chain of lipid II by inhibiting both the D-alanine racemase and the D-ala-D-ala ligase [488-490], and fosfomicin inhibits the synthesis of UDP-MurNAc from UDP-GlcNAc by MurA [304]. DMPI and CDFI are inhibitors of the lipid II flippase, resulting in depletion of the substrate needed for PG synthesis [353]. Like targocil, WTI-11 targets TarGH to inhibit WTA export as well as PG biosynthesis. It is however, structurally unrelated to targocil. WTI-11 was recently identified by Leigh Matano and Heidi Morris in the Walker Lab.

Polymixin B, is thought to be a membrane disrupting agent but a full understanding of its mechanism of action in *S. aureus* is not available. In treatment of Gram-negative infections, polymixin is considered to be the drug of last resort. In these

organisms, the cyclic lipopeptide polymixin binds selectively to lipopolysaccharides lining the outer leaflet of the outer-membrane, inserts its hydrophobic tail into the outer-membrane, eventually destabilizing the outer-membrane, and crossing to the inner membrane which it also destabilizes resulting in lytic cell death [491]. Gram-positive organisms do not synthesize lipopolysaccharides, and are usually less sensitive to polymixin [492]. Nevertheless, it has been observed in Group B *Streptococcus* that lack of D-alanylation on LTAs sensitizes to polymixin [227], suggesting that polymixin can cause damage in Gram-positives as well. In *M. smegmatis*, polymixin has been shown to interact with enzymes involved in the respiratory complex, specifically an NADH dehydrogenase and malate:quinone oxidoreductase [493]. However, there is no knowledge of any additional targets for polymixin in *S. aureus*. Daptomycin is suggested to both disrupt membrane stability and have effects on PG biosynthetic machinery [409, 410, 494], although the exact mechanism of either of those mechanisms remains unknown. Daptomycin is regarded as a drug of last resort in the treatment of MRSA infections.

Table 4.1: Antibiotics tested in Tn-Seq cover a variety of chemical classes and targeted pathways			
Antibiotic	Chemical Class	Target Pathway	Target
Oxacillin	β -lactam	PG biosynthesis	Transpeptidase domain of PBPs
Cefaclor	β -lactam		Transpeptidase domain of PBPs
Moenomycin A	Phosphoglycolipid		Transglycosylases
Vancomycin	Glycopeptide		D-ala-D-ala of lipid II
Ramoplanin	Glycopeptide		Pyrophosphate-sugar moiety of lipid II
Lysobactin	Glycopeptide		Pyrophosphate-sugar moiety of lipid II
D-cycloserine	Amino-acid derivative		Ddl and Alr
Fosfomycin	Phosphonic acid derivative		MurA
DMPI	Indole		Lipid II flippase
CDFI	Indole		Lipid II flippase
Bacitracin	Cyclic peptide		Und-PP
Linezolid	Oxazolidinone	Protein Synthesis	50S subunit of ribosome
Chloramphenicol	Carboxylic acid amide		50S subunit of ribosome
Tetracycline	Polyketide		30S subunit of ribosome
Mupirocin	Monooxycarboxylic acid		Isoleucyl t-RNA synthetase
Rifampicin	Ansamycin	RNA synthesis	DNA-dependent RNA polymerase
Targocil	Triazoloquinazoline	WTA export, PG biosynthesis	TarGH
WTI-11	Furanocoumarin		TarGH
Moxifloxacin	Fluoroquinolone	DNA synthesis	Topoisomerase IV and DNA gyrase
Ciprofloxacin	Fluoroquinolone		Topoisomerase IV and DNA gyrase
Novobiocin	Aminocoumarin		DNA gyrase and topoisomerase IV
Sulfamethoxazole	Sulfonamide	Folate synthesis	Dihydropteroate synthetase
Trimethoprim	Aminopyrimidine		Dihydrofolate reductase
Polymixin B	Cyclic peptide	Membrane disruption	Membrane
Daptomycin	Lipopeptide	Membrane disruption, PG synthesis (hypothesized)	Membrane (other targets possible)

Non-cell envelope antibiotics: In addition to linezolid, mupirocin and rifampicin whose mechanisms of action were discussed in Chapter 3, we also included chloramphenicol, tetracycline, moxifloxacin, ciprofloxacin, novobiocin, sulfamethoxazole and trimethoprim. Chloramphenicol and tetracycline are both protein synthesis inhibitors but while chloramphenicol binds to the 50S subunit of the ribosome inhibiting peptide bond formation [495, 496], tetracycline binds to the 30S subunit inhibiting delivery of the

aa-tRNA [496-498]. Ciprofloxacin, moxifloxacin and novobiocin are all DNA synthesis inhibitors that inhibit DNA gyrase and topoisomerase IV. In *S. aureus*, unlike ciprofloxacin and moxifloxacin which are quinolones that primarily inhibit topoisomerase IV [499], novobiocin is an aminocoumarin that primarily inhibits DNA gyrase [500]. DNA gyrase and topoisomerase IV are both involved in DNA replication and are homologs of each other, however, the latter is better at separating concatenated plasmids and daughter chromosomes than is DNA gyrase [501]. Topoisomerase IV inhibition results in slower inhibition of DNA synthesis than DNA gyrase inhibition [502]. In addition, while novobiocin inhibits the catalytic activity of DNA gyrase, ciprofloxacin stabilizes the gyrase-DNA complex which ultimately leads to multiple DNA breaks and initiates cell death. It has been suggested that this leads to induction of the SOS response, and production of reactive oxygen species [503]. Sulfamethoxazole and trimethoprim inhibit different steps in the folate biosynthesis pathway. Folic acid is used in numerous other metabolic pathways including purine and pyrimidine synthesis. Sulfamethoxazole inhibits dihydropteroate synthetase [504-506] and trimethoprim inhibits the downstream step dihydrofolate reductase [507-509].

This set of antibiotics covers a variety of mechanisms of action and in some cases even when they inhibit the same pathway, they target different steps of the pathway, possibly resulting in slightly different fitness profiles. We wanted to evaluate whether these diverse fitness profiles will be useful in identifying antibiotics which have similar mechanisms of action, and whether this can then be used to predict mechanisms of action for unknown compounds.

4.3 Hierarchical clustering of antibiotic fitness profiles

As a first attempt, we used a hierarchical clustering approach. Hierarchical clustering is a useful statistical tool to determine how different samples compare to each other on a big-picture level. It assigns all samples to one group, then the samples are split into two groups so that the two groups are maximally different from each other. This process is repeated iteratively until all samples are assigned to one cluster where each branch represents a group of samples more similar to each other than they are to the other members of the parent branch [510, 511].

In order to facilitate comparison across all treated antibiotic conditions, we included only one concentration of each antibiotic tested. The "fitness value" described in Chapter 3, section 3.6 were used for this analysis as well. To reduce noise, we only considered the top and bottom 1% of genes, that is, those with the highest and lowest fitness values. As we were considering only the highly affected genes in each sample, we were able to use more selective concentration conditions (including those with <40% of TA sites hit in the treated conditions relative to the untreated condition) for this analysis. Hierarchical clustering was then used to visualize how similar and different the fingerprints for each antibiotic were (Fig. 4.1). As expected, antibiotics with the similar targets or mechanism of action like ramoplanin and vancomycin, ciprofloxacin and moxifloxacin, sulfmethoxazole and trimethoprim, and DMPI and CDFI did cluster together. This implies that the fitness profiles of these antibiotics were more similar to each other and more dissimilar to the fitness profiles of other antibiotics.

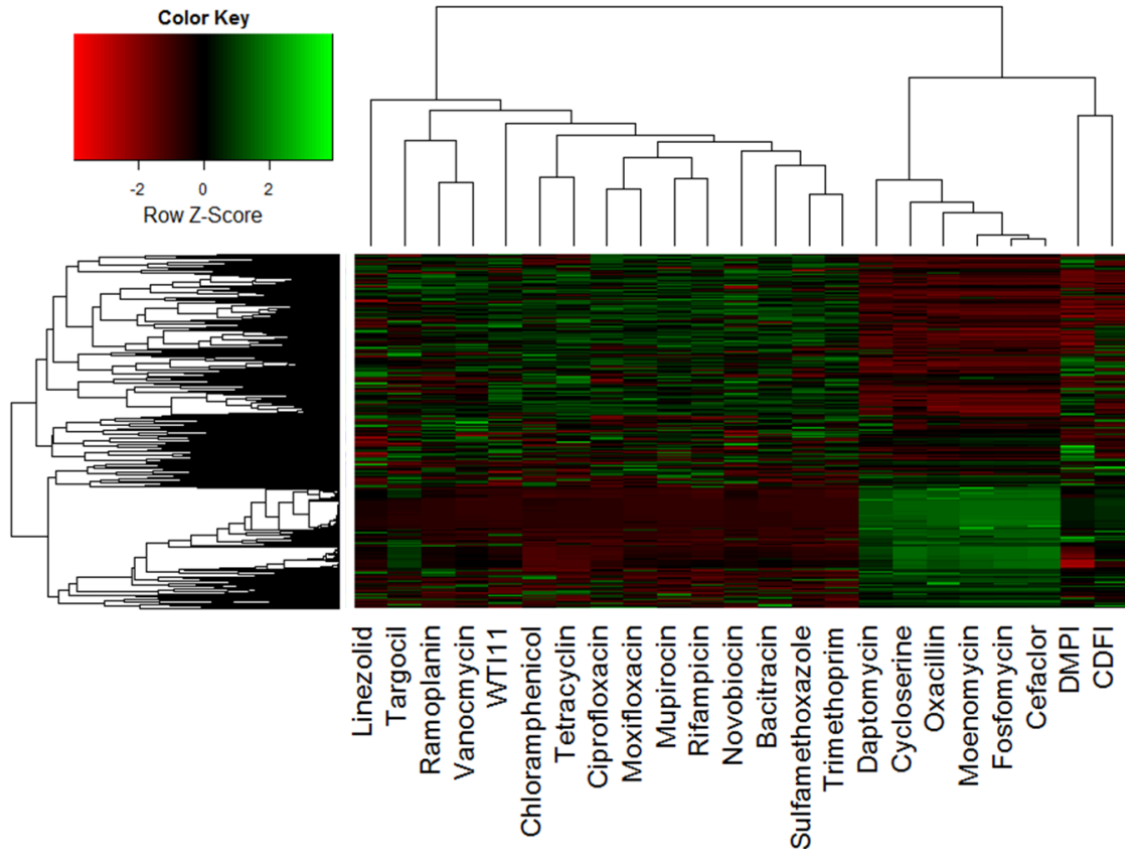


Figure 4.1. Hierarchical clustering showed that antibiotics of similar mechanisms of action have similar profiles and cluster together. This heat map shows fitness profiles of genes (across the vertical axis) under various antibiotics (across the horizontal axis). The colors indicate the spread of fitness of genes with red corresponding to low fitness and green corresponding to high fitness. Antibiotics with similar mechanisms of action such as vancomycin and ramoplanin, and folate synthesis inhibitors, suflamethoxazole and trimethoprim clustered together.

However, there were some instances where clustering did not show the expected result. For instance, targocil and WTI-II have the same target (TarG) but did not cluster closely together. Linezolid, which is also a protein synthesis inhibitor targeting the

ribosome clustered apart from the chloramphenicol-tetracycline subcluster. Bacitracin did not cluster together either with the substrate-binding inhibitors vancomycin and ramoplanin, or the other cell wall inhibitors. While this could possibly be indicative of its unique mechanism of action, we still expect that its fitness profile would be more similar to that of other cell envelope antibiotics than to that of non-cell envelope antibiotics. In order to improve the accuracy of clustering and to develop an approach that can be used to predict mechanism of action of unknown compounds, we used the K-nearest neighbors algorithm.

4.4 K-nearest neighbors algorithm to classify antibiotics by mechanism of action

The K-nearest neighbors algorithm, which was introduced in Chapter 3, section 3.6, is useful for classifying data into multiple classes [482]. This algorithm can be used to classify data in a supervised or unsupervised manner. In the supervised approach, the algorithm "learns" by using a training data set of antibiotic fitness profiles which are manually classified into a specific number of classes. It then compares the fitness profiles an antibiotic of unknown class to this training set and calculates the class of antibiotic that is most similar to this unknown antibiotic using a distance metric (Fig. 4.2). The Minkowski distance metric was used here. In the unsupervised approach, no information is given about antibiotic classes and the algorithm searches for antibiotic fitness profiles that are most similar to each other. It was found experimentally that the supervised approach performs better than the unsupervised approach, which is very similar to hierarchical clustering.

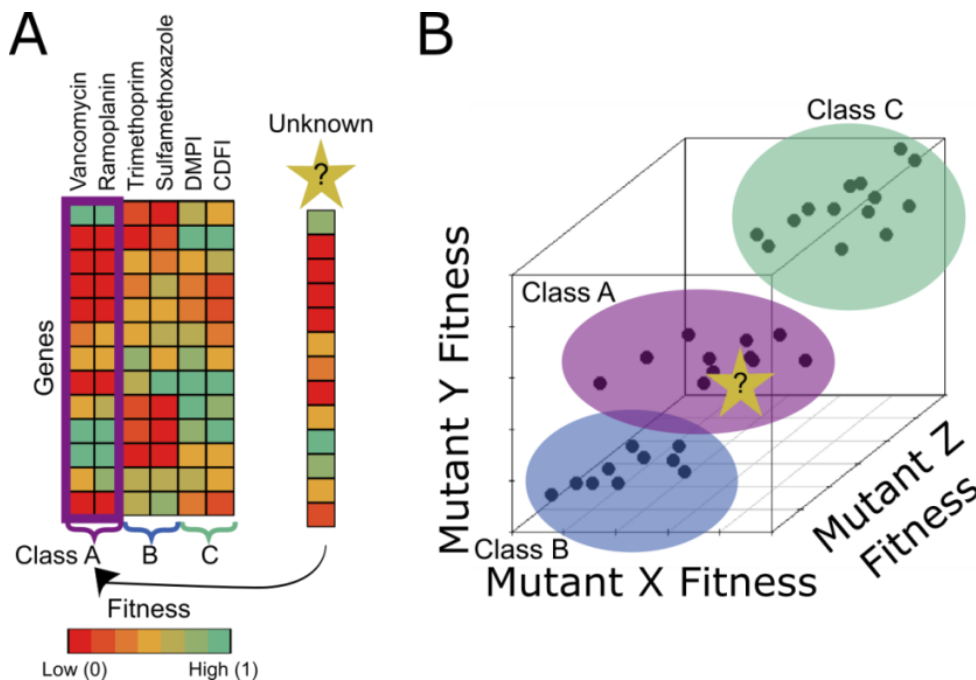


Figure 4.2. A schematic description of the K-nearest neighbors algorithm to predict antibiotic mechanism of action. (A) Antibiotics with the targets in the same pathway have similar fitness profiles, as indicated by the same pattern of red (low fitness) and green (high fitness) for genes across the antibiotic pairs vancomycin and ramoplanin, trimethoprim and sulfamethoxazole, and CDFI and DMPI. The fitness profile of the same set of genes for a new unknown antibiotic can be compared to the known fitness profiles of genes for the known class of antibiotics to identify the known antibiotic with the most similar fingerprint. This allows the prediction of the mechanism of action of the unknown antibiotic. (B). A simplified schematic represents the theory behind the supervised K-nearest neighbors classifier [482]. A training data set is created consisting of known antibiotics classified by their mechanisms of action. The algorithm compares the fitness profile of an unknown antibiotic to the fitness profiles in this training set by calculating the distance of each mutant fitness in that antibiotic to its closest X-number of neighbors. Cumulatively, this allows the prediction of the training

(Continued) class it is most similar to. In this example, the unknown antibiotic is most similar to class A antibiotics, suggesting that it may bind to lipid II like vancomycin and ramoplanin.

Classifying known antibiotics for supervised machine learning:

The number of classes into which antibiotics are classified for the training data set for the K-nearest neighbors algorithm was a parameter that could be optimized to make the results of the algorithm more informative. Antibiotics could be broadly classified into two groups - cell envelope and non-cell envelope antibiotics. However, this will not provide as much information as a more detailed classification according to the target and modes of killing of the antibiotic. The narrower the groups are the better the ability of the algorithm to report on the finer details about the mechanism of action of the antibiotic, but such a narrow classification, while increasing the breadth of classes in the training set, would reduce the depth, that is, many of the classes would have only one representative antibiotic. This would increase the error rate of the algorithm.

For this initial analysis, the antibiotics were classified into broader classes based on the results of hierarchical clustering and unsupervised K-nearest neighbors algorithm (Table 4.2, column 2). While PG biosynthetic inhibitors could be placed into one group, we could also separate lipid II binders and lipid II flippase inhibitors into separate classes because we had sampled more than one antibiotic in these classes. However, as discussed above, due to the lack of more RNA synthesis inhibitors, and other protein synthesis inhibitors that target aminoacyl-t-RNAs, mupirocin and rifampicin had to be placed into a separate category for "other non-cell envelope target".

The concentrations of the antibiotics tested affected how the antibiotics could be classified. For instance, while the higher concentration of WTI-11 exerted more selective pressure and was more closely related to PG biosynthesis inhibitors, the conditions used in targocil treatment exerted less selective pressure and its fitness profile was more similar to that of a lower concentration of WTI-11. Therefore, targocil and other antibiotic conditions which did not result in as high selective pressure, were placed into a separate "Unclassifiable" class. The classification and therefore the performance of the algorithm can be improved if antibiotic conditions included in this analysis result in approximately equivalent levels of selective pressure. This stresses the importance of sampling a range of concentrations and allowing for sufficient number of generations for each antibiotic.

Optimizing the algorithm:

This algorithm was optimized so that the following requirements are satisfied: (1) An antibiotic tested at two different concentrations should be most similar to each other, provided these concentrations are within a 2x window, for instance, moenomycin A tested at 0.16 μ g/mL and 0.32 μ g/mL (2) Two antibiotics of the same chemical class with same target should be most similar to each other for example, CDFI and DMPI, (3) Two antibiotics of different chemical classes with same targets should be similar to each other, for example, targocil and the lower concentration of WTI-11, and (4) two antibiotics that target enzymes in the same pathway should be most similar to each other, for example, trimethoprim and sulfamethoxazole. For each antibiotic, the top 25% and bottom 25% of genes in terms of fitness values were collated, resulting in a unique

set of 1614 total genes. These were then used to evaluate the nearest neighbor to an unknown test antibiotic, that is, the antibiotic class with fitness profiles most similar to the unknown test antibiotic. The optimized algorithm was trained on 24 of the 25 antibiotics and the remaining antibiotic was tested as the "unknown". The algorithm classified the mechanism of action of test antibiotics as per the supplied classification 19 out of 25 or 76% of the time (Table 4.2, column 3).

Table 4.2: Machine learning can predict the class of an unknown antibiotic		
Antibiotic	Class for supervised learning	Predicted class
Oxacillin Cefaclor Moenomycin A Fosfomycin D-cycloserine WTI-11 (via lipid II depletion)	PG Synthesis	PG synthesis PG synthesis PG synthesis PG synthesis PG synthesis PG synthesis
DMPI CDFI	PG Synthesis (Lipid II Flippase)	PG synthesis (Lipid II flippase) PG synthesis (Lipid II flippase)
Vancomycin Ramoplanin	PG Synthesis (Lipid II Binding)	PG synthesis (Lipid II binding) PG synthesis (Lipid II binding)
Polymixin Daptomycin	Membrane Disruption	Protein Synthesis PG Synthesis
Chloramphenicol Tetracycline Linezolid	Protein Synthesis	Protein Synthesis Protein Synthesis Protein Synthesis
Moxifloxacin Ciprofloxacin	DNA Synthesis	DNA Synthesis DNA Synthesis
Trimethoprim Sulfamethoxazole	Folate Synthesis	Folate Synthesis Folate Synthesis
Rifampicin Mupirocin	Other non-cell envelope target	PG synthesis (Lipid II binding) Folate Synthesis
Targocil Bacitracin Lysobactin Novobiocin	Unclassified	PG synthesis (Lipid II binding) Unclassified Folate Synthesis Unclassified

Table 4.2: The table shows 25 antibiotics (column 1) and the categories they were classified into for the training set (column 2). Each antibiotic was used as a test

(Continued) antibiotic for the K-nearest neighbors algorithm trained on the remaining 24 antibiotics. The class predicted for each antibiotic by machine learning is indicated (column 3). The algorithm is able to classify a majority of the antibiotics correctly (shown in green), although there are a some errors (shown in red). There were two antibiotics that was correctly placed into the unclassified category (shown in yellow).

Discussion of the performance of the algorithm:

The errors in prediction by the algorithm can in part be explained by the lack of sufficient number of representatives for each category. For instance, the algorithm incorrectly classified polymixin as a protein synthesis inhibitor. Polymixin results in membrane disruption and the only other inhibitor in this class was daptomycin. However, daptomycin also has effects on PG biosynthesis as discussed earlier, which makes it unlikely that the fingerprints of daptomycin and polymixin will be highly similar. Since we have no other inhibitors that result in membrane disruption alone, polymixin is unlikely to be classified accurately. Our algorithm classified this as a PG synthesis inhibitor, suggesting that daptomycin's fitness profile is closer to that of PG synthesis inhibitors. It is not clear why the algorithm is unable to classify novobiocin accurately as it is a known DNA replication inhibitor. The differences in the mode of killing for novobiocin relative to the quinolones, discussed above, might generate a fitness profile that is dissimilar to those of the quinolones. This could be resolved if more inhibitors whose mode of killing is similar to novobiocin's are included. The algorithm is also unable to classify targocil, bacitracin, and lysobactin accurately. The inclusion of the lower concentration of WTI-11 into a separate "WTA export inhibitor" class, will likely

enable the algorithm to classify targocil correctly into this class. Before the incorrect classification of these antibiotics including lysobactin and bacitracin can be addressed, it would be beneficial to first test the algorithm on fitness profiles generated under more selective treatment conditions, and then obtain biological replicate data to establish that experimental conditions such as concentrations tested being too low or the signature being limited by the fewer number of generations accessible in the small culture volume, do not contribute to the dissimilar fitness profile.

The algorithm could also be optimized by modifying the classification of antibiotics. Bacitracin, fosfomicin, targocil and WTI-11 all deplete lipid II: bacitracin by preventing the recycling of the carrier lipid and therefore the de-novo synthesis of lipid II, fosfomicin by preventing its synthesis, and targocil and WTI-II by sequestering the lipid carrier, preventing its use in PG synthesis [93]. Although they deplete lipid II by different mechanisms of action, classifying bacitracin, fosfomicin, targocil, and WTI-11 into one class, may improve our classification of antibiotics that inhibit PG synthesis by depleting lipid II. The algorithm might also be made more robust by using data from all concentrations of a compound tested so that concentration dependence of classification can be minimized.

Nevertheless, the algorithm correctly placed an antibiotic into the class of its known mechanism of action 68% of the time. Compared with another recently published method, this algorithm performs better. SONAR^G which integrates an antibiotic's synthetic lethal pairs with a genetic interaction network, a system developed for yeast, was able to predict the target of their test compounds 16 out of 27 times, which is a success rate of 59% [512].

4.5 Predicting the mechanism of action of an unknown compound

We next posed the question of whether we can use this algorithm to predict the mechanism of action of an unknown antibiotic. For this we used a series of natural product compounds in the same structural class called WAP compounds (WAP1, WAP2, WAP3), obtained from a collaboration with Dr. Rolf Muller's lab at the Helmholtz Institute for Pharmaceutical Research. We profiled all three of these compounds as they are structurally related compounds, the likelihood that they hit the same target is high and the combined probability of an error by the predictive algorithm will be low. The WAP compounds are natural cyclic-peptide compounds and are therefore broadly in the same structural class as ramoplanin, vancomycin and lysobactin. Relatively little is known about these compounds, except that one related compound, WAP8294A2, is in phase I/II clinical trials as an anti-MRSA compound. Cardiolipin and phosphatidylglycerol are known to antagonize its effects, and it has been suggested that it causes membrane damage [513-515]. These compounds cause rapid lysis of *S. aureus* like lysobactin and ramoplanin. Tn-Seq on the transposon library treated with these compounds and subsequent analysis by the K-nearest neighbors algorithm classified the higher concentrations of WAP2 and WAP3 as PG synthesis inhibitors and WAP1 as Lipid II binding, in the same class as vancomycin and ramoplanin.

Assays conducted by Dr. Wonsik Lee indicate that WAP1 binds lipid II in a ratio of 2:1 inhibiting the processing of lipid II by PBP2. In this assay, purified PBP2 is incubated with different amounts of native lipid II, biotinylated-D-lysine, and the compound. The polymerized product is visualized as laddering in a western blot using

streptavidin-HRP conjugate (Fig. 4.3) [516]. These results confirm that as predicted by the K-nearest neighbors algorithm, WAP1 is a lipid II binding inhibitor.

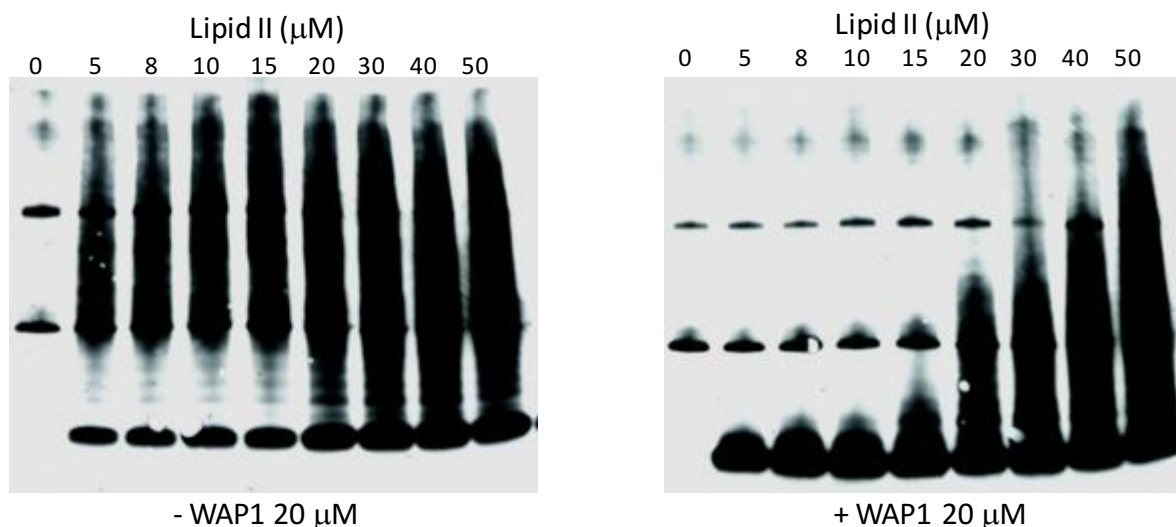


Figure 4.3: WAP1 binds to lipid II inhibiting its polymerization by PBP2. The transpeptidase domain of PBP2 incorporates biotinylated-D-lysine into PG polymers produced from lipid II by its transglycosylase domain. The inhibition of this activity observed by addition of WAP1 suggests that WAP1 is binding to lipid II.

4.6: General discussions on approaches to optimize Tn-Seq based data analysis

In the previous chapter, we discussed various aspects of treatment conditions can be optimized to obtain good quality data sets. In this section, we will discuss ways in which the K-nearest neighbors algorithm can be made more robust and a possible approach to identify more significant hits from Tn-Seq data.

Screening additional compounds will make the K-nearest neighbors algorithm more robust: We showed that the K-nearest neighbors algorithm was able to accurately predict mechanisms of action 68% of the time. Apart from optimizing treatment conditions to obtain equivalent selective pressures across antibiotics and incorporating

data from all concentrations of antibiotics tested to reduce concentration dependence of the algorithm, testing additional compounds to increase representation of unique modes of action might improve the accuracy of the predictions by the algorithm. This will be particularly useful in situations in which compounds exert two different effects on their fitness profiles. For instance, in the case of gentamicin, we found that the inactivation of the oxidative phosphorylation pathway is highly protective. This can mask the fitness profiles that would originate purely from inhibition of protein synthesis by gentamicin, making it difficult for the algorithm to classify gentamicin as a protein synthesis inhibitor. This can, however, be overcome if more compounds which have the same effects on the cell are profiled. For example, if we perform Tn-Seq on other aminoglycosides, we would expect that they would cluster together with gentamicin as they also use the oxidative phosphorylation pathway to enter the cell and inhibit protein synthesis by targeting the ribosome [425]. Polymixin is another antibiotic which would benefit from having fitness profiles of other membrane damaging antibiotics to compare with. The significant hits (p-value <0.05) of polymixin includes *mprF* and the *graXRS/vraFG* operon: reads mapping to these genes were depleted under polymixin treatment. It is known that these factors contribute to resistance to polymixin [35], suggesting that we are able to identify factors that are relevant to the activity of the antibiotic, but as discussed above, we are unable to correctly classify this antibiotic as a membrane damaging agent because the only other membrane damaging agent is daptomycin, which also inhibits PG synthesis. We can increase the scope of this algorithm by profiling more diverse compounds.

Increasing the number of reads in each sample can improve significance of depletion and enrichment fold changes in each gene: The power of next generation sequencing lies in its ability to generate a large number of reads per sample, allowing greater coverage of each gene. Santiago *et al.* reported the construction and characterization of the ultra-high density transposon library used in these experiments [392]. Combined data from sequencing two biological replicates resulted in 23,366,355 reads from 694,755 insertion sites. This library multiplexes six different transposon constructs: four constructs containing outward facing promoters (P_{pen} , P_{cap} , P_{tuf} , P_{erm}), a construct with promoters in both directions (P_{dual}), and an inactivation construct. The number of reads are consequently split among these six different transposon constructs, resulting in only 5,126,052 reads due to the inactivation construct, approximately a fifth of the total number of reads [392]. All our above analyses considered only inactivation constructs, restricting the number of reads used in the analysis to a fraction of that obtained during Illumina sequencing.

Including outward-facing promoter constructs in the library is very useful when looking for genes which are upregulated in the library. Such a strategy can be employed to identify the target of a compound, or to identify resistance mechanism that arise from upregulation of specific genes, and not their inactivation. These constructs have been used to identify several known and unknown mechanisms of resistance for many of the antibiotics discussed here including MurJ upregulation under DMPI treatment and MprF upregulation under daptomycin treatment .

However, outward-facing promoter insertions in one gene need not always upregulate a neighboring gene. Whether or not an insertion of a promoter construct will

be considered as upregulating a neighboring gene depends on the number of insertions in a particular orientation (Fig. 4.4). If a majority of insertions are in the same orientation as the direction of transcription of a neighboring gene, then the insertions are considered to be upregulating a neighboring gene (Fig. 4.4 vi). If on the other hand, there is no preference in orientation of the insertions, then it is unlikely that the insertions are preferentially upregulating a gene (Fig. 4.4 vii). In fact, in this scenario, it is likely that these insertions are acting like the inactivation constructs, interrupting the activity of the gene into which they insert. Moreover, even if the majority of insertions are in the same orientation, the gene into which they insert could still be inactivated. Therefore, it should be possible to include reads from all these constructs in our analysis (Fig. 4.4).

The concern in including reads from all constructs is the inability to distinguish between scenarios IV and V in Fig. 4.4. If the enrichment of insertions in a particular gene is primarily due to outward facing promoters which upregulate downstream genes, then we cannot be sure if the increase in fitness is due to upregulation of the neighboring gene or due to inactivation of the gene in question. Evaluating the promoter data and inactivation data independently, prior to pooling together, will allow us to distinguish between these two scenarios.

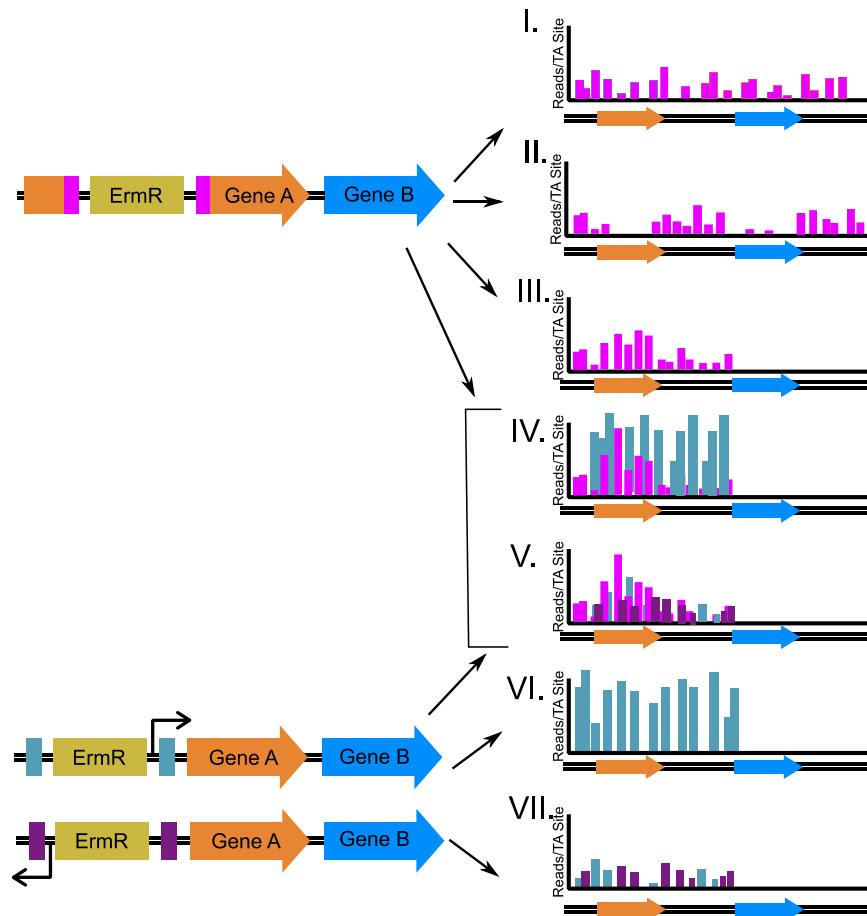


Figure 4.4. Pooling together reads from inactivation and outward facing promoter constructs can improve significance of hits identified. This figure shows the possible situations that can arise due to insertions from inactivation and outward facing promoter constructs. Two neighboring genes A and B in a treated sample are considered. The transposon construct is represented with an erythromycin resistance cassette flanked by colored bands to indicate the nature of the transposon construct - inactivation (pink), outward facing promoter oriented towards gene B (blue) and an outward facing promoter oriented away from gene B (purple). Bars represent the reads in each TA site. Scenarios I, II and III consider only inactivation constructs. (I) A roughly equal distribution of inactivation insertions and number of reads across the two genes indicate that neither of these genes are affected. (II) Both genes have fewer reads

(Continued) mapping to them indicating that these have a fitness defect (III) While gene A has an increase in number of reads, indicating a fitness advantage, gene B has fewer number of reads, indicating a fitness defect. (VI) Gene A and the non-coding region before gene B have a large number of outward facing promoter insertions, indicating that gene B is upregulated. With this high number of insertions, it is likely that gene A is inactivated. (VII) Gene A and the non-coding region before gene B have promoter insertions in both directions, indicating that gene B is unlikely to be upregulated. When reads from promoter data and inactivation constructs are compiled (IV and V), gene A has a large number of reads due to insertions. In comparison to IV and V, enrichment in gene A in scenario III might not be statistically significant due to the fewer number of reads, allowing gene A to be missed as a factor contributing to resistance.

We showed, using two examples, that using reads from all constructs results in lower p-values for hits than obtained when using only blunt inactivation constructs. This results in identification of a larger number of significant genes (Fig. 4.5). Although the fold changes were not dramatically changed when using all constructs or inactivation constructs only, the p-values were very different. For instance, *mprF* (SAOUHSC_01359) which is a known factor contributing to bacitracin resistance [517], was identified as a significant hit both when using only inactivation constructs and when using all constructs, but the p-values (3.93×10^{-18} and 1.48×10^{-39} respectively) are dramatically lower when reads from all constructs are considered. Furthermore, we were able to identify additional significant hits using reads from all constructs, which did

not meet the significance cut-off when using only inactivation constructs. These include *fmtA* (SAOUHSC_00998) and *vraT* (SAOUHSC_02100) under bacitracin treatment, and *mprF* (SAOUHSC_01359), *pbp4* (SAOUHSC_00646), SAOUHSC_01025 and SAOUHSC_01050 under oxacillin treatment. Several of these have been suggested to contribute to resistance to the respective antibiotics previously [24, 357, 441], and we validated above that SAOUHSC_01025 and SAOUHSC_01050 do indeed contribute to oxacillin resistance. This implies that we were able to identify relevant factors as significant by using data from all constructs, which would otherwise have been considered insignificant based on statistical analysis of inactivation constructs alone.

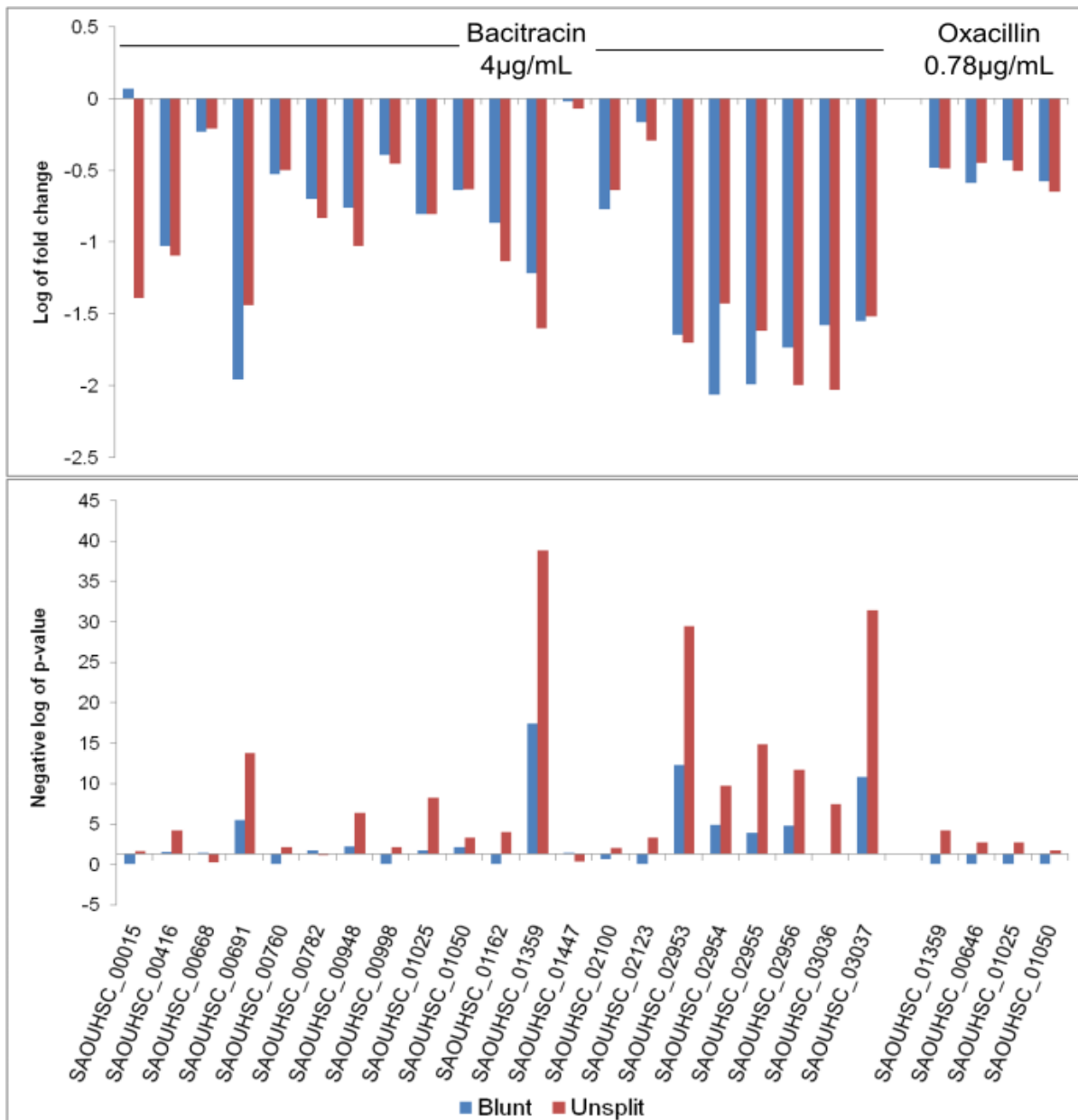


Figure 4.5: Compiling reads from all constructs together resulted in lower p-values and more genes that meet the significance cut off. A cumulative list of significant genes (p-value <0.05) resulting from analysis using reads due to all six constructs (unsplit) and reads due to only (Continued) inactivation constructs (blunt) are shown here. Two samples are considered as an example: bacitracin treated at 4µg/mL

(Continued) and oxacillin treated at 0.78 μ g/mL. Fold changes in reads in the treated sample relative to the untreated control are shown on a log scale (top panel) and p-values corrected for multiple hypothesis testing are shown on a negative log scale (bottom panel). Since p-values are on a negative log scale, a larger value corresponds to a lower p-value. The bars that fall below the horizontal axis are those with p-values >0.05, indicating that these genes were not picked up as significant under the relevant condition. Analysis using unsplit data allows the identification of a larger number of significant genes in both examples.

For future studies, compiled reads from all six constructs can be analyzed in addition to inactivation only constructs to identify significant hits. Furthermore, libraries can be constructed to better align with the goal of the experiment. For instance, if the goal is to study intrinsic resistance factors or identify factors that are synthetically lethal with a mutant, then a library constructed only with inactivation constructs can be more beneficial than a library with all six transposon constructs.

4.7 Methods:

Hierarchical Clustering: Hierarchical clustering was performed using the statistical programming language, R, and visualized using the gplots library. The spearman method was used to measure correlation and complete-linkage clustering to measure distance. We used the unique set of genes which had the largest 99th percentile of the data and smallest changes 1st percentile compared to the control to decrease the

amount of noise in the data, and we used the “fitness value” (described in the previous chapter) for each gene to perform the comparison.

K-Nearest Neighbors Algorithm for predicting mechanism of action: The sci-kit learn Python library was used for this analysis [482]. Normalized fitness values were calculated as described above and the top and bottom 25% of genes were used here. A training set was created with known antibiotics classified into nine separate classes based on hierarchical clustering and unsupervised K-nearest neighbors algorithm. This set is used to train a supervised K-nearest neighbors classifier. We use the Minkowski distance metric, a step size = 0.2, and each antibiotic was weighted uniformly. Two neighbors were used to predict the mechanism of an unknown antibiotic. With a larger training data set, this value could be increased which could result in more accurate predictions.

Chapter 5: Compounds against which inactivation of *mprF* is protective

5.1 Summary

In this chapter, we describe the discovery of a β -lactam potentiator and show that inactivating *mprF* suppresses its activity. MprF is a known intrinsic resistance factor in *S. aureus* and no compounds that select for its inactivation have previously been described. We have discovered other compounds that are lethal to wildtype *S. aureus* but have no activity against a $\Delta mprF$ strain by screening a library of *S. aureus* lethals against both strains. These compounds could provide new insights into the bacterial cell wall, but their targets must be identified. We have established an approach to identify these targets that exploits synthetic lethality to select against inactivating *mprF* mutations. Increased *mprF* activity is important for clinical daptomycin resistance, and inactivation of *mprF* strongly sensitizes *S. aureus* to daptomycin (and several other antibiotics). The discovery of compounds that select for *mprF* inactivation suggests the possibility that these compounds can be combined to delay the development of resistance.

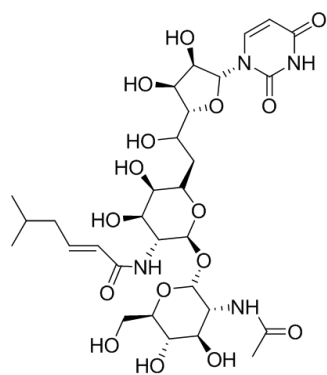
5.2 Targeting intrinsic resistance factors

In the previous chapters we have discussed several examples of intrinsic resistance factors that are important for withstanding antibiotics. Targeting intrinsic resistance factors has been explored as an approach to potentiate (*i.e.*, increase the potency of) existing antibiotics in several studies [518-524]. Potentiators may be particularly useful for overcoming β -lactam resistance in MRSA strains. The β -lactam

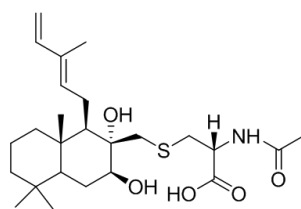
class of antibiotics is widely used to treat bacterial infections. With the rise of resistance to β -lactams, there is an urgent need to look for ways to extend the use of these antibiotics and combat resistance. A successful clinical example of a β -lactam potentiator/ β -lactam combination is Augmentin. Augmentin contains a β -lactam, amoxicillin, and a β -lactamase inhibitor, clavulanic acid, and it was developed to overcome resistance due to β -lactamase-mediated degradation of β -lactams, which is the dominant mechanism of resistance in many organisms [341-343]. β -lactamase inhibitors have been developed for use in combination with β -lactams to treat both Gram-positive and Gram-negative infections [525-529]. Unfortunately, β -lactamase/ β -lactam combinations are not effective against MRSA because clinical resistance is not primarily due to β -lactamases, but due to the acquired resistance protein PBP2A [95, 100, 346].

There are several intrinsic resistance factors that contribute to β -lactam resistance in MRSA, and all of these are possible targets for compounds that overcome β -lactam resistance. Only a few of these targets have been explored in the context of β -lactam potentiation. TarO, which catalyzes the first step in WTA biosynthesis, is among these targets; and inhibitors of TarO have been shown to synergize with β -lactams in MRSA (Fig. 5.1) [200, 530, 531]. Some compounds that inhibit lethal targets in the PG biosynthetic pathway have also been identified as β -lactam potentiators, but because these compounds are lethal on their own, they belong in a different category from compounds that inhibit non-essential targets. For example, the Lipid II flippase inhibitors, DMPI and CDFI, have been described as β -lactam potentiators [353], but also have antibacterial activity. Inhibitors of FtsZ, the essential protein that forms the Z-ring

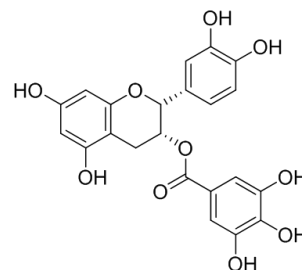
during cell division, have also been identified as potentiators of β -lactams [532, 533]. Cyslabdan, a small molecule produced by *Streptomyces* (Fig. 5.1), was shown to potentiate β -lactams by inhibiting FemA and preventing the synthesis of the pentaglycine bridge [534]. MRSA strains lacking FemA are viable and capable of forming crosslinked PG from cell wall precursors containing monoglycine rather than pentaglycine, but these strains have growth defects [535]. It has been suggested that *femA* deletion mutants are sensitive to β -lactams because PBP2A is unable to crosslink stem peptides containing only monoglycine, however the substrate specificity of PBP2A has not yet been established. Apart from these examples, several natural compounds that potentiate β -lactams have been characterized, but their targets have not been elucidated [536-539]. One of these, epicatechin gallate, a component of green tea, is proposed to insert into the membrane, release LTA, and delocalize PG synthesis machinery [540-542]. While β -lactam potentiators for MRSA infections have yet to reach the clinic, they can be useful tool compounds to explore the impact of inhibiting their targets on cell physiology. Tunicamycin, for example, has been useful in a number of studies to explore the effects of preventing WTA synthesis [204, 367].



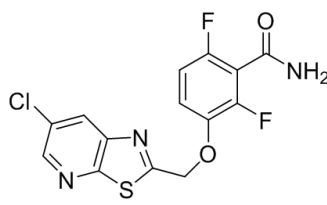
Tunicamycin
TarO inhibitor



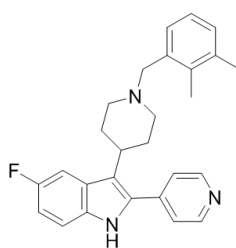
Cyslabdan
FemA inhibitor



Epicatechin Gallate
Delocalization of PG machinery



PC190723
FtsZ inhibitor



DMPI
MurJ inhibitor

Figure 5.1: Examples of compounds that potentiate the activity of β -lactams

We report here the identification of a β -lactam potentiator in a high-throughput screen of 43,648 compounds. We found that inactivating *mprF* confers a large fitness advantage in the presence of the compound. We have also identified structurally related compounds by screening a \sim 600-compound library of lethal anti-Staphylococcal agents against a $\Delta mprF$ strain. Finally, we have developed a strategy to identify the targets of these compounds, but have not yet validated it.

5.3 High-throughput screening for β -lactam potentiators

We set out to identify compounds that would sensitize MRSA strains to β -lactams using a cell-based high-throughput screening approach. I carried out a high-throughput

screen in collaboration with Dr. Jennifer Campbell, a former post-doc in the Walker Lab. The screen design is shown in table 5.1. Compounds were screened against a MRSA strain under two conditions: in the absence of a β -lactam and in the presence of a sub-minimum inhibitory concentration (sub-MIC) of a β -lactam. At the concentration of β -lactam used, the MRSA strain will grow unless sensitized to the β -lactam by a potentiator. Screening two conditions in parallel allows us to weed out those small molecules that are toxic to MRSA on their own.

Table 5.1: Predicted outcomes for small molecules screened

	MRSA + β -lactam	MRSA - β -lactam
No Effect	High OD600	High OD600
Toxic small molecule	Low OD600	Low OD600
β -lactam potentiator targeting non-essential factors	Low OD600	High OD600

Screening conditions:

The appropriate concentration of β -lactam was selected as the concentration at which a Z' score >0.5 was obtained under test conditions (see Methods). Z' is an indicator of the robustness of the assay and a score >0.5 is considered to be suitable for high-throughput screening [543]. Initially, we screened 23,232 compounds against MW2, a community acquired MRSA strain [458], using a sub-MIC concentration of methicillin. In the middle of the screen, we decided to change the screening strain and the β -lactam. We changed the strain because we were displeased with the high level of variability in the screen, which we ascribed to the fact that MW2 shows heterogeneous

resistance. We chose a hospital-acquired clinical strain, 1784A, as an alternative because we found that it displayed more homogenous resistance to β -lactams, and the Z' score improved. Because 1784A had not previously been sequenced or characterized in any way, we asked Dr. Veronica Kos in Dr. Michael Gilmore's lab to sequence the strain. The sequence data showed that 1784A belongs to the multilocus sequence type 8 (MLST 8) so it has the same sequence type as strain Newman, NCTC8325, and USA300 (which is the epidemic community-acquired MRSA strain). An additional 20,416 compounds were screening against 1784A using a sub-MIC concentration of oxacillin. All 43,648 compounds screened were included in our analysis to identify hits.

Classification of hits:

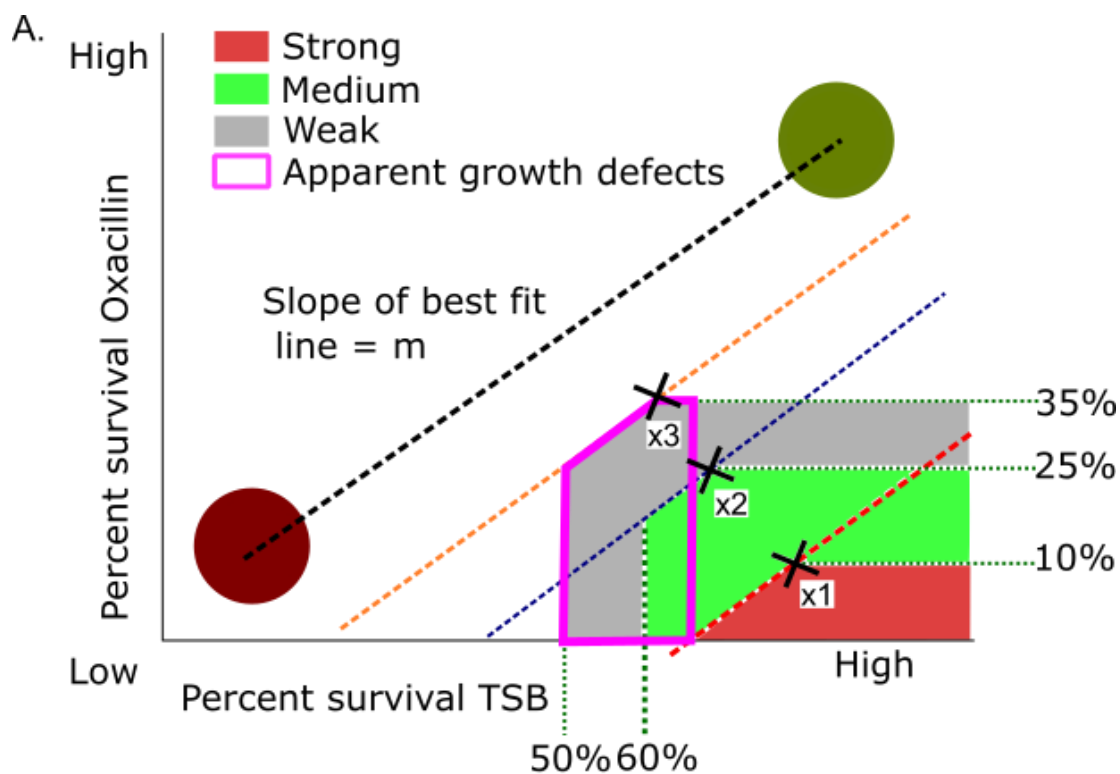
We converted end-point OD₆₀₀ values to normalized percent survival based on the positive and negative controls (see Methods). As compounds were tested in duplicate, we had two values for each compound under each condition, and we averaged these values. We were initially interested in compounds that resulted in little to no effect on apparent survival of the wildtype strain; therefore, compounds were classified into three categories, strong, medium, and weak, based on the average percent survival in the presence and in the absence of oxacillin (Fig. 5.1A). Classifying compounds into three categories allowed us to prioritize compounds for follow-up. We found that it was not possible to categorize compounds based on strict numerical cutoffs because this approach resulted in misclassification of some compounds. For instance, a compound that results in a very high percent survival (>95%) in the absence of oxacillin

and a very low percent survival (<10%) in the presence of oxacillin, is obviously a strong hit. Likewise, a compound that results in a moderate percent survival (~80%) in the absence of oxacillin and a moderately low percent survival (20%) in the presence of oxacillin, can readily be classified in the medium category. However, classification problems arose for compounds that resulted in, for example, 85% survival in the absence of oxacillin but only 5% percent survival in the presence of oxacillin. We needed a standard approach to classify compounds that did not fit neatly into a given category.

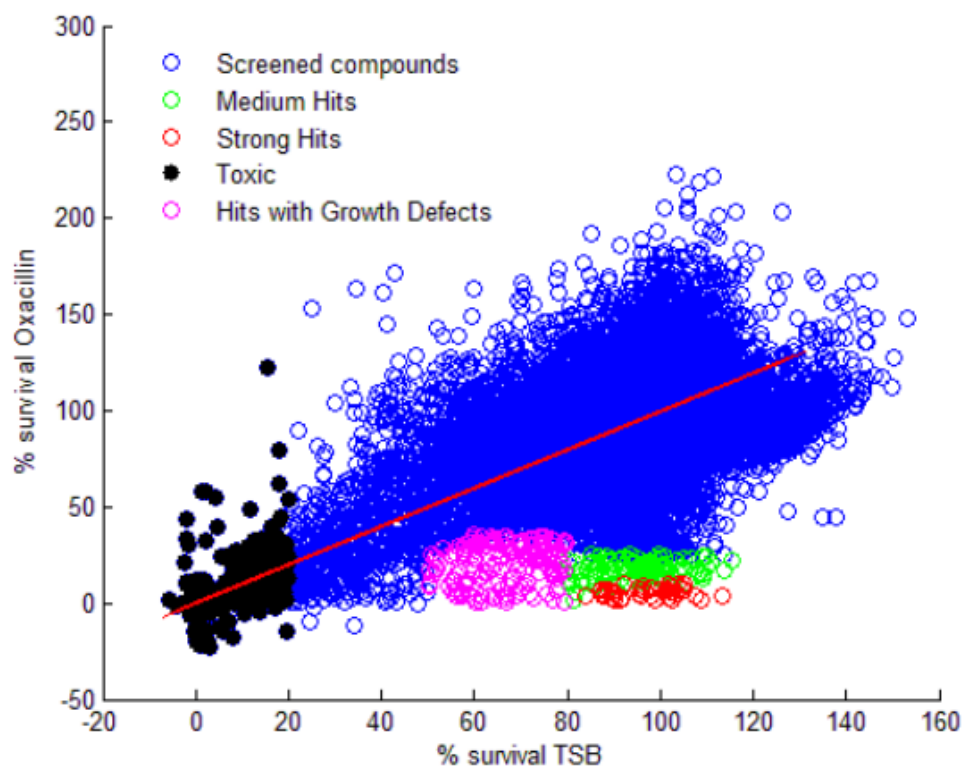
We classified compounds as follows: First, the best fit line between the percent survivals of positive and negative controls was determined. The slope of this line describes how our data can vary in a best case scenario. Next, we solved for the equation $y=mx+c$ using the value for m from the slope of the best fit line. Values for y and x were specified manually. We solved for the intercept, c , to generate an equation for a line that was then used as an upper limit cut-off. Such a line was generated for each category: strong, medium and weak. All data points below these category lines, which also fell between a minimum and maximum prescribed percent survival in each condition, were assigned to that category (Fig. 5.2A). This process was applied to all the compounds screened, and compounds in each category were identified (Fig.5.2B).

Figure 5.2: Compounds were classified into three categories. (A) Schematic of algorithm used for classification. A least squares best fit line (black) was determined between positive (green circle) and negative (brown circle) controls. The slope of this line was determined. Here it is denoted as 'm'. Using this slope and manually specified percent survival values for y and x, cut-off lines with the equation $y = mx + c$ were plotted for each of the three criteria: Strong (red line), Medium (blue line) and Weak (orange line). Manually specified percent survivals are indicated as black crosses on the cut-off lines. The values used are $x_1 = 90\%$ survival in TSB (absence of oxacillin), 10% survival in the presence of oxacillin; $x_2 = 75\%$ survival in TSB, 25% survival in oxacillin; $x_3 = 60\%$ survival in TSB, 35% survival in oxacillin. These points were chosen as the outer-limits for each category. Outer-bounds were specified for these cut-off lines as we did not want to consider compounds with percent survivals in TSB below 60% for medium and strong compounds, or below 50% for weak compounds, as these compounds would be fairly lethal. Likewise, we did not want to consider compounds which resulted in a percent survival $> 35\%$ in oxacillin as these compounds are likely not potent. Therefore, while outer-bound cut-offs had to be prescribed manually, this approach enables us to capture more compounds in each criteria than using a strict percent survival cut-off would have. Another category of compounds that possibly cause growth defects (compounds causing between 50% and 80% survival in TSB) was also identified. This category will include compounds from both the medium and weak hits categories and is demarcated by a purple outline. (B) A scatter plot of the compounds screened with strong (red), medium (green) and hits with apparent growth defects (purple) is shown.

Figure 5.2 (Continued):



B.



We also wanted to capture potentiators that affected growth of the wildtype strain by inhibiting non-essential targets. Inhibition of some targets, for example, TarO or LcpA in the WTA pathway, results in reduced stationary phase density that can be mistaken for compound toxicity in a screen that uses an end-point OD₆₀₀ as the indicator of compound activity. Therefore, we also included those compounds that moderately affected apparent survival of the wildtype strain (50-80% survival in the absence β -lactam). These compounds overlapped with medium and weak hits categories (see Fig. 5.3), although it should be noted that some have β -lactam potentiation activity that would have classified them in the strong category if it were not for the reduced percent survival. We considered compounds that were in the strong and medium categories to be hits in this assay. Of the 163 compounds that possibly cause growth defects, we considered compounds that would have been classified in the strong or medium categories if it were not for the reduced survival, as hits. There were 93 hits in this category, 33 of which would have been classified in the strong category (Fig. 5.3B). Hits are provided in Appendix 2.

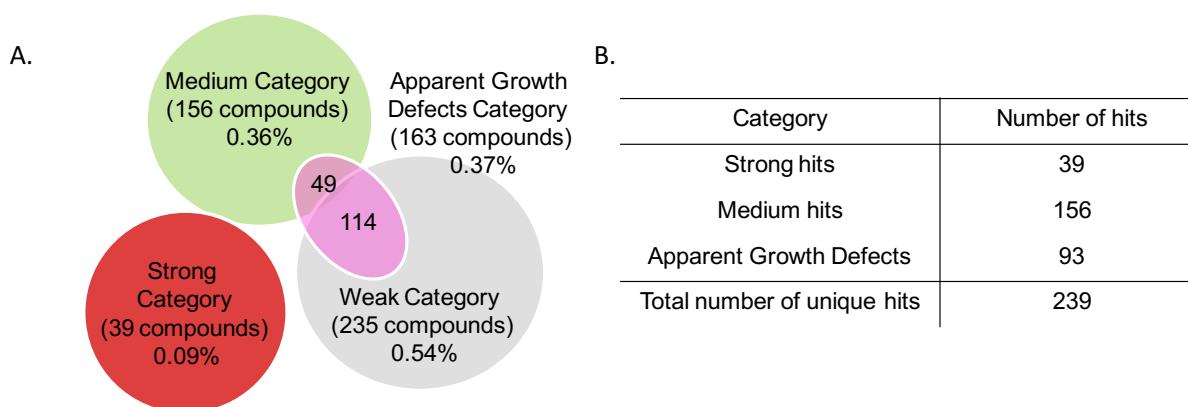


Figure 5.3: Number of compounds and hits identified in each category. (A) The number of compounds identified in each category are shown. (B) The number of those

(Continued) compounds considered as hits are shown here. If we consider all these hits, our screen had a hit rate of 0.55%. Considering the strong and medium hits only, our hit rate is 0.45%, which is in line with the typical high-throughput screening hit rate [543].

5.4 Characterization of lead compounds MR100 and MR101

We chose to focus on a subset of the strong hits that showed high potency in the screen, and we purchased eight compounds for retesting in β -lactam potentiation assays against the two screening strains, MW2 and 1784A. Four of these compounds sensitized the screening strains to oxacillin, but only three of these showed activity against at least one other MRSA strain. Of these three, two compounds were structurally related, and one analog showed superior potency and activity against all four MRSA strains tested. This compound, MR100, sensitized oxacillin in secondary dual dose response assays against community-acquired strain MW2 (USA400), and hospital acquired strains USA200, 1784A and B5340A (Fig. 5.4 A-C, and Appendix 3). We defined a minimum sensitization concentration (MSC) as the concentration of compound at which maximum reduction is observed in β -lactam MIC in that assay. The MSC of the compound varied depending on the MRSA strain tested. The lowest MSC we observed (0.39 μ g/mL or 0.74 μ M) was to 1784A, but other strains were sensitized at only slightly higher concentrations (1.5 μ g/mL). MR100 thus had excellent potency. Fold changes evaluated for these strains with dual dose response assays could be an underestimate because the lowest concentration of oxacillin tested in these assays was 3.125 μ g/mL for 1784A, MW2, and USA200 and 50 μ g/mL for B5340A. Therefore, fold

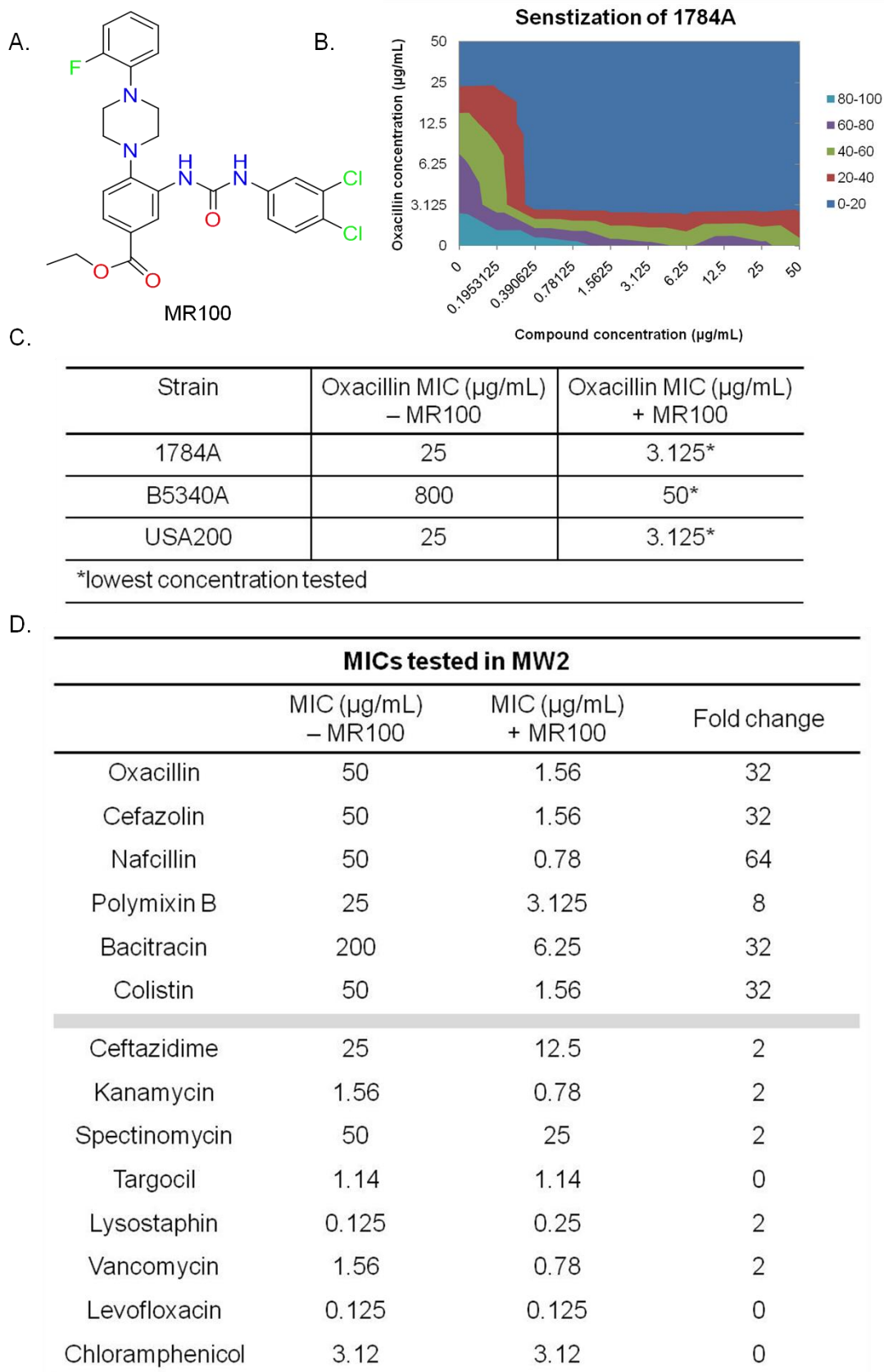
changes were not calculated for these assays. When we tested MR100 on an expanded concentration range for three other β -lactams in addition to oxacillin for sensitization in MW2, we found that MR100 sensitized MW2 to cefazolin, nafcillin and oxacillin by 32x. We did not see sensitization to ceftazidime (Fig. 5.4D). While cefazolin, nafcillin, and oxacillin are non-specific in their selectivity for PBPs [544], ceftazidime has higher binding affinity for PBP 1 and PBP 2 [545]. There is a possibility that the sensitization of β -lactams by MR100 depends on the PBP specificity of the β -lactam, but a larger panel of β -lactams must be tested in order to draw conclusions about the specificity of the sensitization by MR100.

We investigated whether MR100 also affected the MIC of other antibiotics in MRSA strains. While the compound had no effect (only a 2x change, if any) on the MIC of most antibiotics, we observed strong sensitization to bacitracin (32x), colistin (32x) and polymixin B (8x). Bacitracin forms a complex with undecaprenyl pyrophosphate and a metal ion (Zn^{2+} or Ca^{2+}), which prevents carrier lipid from being flipped back inside the cell and used to make the peptidoglycan precursor, Lipid II [93, 546]. Polymixin B and colistin are membrane damaging antibiotics. All three of the antibiotics whose activity was potentiated by MR100 function at the membrane. We considered the possibility that MR100 sensitizes to these antibiotics by reducing membrane stability. However, because the compound did not significantly sensitize to antibiotics with intracellular targets, it is unlikely that MR100 affects a target that makes the membrane generally leaky. Notably, the compound did not strongly potentiate the activity of daptomycin, which also forms a Ca^{2+} complex and interacts with the membrane [477, 478]. A full

understanding of how the compound sensitizes MRSA to bacitracin will require identifying the target.

Figure 5.4: MR100 is a potent β -lactam potentiator for numerous strains. (A) Structure of MR100. (B) A sample of the dual dose response plot for sensitization of 1784A to oxacillin. Oxacillin concentration varies along the vertical axis while MR100 concentration varies across the horizontal axis. Percent survivals are shown in different colors, with dark blue being <20% survival. In this plot, when no compound is added, the MIC of oxacillin for this strain is 25 μ g/mL, but in the presence of 0.39 μ g/mL (=0.74 μ M) the MIC of oxacillin drops to 3.12 μ g/mL, which is the lowest concentration tested in this assay. (C) The potentiation of oxacillin by this compound to various hospital acquired strains (1784A, USA200, B5340A, USA200) were determined by dual dose response assays. The MIC values in the presence and absence of MR100 are shown in the table. Dual dose response plots for all strains are shown in Appendix 3. As these assays were limited in the lowest concentration of oxacillin tested, fold changes in the MIC of oxacillin caused by the compound in these assays could be an underestimate. (D) The MIC values of a set of antibiotics of different classes were measured in the presence and absence of MR100. These MIC's were measured using MW2 in MHB2 because greater potentiation to antimicrobial peptides with this media.

Figure 5.4 (Continued):



To characterize MR100 further, we explored its effects on cells in a number of different assays. In the course of our experiments, we tested its effects on an MSSA strain, HG003, and found that it inhibited growth at concentrations greater than 6 μ g/mL (Fig. 5.5A). We initially ascribed this effect to the possibility that MSSA strains are more sensitive to this compound; however, when we subsequently tested a new batch of custom-synthesized compound, we discovered that it was not lethal against HG003 (Fig. 5.5B). This result suggested that MR100 had an impurity that inhibited growth. The resynthesized batch of the compound will henceforth be referred to as MR101. An NMR of MR101 was taken to confirm the structure of the compound (Appendix 4). We then examined MR100 with HPLC to determine whether it had impurities. HPLC characterization of MR100 revealed that it had some impurities that were not detected in MR101 (Appendix 4). We could not identify the impurities in MR100 due to the limited amounts of compound that remained, but we think an impurity likely accounts for the the lethal MSSA activity observed with this compound.

We sought to determine if any other phenotypes we had observed with MR100 were due to the impurities, so we tested MR101 for its ability to potentiate several antibiotics. We found that like MR100, MR101 sensitized MRSA strains to oxacillin, although the MSC was shifted to 1.5 μ g/mL (Fig. 5.5C and Appendix 3). Because MR101 was not toxic to MSSA strains, its sensitization profile could be evaluated against an MSSA strain. MR101 sensitized to colistin, polymixin and bacitracin in MSSA strain HG003 (Fig. 5.5 D), but we did not observe additional sensitivity to any other cell envelope or non-cell envelope antibiotics tested. It should be noted that β -lactam sensitization is not typically observed in MSSA strains, at least in end-point MIC assays.

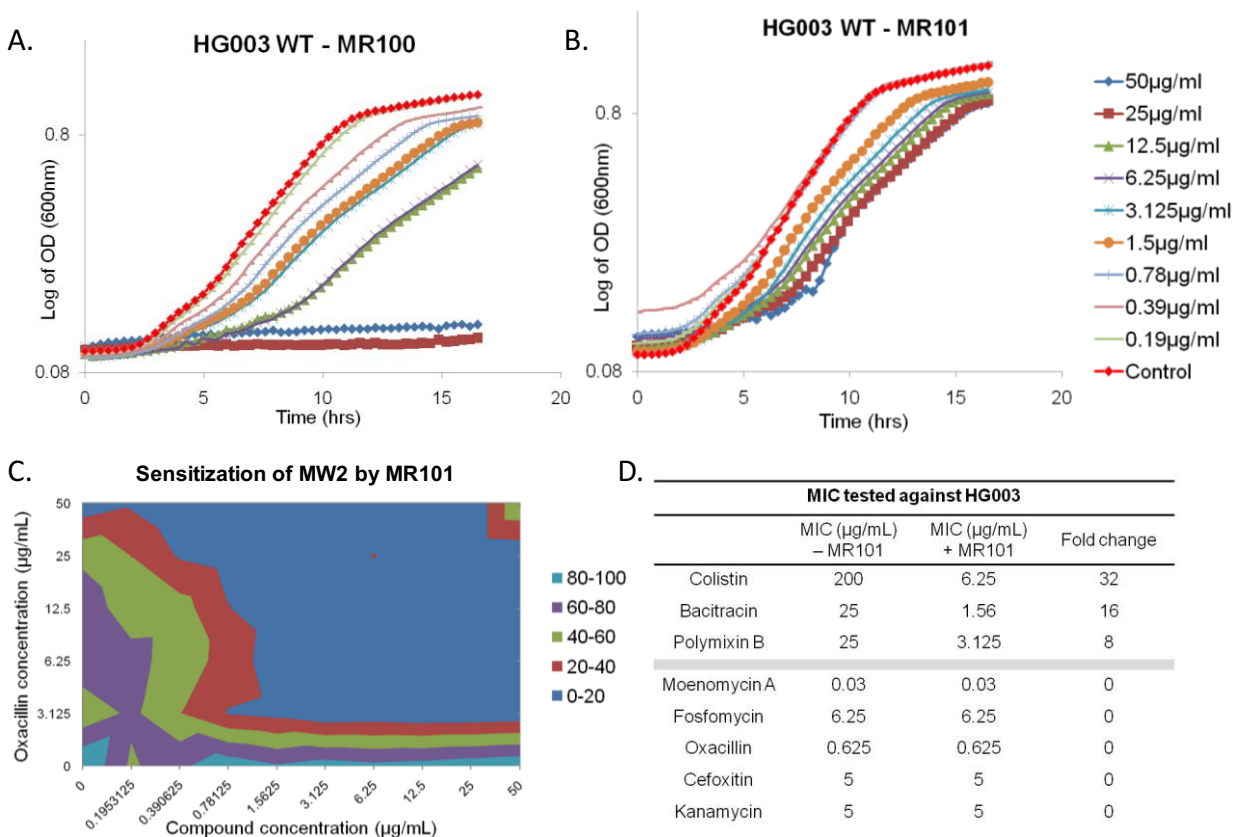


Figure 5.5: Characterization of MR101. (A) MR100 showed lethality to HG003 WT, but (B) MR101 did not show as much lethality, although some growth rate reduction was observed. (C) MR101 continued to sensitize MRSA strains to oxacillin as shown in the sample dual dose plot for MW2. Percent survivals are shown in different colors, with dark blue being <20% survival. (D) MICs for a panel of antibiotics are shown in the presence and absence of MR101. These MICs were tested against HG003. Since HG003 is an MSSA strain we do not see additional sensitization to β -lactams. We see dramatic sensitization to colistin, bacitracin, and polymixin as with MR100.

The recapitulation of all sensitization effects of MR100 by MR101 was puzzling. If the impurities in MR100 accounted for some of its biological activity, and these are no longer present in MR101, we would expect that we would not be able to observe the same sensitization effects. There are two possible interpretations: first, that there are two targets, one that is essential in MSSA strains and is targeted by the impurities, and the second that results in sensitization effects and is targeted by the main compound. The other possible interpretation is that the same impurities are also present in MR101, but are undetectable. Because the amount of impurities in MR100 was already low (see appendix 4), we cannot rule out the possibility that MR101 contains a bioactive impurity that is undetectable by HPLC. MR101 should be examined by mass-spectrometry (Selected-ion monitoring) for the presence of the impurities known to be present in MR100. It is possible that lower levels of the impurity in MR101 accounts for the reduced growth inhibition in MSSA strains by this compound compared to MR100. We wanted to determine the target(s) of MR100/MR101 because the sensitization profile suggests that it has an interesting target that we could subsequently develop pure inhibitors for.

5.5 Inactivation of *mprF* is strongly protective against MR100/MR101

To identify the target of our compounds, we first tried raising resistant mutants in a MRSA strain on agar plates containing oxacillin and MR100. (These experiments were done prior to our discovery that MR100 contained impurities). However, substantially higher concentrations of MR100 were required on plates than in liquid, and the colonies isolated did not prove resistant when tested in liquid cultures. Other researchers have observed similar problems when raising resistant mutants to

potentiators in combination with β -lactams (Professor Xiang Wang, University of Colorado, Boulder, personal communication). This problem could be due to changes in expression levels of genes that constitute a transient stress response. Another concern with raising resistant mutants to a combination of compounds was that we could obtain resistant mutants to either compound. It is possible that a majority of the mutations isolated from a combination with oxacillin would be protective to oxacillin but not the compound of interest. Another lab member, Marina Santiago, found this to be the case when she tested a combination of epicatechin gallate and oxacillin in Tn-Seq, and found all the mutants had previously described β -lactam resistance mutations.

For these reasons, we decided to take advantage of transposon-based methods to gain insight into the target of MR100/MR101. Tn-seq can help in identifying genes whose inactivation sensitizes to the compound. Inactivation mutants of these genes could then be used to raise resistant mutants to this compound, in a similar approach to that described in Pasquina *et al.* [367]. We initially used MR100 in Tn-Seq experiments, but repeated the experiments with MR101. Data was analyzed as described in previous chapters. The full list of significant hits for both compounds is provided in Appendix 5.

Tn-Seq with MR100 and MR101 showed that reads mapping to *mprF* were significantly enriched relative to the untreated control at all concentrations of the compound, suggesting that inactivation of *mprF* provided a strong fitness advantage in the presence of the compound (Fig. 5.8A). In fact, reads mapping to *mprF* at 12.5 μ g/mL, the highest concentration of MR100 tested, was almost 1000x greater than in the control. We determined manually that insertions due to overexpression and inactivation constructs were distributed throughout the length of *mprF*, implying they are all resulting in inactivation phenotypes. There was a concentration dependent increase

in the fold change of reads mapping to *mprF* in treated samples relative to untreated samples (Fig. 5.6B). Furthermore, at 12.5µg/mL, 90% of the total number of reads in that sample were due to insertions in *mprF* (Fig. 5.6C). In addition, reads due to insertions in components of the multi-component sensing system that regulates *mprF* (*graRS/vraFG*) were also highly enriched relative to untreated control in samples treated with lower concentrations of MR100 (Fig 5.6A). Enrichment in reads mapping to *mprF*, and components of *graRS/vraFG* was also observed in the presence of MR101, although the fold change in reads was lower, consistent with reduced compound toxicity and therefore, reduced selective pressure due to MR101 (Fig. 5.6A). In fact, *mprF* remained among the top three most enriched hits for MR101 under both treatment conditions. These results strongly suggested that inactivation of *mprF* is a major resistance mechanism to MR100/MR101.

We validated that inactivation of *mprF* is indeed protective by evaluating the growth of a $\Delta mprF$ strain in the presence of MR100 and MR101. HG003 $\Delta mprF$ was independently constructed by Dr. Ting Pang, a post-doc in the Bernhardt Lab, and Dr. Samir Moussa, a post-doc in the Walker Lab. We found that as predicted by transposon results, $\Delta mprF$ is protective against all concentrations of MR100 and MR101 (Fig. 5.6D). Due to the greater lethality of MR100, the protective effect of $\Delta mprF$ is more dramatic than in MR101.

Figure 5.6: Inactivation of *mprF* has a fitness advantage in the presence of MR100

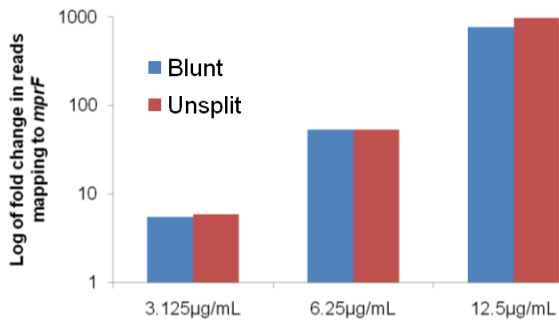
and MR101. (A) Fold changes in reads mapping to *mprF* and the multi-component sensing system *graRS/vraFG* were significantly (corrected p-value <0.05) enriched under the lower concentrations of treatment with MR100 and under treatment with MR101. The table shows results obtained when considering all constructs (B) Log of fold change of reads mapping to *mprF* in treated conditions relative to untreated control for each concentration of MR100 is shown for both inactivation constructs only (blunt) and for all constructs combined (Unsplit). Reads due to insertions in *mprF* are dramatically enriched in the presence of compound relative to the control. At 12.5µg/mL, the fold change in reads mapping to *mprF* was 987. There is a concentration dependent increase in fold change of reads mapping to *mprF* (C) As the concentration at which the sample is treated increases, reads due to insertions in *mprF* account for increasing percentages of total reads in the respective sample. At 12.5µg/mL, reads due to insertions in *mprF* account for almost all the reads (90%) in the sample. (D) Growth curves indicate that HG003 $\Delta mprF$ is more resistant than WT to both MR100 and MR101.

Figure 5.6 (Continued):

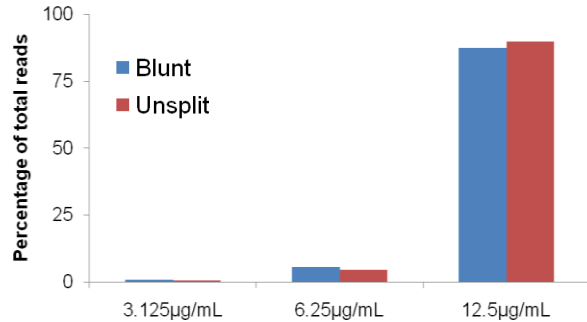
A.

		MR100 6.25µg/mL		MR101 12.5µg/mL		MR101 25µg/mL	
		Fold change	P-value	Fold change	P-value	Fold change	P-value
SAOUHSC_01359	<i>mprF</i>	53.02441	8.68E-26	7.83721	1.35E-17	17.43274	1.28E-26
SAOUHSC_00665	<i>graR</i>	38.94515	2.40E-05	6.31894	0.00421	10.67862	3.12E-05
SAOUHSC_00667	<i>vraF</i>	36.68268	1.34E-06	6.65414	0.00097	11.93893	6.22E-06
SAOUHSC_00668	<i>vraG</i>	35.98589	1.33E-17	6.76380	1.87E-14	12.42393	6.26E-24
SAOUHSC_00666	<i>graS</i>	33.25315	1.72E-09	7.36648	5.91E-06	13.85491	2.46E-09

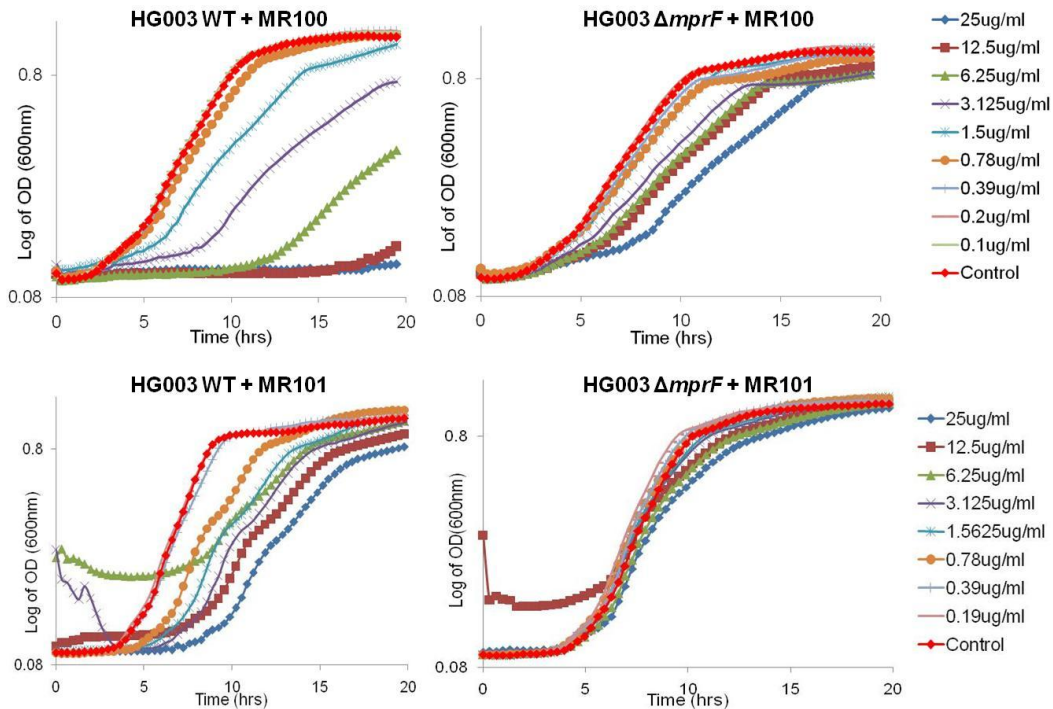
B.



C.



D.



5.6 Identifying other compounds that are also protected by the inactivation of *mprF*

The finding that inactivation of *mprF* was so protective to a compound was surprising because, as discussed in previous chapters, *mprF* is a major intrinsic resistance factor for antibiotics of many different classes including cationic antimicrobial peptides, cationic aminoglycosides, bacitracin and oxacillin [23, 24, 517]. We also identified in our Tn-Seq analysis of PG biosynthesis inhibitors that inactivation of *mprF* had reduced fitness in the presence of cell-wall active antibiotics like ramoplanin and vancomycin. Inactivation of *mprF* also sensitizes to daptomycin, and increased *mprF* activity is observed in clinical resistance to daptomycin, the antibiotic of last resort in treating MRSA infections [25, 27, 28, 36, 226, 547, 548]. Given that *mprF* inactivation potentiates the activity of so many compounds, and so far no cases have been reported where inactivation of *mprF* suppresses bioactivity, the compounds described here might belong to a new class of inhibitors. Inhibitors of previously unexplored targets would have considerable value as tool compounds to further investigate *S. aureus* biology, and may be useful in a clinical setting. For example, compounds that select for inactivation of *mprF*, could be useful in delaying *mprF*-mediated resistance to daptomycin. The merits of such compounds in daptomycin combination therapies still have to be evaluated, but the possibility that such a compound combination could be useful is exciting.

We wondered if we could find other compounds against which *mprF* inactivation mutants are protective. Leigh Matano and Heidi Morris carried out a ~250,000 compound screen against an MSSA strain of *S. aureus* and identified 600 compounds

that killed WT *S. aureus*. Those compounds were then screened against a $\Delta mprF$ strain in order to identify those compounds that kill WT but not $\Delta mprF$. Three confirmed lethal compounds that were inactive against the $\Delta mprF$ strain were identified. Two of the three compounds had structural similarities to MR100/MR101 (Fig. 5.7). 1838 M10 and 1841 C20 both have a core urea group with halogen substituted benzene rings like MR101. 1841 C20 also has the presence of the aromatic group substituted with an ester moiety, which is present in MR101. The structural similarity suggests that these compounds could share the same target as MR100/MR101. It was exciting to find that other compounds against which the inactivation of *mprF* is protective could be identified. Access to other such compounds increases the number of tool compounds we can use to study the effects of *mprF* on the cell wall. Henceforth, we will refer to compounds against which *mprF* inactivation is protective as BSIM compounds (**B**ioactivity **S**uppressed by Inactivation of *mprF*).

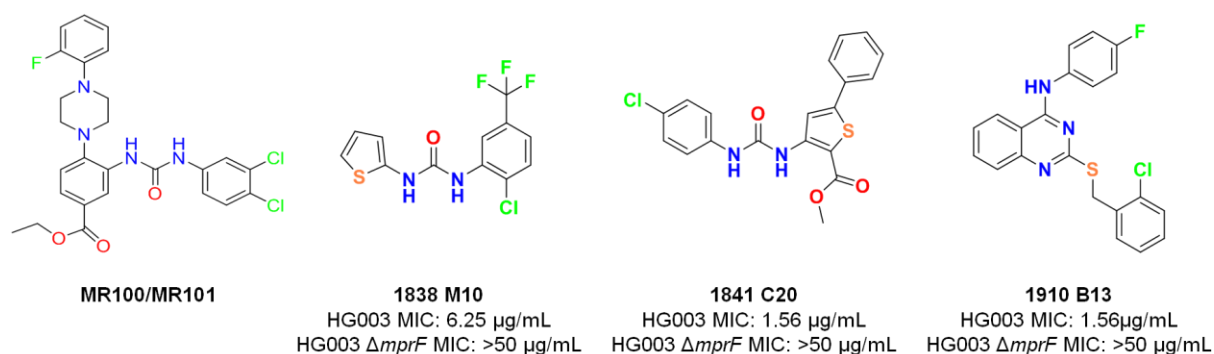


Figure 5.7: Structures of three lethal compounds whose bioactivity is suppressed by *mprF* inactivation (BSIM compounds). Two of the three compounds, 1838 M10 and 1841 C20, are structurally similar to MR100/MR101.

5.7 Strategy for target identification

The identification of other BSIM compounds spurred our interest in identifying the targets of these compounds. BSIM compounds posed an intriguing problem: how do we identify the target of a compound when any attempts to raise resistant mutants in a wildtype strain select for *mprF* inactivation mutants. When we mapped mutants isolated from screening a transposon library on agar plates containing MR100, all of the mapped mutants contained insertions in *mprF* (see Appendix 5). We needed a strategy to identify the resistant mutants to our BSIM compounds that are not *mprF* nulls.

To counter-select against *mprF* null mutants, we needed to identify a condition under which inactivation of *mprF* is not favored. As mentioned above, inactivation of *mprF* sensitizes to several antibiotics and we could use a combination of one of these antibiotics, like bacitracin, with MR100 and attempt to raise resistant mutants. However, as discussed previously, such compound combinations could result in selecting for upregulation of stress responses, or mutations that only protect from bacitracin, and fail to yield target mutations.

In order to increase the chances of finding target mutations, we sought to identify genes that cause lethality when both the gene (say, gene X) and *mprF* are inactivated, that is, genes that are synthetically lethal with *mprF*. In the case of the lethal compounds identified above, resistant mutants can directly be raised on a $\Delta geneX$ background (Fig. 5.8), once it is confirmed that $\Delta geneX$ is not protective against the compound.

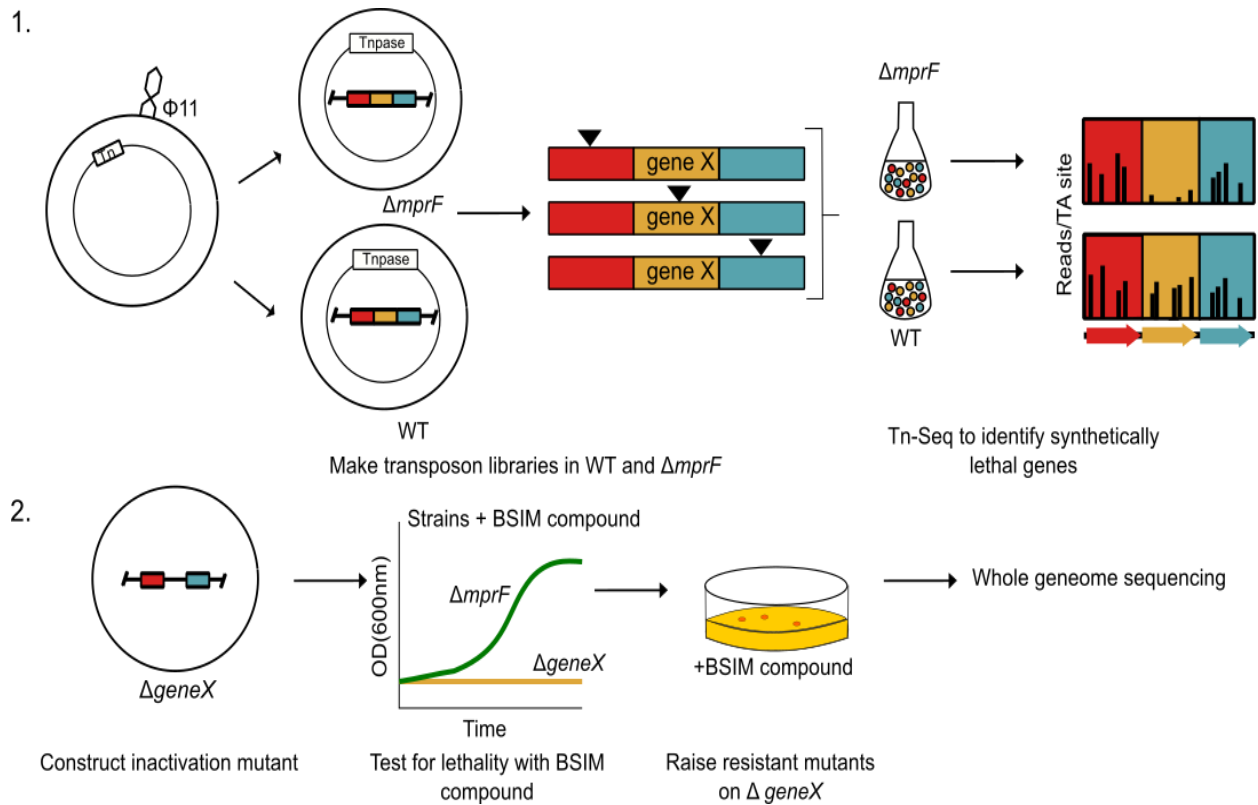


Figure 5.8: Strategy to identify resistant mutants to BSIM compounds that are not *mprF* nulls. This strategy requires two steps: (1) A transposon library in $\Delta mprF$ can be constructed using the phage-based transposition system, where donor strains with the transposon construct is infected with phage. Phage lysates with packaged transposon constructs can then be used to move the transposon to a recipient strain containing a transposase plasmid [392]. This library can be subjected to Tn-Seq and compared with Tn-Seq conducted on a WT library. Genes that have fewer insertions in the $\Delta mprF$ background relative to the WT background are synthetically lethal with *mprF*. In this example, *geneX* is synthetically lethal with *mprF*. (2) An inactivation mutant of *geneX* can be constructed. This mutant strain should first be tested against the BSIM compound to ascertain that it is sensitive to the compound. This can be done using

(Continued) growth curves. In the example shown here, $\Delta mprF$ (in green) grows normally in the presence of the compound, but $\Delta geneX$ (in orange) shows no growth. Resistant mutants can then be raised to the compound in $\Delta geneX$ background and subjected to whole genome sequencing.

5.7.1 Identifying genes that are synthetically lethal with *mprF*

To identify genes that are synthetically lethal with *mprF* we constructed a transposon library in HG003 $\Delta mprF::KanR$ strain using the phage-based transposition system [392]. This system has been adapted for use with HG003 in a number of ways. We used a recipient strain in which the resident $\Phi 11$ prophage was removed by *att:FRT* exchange, as described in Santiago *et al.* [392]. The marked *mprF* deletion was transduced into an HG003 $\Delta \Phi 11:FRT$ strains which contained either a functional transposase or a truncated transposase. The latter served as a negative control for the transposition. Subsequent steps followed the same protocol as described in Santiago *et al.* (See Methods) [392]. For this library, we used the blunt, P_{pen} , P_{tuf} and P_{cap} transposon constructs. We chose to include the overexpression constructs in case we choose to test this library under pressure of other antibiotics in the future. 601,000 colonies were harvested from these four donor constructs to make this library. This library and the HG003 WT library constructed using six different transposon constructs, described in Santiago *et al* [392], were subjected to Tn-Seq. Tn-Seq revealed that there were 353,356 unique mutants in the *mprF* library.

As *mprF* is a gene that when inactivated sensitizes to so many antibiotics, we expected several genes to be important in the absence of *mprF*, but we found very few synthetically lethal genes. The Mann-Whitney U analysis revealed very few significant

hits when only the blunt constructs were considered, so we used data with all the constructs combined (unsplit). This resulted in a few more hits that met our cut-offs (See Chapter 4, section 4.6) (Fig. 5.9). As a positive control we found reads mapping to *mprF* to be depleted in our deletion library, as expected. We found that the reads mapping to genes involved in LTA synthesis (*ugtP* and *ltaA*) were significantly depleted. LTA synthesis was discussed in detail in Chapter 1. Briefly, UgtP uses UDP-glucose to make Glc₂DAG, the glycolipid anchor of LTA. LtaA flips this across the membrane and LtaS subsequently synthesizes the complete LTA polymer on this anchor [168]. We also found that reads mapping to *SAOUHSC_00718*, a gene encoding a hypothetical transmembrane protein, were also depleted.

A.

Locus	Gene	P-value	Fold change
SAOUHSC_01359	<i>mprF</i>	4.71E-46	0.038271
SAOUHSC_00718	hypothetical	7.12E-11	0.042821
SAOUHSC_00952	<i>ltaA</i>	4.89E-09	0.134467
SAOUHSC_00953	<i>ugtP</i>	0.03804	0.136

B.

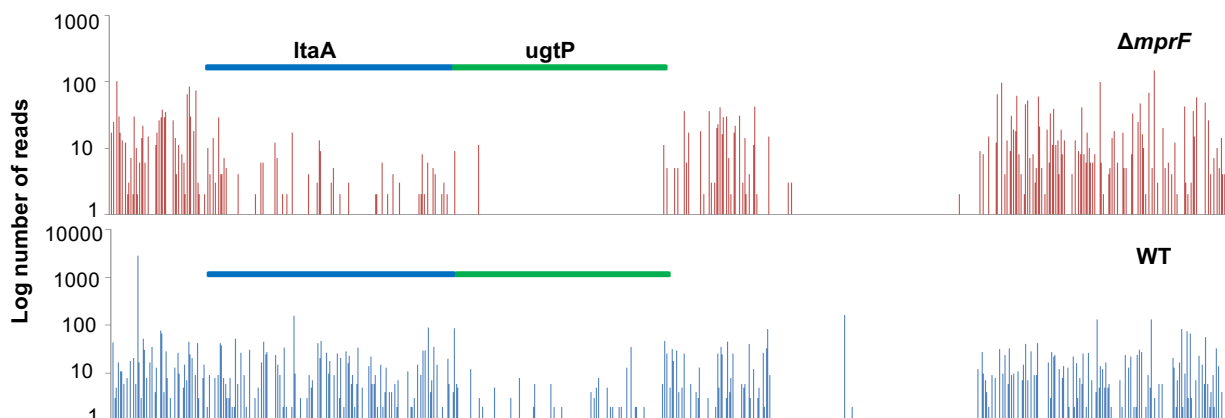


Figure 5.9: LTA synthesis genes are synthetically lethal with *mprF*. (A) The few significant depleted hits include *mprF*, *ugtP* and *ltaA*. All significant hits, their fold

(Continued) changes and p-values are shown. (B) Log of number of reads/TA site across the genomic context of *ItaA* and *ugtP* in the $\Delta mprF$ (top) and WT (bottom) backgrounds are represented by vertical lines. The regions before *ItaA* and after *ugtP* show similar read count but the regions of *ItaA* (blue bar) and *ugtP* (green bar) have significantly fewer genes.

This synthetic lethality of *mprF* with *ugtP* and *ItaA* was validated using an inducible promoter construct. *MprF* was cloned into the pTP63 plasmid with its native ribosome binding site, which integrates into the genome to give a stable single copy of *MprF*. This construct is inducible with anhydrous tetracycline. The expression of this construct was validated by looking for increased resistance of the complemented HG003 $\Delta mprF$ to gentamicin, a cationic aminoglycoside (Fig. 5.10A). Once expression was confirmed, transposon mutants of *ugtP* and *ItaA* from the Nebraska library were also transduced into this strain, and lethality was evaluated by plating in the presence and absence of inducer (Fig. 5.10B). The results showed that the *ugtP* and *ItaA* transposon mutant were indeed synthetically lethal/sick with $\Delta mprF$. These may be good strain backgrounds in which to raise resistant mutants. The *ItaA* mutant appears to grow better than the *ugtP* mutant, suggesting that the *ItaA* mutant strain might be an easier strain to work with than the *ugtP* mutant.

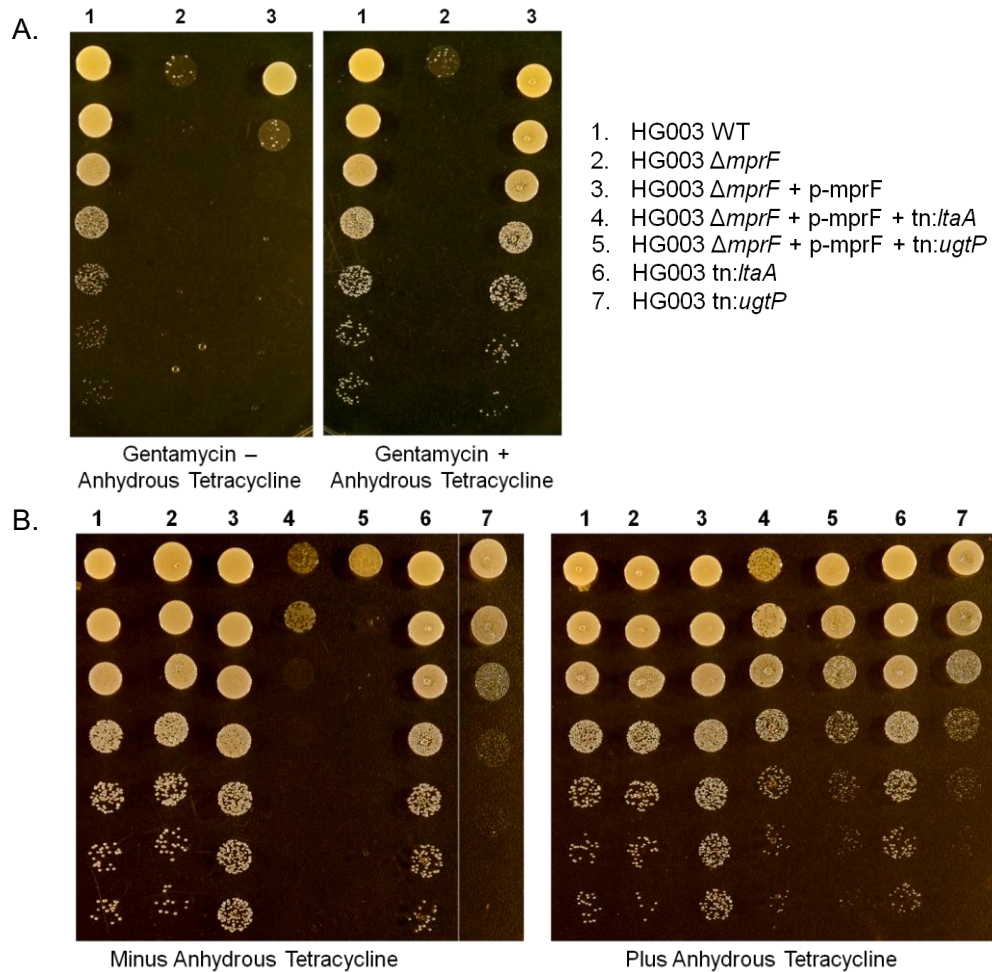


Figure 5.10: Validation of synthetic lethality of *ItaA* and *ugtP* with *mprF*. (A) HG003 WT (lane1), HG003 $\Delta mprF$ (lane2) and the complemented HG003 $\Delta mprF$ (lane 3) was first tested with gentamycin. In the absence of inducer both $\Delta mprF$ and the complemented strain are more sensitive than WT. In the presence of inducer, while the $\Delta mprF$ strain remains sensitive, the complemented strains grows to WT levels, showing that the complementation is successful. (B) *UgtP* and *ItaA* inactivation combined with *mprF* deletion mutants are highly lethal when grown in the absence of inducer (lanes 4 and 5, left panel). In the presence of inducer these strains grow to the same extent as the single inactivation mutants of *ItaA* and *ugtP*.

We suggest that resistant mutants to the lethal BSIM compounds identified here, can be raised in *ugtP* or *ItaA* inactivation mutant strain, once it is confirmed that the BSIM compounds remain lethal in the *ugtP* or *ItaA* inactivation mutant strains.

5.7.2 Raising resistant mutants to MR101

Unlike the other BSIM compounds identified, MR101 is not lethal and therefore, we had to determine whether the inactivation of *ugtP* was lethal prior to raising resistant mutants to MR101 in the *ugtP* inactivation background. However, although a transposon inactivation mutant of *ugtP* (*tn::ugtP*) had a slightly depleted growth rate at higher concentrations compared to WT, it was not sensitive enough to use for raising resistant mutants (Fig. 5.11B). Therefore, we went back to our Tn-Seq results to identify other sensitive mutants. From these list of depleted hits (Appendix 4), we found that *SAOUHSC_00948* was among the most depleted hits under all treatment conditions of the compound. *SAOUHSC_00948* encodes for a transmembrane protein of unknown function. We tested the transposon inactivation mutant of *SAOUHSC_00948* (*tn::948*) in a growth curve assay, and found that this mutant was completely killed by the compound (Fig. 5.11C).

Unfortunately, this mutant does not allow us to counter-select for mutations inactivating *mprF*. In fact, inactivating *mprF* in *tn::948* background increased the MIC by at least 4x (Fig. 5.11D). This suggests, that although we cannot say with certainty that inactivation of *mprF* will be the primary mechanism of resistance in the *tn::948* background, the likelihood of this exists.

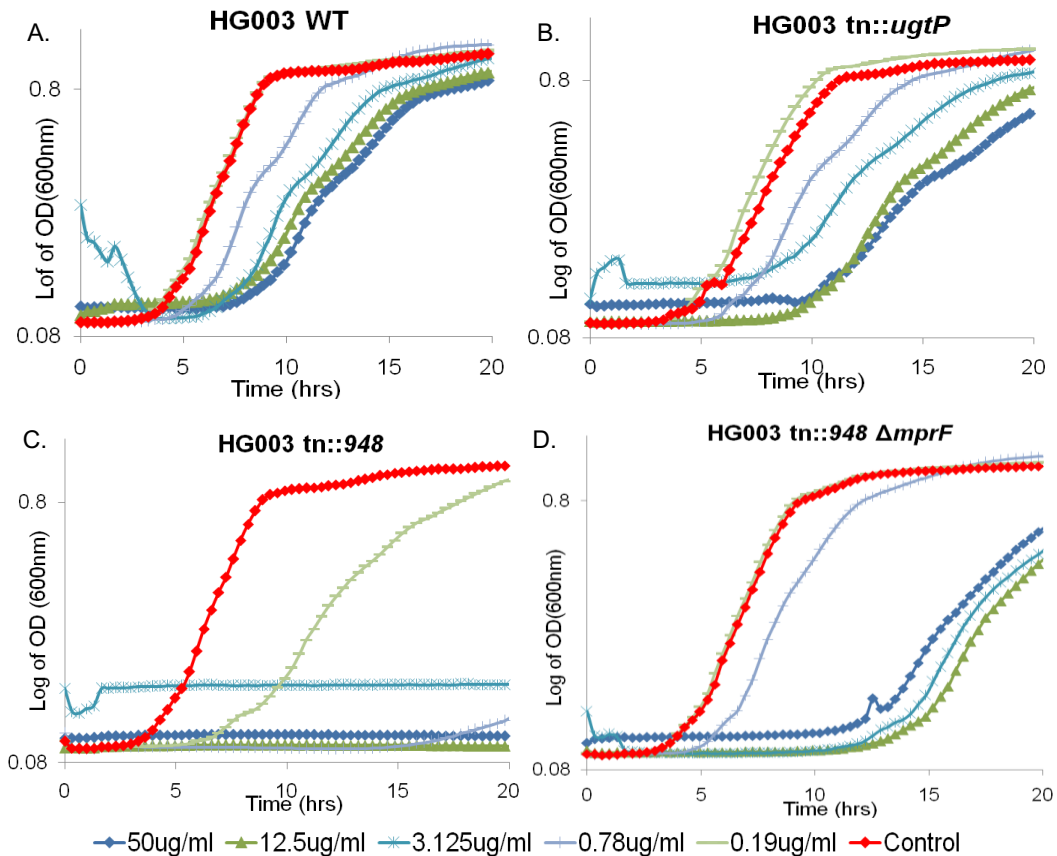


Figure 5.11: Tn::948 is more sensitive to MR101 than *tn::ugtP*. Growth curves of (A) HG003 WT, (B) HG003 *tn::ugtP*, (C) HG003 *tn::948* and (D) HG003 *tn::948 ΔmprF* strains in the presence of varying concentrations of MR101 at 37°C. This indicates that while *tn::ugtP* has minor growth defect compared to WT, *tn::948* is far more sensitive to MR101, and a better strain to raise resistant mutants in. Inactivation of *mprF* in this strain was still protective by at least 4x.

In order to overcome the possibility of *mprF* inactivation mutants arising in the *tn::948* background, we made a HG003 *tn::948 ΔugtP* strain, and raised resistant mutants in that background. Bacterial cultures of both HG003 *tn::948* and HG003 *tn::948 ΔugtP* were inoculated at an OD₆₀₀ of 0.1 in 96 well format with varying

concentrations of MR101 and MIC was monitored. A lower starting inoculum was found to not show any increase in MIC after 2 days of incubation. MIC was visually measured after 8 hours, 24 hours and 36 hours of incubation of HG003 tn::948 and HG003 tn::948 Δ ugtP at 30°C. Resistance experiments were conducted at 30°C in order to reduce background mutations. HG003 tn::948 gains resistance to a much higher concentration, whereas HG003 tn::948 Δ ugtP only increases by 2-4x in the same time period (Fig.5.12). The cultures from the wells that showed growth can be diluted and plated to single colonies. After confirmation of resistance, these colonies can be whole genome sequenced to identify resistant mutations. Resistance experiments were done in collaboration with Dr. Michael Welsh, a post-doc in the Walker Lab and this work is ongoing.

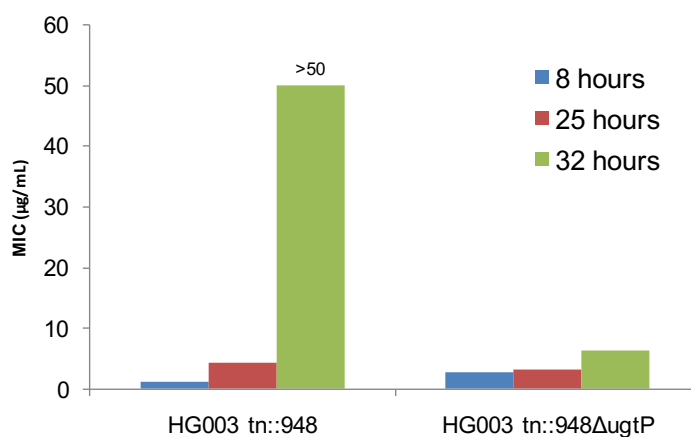


Figure 5.12: A larger increase in MIC of MR101 developed in HG003 tn::948. MIC measurements shown here are an average of 3 independent starter cultures. HG003 tn::948 appears to gain resistance much faster and to a higher concentration than HG003 tn::948 Δ ugtP.

The reason HG003 tn::948 shows an increase in MIC faster than the HG003 tn::948 Δ *ugtP* strain could be due to the fact that *mprF* null mutations can arise in the former strain whereas such mutations cannot occur in the latter strain. This can be confirmed by targeted sequencing of *mprF* in the resistant mutants isolated from HG003 tn::948.

We cannot rule out the possibility of suppressors arising to the double inactivation mutant strain. Suppressors to the inactivation of *ugtP* is unlikely to be selected for since tn::948 will still be susceptible to MR101. Should these occur, we can counter-screen the resistant colonies with tunicamycin, since *ugtP* is sensitive to tunicamycin, mutations that compensate for inactivation of *ugtP*, will likely protect against tunicamycin [171, 180, 204]. Suppressors of the inactivation of 948 is much more likely. However, Tn-Seq of the numerous antibiotics we described in previous chapters shows that tn::948 has similar antibiotics sensitivities as does treatment with MR101. This suggests that even if we find suppressor mutations to tn::948, they would be of interest and possibly in the same genetic network as the target of the compound.

5.8 Conclusions and Future Directions

In this chapter, we described the identification of a small molecule (MR100/MR101) that potentiates the activity of the β -lactam in a number of MRSA strains, and also sensitizes to antimicrobial peptides colistin, polymixin and bacitracin. The presence of impurities in MR100 was an unexpected challenge, and stresses the importance of confirming the purity and identity of purchased compounds as well as re-synthesizing any compounds that look significantly promising. Nevertheless, studies on

this compound led us to the finding that inactivation of *mprF* was protective. Based on this finding, we could identify bioactive compounds that are suppressed by *mprF* inactivation. We identified three such BSIM compounds from a screen of 600 lethal compounds. Compounds like these could be useful not only as tool compounds to further understand *S. aureus* cell biology, but might also be used in compound combinations to delay *mprF*-mediated clinical resistance to daptomycin. In the face of a dwindling store of effective antibiotics, the importance of multiple approaches to increase the life-span of daptomycin cannot be understated.

We have developed a possible strategy to identify the targets of compounds of this category, which can begin to be applied to the additional compounds identified here. This strategy is also generalizable to other compounds (lethal, or non-lethal) against which an inactivation mutant is protective.

As a part of this work, we identified that *mprF* is synthetically lethal with LTAs. This has not been previously observed and the basis for this lethality is not understood. We found that *mprF* is not synthetically lethal with WTAs. Transmission electron microscopy images showed increased cell division defects in the *ltaA*, *mprF* double inactivation mutant that are not observed in the *ltaA* inactivation mutant alone (Appendix 6). This suggests that *mprF* may, like *ugtP* and *ltaS*, have a possible role in cell division. MprF is an important intrinsic resistance factor and a full understanding of its impact on cell physiology will be useful in a more detailed picture of the cell envelope interaction network. This picture will enable the identification of more critical pathways that can be targeted by new antimicrobials.

5.9 Methods

Bacterial strains and compounds: A list of strains and primers used is provided in Appendix 7. MRSA strains USA400 (MW2) and USA200 were obtained from Dr. David Hooper at the Massachusetts General Hospital. HG003 tn::948 (MR087) and HG003 tn::ugtP (WL006) were constructed by phage transduction of Nebraska library transposon mutations using phage variant ϕ 11:FRT or ϕ 85. HG003 tn::ugtP was made by Dr. Wonsik Lee. HG003 tn::948 Δ mprF:KanR (MR108) and HG003 tn::948 Δ ugtP:KanR was made by phage transduction of marked deletion of *mprF* into MR087, and a marked deletion of *ugtP* from RN4220 Δ ugtP:KanR (WL077) into MR087. Plasmid for inducible *mprF* expression from pTP63 was constructed by amplifying *mprF* from HG003 WT genomic DNA using primers i-mprFpTP63F and mprFpTP63R, and ligated into the KpnI and EcoRI restriction sites of pTP63 vector using T4 DNA ligase. In order to include the native ribosome binding site of *mprF*, the forward primer anneals 25 bp ahead of the start of the gene. The plasmid was transformed into Stellar competent cells and confirmed by sequencing with Cm_to_HindIII primer. The confirmed plasmid was then electroporated into RN4220 competent cells which contains the helper plasmid pTP44 that is necessary for pTP63 to integrate (SHM 188). This was transduced using phage variant ϕ 11:FRT into HG003 Δ mprF:KanR (MR107). Transposon mutants tn::ugtP and tn::ltaA from the Nebraska library were then transduced into MR107. Anhydrous tetracycline inducer was maintained at 0.4 μ M throughout the transduction process. All transductants were verified by PCR with the following primers: pTP63_mprF_F and pTP63_B_mprF_R (for *mprF*); ugtP_orf_F and ugtP_orf_R (for tn::ugtP); ugtP_CA and ugtP_CB (for Δ ugtP); 948_F and 948_R (for 948) and

Cm_to_hindIII and mprF_CB_pTP63R (for p-*mprF*). All transposon mutants are marked with erythromycin. Strains were maintained with following antibiotics as necessary: Erythromycin at 5µg/mL, Kanamycin and Neomycin at 50 µg/mL each, Chloramphenicol at 10µg/mL, anhydrous tetracycline inducer was used at 0.4µM to induce expression of *mprF* from pTP63. Screening compounds were ordered from ChemDiv.

High-throughput screening: First, positive and negative controls were set up to determine robust screen conditions as indicated by Z'. 384 well plates for each of the screening conditions (see Table 5.2) were used to determine Z'. Half the plate was filled with 30µL of TSB with or without β-lactams. The remaining half of the plate was filled with 30µL of TSB containing erythromycin or β-lactams and tunicamycin. The wells were then topped with 30µL of overnight culture of MRSA strains 1784A or MW2 diluted 1:1000 into fresh TSB. Final concentrations are shown below. Plates were incubated at 30°C and OD₆₀₀ was measured after 16-17 hours of incubation. Z' was calculated as previously reported [543]. Z' measured was >0.5, suitable for high-throughput screening. Screening of compounds at the Institute for Chemical Genetics (ICCB - Longwood) was carried out same as above. 300nL of test compounds were pin-transferred into the plates pre-filled with erythromycin or oxacillin as necessary, and then topped with bacterial culture. This gave a final compound test concentration of 25µg/mL. Each compound was tested in replicate for each condition. 43,648 compounds from the ChemDiv6 library were screened in duplicate. All assays were performed in the bio-hood following protocols for BSL2 pathogen screening.

Table 5.2: Conditions for high-throughput screening for β -lactam potentiators

		Positive control	Negative control	Test wells
1784A	For lethality test	No antibiotic	Oxacillin 1.2 μ g/mL	No antibiotic
	For potentiator test	Oxacillin 1.2 μ g/mL	Oxacillin 1.2 μ g/mL + Tunicamycin 0.4 μ g/mL	Oxacillin 1.2 μ g/mL
MW2	For lethality test	No antibiotic	Methicillin 10 μ g/mL	No antibiotic
	For potentiator test	Methicillin 10 μ g/mL	Methicillin 10 μ g/mL + Tunicamycin 10 μ g/mL	Methicillin 10 μ g/mL

Data analysis: Average values for OD₆₀₀ measurements for positive and negative controls for each of the plates screened was calculated. A normalized percentage survival for each well was calculated as

$$\frac{(\text{OD}_{600} \text{ of each well} - \text{average of positive controls})}{(\text{average of positive controls} - \text{average of negative controls})} \times 100.$$

Subsequent analysis was

completed in MATLAB. First, replicate data was evaluated and those wells which did not replicate were removed. This was done by plotting one replicate of each data point against the other. Then a least squares best fit line was calculated. The standard deviations of all the data points from this best fit line was calculated and those data points that were greater than five times the standard deviation away from this line were removed. Exceptions to this were if percentage survival in TSB alone was >85% and percentage survival in oxacillin was <20%. In these two scenarios, both replicates were included without calculating standard deviations. These steps were done for positive controls, negative controls and all compound wells separately. The adjusted data for positive and negative controls were then plotted and a least squares best fit line was

calculated for the controls. Then, using this slope, three different cut-off planes were plotted using the $y = mx + c$ equation. Values for y and x were manually specified and cut-off planes with the equation $y = mx+c$ were plotted for each of three criteria: Strong, Medium and Weak. The values used are 90% survival in TSB, 10% survival in the presence of oxacillin for strong hits; 75% survival in TSB, 25% survival in oxacillin for medium hits; 60% survival in TSB, 35% survival in oxacillin for weak hits. Outer-bounds were specified for these cut-off planes as we did not want to consider compounds with percent survivals in TSB below 60% for medium and strong hits, or below 50% for weak hits, as these compounds would be fairly lethal. Likewise, we did not want to consider compounds which resulted in a percent survival $> 35\%$ in oxacillin as these compounds are likely not potent. Therefore, while outer-bound cut-offs had to be prescribed manually, this approach enables us to capture more compounds in each criteria than using a strict percent survival cut-off would have.

Checkerboard and MIC assays: Dual dose response checkerboard assays as well as single compound MIC assays were conducted using tryptic soy broth (TSB) for MR100 or cation-adjusted Mueller Hinton broth (MHB2) for MR101 at 30°C with a starting inoculum of $\sim 10^6$ cfu/mL. Antibiotic concentrations tested varied by 2x across all the tested wells. MICs were tested in 96 well plates with an assay volume of 150 μ L. Plates were incubated for 16-20 hours after which OD₆₀₀ was read using a plate reader. MICs for USA200 were measure after 19 hours (in TSB) and 24 hours (in MHB2) since this strain grows more slowly than others. MICs were recorded as the lowest concentration at which survival was $< 20\%$ of control. For testing sensitization to an antibiotic panel in MW2 a single concentration of MR100 was used, 10 μ g/mL for MRSA strains.

Sensitization by MR101 to the antibiotic panel in Newman was tested at 3µg/mL MR101.

Growth curves: Assays were conducted in 96 well plates with a total assay volume of 150µL. Strains were diluted to $\sim 10^5$ cfu/mL in MHB2 and incubated at 37°C with shaking in a plate reader. OD₆₀₀ was read every 20min for 20 hours and plotted on a log scale.

Identifying resistant mutants by plating: Two transposon libraries constructed by Dr. Timothy Meredith were used. One library (Library 3) with inactivation (blunt) and overexpression (P_{pen} , P_{tuf} , P_{cap} , P_{Erm} , P_{tuf}) constructs was combined with the another library (Library 4) constructed with transcription terminator (TT) constructs of varying strengths (weak, good, medium and strong). Based on number of colonies that were harvested in both libraries, they were combined in 2:1 ratio. Then diluted 1:100 in TSB and incubated at 30°C with shaking until OD₆₀₀ doubled. Library 3 and Library 4 were combined in 2:1 ratio. Cultures diluted to 0.01 OD₆₀₀ and $\sim 10^5$ cfu's were plated on MHB2 agar containing 50µg/mL MR100. Plates were incubated at 30°C overnight. Resistance was re-tested in growth curves and mutants which were resistant were mapped using inverse PCR. Resistant mutants were purified to single colonies and were mapped using inverse PCR [549]. All overnight cultures of mutants were maintained with Erythromycin 5µg/mL. Briefly, genomic DNA from 1mL overnight cultures was prepared using the Wizard genomic purification kit, and then 5µL of DNA was digested with Acil for 4 hours at 37°C. This was heat inactivated at 65°C for 20min and self-ligated with T4 DNA ligase at 16°C overnight. Ligation reactions were PCR purified. PCR reactions were set up using primers HGTnInvPCROUTF and

HGTnInvPCRoutR with 50°C annealing temperature and a 2 min extension time. Reactions were sequenced with HGTnInvPCRseq at Dana Farber Sequencing Facility. After identifying two mutants as insertions in *mprF*, PCR was conducted on six other mutants using MprFdccfwd2 and MprFdccrev2 primers and sequenced with TM168 at Genewiz Sequencing facility in order to map the location of the insertion and the type of transposon construct.

Tn-Seq: Tn-Seq was performed as described in Chapter 3 with some modifications. For MR100, Libraries 3 and 4 were combined in a 2:1 ratio and then diluted as previously described (Chapter 2), except a starting inoculum of 10^6 cfu's/2mL was used. Diluted transposon library aliquots were treated with 12.5µg/mL, 6.25µg/mL and 3.125µg/mL of MR100 and incubated at 37°C with shaking, and harvested when it reached stationary phase. For MR101, the library with only inactivation and upregulation constructs, library 2, described in Santiago *et al.* was used [392]. The library was treated with 6.25µg/mL, 12.5µg/mL and 25µg/mL. Samples were prepared for Tn-Seq and after Illumina sequencing at Biopolymers Sequencing facility. Sample preparation and data analysis was conducted as previously described [392] with one exception. Since the number of TA sites hit under 12.5µg/mL of MR100 was very low (only 15,305) compared to the number of TA sites hit in the control condition (168,848), this data set was normalized only by number of reads and not by simulation-based resampling, which also takes into account number of TA sites hit. Donor barcodes for each construct are pen: ATTCG, cap: CCACG, tuf: ATCCG, blunt: TACCG, dual: AATCG, erm: TGCCG, weak TT: GTACG, medium TT: CGTCG, good TT: AGACG, strong TT: ATACG.

HPLC: HPLC was performed using a C18 column and water with 0.1% formic acid and acetonitrile with 0.1% formic acid as solvents. Solvents were varied with time as follows: for the first 2min, 5% acetonitrile, 2min-8min, ramp to 95% acetonitrile, 8min - 20min, maintain at 95% acetonitrile, 20-22min ramp down to 5% acetonitrile. Mass spectrometry of collected fractions was completed in the Kahne lab in Cambridge.

Construction of HG003 $\Delta mprF$ transposon library: Antibiotic resistance cassettes of plasmids (TM174 and TM175) containing functional and truncated transposases were switched from kanamycin to chloramphenicol and moved to the HG003 strain with resident $\phi 11$ prophage deleted (SHM062 and SHM063) by Dr. Samir Moussa, a post-doc in the Walker Lab. The kanamycin marked *mprF* deletion was moved into these strains by $\phi 85$ transduction (MR039 and MR040). Transductions were confirmed using MprFdccfwd2 and MprFdccrev2 primers. Donor lysates were made using ϕ -11 FRT phage variant from donor strains TCM239, TCM240, TCM241, TCM242 to obtain phage packaged with blunt, P_{pen} , P_{cap} , P_{tuf} , transposon constructs respectively. Phage were titred and packaging efficiency was determined on RN4220 and TM19 respectively. A high phage titre ($\sim 10^9$ pfu/mL) is desired. We obtained a packaging efficiency of 37-88% from our phage lysates. These lysates were used to infect the recipient strains (MR039 and MR040). A test transposition was conducted to determine phage:cell ratio that was suitable. We obtained ~ 500 colonies from MR039 with the functional transposase and no colonies in MR040 with truncated transposase at 5 MOI (multiplicity of infection). This was scaled up to construct the full library. We harvested a total of 601,000 colonies. Tn-Seq sample preparation and harvesting was conducted at 37°C following the same protocol as described previously. Data analysis was also conducted as

previously, with normalization of samples by read count. All TCM strains are described in Santiago *et al.* [392].

Spot dilution assays: All strains were diluted from overnight cultures into fresh media with appropriate antibiotics (and anhydrous tetracycline inducer if necessary) and grown at 30°C until an OD₆₀₀ of 1. These were then serially diluted and 5µL were spotted on agar plates with or without 0.4 µM anhydrous tetracycline and incubated at 37°C overnight. For assays with tunicamycin or gentamicin, tunicamycin was used at 1µg/mL and gentamicin at 1.2µg/mL. Plates were imaged after overnight incubation.

Transmission electron microscopy: Overnight cultures were diluted 1/100 in fresh TSB with the presence of appropriate antibiotics or anhydrous tetracycline inducer, if desired, grown at 30°C until an OD₆₀₀ 0.3. Samples were outgrown for 2 hours or 4 hours after this point. Cells were harvested by centrifuging at 14,000xg for 3min, and resuspended in 50µL water. 50µL of 4 parts fixative solution and 1 part glutaraldehyde, provided by the Electron Microscopy facility was added to the samples. Samples were allowed to fix at room temperature for 30min and submitted for sectioning to the Electron Microscopy facility. After staining, the samples were imaged using JEOL 1200EX-80kV microscope.

Appendix 1: MATLAB code for analyzing high-throughput screening data

```
1 - a = xlsread ('1070_total');
2
3 - %size(a)
4 - SCREEN_SIZE=47616;
5
6 - % make controls file
7
8 - %remove the wells which do not replicate
9 - x_con1=[];y_con1=[];
10 - for i = 1:SCREEN_SIZE
11 -     if mod(i+1,24)==0 || mod(i,24)==0
12 -         x_con1(i,1)= a(i,3);
13 -         y_con1(i,1)= a(i,4);
14 -     else
15 -         x_con1(i,1)=nan;
16 -         y_con1(i,1)=nan;
17 -     end
18 - end
19 - % least squares best fit of the replicates
20 - X_TSB=x_con1(:,1);
21 - Y_TSB=y_con1(:,1);
22 - q=~(isnan(X_TSB)|isnan(Y_TSB));
23 - p_con=polyfit(X_TSB(q),Y_TSB(q),1);
24 - y_con=polyval(p_con,x_con1);
25 - offset_con=y_con1-y_con;
26 - figure
27 - scatter(x_con1,y_con1,'b')
28 - hold on
29 - plot(x_con1,y_con,'r--')
30 - title ('TSB1 against TSB2')
31 - xlabel('Avg % survival TSB1')
32 - ylabel('Avg % survival TSB2')
33 -
34 -
35 - %calculate std dev of offsets
36 - X_offsetcon = offset_con(:,1);
37 - q_offsetcon = ~(isnan(X_offsetcon));
38 - absX = abs(X_offsetcon(q_offsetcon));
39 - stdev_offsetcon = std(absX);
40 -
41 - % remove the wells that are too different in replicates
42 - corr_TSB_con=[];
43 - for i = 1:SCREEN_SIZE
44 -     corr_TSB_con(i,1:2)=a(i,1:2);
45 -     if mod(i+1,24)==0 || mod(i,24)==0
46 -         if x_con1(i,1)>85 & y_con1(i,1) > 85
47 -             corr_TSB_con(i,3)=(x_con1(i,1)+y_con1(i,1))/2;
48 -         elseif x_con1(i,1)<20 & y_con1(i,1)<20
49 -             corr_TSB_con(i,3)=(x_con1(i,1)+y_con1(i,1))/2;
50 -         elseif abs(offset_con(i))<5*stdev_offsetcon
51 -             corr_TSB_con(i,3)=(x_con1(i,1)+y_con1(i,1))/2;
52 -         else
53 -             corr_TSB_con(i,3) = nan;
54 -         end
55 -     else
56 -         corr_TSB_con(i,3) = nan;
57 -     end
58 - end
59 -
60 - %do the same for oxacillin control wells
61 - x_con2=[];y_con2=[];
62 - for i = 1:SCREEN_SIZE
63 -     if mod(i+1,24)==0 || mod(i,24)==0
64 -         x_con2(i,1)= a(i,5);
```

```

65 -     y_con2(i,1)= a(i,6);
66 -     else
67 -     x_con2(i,1)=nan;
68 -     y_con2(i,1)=nan;
69 -     end
70 - end
71 - X_OX=x_con2(:,1);
72 - Y_OX=y_con2(:,1);
73 - q2=~(isnan(X_OX)|isnan(Y_OX));
74 - p2_con=polyfit(X_OX(q2),Y_OX(q2),1);
75 - y2_con=polyval(p2_con,x_con2);
76 - offset_ox_con=y_con2-y2_con;
77 - figure
78 - scatter(x_con2,y_con2,'b')
79 - hold on
80 - plot(x_con2,y2_con,'r--')
81 - title('Ox1 against Ox2')
82 - xlabel('Avg % survival ox1')
83 - ylabel('Avg % survival ox2')
84 - hold off
85
86 %calculate std dev of offsets
87 - X_offsetoxcon = offset_ox_con(:,1);
88 - q_offsetoxcon = ~(isnan(X_offsetoxcon));
89 - absXox = abs(X_offsetoxcon(q_offsetoxcon));
90 - stdev_offsetoxcon = std(absXox);
91
92 %remove the wells that are too different in replicates
93 - corr_ox_con=[];
94 - for i = 1:SCREEN_SIZE
95 -     corr_ox_con(i,1)=a(i,1);
96 -     corr_ox_con(i,2)=a(i,2);
97 -
98 -     if mod(i+1,24)==0 || mod(i,24)==0
99 -         if x_con2(i,1)>85 & y_con2(i,1) > 85
100 -             corr_ox_con(i,3)=(x_con2(i,1)+y_con2(i,1))/2;
101 -         elseif x_con2(i,1)<20 & y_con2(i,1)<20
102 -             corr_ox_con(i,3)=(x_con2(i,1)+y_con2(i,1))/2;
103 -         elseif abs(offset_ox_con(i))<5*5.79
104 -             corr_ox_con(i,3)=(x_con2(i,1)+y_con2(i,1))/2;
105 -         else
106 -             corr_ox_con(i,3) = nan;
107 -         end
108 -     else
109 -         corr_ox_con(i,3) = nan;
110 -     end
111 - end
112 %controls final with replicates removed - removes 28 out of 3968 controls
113 %=0.7%
114 %
115 con_final=[];
116 - for i = 1:SCREEN_SIZE
117 -     con_final(i,1:2)=a(i,1:2);
118 -     if isfinite(corr_TSB_con(i,3)) || isfinite(corr_ox_con(i,3))
119 -         con_final(i,3)=corr_TSB_con(i,3);
120 -         con_final(i,4)=corr_ox_con(i,3);
121 -     else
122 -         con_final(i,3:4)=nan;
123 -     end
124 - end
125
126 count_con=0;
127 - for i = 1:SCREEN_SIZE
128 -     if isfinite(con_final(i,3)) & isfinite(con_final(i,4))

```

```

129 -     count_con = count_con+1
130 - end
131 - end
132 - %least squares best fit of adjusted controls - but first remove nans
133 - X=con_final(:,3);
134 - Y=con_final(:,4);
135 - q3=~(isnan(X)|isnan(Y));
136 - p_con_final = polyfit(X(q3),Y(q3),1);
137 - y_con_final = polyval(p_con_final,X);
138 - figure
139 - scatter(con_final(:,3),con_final(:,4))
140 - hold on
141 - plot(con_final(:,3),y_con_final,'r--')
142 -
143 - %for actual library compounds
144 - %TSB
145 - x_coll=[];y_coll=[];
146 - for i = 1:SCREEN_SIZE
147 -     if mod(i+1,24)~=0 & mod(i,24)~=0
148 -         x_coll(i,1)= a(i,3);
149 -         y_coll(i,1)= a(i,4);
150 -     else
151 -         x_coll(i,1)=nan;
152 -         y_coll(i,1)=nan;
153 -     end
154 - end
155 - X_TSB_sc=x_coll(:,1);
156 - Y_TSB_sc=y_coll(:,1);
157 - q_TSB_sc=~(isnan(X_TSB_sc)|isnan(Y_TSB_sc));
158 - p_TSB_sc=polyfit(X_TSB_sc(q_TSB_sc),Y_TSB_sc(q_TSB_sc),1);
159 - y_TSB_sc=polyval(p_TSB_sc,x_coll);
160 - offset_TSB_sc=y_coll-y_TSB_sc;
161 - figure
162 - scatter(x_coll,y_coll,'b')
163 - hold on
164 - plot(x_coll,y_TSB_sc,'r--')
165 - title ('TSB1 against TSB2')
166 - xlabel('Avg % survival TSB1')
167 - ylabel('Avg % survival TSB2')
168 - hold off
169 -
170 - %calculate std dev of offsets
171 - X_offsetTSBsc = offset_TSB_sc(:,1);
172 - q_offsetTSBsc = ~(isnan(X_offsetTSBsc));
173 - absXTSBsc = abs(X_offsetTSBsc(q_offsetTSBsc));
174 - stdev_offsetTSBsc = std(absXTSBsc);
175 -
176 - %remove the wells that are too different in replicates
177 - corr_TSB=[];
178 - for i = 1:SCREEN_SIZE
179 -     corr_TSB(i,1)=a(i,1);
180 -     corr_TSB(i,2)=a(i,2);
181 -     if mod(i+1,24)~=0 & mod(i,24)~=0
182 -         if x_coll(i,1)>85 & y_coll(i,1) > 85
183 -             corr_TSB(i,3)=(x_coll(i,1)+y_coll(i,1))/2;
184 -         elseif x_coll(i,1)<20 & y_coll(i,1)<20
185 -             corr_TSB(i,3)=(x_coll(i,1)+y_coll(i,1))/2;
186 -         elseif abs(offset_TSB_sc(i))<6*stdev_offsetTSBsc
187 -             corr_TSB(i,3)=(x_coll(i,1)+y_coll(i,1))/2;
188 -         else
189 -             corr_TSB(i,3) = nan;
190 -         end
191 -     else
192 -         corr_TSB(i,3) = nan;

```

```

193 -         corr_TSB(i,3) = nan;
194 -     end
195 - else
196 -     corr_TSB(i,3) = nan;
197 - end
198 - end
199 -
200 - %determines how many wells were rejected at this step; was 3989 minus 3968
201 - %controls = 21 experimental wells
202 - count_tsb=0;
203 - count_tsbrejects=0;
204 - for i = 1:SCREEN_SIZE
205 -     if isfinite(corr_TSB(i,3))
206 -         count_tsb = count_tsb+1;
207 -     elseif isnan(corr_TSB(i,3))
208 -         count_tsbrejects = count_tsbrejects + 1;
209 -     end
210 - end
211 -
212 - x_col2=[];y_col2=[];
213 - for i = 1:SCREEN_SIZE
214 -     if mod(i+1,24)~=0 & mod(i,24)~=0
215 -         x_col2(i,1)= a(i,5);
216 -         y_col2(i,1)= a(i,6);
217 -     else
218 -         x_col2(i,1)=nan;
219 -         y_col2(i,1)=nan;
220 -     end
221 - end
222 - X_OX_sc=x_col2(:,1);
223 - Y_OX_sc=y_col2(:,1);
224 - q_OX_sc=~(isnan(X_OX_sc)|isnan(Y_OX_sc));
225 - p_OX_sc=polyfit(X_OX_sc(q_OX_sc),Y_OX_sc(q_OX_sc),1);
226 - y_OX_sc=polyval(p_OX_sc,x_col2);
227 - offset_OX_sc=y_col2-y_OX_sc;
228 - figure
229 - scatter(x_col2,y_col2,'b')
230 - hold on
231 - plot(x_col2,y_OX_sc,'r--')
232 - title ('Ox1 against Ox2')
233 - xlabel('Avg % survival ox1')
234 - ylabel('Avg % survival ox2')
235 - hold off
236 -
237 - %calculate std dev of offsets
238 - X_offsetOXsc = offset_OX_sc(:,1);
239 - q_offsetOXsc = ~(isnan(X_offsetOXsc));
240 - absXOXsc = abs(X_offsetOXsc(q_offsetOXsc));
241 - stdev_offsetOXsc = std(absXOXsc);
242 -
243 - %determines how many wells were rejected at this step; was 4037 minus 3968
244 - %controls = 69 experimental wells
245 -
246 - corr_ox=[];
247 - for i = 1:SCREEN_SIZE
248 -     corr_ox(i,1)=a(i,1);
249 -     corr_ox(i,2)=a(i,2);
250 -     if mod(i+1,24)~=0 & mod(i,24)~=0
251 -         if x_col2(i,1)>85 & y_col2(i,1) > 85
252 -             corr_ox(i,3)=(x_col2(i,1)+y_col2(i,1))/2;
253 -         elseif x_col2(i,1)<20 & y_col2(i,1)<20
254 -             corr_ox(i,3)=(x_col2(i,1)+y_col2(i,1))/2;
255 -         elseif abs(offset_OX_sc(i))<6*stdev_offsetOXsc
256 -             corr_ox(i,3)=(x_col2(i,1)+y_col2(i,1))/2;
257 -         else
258 -             corr_ox(i,3) = nan;
259 -         end
260 -     else

```

```

261 -     corr_ox(i,3) = nan;
262 -     end
263 - end
264
265 -     count_ox = 0;
266 -     count_oxrejects=0;
267 - for i = 1:SCREEN_SIZE
268 -     if isfinite(corr_ox(i,3)) & isfinite(corr_ox(i,3))
269 -         count_ox = count_ox+1;
270 -     elseif isnan(corr_ox(i,3)) & isnan(corr_ox(i,3))
271 -         count_oxrejects = count_oxrejects+1;
272 -     end
273 - end
274
275 - %file of screened compounds without rejected wells
276 - screen_adjusted = [];
277 - for i = 1:SCREEN_SIZE
278 -     screen_adjusted(i,1:2)=a(i,1:2);
279 -     if isfinite(corr_TSB(i,3)) & isfinite(corr_ox(i,3))
280 -         screen_adjusted(i,3)=corr_TSB(i,3);
281 -         screen_adjusted(i,4)=corr_ox(i,3);
282 -     else
283 -         screen_adjusted(i,3:4)=nan;
284 -     end
285 - end
286 - % 87 wells in addition to controls were removed = 0.19%
287 - count_screenedcmpds = 0;
288 - count_rejectedcmpds = 0;
289 - for i = 1:SCREEN_SIZE
290 -     if isfinite(screen_adjusted(i,3:4))
291 -         count_screenedcmpds = count_screenedcmpds + 1;
292 -     elseif isnan(screen_adjusted(i,3:4))
293 -         count_rejectedcmpds = count_rejectedcmpds + 1;
294 -     end
295 - end
296 - %%
297 - %Identify only toxic hits, excluding negative controls which are in the
298 - %24th column of each plate
299 - Toxic = [];
300 - for i=1:SCREEN_SIZE
301 -     Toxic(i,1)=a(i,1);
302 -     Toxic(i,2)=a(i,2);
303 -     if screen_adjusted(i,3)<20
304 -         Toxic(i,3:4)= screen_adjusted(i,3:4);
305 -     else
306 -         Toxic(i,3:4)= nan;
307 -     end
308 - end
309 - % gives the total number of lethal hits - for screen 1070, this was 472=1.08%
310 - count_toxic = 0;
311 - for i = 1:SCREEN_SIZE
312 -     if isfinite(Toxic(i,3))
313 -         count_toxic = count_toxic + 1;
314 -     end
315 - end
316 - %%
317 - %Sorting hits
318 - weak_hits=[];
319 - medium_hits=[];
320 - strong_hits=[];
321 - y_weak=[];
322 - y_medium=[];
323 - hits_withgd=[];
324 - for i=1:SCREEN_SIZE
325 -     weak_hits(i,1:2)=a(i,1:2);
326 -     medium_hits(i,1:2)=a(i,1:2);
327 -     strong_hits(i,1:2)=a(i,1:2);
328 -     hits_withgd(i,1:2)=a(i,1:2);

```



```

329 - strong_hits(i,3:4)=nan;
330 - medium_hits(i,3:4)=nan;
331 - weak_hits(i,3:4)=nan;
332 - hits_withgd(i,3:4)=nan;
333 - %intercepts were determined by using the cut off values below for TSB and ox; and
334 - %solving the equation y=mx+c where m= slope of best fit line of controls.
335 - y_weak(i,1)= 0.9958*(screen_adjusted(i,3))-24.748;
336 - y_medium(i,1)=0.9958*(screen_adjusted(i,3))-49.685;
337 - y_strong(i,1)=0.9960*(screen_adjusted(i,3))-79.622;
338 - %if TSB>60 and oxa <35 then weak; if TSB>75 and oxa<25, then medium; if
339 - %TSB>90 and oxa<10, then strong
340 - if screen_adjusted(i,4)<y_strong(i,1) & screen_adjusted(i,3) > 60 & screen_adjusted(i,4)<10
341 -     strong_hits(i,3)=screen_adjusted(i,3);
342 -     strong_hits(i,4)=screen_adjusted(i,4);
343 - else
344 -     strong_hits(i,3:4)=nan;
345 - end
346 - if screen_adjusted(i,4)<y_medium(i,1) & screen_adjusted(i,3) > 60 & screen_adjusted(i,4)<25 & isnan(strong_hits(i,3))
347 -     medium_hits(i,3)=screen_adjusted(i,3);
348 -     medium_hits(i,4)=screen_adjusted(i,4);
349 - else
350 -     medium_hits(i,3:4)=nan;
351 - end
352 - if screen_adjusted(i,4)<y_weak(i,1) & screen_adjusted(i,3)>50 & screen_adjusted(i,4)<35 & isnan(medium_hits(i,3)) & isnan(strong_hits(i,3))
353 -     weak_hits(i,3)=screen_adjusted(i,3);
354 -     weak_hits(i,4)=screen_adjusted(i,4);
355 - else
356 -     weak_hits(i,3:4)=nan;
357 - end
358 - if screen_adjusted(i,3)>45 & screen_adjusted(i,3)<80
359 -     if isfinite(medium_hits(i,3)) || isfinite(strong_hits(i,3)) || isfinite(weak_hits(i,3))
360 -         hits_withgd(i,3)=screen_adjusted(i,3);
361 -         hits_withgd(i,4)=screen_adjusted(i,4);
362 -     else
363 -         hits_withgd(i,3:4)=nan;
364 -     end
365 - else
366 -     hits_withgd(i,3:4)=nan;
367 - end
368 - end
369 - %number of hits - medium and weak hits will have some overlap with hits
370 - %with growth defect
371 - count_strong = 0;
372 - count_weak = 0;
373 - count_medium=0;
374 - count_gd = 0;
375 - for i = 1:SCREEN_SIZE
376 -     if isfinite(strong_hits(i,3:4))
377 -         count_strong = count_strong + 1;
378 -     end
379 -     if isfinite(weak_hits(i,3:4))
380 -         count_weak = count_weak+1;
381 -     end
382 -     if isfinite(medium_hits(i,3:4))
383 -         count_medium = count_medium + 1;
384 -     end
385 -     if isfinite(hits_withgd(i,3:4))
386 -         count_gd = count_gd+1;
387 -     end
388 - end
389 - %%
390 - %Plotting
391 - %plot all adjusted data
392 - figure
393 - scatter(corr_TSB(:,3), corr_ox(:,3), 'b')
394 - hold on
395 - scatter(medium_hits(:,3), medium_hits(:,4),'g')
396 - hold on
397 - scatter(strong_hits(:,3), strong_hits(:,4), 'r')
398 - hold on
399 - scatter(Toxic(:,3), Toxic(:,4), 'k', 'filled')
400 - hold on
401 - scatter(hits_withgd(:,3), hits_withgd(:,4), 'm')
402 - hold on
403 - plot(con_final(:,3), y_con_final, 'r--')
404 - title ('')
405 - xlabel('% survival TSB')
406 - ylabel('% survival Oxacillin')
407 - axis([-20,160,-50,300])
408 - lgnd = legend('Screened compounds','Medium Hits', 'Strong Hits', 'Toxic', 'Hits with Growth Defects','Location','Northwest')
409 - set(lgnd, 'Color','none')
410 - legend('boxoff')

```

Appendix 2: Hits identified in high-throughput screening for β -lactam potentiators

Table A2.1: High-throughput screening hits identified in the strong category

Plate	Well	Average percent survival		SMILES	Annotations
		minus β -lactam	plus β -lactam		
1842	P13	95.50	4.75	<chem>n(c(cccc1)c1n2CCCCO(c(cc3)ccc3C)c2CC</chem>	
1870	F18	88.76	7.17	<chem>S(=O)(=O)(NC1CCCC1)c(ccc(c23)OCC(=O)N2CC(=O)Nc(ccc(c4Cl)C)c4)c3</chem>	
1871	P17	101.76	9.66	<chem>N1(c2ccc(cc2)Cl)C(=O)C(N(Cc(c(cc3)ccn3)C1=O)CC(=O)Nc(cc4)ccc4OCCC</chem>	
1879	N13	96.67	5.75	<chem>c1(C(F)(F)F)nc(cccc2)c2nc1N(CC3)CCC3C(=O)Nc4cccc(F)c4</chem>	Did not retest
1891	B17	104.00	9.45	<chem>c1(c(cc2c(ccc(C)c2)n1)cc3C(NCCCN(C)c4cccc4)=O)s3</chem>	Retested - sensitizes only 1784A and MW2
1891	I21	97.84	7.90	<chem>S(NCCc1csc(c2ccc(cc2)Cl)n1)(=O)(=O)c3c(OC)ccc(F)c3</chem>	
1891	M21	96.26	9.34	<chem>S(NCCc1csc(c2ccc(cc2)Cl)n1)(=O)(=O)c3cc(C)ccc3C</chem>	
1893	P10	102.70	6.14	<chem>C(CO(c(c12)ccc(Br)c1)(C(=O)NCc3cccc3Cl)=C2</chem>	
1895	D02	87.97	7.22	<chem>C(NC(=O)c(cccc1[N+](=O)[O-])c1C)(=C(C)N=C(N23)C=C(C=C2)C)C3=O</chem>	
1898	J05	92.37	9.70	<chem>c1(N(CC2)CCC2C(=O)N(CC3)CCN3c4cc(C)ccc4C)[nH]c5c(ccc(C)c5)n1</chem>	
1902	B07	104.53	7.95	<chem>n1c(CCNc(=O)c2cc(OC)cc(OC)c2)esc1c(cc3)ccc3C(F)(F)F</chem>	
1903	I18	101.61	2.55	<chem>n1c(c2ccc(cc2)Cl)nn(c(cs3)CCNS(=O)(=O)c(c4C)c(C)on4)c13</chem>	
1905	A10	87.54	4.01	<chem>c1(sc(c2C)CCNS(c3cccc3)(=O)=O)n2nc(c4ccc(cc4)Cl)n1</chem>	
1906	I21	105.09	6.42	<chem>C1(=CC=CN(Cc(cccc2[N+](=O)[O-])c2)C1=O)C(=O)Nc(cc3)ccc3CC</chem>	
1908	O07	104.89	9.97	<chem>c1(C(=O)Nc(ccc(c2C(F)(F)F)Cl)c2)nc(cccc3)c3nc1N4CCCC4</chem>	
1910	O11	102.51	1.94	<chem>n1(nc(n2)CCn(c3)c(C)cn3)c2c4c(ccc4)nc1SCC(=O)Nc5cccc(Cl)c5</chem>	
1911	H11	100.05	6.32	<chem>n1(c2cccc(Cl)c2)nce3e1nenc3NCCC(C)C</chem>	
1911	K02	101.74	6.30	<chem>n1(c2ccc(cc2)F)nce3c1nenc3Nc(cc4)ccc4Oc(cc5)ccc5Cl</chem>	
1912	H20	95.85	3.80	<chem>S(=O)(=O)(N(Cc1cccc1)c2c(F)ccc(c2)C(=O)Nc3cc(Cl)cc(Cl)c3</chem>	Retested
1912	P18	103.21	4.75	<chem>S(=O)(=O)(N1CCCCC1)c2c(F)ccc(c2)C(=O)Nc3cc(Cl)cc(Cl)c3</chem>	Inconclusive
1913	E16	98.83	1.82	<chem>c1(cc(ccc1N(CC2)CCN2c3cccc3F)C(OCC)=O)NC(=O)Nc(ccc(c4Cl)Cl)c4</chem>	MR101/MR100
1913	K22	98.10	3.41	<chem>c1(cc(ccc1N(CC2)CCN2c3cccc(Cl)c3)C(OCC)=O)NC(=O)Nc(cc4)ccc4Cl</chem>	Structural analog of 1913 E16, retested - 4-8x weaker
1914	B14	101.45	7.29	<chem>c(cc1Sc2cccc(Cl)c2)(c3c(n1)cccc3)C(NCCCN4CCCC4C)=O</chem>	
1914	C14	90.25	4.71	<chem>c1(Cl)cc(F)ccc1CNc(=O)CCSCc(cc2)ccc2Cl</chem>	
1914	F09	87.28	7.12	<chem>c1(Cl)cc(F)ccc1CNc(=O)CCSCc2cccc(Cl)c2</chem>	
1914	P15	102.39	8.73	<chem>c1(Cl)cc(ccc1Cl)CNC(CSCc2cccc2Cl)=O</chem>	
1915	B09	102.09	5.43	<chem>C(=O)(Nc(ccc(c1Cl)Cl)c1)N2CCC(c3ccc(cc3)C)C2</chem>	
1915	B11	91.68	2.24	<chem>S(=O)(=O)(c(cccc1)c1C(N2Cc3cccc(Cl)c3)=O)c(ccc(c4)C(NCCCN5CCCC(C)C5)=O)c24</chem>	
1915	D20	107.61	3.27	<chem>c1(c2c(sc1Nc3cccc3)CCCC2)C(=O)Nc(cc4)ccc4C(OCC)=O</chem>	Did not retest
1915	H20	91.16	1.31	<chem>c1(c2c(sc1Nc3cccc(F)c3)CCCC2)C(=O)Nc(cc4)ccc4C(OC)=O</chem>	
1915	O17	108.61	1.61	<chem>N1(Cc2cccc2C)C(=O)CN=C(c3cccc3)c(cc(Cl)cc4)c14</chem>	
1916	B12	94.93	7.77	<chem>n(CCC(=O)Nc(cc(C)cc1C)c1)(c2C)c(c3cccc3)cc2C(C)=O</chem>	
1916	P21	84.08	3.69	<chem>c(C(OCC)=O)(cc(n1CCC(=O)Nc(cc2)ccc2C(F)(F)F)c3cccc3)c1C</chem>	
1917	A15	95.95	6.67	<chem>S(=O)(=O)(c(ccc1c2c3c([nH]1)CCCC3)c2)NC(c4cccc4Cl)CC(OCC)=O</chem>	
1917	K05	87.72	4.74	<chem>n(CCC(=O)Nc(ccc(c1Cl)C)c1)(c2C)c(c3ccc(cc3)OC)cc2C(C)=O</chem>	
1918	P20	113.26	3.38	<chem>C(=O)(C(c1ccc(cc1)Cl)=Cc(c23)ccc(O)c2CN(CC4)CCO4)O3</chem>	Did not retest
1919	G16	89.76	5.42	<chem>S(NCCc1c1c([nH]2)ccc(C)c1)c2C(=O)(=O)c3ccc(c(OC)c3)Br</chem>	
1919	M04	89.62	2.53	<chem>S(c1cccc1)(=O)(=O)N(c(cccc2C(F)(F)F)c2)CC(=O)Nc3cccc(Cl)c3</chem>	
1919	P17	90.15	1.35	<chem>c1(Nc2c(OC)ccc(OC)c2)c3c(cccc3)nc(c4ccc(cc4)C)n1</chem>	

Table A2.2: High-throughput screening hits identified in the medium category

Plate	Well	Average percent survival		SMILES	Annotation
		minus β -lactam	plus β -lactam		
1919	L04	66.79	0.26	<chem>n1(C)c(c2ccc(cc2)Br)enc1NCCc3cccc(OC)c3</chem>	
1877	D02	79.44	0.61	<chem>c(C)(NCCCN(CCC(c12)cccc1)C2=O)(cnn3c4ccc(c(C)c4)C)c3C(CC5)CCN5C(=O)OC(C)(C)C</chem>	
1912	J18	60.07	0.71	<chem>S(=O)(=O)(NC1CCCC1)c(ccc(c2C(=O)Nc(cc3)ccc3Br)F)c2</chem>	
1877	M05	61.49	0.72	<chem>c1(C(=O)N(CCN(C)C)Cc2ccc2)oc(c3c1NC(=O)c4cccc4OC)cccc3</chem>	
1912	D20	81.27	1.42	<chem>S(NCCc1cccc1)(=O)(=O)c(ccc(c2C(=O)Nc(cc3)ccc3C(C)C)F)c2</chem>	
1903	E16	65.66	1.87	<chem>n1c(c2ccc(cc2)Cl)nn(c(cs3)CCNS(=O)(=O)c4c(C)cc(cc4C)C)c13</chem>	
1876	J18	76.75	1.94	<chem>c1(C(=O)N(CC2)CCN2c(ccc3C(F)(F)F)c3)c(C)oc(ncnc4N5CCCC5)c14</chem>	
1876	J08	76.86	2.04	<chem>[nH]1c2c(cc1C(=O)NCC(C)CCN3C4cc(C)ccc4C)ccc(cccn5)c25</chem>	
1876	E20	67.02	2.87	<chem>c(C)(NCCCN(CC1)CCN1c2cccc2OC=O)(cnn3c4ccc(Cl)c4)c3C(CC5)CCN5C(=O)OC(C)(C)C</chem>	
1912	M07	64.04	3.08	<chem>S(=O)(=O)(c1c(F)ccc(c1)C(=O)Nc2cc(Cl)cc(Cl)c2)N3CCc(ccc4)c34</chem>	
1897	M02	72.57	3.10	<chem>c1(sc(c2n1)ccc(C)c2C)NC(=O)c(ccc(c34)OCCO3)c4</chem>	
1914	P22	69.08	3.28	<chem>N1(Cc2cc(C)ccc2C)c3c(ccc(c3)C(=O)NCC4cccc4)Sc(cccc5)c5C1=O</chem>	
1876	F20	63.01	3.59	<chem>c(C)(NCCN1CCC(CC1)Cc2cccc2=O)(cnn3c4ccc(cc4)F)c3C(CC5)CCN5C(=O)OC(C)(C)C</chem>	
1902	A02	61.44	4.07	<chem>c1(ccc(c2c1O)ccc2)C(Nc3cccc3)c4cccc4F</chem>	
1898	H05	75.73	4.37	<chem>n1c(c2ccc(cc2)F)nn(c(cs3)CCNC(=O)c(cccc4C(F)(F)F)c4)c13</chem>	
1915	F19	66.75	4.38	<chem>c(c1)(c2c(nc1Nc3cccc3OC)cccc2)C(NCCCN(CC4)CCN4c5ccc(cc5)OC)=O</chem>	
1898	F05	71.76	5.14	<chem>c1(N(CC2)CCC2C(=O)N(CC3)CCN3c4cccc(Cl)c4)[nH]c5c(ccc(C)c5)n1</chem>	
1915	E03	81.92	5.70	<chem>C(=O)(Nc(cc1)ccc1Cl)N2CCC(c3cccc3)C2</chem>	
1910	D13	69.92	6.16	<chem>c1(Nc(cc2)ccc2F)c3c(cccc3)nc(SCc(cc4)ccc4Cl)n1</chem>	
1913	D15	77.54	6.37	<chem>N1(Cc(cc2)ccc2F)C(=O)CScc(ccc3)C(NCCc(cc4)ccc4Cl)=O)c13</chem>	
1910	P13	65.77	6.88	<chem>c1(Nc(cc2)ccc2F)c3c(cccc3)nc(SCc4cccc(Cl)c4)n1</chem>	
1875	H01	70.07	7.94	<chem>c1(c2c3ccc(cc3)F)c(on2)N=CN(CCC(=O)Nc4c(OC)cc(c(Cl)c4)OC)C1=O</chem>	
1910	N18	67.22	8.86	<chem>c(c1C)(C(=O)N(CCc2cccc2)C(N3Cc4cccc(Cl)c4)=O)c3sc1C(=O)N(CC)CC</chem>	
1872	M15	85.94	9.08	<chem>c1(c2c([nH]c1)cccc2)C(CC3)=CCN3C(=O)Nc(ccc(c4Cl)F)c4</chem>	
1871	B12	70.84	9.28	<chem>N1(c2ccc(cc2)Cl)C(=O)C(N(C3CCCC3)C1=O)CC(=O)Nc(cccc4C(OCC)=O)c4</chem>	
1910	F13	89.19	9.34	<chem>n1c(SCc(c(OC)ccc2C(C)=O)c2)nc(c3c1NCCc4cccc4)cccc3</chem>	
1911	L21	96.69	10.64	<chem>n1(c2c(C)ccc(Cl)c2)nc3c1nnc3NCCCc4cccc4</chem>	
1912	B20	106.04	10.69	<chem>c1(ccccc1F)(nc(cccc2)c2c3Nc4cccc4OC)n3</chem>	
1916	O21	88.07	10.77	<chem>c1(C(=O)Nc2c(OC)ccc(Cl)c2)c3c(sc1NCCc4cccc4)CC(C)CC3</chem>	
1809	M02	65.40	10.80	<chem>c1(SCCN([H])Cc2cccc(OC)c2OCc3ccc(cc3Cl)Cl)nnnn1C</chem>	
1912	C19	93.17	10.81	<chem>S(=O)(=O)(NCCc(ccc(c12)OCO1)c2)c(ccc(c3C(=O)Nc(ccc(c4Cl)F)c4)F)c3</chem>	
1893	C11	84.46	10.90	<chem>S(=O)(=O)(N(CC1)CCC1C(=O)Nc(ccc(c2C(F)(F)F)Cl)c2)c3c(C)noc3\C=C\c4c(C)cc(cc4C)C</chem>	
1897	G14	96.29	10.91	<chem>c1(cnc(c(cccc2)c12)NCCc(cc3)ccc3Cl)C(OCC)=O</chem>	
1912	I10	82.86	10.93	<chem>n1(c2c(nc1\C=C\c3)ccc3SC)cccc2)S(=O)(=O)c4ccc(c(C)c4)F</chem>	
1811	A21	81.15	10.95	<chem>c1(Nc2ccc(c(OC)c2)OC)c3c(CCCC3)nc(ccc(c4)NC(=O)c5cc(OC)cc(OC)c5)c14</chem>	
1875	M16	71.51	11.03	<chem>c1(c(C)[nH]c(C)c1C(OCC)=O)S(=O)(=O)N(CC2)CCN2c(cccc3C(F)(F)F)c3</chem>	
1876	P04	71.38	11.11	<chem>c(C(=O)NCC(CC1)CCN1CCc(cc2)ccc2OC)(cnn3c4ccc(Cl)c4)c3C(CC5)CCN5C(=O)OC(C)(C)C</chem>	
1912	O14	86.14	11.17	<chem>S(=O)(=O)(N1CCCC1)c2c(F)ccc(c2)C(=O)Nc3cc(Cl)cc(Cl)c3</chem>	
1900	C04	80.04	11.17	<chem>C1(=O)c2c(cccc2)Sc(ccc(c3)NC(=O)Nc4cccc(c4C)[N+](=O)[O-])c3N1CC</chem>	
1919	D22	96.68	11.70	<chem>C1(=N)N(CC)c2c(cccc2)N1CCOc(cc3)ccc3Br</chem>	
1878	B09	98.06	12.20	<chem>c1(nc(C)cc2C(=O)Nc(cccc3C(F)(F)F)c3)c2c(nn1c4ccc(cc4)CC)C</chem>	
1912	M20	83.22	12.24	<chem>S(=O)(=O)(NC1CCCCC1)c2c(F)ccc(c2)C(=O)Nc(cc3)ccc3Br</chem>	
1878	H05	91.94	12.53	<chem>S(=O)(=O)(N(C)Cc1cccc1)c(ccc2c3c4c([nH]2)CCCC4)c3</chem>	
1915	N22	109.11	12.59	<chem>S(=O)(=O)(c(cccc1)c1C(N2Cc3cccc(Cl)c3)=O)c(ccc(c4)C(NCCCN5CCCC5CC)=O)c24</chem>	
1893	F12	100.83	12.68	<chem>C(CO(c12)ccc(Br)c1)(C(=O)NCCc3cccc(F)c3)=C2</chem>	
1911	D11	97.66	12.69	<chem>c1(N([H])C(=O)c(cc2)ccc2S(=O)(=O)N(CCC)CCC)sc(c(CCN3CC)c1C(OC)=O)C3</chem>	
1911	B16	89.36	12.70	<chem>n1(c2cccc2)nc3c1nnc3NNC(=O)c(cc4)ccc4C(C)(C)C</chem>	
1876	F06	99.42	12.87	<chem>c(C(=O)NCC(CC1)CCN1Cc2cccc2OC)(cnn3c4ccc(Cl)c4)c3C(CC5)CCN5C(=O)OC(C)(C)C</chem>	
1911	N17	96.72	12.95	<chem>n1(c2cccc(Cl)c2)nc3c1nnc3NCCCc4cccc4</chem>	
1875	N12	77.50	13.03	<chem>c1(cc(C)c2c(ccc(c2)NC(=O)Nc(cc3)ccc3Cl)n1)N(CC4)CCN4C</chem>	
1898	I02	95.20	13.41	<chem>c1(N(CC2)CCC2C(=O)Nc(ccc(c3Cl)C)c3)[nH]c(c4n1)cccc4</chem>	
1912	B13	67.54	13.43	<chem>S(=O)(=O)(NCC1cccc1Cl)c2c(F)ccc(c2)C(=O)Nc3cc(Cl)cc(Cl)c3</chem>	
1916	I02	96.28	13.43	<chem>N1(c2cccc(Cl)c2)C(=N)c(c(C)[nH]3)c3N=C1SCC(=O)Nc4cccc(C)c4</chem>	
1900	A04	100.61	14.04	<chem>C1(=O)c2c(cccc2)Sc(ccc(c3)NC(=O)Nc(ccc(c4C)Br)c4)c3N1CC</chem>	
1916	P08	102.20	14.12	<chem>N1(c2ccc(c(C)c2)C)C(=O)c(c3)c(N=C1SCc4cccc(F)c4)[nH]n3</chem>	
1912	B07	76.99	14.14	<chem>S(=O)(=O)(NCC1cccc1OC)c2c(F)ccc(c2)C(=O)Nc(cccc3C(F)(F)F)c3</chem>	
1913	B21	85.43	14.25	<chem>N1(Cc2cccc(C)c2)c3c(ccc(c3)C(NCCCN(CC4)CCO4)=O)Sc(cccc5)c5C1=O</chem>	
1872	N09	81.48	14.62	<chem>n1(CC2C)c(c(S2)ccc3)c3cc1C(=O)NCCc4cccc(Br)c4</chem>	

Table A2.2 (Continued)

Plate	Well	Average percent survival		SMILES	Annotation
		minus β-lactam	plus β-lactam		
1916	D05	77.12	14.74	<chem>N1(c2ccc(cc2)CC)C(=O)c(c3)c(N=C1SCc4cccc4F)[nH]n3</chem>	
1895	E15	87.24	14.79	<chem>c1(C(OCC)=O)c(C)c([nH]c1C)CCC(NCCCN(CC2)CCN2c3c(C)ccc(Cl)c3)=O</chem>	
1898	C07	88.15	14.83	<chem>c1(N2CCC(CC2)C(=O)NCC3cccc(C)c3)[nH]c4c(ccc(Cl)c4)n1</chem>	
1897	N02	96.61	15.04	<chem>c1(NC(CSc2nccn2Cc(cc3)ccc3Cl)=O)sc(c4n1)cccc4</chem>	
1911	N18	78.08	15.20	<chem>n1(c2cccc(Cl)c2)ncc3c1nenc3NCCC4=CCCC4</chem>	
1877	C19	109.06	15.23	<chem>c12n(ncc1C(=O)Nc(cc3)ccc3F)C(C=C(c4cccc(OC)c4)N2)c5cccc5F</chem>	
1902	K05	108.40	15.29	<chem>n1c(CCN(C(=O)c2ccc(c(C)C)c2)C)Csc1c3ccc(cc3)C</chem>	
1914	H05	76.97	15.34	<chem>c1(cc(Br)ccc1OC)CNC(=O)CCSCc(cc2)ccc2Cl</chem>	
1906	E07	78.16	15.42	<chem>N1=C(SCC(=O)Nc2c(C)cc(cc2C)C)C3=C(N(Cc4ccco4)C1=O)CCC3</chem>	
1900	F01	89.34	15.44	<chem>n1c(C)onc1c2cccc(c2)NC(=O)Nc(cc3)ccc3[N+](=O)[O-]</chem>	
1917	B21	108.31	15.53	<chem>c1(C(F)(F)F)c2c(n(CC(=O)Nc3cccc(Cl)c3)n1)CCCC2</chem>	
1912	N18	76.50	15.57	<chem>N1(c2ccc(c(Cl)c2)OC)C\C=C(c(cccc3C(F)(F)F)c3)=Nc(c4C1=O)cccc4</chem>	
1911	D15	98.43	15.75	<chem>S(=O)(=O)(c(cc1)ccc1C(=O)N([H])c2sc(c(CCN3CC)c2C(OC)=O)C3)N4CCCC(C)C4</chem>	
1911	K20	103.92	16.11	<chem>n1(c2ccc(c(Cl)c2)C)ncc3c1nenc3NC4CCCCC4</chem>	
1911	M16	93.08	16.11	<chem>n1(c2cccc(Cl)c2)ncc3c1nenc3NC4CCCCC4</chem>	
1895	I16	81.67	16.16	<chem>[nH]1c(SCC(=O)NCc2cc(Br)ccc2OC)nnc1c3cccc3</chem>	
1911	F15	101.98	16.17	<chem>n1(c2cccc(Cl)c2)ncc3c1nenc3NCCc(cc4)ccc4OC</chem>	
1911	D16	88.16	16.18	<chem>S(=O)(=O)(c(cc1)ccc1C(=O)N([H])c2sc(c(CCN3C(C)C)c2C(OC)=O)C3)N4CCCC(C)C4</chem>	
1909	H22	92.68	16.18	<chem>N12C(c3c(ccc3)N=C1SCC(=O)Nc(cc4)ccc4C(C)C)=NC(CC(=O)NCCc5cccs5)C2=O</chem>	
1917	E02	73.94	16.26	<chem>S(=O)(=O)(NCc1cccc1)c2c(Br)ccc(c2)C(=O)Nc(cc3)ccc3Br</chem>	
1911	N09	93.14	16.31	<chem>n1(c2ccc(c(C)C)c2)C)ncc3c1nenc3Nc(cccc4C(F)(F)F)c4</chem>	
1902	B03	101.71	16.59	<chem>n1(ccnc1SCC(=O)Nc2cccc(ccc3)c23)c4cccc(Cl)c4</chem>	
1915	E02	71.14	16.62	<chem>c1(c2c(sc1NCc(ccc(c3OC)OC)c3)CCCC2)C(=O)Nc(cc4)ccc4C(OC)=O</chem>	
1909	N22	101.33	16.68	<chem>N12C(c3c(ccc3)N=C1SCC(=O)Nc(cc4)ccc4C(C)C)=NC(CC(=O)NCCc5cccs5)C2=O</chem>	
1890	N15	79.18	16.75	<chem>c1(C2c3ccc(cc3)F)c(CCN2C(=O)Nc(ccc(c4Cl)F)c4)c(c(C)s1)CC</chem>	
1878	O21	96.76	16.86	<chem>n1(c2cccc(F)c2)nc(c3c1nc(C)cc3C(=O)NCC4cccc4)C</chem>	
1911	H15	99.20	16.86	<chem>c1(c(c2cccc2)cn3c4ccc(c(Cl)c4)C)c3nenc1N([H])c(cc5)ccc5NC(C)=O</chem>	
1876	P14	104.06	16.88	<chem>[nH]1c2c(cc1C(=O)NCC(CC3)CCN3Cc(cc4)ccc4C)ccc(cccn5)c25</chem>	
1866	K19	83.05	17.10	<chem>n(CCC(=O)N1CCCCC1)(c(ccc2)c2c3SCc(cc4)ccc4F)c3</chem>	
1871	D15	96.07	17.13	<chem>c1(n2cccc2)c(C(NCCCN(CC3)CCN3c4cccc(Cl)c4)=O)c(nn1c5ccc(cc5)F)C</chem>	
1872	G19	86.09	17.20	<chem>n1(CC2C)c(c(S2)ccc3)c3cc1C(NCCc(cc4)ccc4Cl)=O</chem>	
1892	A17	107.62	17.22	<chem>S(=O)(=O)(Nc(cccc1c2ccc(nn2)OC)c1)c3c(C)cc(c(C)c3)Cl</chem>	
1871	C16	69.23	17.23	<chem>S(=O)(=O)(c(cc1)ccc1n2cccn2)Nc3ccc(cc3F)F</chem>	
1902	N16	91.82	17.26	<chem>N(CC1)(CCN1c2cccc2)C(CNC(=O)c(ccc(c3F)F)c3)c(ccc(c45)OCO4)c5</chem>	
1872	K17	98.46	17.40	<chem>S(=O)(=O)(c(cc1)ccc1c(cc(n2)C)o2)Nc3ccc(cc3C)Cl</chem>	
1911	A22	113.71	17.51	<chem>n1(c2ccc(cc2C)C)ncc3c1nenc3Nc4cccc(Cl)c4</chem>	
1876	N18	96.59	17.71	<chem>c(C(=O)NCC(CC1)CCN1c2cccc2OC)(cnn3c4ccc(cc4)Cl)c3C(CC5)CCN5C(=O)OC(C)(C)C</chem>	
1911	K17	97.49	17.77	<chem>n1(c2c(C)ccc(Cl)c2)ncc3c1nenc3NCC4cccc4</chem>	
1905	M06	95.37	17.86	<chem>c1(sc(c2C)CCNC(=O)c3ccc(Br)o3)n2nc(c4ccc(cc4)Cl)n1</chem>	
1904	M22	76.80	18.08	<chem>c1(c(CC2)c(sc1NC(CSc3cccc3)=O)CN2CC)c4sc(c5n4)cccc5</chem>	
1909	B16	104.84	18.38	<chem>N12C(c3c(ccc3)N=C1SCC(=O)Nc(cc4)ccc4C(C)C)=NC(CC(=O)NCCc5cccs5)C2=O</chem>	
1875	N16	96.20	18.62	<chem>[nH]1c2c(cc1C(=O)NCC3cccc3OC)ccc(ccc(C)n4)c24</chem>	
1910	L04	78.20	18.72	<chem>c1(Nc2cc(OC)cc(OC)c2)c3c(ccc3)nc(SCC(=O)c(ccc(c4Cl)Cl)c4)n1</chem>	
1918	D01	99.87	18.72	<chem>c12c(c(nnc1N3CCC(CC3)C(=O)NCC4cccc(Cl)c4)C)c(n(c5cccc5)n2)C</chem>	
1917	N12	91.81	18.81	<chem>N(Cc1cccc1C)(c2c(C3(O)CC(c4cccc4)=O)cc(Cl)c2)C3=O</chem>	
1911	E20	110.12	19.02	<chem>n1(c2ccc(cc2)Cl)ncc3c1nenc3NC4CCCC4</chem>	
1873	A14	101.44	19.13	<chem>n1(Cc(cc2)ccc2C=C)c(cc(C)cc3)c3c(CNCc4cccc4)c1C(O)=O</chem>	
1866	K21	75.95	19.35	<chem>n(CCC(=O)N1CCCCC1)(c(ccc2)c2c3SCc(cc4)ccc4C(F)(F)F)c3</chem>	
1891	D18	100.68	19.36	<chem>n1(nc(n2)c3ccc(cc3)C)c2nc(C)cc1NCc4cccc(OC)c4</chem>	
1913	J21	104.51	19.51	<chem>N1(Cc2cccc2)C(=O)CSc(ccc(c3)C(NCCc(cc4)ccc4Cl)=O)c13</chem>	
1900	K08	86.98	19.65	<chem>S(=O)(=O)(Nc(cccc1C(C)=O)c1)c(ccc2c3c4c([nH]2)CCCCC4)c3</chem>	
1910	N13	78.97	19.82	<chem>n1(c2cccc(C)c2)ncc3c1nenc3Nc(cc4)ccc4Oc(cc5)ccc5Cl</chem>	
1894	E22	100.51	20.37	<chem>S(=O)(=O)(N(CC1)CCN1c2cccc(C)c2)C3n[nH]c(C(OC)=O)c3</chem>	
1911	P01	98.48	20.46	<chem>n1(c2ccc(c(Cl)c2)C)ncc3c1nenc3NCCN(ccn4)c4</chem>	
1911	H18	84.82	20.50	<chem>n1(c2cccc(Cl)c2)ncc3c1nenc3NCCc4cccc4</chem>	
1913	M05	74.68	20.62	<chem>c1(nc2C)n(nc(SCC(=O)NC3CCC(CC3)C)n1)c(c2Cc4cccc4Cl)C</chem>	
1911	I04	96.85	20.81	<chem>n1(c2ccc(cc2)Cl)ncc3c1nenc3NNC(=O)c(cc4)ccc4C(C)C</chem>	
1870	J04	93.80	20.84	<chem>c1(cnc(nc1C(F)F)F)SC(=O)NCC2cccc2Cl</chem>	
1857	P01	87.25	21.00	<chem>C1(=O)c2c(ccc2)Sc(ccc(c3)NC(NCCC(C)C)=O)c3N1C</chem>	

Plate	Well	Average percent survival		SMILES	Annotation
		minus β-lactam	plus β-lactam		
1911	B17	98.14	21.01	S(=O)(=O)(c(cc1)ccc1C(=O)N([H])c2sc(c(CCN3C(C)C)c2C(N)=O)C3)N(C)C4CCCC4	
1912	D01	94.61	21.03	n1c(c2ccc(cc2)Br)nc(c3c1N4CCC(CC4)C(OCC)=O)cccc3	
1877	D19	110.77	21.06	c(C(NCCN(CCc(c12)cccc1)C2)=O)(cnn3c4ccc(c(C)c4)C)c3C(CC5)CCN5C(=O)OC(C)(C)C	
1912	M19	97.56	21.16	S(=O)(=O)(NC1CCCCC1)c(ccc(c2C(=O)Nc(ccc(c3F)F)c3)F)c2	
1910	N07	86.44	21.30	c1(Nc2cc(OC)cc(OC)c2)c3c(cccc3)nc(SCc4cccc4F)n1	
1833	K07	75.15	21.35	c12n(c(c3c(NC4CCCC4)n1)cccc3)nnc2c5ccc(cc5)Cl	
1878	O02	85.34	21.39	c1(cn(cc1S(=O)(=O)NC(C)(C)C)CC(=O)Nc(cc(C)cc2C)c2)S(=O)(=O)NC(C)(C)C	
1907	D16	89.13	21.57	n1(Cc(cc2)ccc2C)c3c(cc1CN(CC4)CCC4C(=O)NCc5cccc5C)cccc3	
1912	D14	81.49	21.63	S(=O)(=O)(NCc(cc1)ccc1OC)c2c(F)ccc(c2)C(=O)Nc3cc(Cl)cc(Cl)c3	
1905	G21	88.73	21.70	c1(sc(c2C)CCN5(=O)=O)c3c(F)ccc(F)c3)n2nc(c4ccc(cc4)C)n1	
1918	J03	90.88	21.78	S(=O)(=O)(Nc(cc1)ccc1OCC)c(ccc(c23)SCCC(=O)N2)c3	
1907	J19	91.51	21.83	c1(c(cc2)cc(c2NC(Cc(cc3)ccc3OC)=O)Cl)sc(c4n1)cccc4	
1826	I05	80.25	22.05	c1(SCC(=O)N(CCCC)CC)c2c(CCCC2)nc(ccc(Cl)c3)c13	
1823	N13	93.00	22.20	N1(Cc2c(cccc2Cl)F)c(c3)c(ccc3C(=O)N4CCCC4)Sc(cccc5)c5C1=O	
1807	C05	73.60	22.25	n1(C)c(NCc(cc2)ccc2CC)ncc1c3cccc(OC)c3	
1878	C21	115.62	22.30	n1(c2cccc(F)c2)nc(c3c1nc(C)c3C(NCCc(cc4)ccc4Cl)=O)C	
1898	F13	103.42	22.33	S(=O)(=O)(c1ccc(cc1)Cl)C(CNC(Cc(cc2)ccc2Cl)=O)c3cccc3	
1913	H13	88.85	22.46	S(NCCc(cc1)ccc1Cl)(=O)(=O)c(ccc(c2C(=O)Nc(cc3)ccc3C)F)c2	
1865	L03	72.60	22.60	c12n(c(c3c(NC4CCCC4)n1)ccc3)nnc2S(=O)(=O)c5ccc(c(C)c5)C	
1898	F11	91.55	22.79	c1(N(CC2)CCC2C(=O)N(CC3)CCN3c4cccc(C)c4C)[nH]c5c(ccc(C)c5)n1	
1918	K16	74.27	22.84	c12n(c3c(cccc3)nc1Nc(ccc(c4C)Br)c4)c(nn2)CC	
1812	O19	77.00	22.95	c1(OC(=O)c2cccc(OC)c2OC)n(C(C)(C)C)nc(C)c1Sc(cc3)ccc3C	
1915	L20	104.85	23.05	c1(C(=O)Nc2cccc2OC)c3c(sc1NCc4ccc(C)o4)CC(C)CC3	
1917	L05	99.91	23.15	n1(C)c(c2cccc2)cnc1NCc(cc3)ccc3SC	
1871	B03	94.99	23.19	N1(c2ccc(cc2)Cl)C(=O)C(N(Cc3ccco3)C1=O)CC(=O)Nc(cc4)ccc4C(OC)=O	
1878	D05	95.01	23.51	S(=O)(=O)(Nc(cccc1C(C)=O)c1)c(ccc2c3c4c([nH]2)CCCC4)c3	
1912	K02	106.77	23.53	S(NCCc1cccc1)(=O)(=O)c2c(F)ccc(c2)C(=O)Nc(ccc(c3F)C)c3	
1907	J21	98.63	23.54	c1(c2ccc(cc2C)NC(=O)c3cccc3OC)sc(c4n1)cccc4	
1911	K03	93.06	23.56	n1(c2c(C)ccc(Cl)c2)ncc3c1nnc3NCCc(cc4)ccc4OC	
1877	E19	109.11	24.07	c(C(NCCN1CCC(CC1)Cc2cccc2)=O)(cnn3c4cccc4)c3C(CC5)CCN5C(=O)OC(C)(C)C	
1918	M09	86.63	24.11	n1(CC2)c(c(S2)ccc3)c3cc1C(=O)NCc(cc4)ccc4F	
1918	D15	78.19	24.11	n1c(c2cccc(c2)NC(C)=O)onc1c3cccc3	
1916	C03	88.55	24.25	n(CCC(=O)Nc(cc1)ccc1C(C)C)(c2C)c(c3cccc3)cc2C(C)=O	
1898	G05	110.16	24.31	c1(c(C)onc1c2ccc(cc2F)F)C(=O)Nc(cccc3C(F)F)F)c3	
1915	O14	101.09	24.34	c1(ccc(CSCc2cccc(Cl)c2)o1)C(NCCc(cc3)ccc3Cl)=O	
1878	G07	99.62	24.87	S(=O)(=O)(c(ccc1c2c3c([nH]1)CCCC3)c2)N(CC4)CCN4c5cccc(C)c5C	
1875	C20	76.56	24.90	N1(CC(C)C)C=C(c(c2C1=O)cccc2)NC(=O)N(CC3)CCN3c4cccc(C)c4C	
1914	O22	85.29	24.97	C(=O)(Nc(ccc(c1Cl)Cl)c1)N(CCC(C)C)C(C)c2cccs2	
1871	P01	93.28	24.99	N1(c2ccc(cc2)Cl)C(=O)C(N(C3CCCC3)C1=O)CC(=O)Nc(cc4)ccc4CC	

Table A2.3: High-throughput screening hits identified as potentially causing growth defects, prioritized by percent survival in the presence of β -lactam.

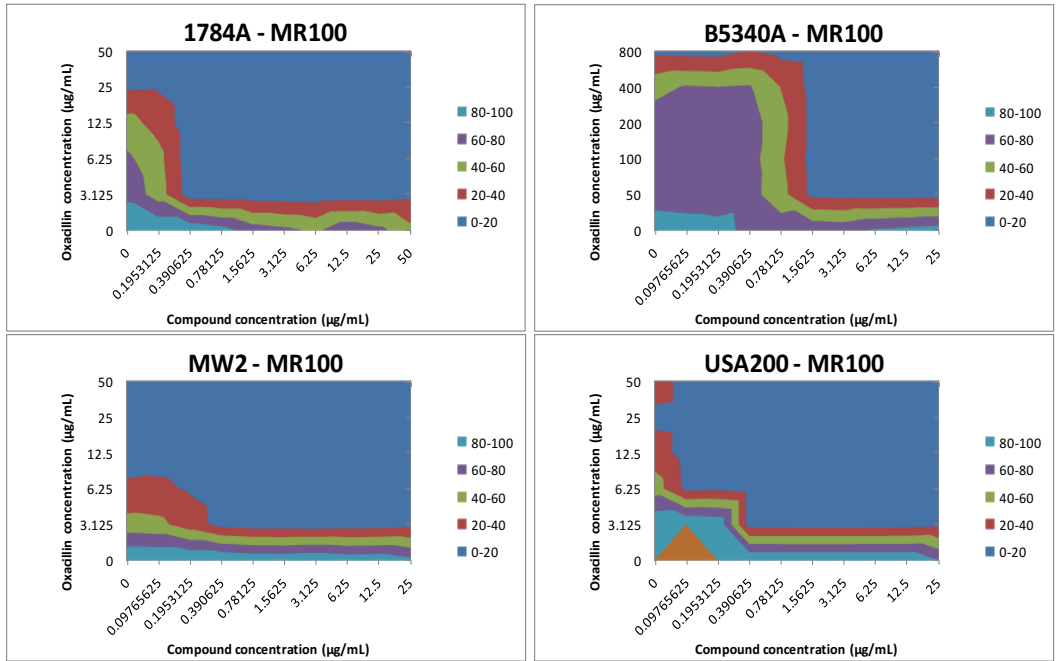
Plate	Well	Average percent survival		SMILES	Annotation
		minus β -lactam	plus β -lactam		
1919	L04	66.79	0.26	<chem>C1(=N)N(CC)c2c(cccc2)N1CCOC(cc3)ccc3Br</chem>	
1877	D02	79.44	0.61	<chem>c1(C(=O)N(CCN(C)C)Cc2ccco2)oc(c3c1NC(=O)c4cccc4OC)cccc3</chem>	
1912	J18	60.07	0.71	<chem>S(=O)(=O)(NC1CCCC1)c(ccc(c2C(=O)Nc(cc3)ccc3Br)F)c2</chem>	
1877	M05	61.49	0.72	<chem>c(C(NCCN1CCC(CC1)Cc2ccccc2)=O)(cnn3c4cccc4)c3C(CC5)CCN5C(=O)OC(C)(C)C</chem>	
1903	E16	65.66	1.87	<chem>n1c(c2ccc(cc2)Cl)nn(c(cs3)CCNS(=O)(=O)c4c(C)cc(cc4C)C)c13</chem>	
1876	J18	76.75	1.94	<chem>c1(C(=O)N(CC2)CCN2c(cccc3C(F)(F)F)c3)c(C)oc(ncn4N5CCCC5)c14</chem>	
1876	J08	76.86	2.04	<chem>c(C(NCCCN(CC1)CCN1c2ccccc2OC)=O)(cnn3c4cccc(Cl)c4)c3C(CC5)CCN5C(=O)OC(C)(C)C</chem>	
1894	B06	59.74	2.77	<chem>n1c(cc2)c(ccc1CCc3ccccc3)cc2C(NCCCN(CC4)CCN4c5ccccc5F)=O</chem>	
1876	E20	67.02	2.87	<chem>c1(cc(c2[nH]1)ccc(cccn3)c23)C(=O)N(C(C)C)Cc4cccc4</chem>	
1912	M07	64.04	3.08	<chem>S(NCCc1ccccc1)(=O)(=O)c(ccc(c2C(=O)Nc(cc3)ccc3C(C)C)F)c2</chem>	
1897	M02	72.57	3.10	<chem>c1(cnc(c(ccccc2)c12)NCC(cc3)ccc3Cl)C(OCC)=O</chem>	
1914	P22	69.08	3.28	<chem>N1(Cc2cc(C)ccc2C)c3c(ccc(c3)C(=O)NCC4cccc4)Sc(cccc5)c5C1=O</chem>	
1874	C04	56.06	3.38	<chem>c1(C2=O)c(c3c(ccccc3)n1C)C(N2CC(NCCC)=O)c4ccc(cc4)OC</chem>	
1876	F20	63.01	3.59	<chem>c(C(NCCN1CCC(CC1)Cc2ccccc2)=O)(cnn3c4ccc(cc4)F)c3C(CC5)CCN5C(=O)OC(C)(C)C</chem>	
1902	A02	61.44	4.07	<chem>c1(ccc(c2c1O)cccn2)C(Nc3cccn3)c4cccc4F</chem>	
1871	N21	57.20	4.07	<chem>N1(c2ccccc2)C(=O)C(N(Cc(cc3)ccc3F)C1=O)CC(=O)Nc(cc4)ccc4OCCCC</chem>	
1898	H05	75.73	4.37	<chem>c1(N(CC2)CCC2C(=O)N(CC3)CCN3c4cccc(Cl)c4)[nH]c5c(ccc(C)c5)n1</chem>	
1915	F19	66.75	4.38	<chem>c1(c2c(sc1NCc3cc(OC)ccc3OC)CCCC2)C(=O)Nc4c(OC)ccc(OC)c4</chem>	
1913	K05	57.45	5.01	<chem>N1(Cc2cccc(C)c2)c3c(ccc(c3)C(NCCCN(CC4)CCO4)=O)Sc(cccc5)c5C1=O</chem>	
1898	F05	71.76	5.14	<chem>c1(N(CC2)CCC2C(=O)N(CC3)CCN3c4cccc(Cl)c4)[nH]c5c(ccc(C)c5)n1</chem>	
1870	J16	58.78	5.23	<chem>S(=O)(=O)(NC1CCCC1)c(ccc(c23)OCC(=O)N2CC(=O)Nc(cc4)ccc4Cl)c3</chem>	
1890	L09	57.42	5.49	<chem>c1(C2c3ccccc3)c(CCN2Cc4cccc(OC)c4)c(c(C)s1)CC</chem>	
1910	L11	55.46	5.78	<chem>c1(Nc2cc(OC)cc(OC)c2)c3c(cccc3)nc(SCc4cccc4Cl)n1</chem>	
1910	D13	69.92	6.16	<chem>N1(Cc2cccc(Cl)c2)C(=O)N(c3ccc(c(C)c3)C)C(c(c(c4C(=O)N(CC)CC)C)c1s4)=O</chem>	
1913	D15	77.54	6.37	<chem>S(=O)(=O)(NC1CCCC1)c2c(F)ccc(c2)C(=O)Nc3cc(Cl)cc(Cl)c3</chem>	
1912	N22	56.19	6.65	<chem>S(=O)(=O)(NCC1ccccc1Cl)c2c(F)ccc(c2)C(=O)Nc3cc(Cl)cc(Cl)c3</chem>	
1910	P13	65.77	6.88	<chem>c1(Nc(cc2)ccc2F)c3c(cccc3)nc(SCc(cc4)ccc4Cl)n1</chem>	Analog of 1910B15
1875	H01	70.07	7.94	<chem>c1(c2c3ccc(cc3)F)c(on2)N=CN(CCC(=O)Nc4c(OC)cc(c(Cl)c4)OC)C1=O</chem>	
1910	B15	50.21	8.72	<chem>N1(Cc2ccc(cc2Cl)F)C(=O)N(CCC3ccccc3)C(c(c(c4C(=O)N(CC)CC)C)c1s4)=O</chem>	Reconfirmed
1910	N18	67.22	8.86	<chem>c(c1C)C(=O)N(CCc2ccccc2)C(N3Cc4cccc(Cl)c4)=O)c3sc1C(=O)N(CC)CC</chem>	
1878	G06	54.62	8.99	<chem>S(=O)(=O)(c(ccc1c2c3c([nH]1)CCCC3)c2)Nc4ccccc4C</chem>	
1871	B12	70.84	9.28	<chem>c1(n2ccccc2)c(C(NCCCN(CC3)CCN3c4cccc(Cl)c4)=O)c(nn1c5ccc(cc5)F)C</chem>	
1807	I03	50.50	9.80	<chem>n1(C)c(NCc(cc2)ccc2CC)nc1c3cccc(OC)c3</chem>	
1908	D19	57.78	10.26	<chem>C1(=Cc(cc(C)(C)C)cc2C(C)C)c2OC1=O)c3[nH]c(c(ccc4C(O)=O)n3)c4</chem>	
1912	L06	58.21	10.69	<chem>S(=O)(=O)(c1ccc(cc1)NC(C)=O)N(Cc(cc2)ccc2C(OCC)=O)Cc(cc3)ccc3C</chem>	
1809	M02	65.40	10.80	<chem>c1(SCCN([H])Cc2cccc(OC)c2OCc(cc3)ccc3Cl)nnnn1C</chem>	
1875	M16	71.51	11.03	<chem>c1(c(C)[nH]c(C)c1C(OC)=O)S(=O)(=O)N(CC2)CCN2c(cccc3C(F)(F)F)c3</chem>	
1876	P04	71.38	11.11	<chem>c(C(=O)NCC(CC1)CCN1CCc(cc2)ccc2OC)(cnn3c4cccc(Cl)c4)c3C(CC5)CCN5C(=O)OC(C)(C)C</chem>	
1900	I08	55.26	11.54	<chem>S(=O)(=O)(Nc(ccc(c1C)C)c1)c(ccc2c3c4c([nH]2)CCCCC4)c3</chem>	
1827	P14	55.70	12.05	<chem>S(=O)(=O)(c(cccc1)c1C(N2Cc(cc3)ccc3Cl)=O)c(ccc(c4)C(NCCCN5CCCC(C)C5)=O)c24</chem>	
1890	J09	60.92	12.72	<chem>c1(C2c3ccccc3)c(CCN2Cc4cccc4)c(c(C)s1)CC</chem>	
1875	N12	77.50	13.03	<chem>c1(cc(C)c2c(ccc(c2)NC(=O)Nc(cc3)ccc3Cl)n1)N(CC4)CCN4C</chem>	
1912	B13	67.54	13.43	<chem>S(NCCC1=CCCC1)(=O)(=O)c(ccc(c2C(=O)Nc(cc3)ccc3C(C)C)F)c2</chem>	Did not retest
1850	F17	61.35	13.60	<chem>C(=O)(NCC(CCN1Cc(cc2)ccc2C)C1)Nc(cc3)ccc3Cl</chem>	
1912	B07	76.99	14.14	<chem>N1(c2ccc(c(Cl)c2)OC)C(\C=C\c(cccc3C(F)(F)F)c3)=Nc(c4C1=O)cccc4</chem>	
1907	B21	56.07	14.63	<chem>c1(c2ccc(cc2C)NC(Cc(ccc(c3OC)OC)c3)=O)sc(c4n1)cccc4</chem>	
1916	D05	77.12	14.74	<chem>N1(c2ccc(cc2)C)C(=N)c(C)N[nH]3)c3N=C1SCC(=O)Nc4cccc(Cl)c4</chem>	
1911	N18	78.08	15.20	<chem>S(=O)(=O)(c(cc1)ccc1C(=O)N([H])c2sc(c(CCN3C(C)C)c2C(N)=O)C3)N(C)C4CCCC4</chem>	

Table A2.3 (Continued)

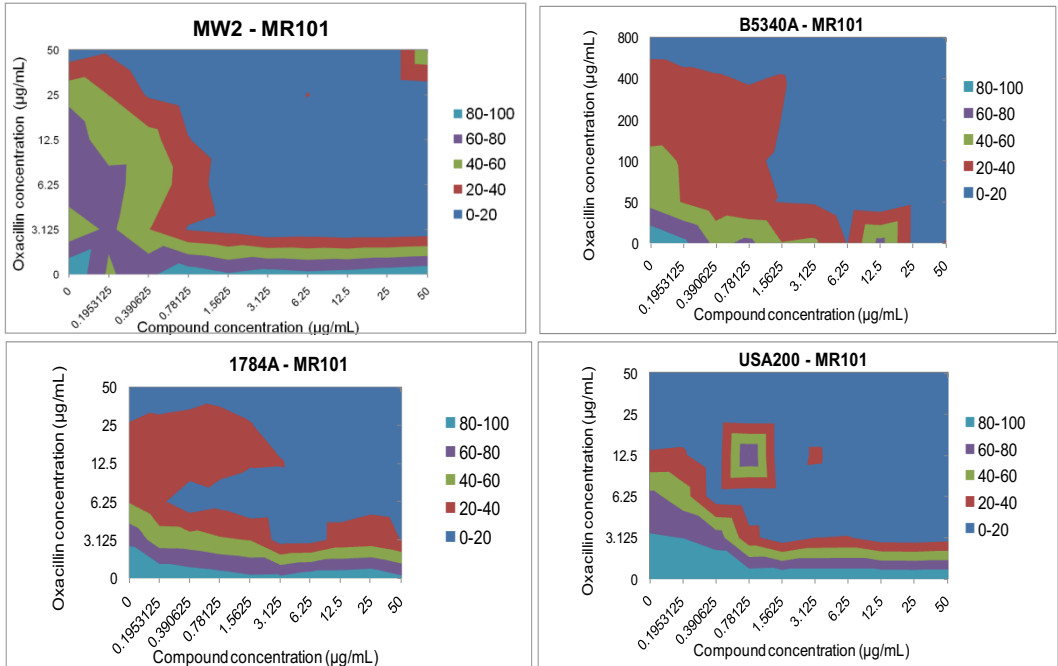
Plate	Well	Average percent survival		SMILES	Annotation
		minus β-lactam	plus β-lactam		
1806	G22	51.05	15.20	<chem>C(F)(F)(F)c(cc1cccc1)nc2SCCC(=O)Nc3cccc(O)c3)n2</chem>	
1914	H05	76.97	15.34	<chem>N1(Cc2cc(C)ccc2C)c3c(ccc(c3)C(=O)Nc4cccc4)Sc(cccc5)c5C1=O</chem>	
1906	E07	78.16	15.42	<chem>N1=C(SCC(=O)Nc2c(C)cc(cc2C)C)C3=C(N(Cc4cccc4)C1=O)CCC3</chem>	
1912	N18	76.50	15.57	<chem>S(=O)(=O)(NCc(cc1ccc1OC)c2c(F)ccc(c2)C(=O)Nc3cc(Cl)cc(Cl)c3</chem>	
1889	P22	61.94	15.75	<chem>c1(ncc(c(CCN2C(c3)ccc3C)n1)C2)N(CC4)CCN4c5ncccc5</chem>	
1869	O08	62.65	16.10	<chem>c1(sc(c2n1)ccc(C)c2C)N(CCN(CC)CC)C(=O)c3cccc3</chem>	
1917	E02	73.94	16.26	<chem>S(=O)(=O)(NCc1cccc1)c2c(Br)ccc(c2)C(=O)Nc(cc3)ccc3Br</chem>	
1851	O07	56.95	16.50	<chem>c1(SCCCN([H])Cc(ccc2c3cccc(Cl)c3C)o2)nnnn1C</chem>	
1915	E02	71.14	16.62	<chem>c(c1)(c2c(nc1Nc3cccc3OC)cccc2)C(NCCCN(CC4)CCN4c5ccc(cc5)OC)=O</chem>	
1890	N15	79.18	16.75	<chem>c1(C2c3ccc(cc3)F)c(CCN2C(=O)Nc(ccc(c4Cl)F)c4)c(c(C)s1)CC</chem>	
1854	F15	65.65	16.85	<chem>S(=O)(=O)(c1ccc(cc1)Cl)Nc(ccc2c3oc(n2)c4ccc(cc4)OC)c3</chem>	Did not retest
1878	G02	59.93	17.07	<chem>S(=O)(=O)(NCc(cc1ccc1N(C)C)c(ccc2c3c4c([nH]2)CCCC4)c3</chem>	
1871	C16	69.23	17.23	<chem>S(=O)(=O)(c(cc1)ccc1n2cccn2)Nc3ccc(cc3F)F</chem>	
1808	F17	50.40	17.25	<chem>c1(c(nc(CCN2C(C)=O)c(C2)c1C(F)(F)F)sc3C(=O)c4ccc(cc4)F)c3N</chem>	
1901	G20	52.02	17.61	<chem>c1(C2=O)c(c3c(cccc3)[nH]1)N=C(SCC(=O)Nc(cccc4C(F)(F)F)c4)N2c5cccc5</chem>	
1817	O09	63.60	17.70	<chem>c(c1c2cccc1)(cc(n2)c3ccc(Cl)s3)C(=O)Nc(cccc4C(F)(F)F)c4</chem>	
1904	M22	76.80	18.08	<chem>c1(sc(c2n1)cccc2)N(Cc(cccn3)c3)C(C4CCCC4)=O</chem>	
1820	J06	51.45	18.55	<chem>c1(nc2c(nc1Nc(ccc(c3Cl)OC)c3)ccc(C)c2)n4c(C)cc(C)n4</chem>	
1910	L04	78.20	18.72	<chem>c1(Nc(cc2)ccc2F)c3c(cccc3)nc(SCc4ccc(F)c4)n1</chem>	
1866	K21	75.95	19.35	<chem>n(CC(=O)N1CCCCC1)(c(cccc2)c2c3SCc(cc4)ccc4C(F)(F)F)c3</chem>	
1910	N13	78.97	19.82	<chem>c1(Nc2cc(OC)cc(OC)c2)c3c(cccc3)nc(SCC(=O)c(ccc(c4Cl)Cl)c4)n1</chem>	
1806	D10	59.55	19.90	<chem>c1(c(ccc(c2NC(=O)c3cccc3OC)OC)c2)sc(c4n1)cccc4</chem>	
1809	N04	69.75	19.90	<chem>c1(c(cccc2NC(=O)c3cccc(cccc4)c34)c2)oc5c(ccc(C)c5)n1</chem>	
1864	E17	64.55	20.55	<chem>c1(ccc(CS(=O)c2ccc(cc2)C)o1)C(=O)Nc(cc3)ccc3OC(C)C</chem>	
1913	M05	74.68	20.62	<chem>S(NCCc(cc1)ccc1Cl)(=O)(=O)c(ccc(c2C(=O)Nc(cc3)ccc3C)F)c2</chem>	Did not retest
1838	O07	52.25	21.15	<chem>c1(n2cccc2)sc(c(C)c1C(C)NC(=O)Nc(cc3)ccc3C(OC)=O)C</chem>	
1833	K07	75.15	21.35	<chem>c12n(c(c3c(NC4CCCC4)n1)cccc3)nnc2c5ccc(cc5)Cl</chem>	
1868	D07	69.05	21.80	<chem>C(=O)(Nc(ccc(c1C)Br)c1)N(Cc(ccc(c23)OCO2)c3)C(CC4)CCN4CC</chem>	
1807	C05	73.60	22.25	<chem>n1(C)c(c2ccc(cc2)Cl)cnc1NCc3cc(OC)ccc3OC</chem>	
1865	L03	72.60	22.60	<chem>n1oc(c2c1CNC(=O)N(CC3)CCN3c4cc(C)ccc4C)cccc2</chem>	
1918	K16	74.27	22.84	<chem>S(=O)(=O)(Nc(cc1)ccc1OCC)c(ccc(c23)SCCC(=O)N2)c3</chem>	
1812	O19	77.00	22.95	<chem>c(NCc(cc1)ccc1F)(nc(c2ccc(cc2)Cl)cc3C(F)(F)F)n3</chem>	
1918	N11	70.99	23.26	<chem>n1(CC2)c(c(S2)ccc3)c3cc1C(=O)Nc(cc4)ccc4F</chem>	
1875	O18	60.30	23.32	<chem>[nH]1c2c(cc1C(=O)Nc3cccc3OC)ccc(ccc(C)n4)c24</chem>	
1849	L05	71.45	23.50	<chem>c1(nnc(CC)s1)N([H])C(=O)c2c(Cl)cnc(SCc(cc3)ccc3F)n2</chem>	
1869	G18	51.95	23.50	<chem>c(c1c(n2CC(=O)Nc(ccc(c3Cl)F)c3)cccc1)(c2)S(=O)(=O)Cc4cccc4F</chem>	
1851	E17	60.00	23.55	<chem>n1(c2cccc2)nnnc1SCCCN([H])Cc(cc3)ccc3Br</chem>	
1876	J20	65.60	23.69	<chem>c(cnn1c2cccc(Cl)c2)(C(=O)N3CCC(c4ccc(cc4)C)C3)c1C(CC5)CCN5C(=O)OC(C)(C)C</chem>	
1910	J04	73.03	23.90	<chem>n1(c2cccc(C)c2)ncc3c1nnc3Nc(cc4)ccc4Oc(cc5)ccc5Cl</chem>	
1918	D15	78.19	24.11	<chem>[nH]1c2c(cc1C(=O)Nc3cccc3OC)ccc(cccn4)c24</chem>	
1832	D11	55.15	24.55	<chem>n(oc(c12)ncnc1NCC(CC3)CCN3Cc(cc4)ccc4Cl)c2c5ccc(cc5)Cl</chem>	
1855	C12	51.55	24.55	<chem>n1c(c(ccc(c2[N+](=O)[O-])N(CC3)CCN3C)c2)onc1c4cccc4</chem>	
1915	J14	57.56	24.75	<chem>S(=O)(=O)(c(cccc1)c1C(N2Cc3cccc(Cl)c3)=O)c(ccc(c4)C(NCCCN5CCCC5CC)=O)c24</chem>	
1875	C20	76.56	24.90	<chem>c1(c2c3ccc(cc3)F)c(on2)N=CN(CCC(=O)Nc(ccc(c4Cl)F)c4)C1=O</chem>	
1866	I15	50.55	24.95	<chem>n(CC(=O)N(CC1)CCO1)(c(cccc2)c2c3SCc(cc4)ccc4C(F)(F)F)c3</chem>	

Appendix 3: Dual dose response assays

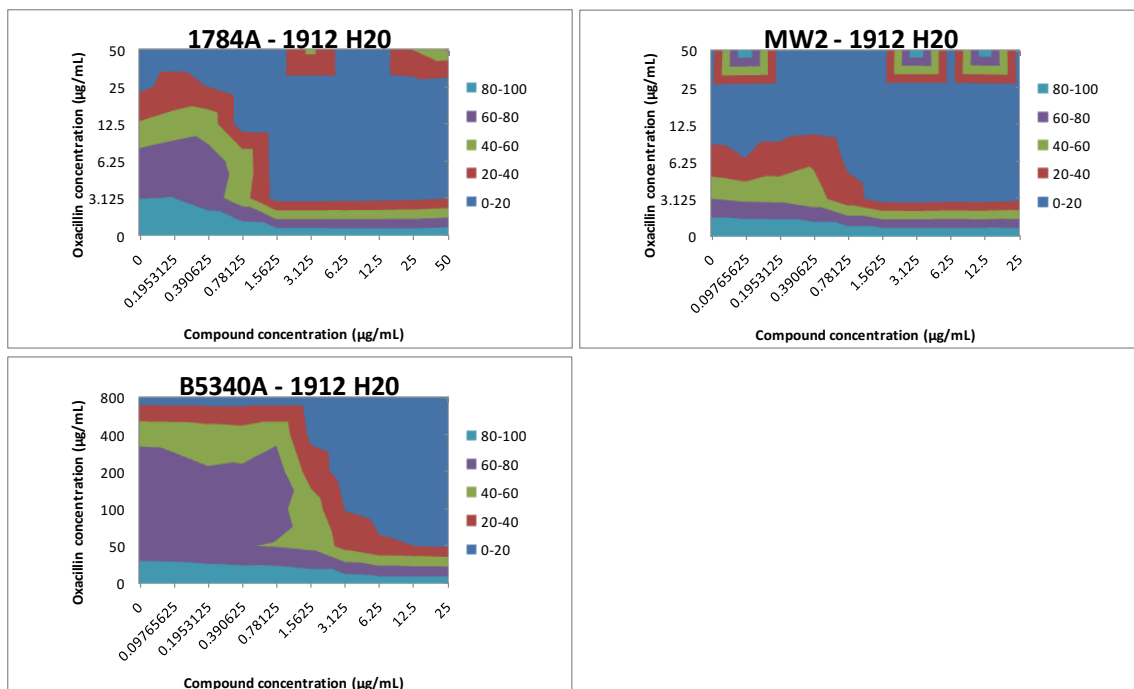
MR100



MR101

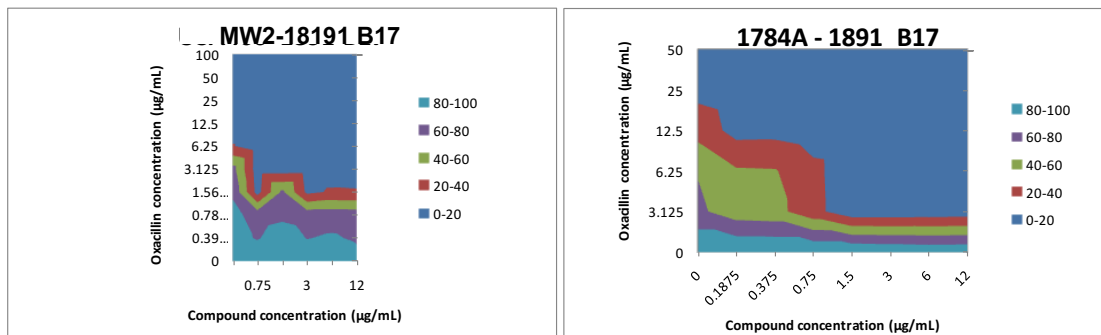


1912 H20 (a hit from the strong category)



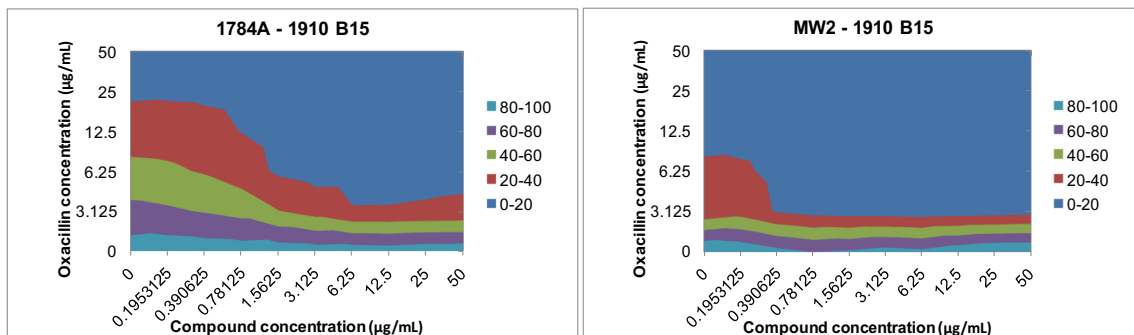
Tests against USA200 were inconclusive.

1891 B17 (a hit from the strong category)



No activity in any other strain or against any other β -lactam except nafcillin

1910 B15 (a hit from the apparent growth defects category)



Appendix 4: HPLC and NMR analyses

Figure A4.1: HPLC showed that MR100 had contaminants. The HPLC trace of MR100 (top) showed two additional peaks of very small percentage area in addition to the main compound peak. The fractions were collected and analyzed by mass spectrometry. Percent areas are shown in blue and the m/z value from mass spectrometry of those fractions are shown in red. M/z values showed that the highest percent area (79.8%) corresponded to the predicted compound. Based on the hypothesis that the impurity is likely a by-product of the synthesis process, we were able to assign a tentative structure to one of the fractions with 2% area. It could not be assigned a structure with more certainty since more compound was not available for analysis. The other fractions could not be assigned a structure as the m/z values did not correspond to any intermediate in the synthesis. The HPLC trace of MR101 (bottom) showed no additional peaks apart from the main compound peak, indicating that it is a pure sample.

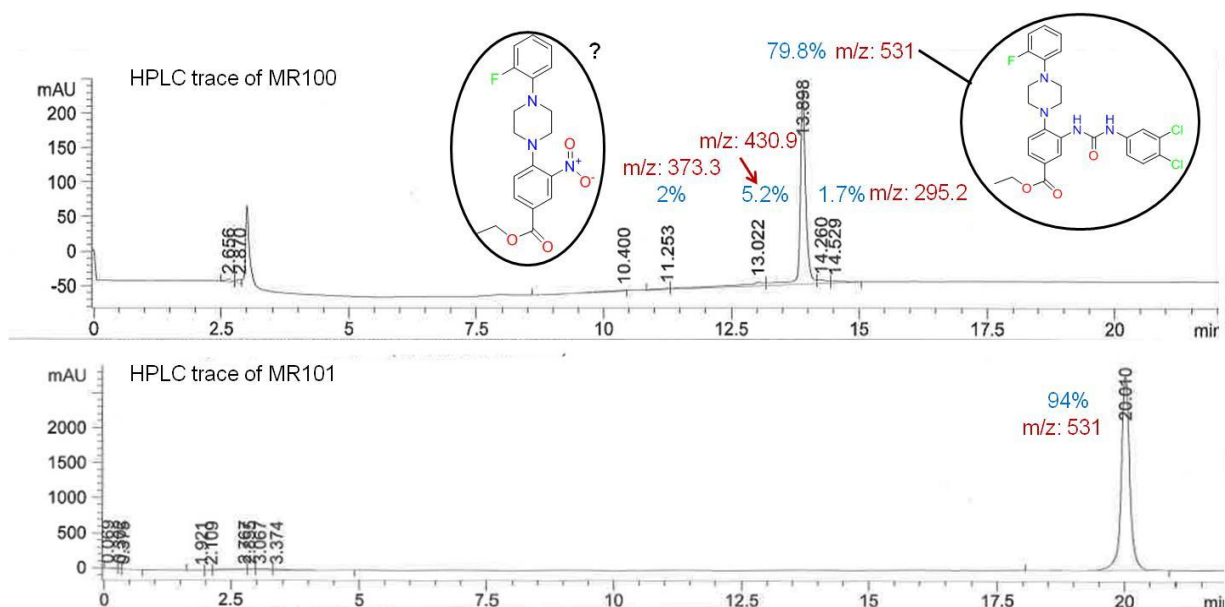
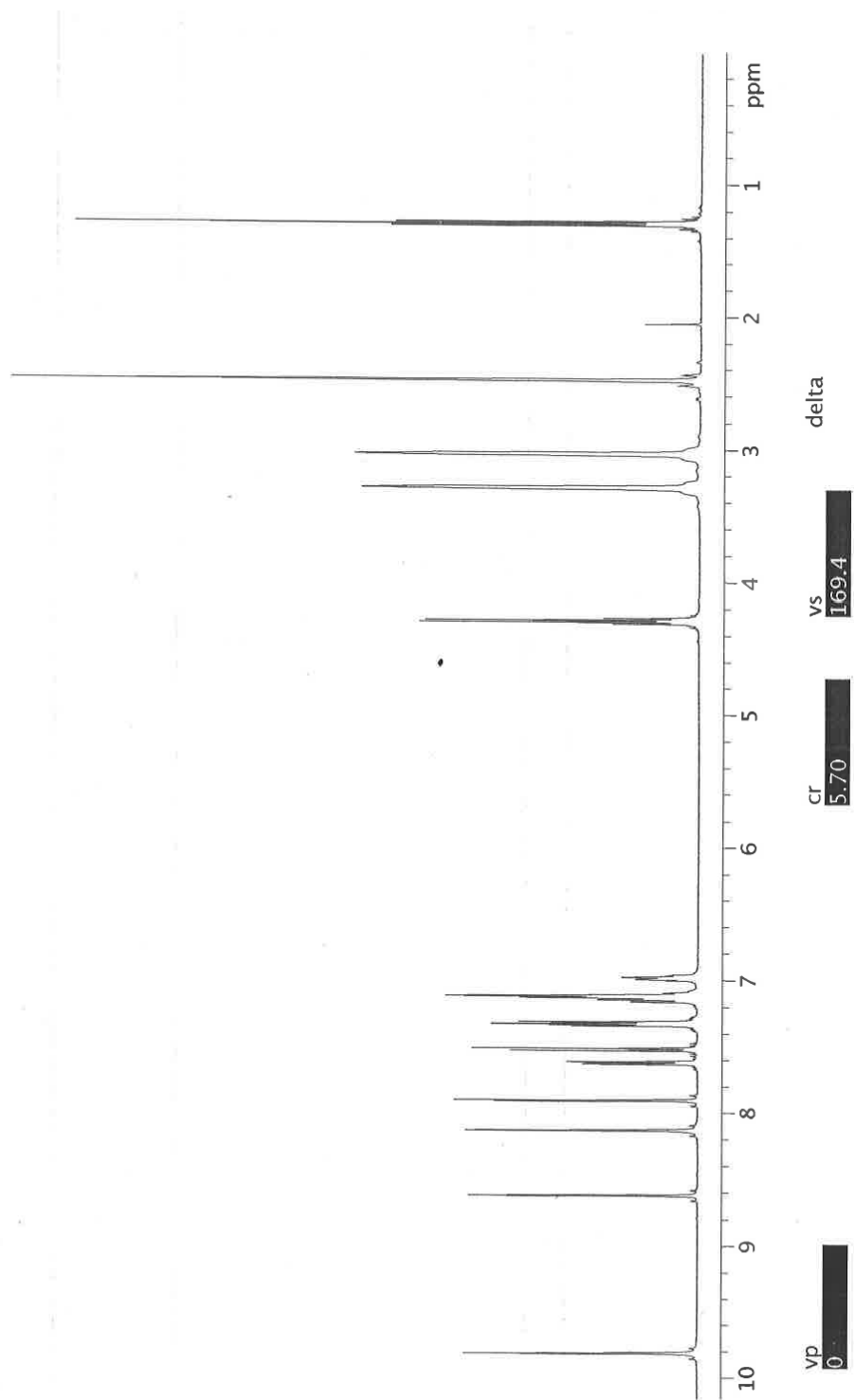


Figure A4.2 H1-NMR of MR101

H1-NMR of MR101 conducted in the Chemistry Department NMR facility using Varian Unity/Inova 500B (1500B) NMR.



Appendix 5: Results from transposon-based experiments on MR100/MR101

Tables A5.1 and 5.2: Tn-Seq hits identified as significant in MR100 6.25µg/mL, MR101 12.5µg/mL or MR101 25µg/mL, and that had fold changes <0.2 or >5 in at least one of these conditions are provided below. Significant fold changes showing enrichment are shown in green, significant fold changes showing depletion are shown in red, interesting genes are highlighted in red boxes, and *'s indicate possible jackpotting errors.

Table A5.1: Hits that are >5x enriched under MR100 or MR101 and that were significant in at least one condition

		MR100		MR101			
		6.25µg/mL		12.5µg/mL		25µg/mL	
		Fold change	P-value	Fold change	P-value	Fold change	P-value
SAOUHSC_00427	sleI	6.61150907	0.000464	2.95747893	0.001325	6.64097348	2.29E-06
SAOUHSC_00665	graR	38.9451537	2.40E-05	6.31894279	0.004211	10.6786171	3.12E-05
SAOUHSC_00666	graS	33.2531477	1.72E-09	7.36647635	5.91E-06	13.8549086	2.46E-09
SAOUHSC_00667	vraF	36.6826783	1.34E-06	6.65414307	0.000969	11.9389336	6.22E-06
SAOUHSC_00668	vraG	35.9858882	1.33E-17	6.76380014	1.87E-14	12.4239302	6.26E-24
SAOUHSC_00789		7.84285714	0.049478	5.05580177	0.0499	12.1522441	0.004151
SAOUHSC_01193		10.9976777	0.000405	6.5420062	3.50E-06	19.2231159	2.17E-11
SAOUHSC_01359	mprF	53.0244104	8.68E-26	7.83721464	1.35E-17	17.4327433	1.28E-26
SAOUHSC_01433		9.88235294	6.04E-05	5.71116667	5.09E-05	16.4518274	3.33E-09
SAOUHSC_01472		5.39812749	1.19E-12	2.07704777	0.000969	2.30914831	2.94E-05
SAOUHSC_01974		9.193	1.72E-09	2.51282772	4.94E-05	5.00652828	3.16E-11
SAOUHSC_01975		10.5404399	0.000382	4.1009825	0.049177	8.57813825	0.000423
SAOUHSC_02149		17.9069174	0.035018	6.72142466	0.096299	20.212317	0.005168
SAOUHSC_02369		9.32706767	0.041735	4.19229481	0.083928	6.05231961	0.108343
SAOUHSC_02481		23.6708861	9.36E-05	4.38932787	0.5	7.55644803	0.0683
SAOUHSC_02482		26.4651163	0.007185	4.55360381	0.170851	7.41209244	0.014911
SAOUHSC_02483		13.1832884	0.001431	6.63504878	0.003337	10.5301542	0.001257
SAOUHSC_02664		6.99553911	1.21E-11	3.67384609	3.98E-07	5.81755898	1.20E-12

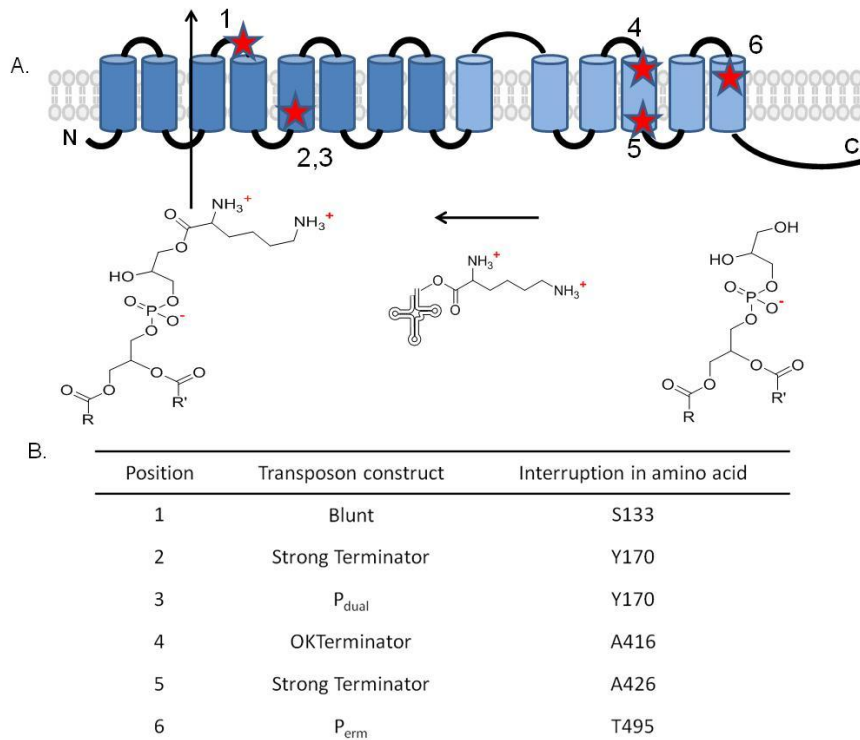
Table A5.2: Hits that are >5x depleted under MR100 or MR101 and that were significant in at least one condition

		MR100		MR101			
		6.25µg/mL		12.5µg/mL		25µg/mL	
		Fold change	P-value	Fold change	P-value	Fold change	P-value
SAOUHSC_00015		0.19069767	1.54E-05	0.1675272	0.161967	*13.6830091	0.5
SAOUHSC_00022		0.07036115	0.00039	0.66427222	0.5	0.42672293	0.272584
SAOUHSC_00023		0.07142857	0.008283	0.53976741	0.5	0.47988196	0.5
SAOUHSC_00469		0.08746736	0.033054	0.15724911	0.186694	0.17560911	0.183326
SAOUHSC_00541		0.03	3.29E-05	0.05711478	0.273881	0.05043821	0.213573
SAOUHSC_00616		0.25007795	0.135487	0.24005943	0.049177	0.19602013	0.0683
SAOUHSC_00618		0.13055003	0.000164	0.83938057	0.5	0.63468039	0.5
SAOUHSC_00746	sstA	0.04037491	4.41E-11	0.11845304	0.000224	0.18404596	0.006545
SAOUHSC_00747	sstB	0.0180018	7.71E-18	0.10639675	5.43E-09	0.25745949	0.000331
SAOUHSC_00748	sstC	0.03813104	1.81E-08	0.10770894	2.87E-05	0.22609531	0.026438
SAOUHSC_00749	sstD	0.0152484	2.66E-15	0.14035769	2.19E-06	0.25104296	0.014182
SAOUHSC_00760		0.06769231	1.64E-07	0.27376564	0.001802	0.08304362	3.77E-08
SAOUHSC_00878		0.05504587	0.000852	0.57181274	0.5	1.27845306	0.5
SAOUHSC_00895		0.02132196	2.63E-11	0.05204123	0.111278	1.05261184	0.5
SAOUHSC_00948		0.00384202	4.75E-23	0.00248289	4.02E-20	0.1285998	1.67E-16
SAOUHSC_00953	ugtP	0.21157324	0.001351	0.63609847	0.5	0.17475212	0.004282
SAOUHSC_00982		0.16788321	1.92E-05	0.31965391	0.5	1.67901057	0.5
SAOUHSC_00983		0.04115854	0.011951	0.05853337	0.5	0.04818354	0.5
SAOUHSC_00984		0.15479115	0.000987	0.5179789	0.5	0.67830722	0.5
SAOUHSC_00997	lcpB	0.07515337	1.34E-07	0.21658265	1.64E-06	0.1150935	2.94E-05
SAOUHSC_00998	fmtA	0.18324861	0.009249	1.12571532	0.5	0.78740783	0.5
SAOUHSC_01002		0.14285714	0.007185	0.2104465	0.5	*14.5691936	0.5
SAOUHSC_01040		0.05925926	0.005771	*2.339833846	0.207692	1.56379308	0.365983
SAOUHSC_01042		0.13846154	0.001397	0.73282391	0.5	0.91419109	0.5
SAOUHSC_01043		0.01712329	0.007185	1.24767043	0.5	1.68229304	0.5
SAOUHSC_01062		0.07228916	0.013395	0.18088822	0.5	0.26025807	0.5
SAOUHSC_01067		0.04032258	0.027727	0.24978953	0.5	0.82604058	0.5
SAOUHSC_01069		0.04752252	4.60E-07	0.24720876	0.078121	0.25327849	0.5
SAOUHSC_01103		0.08974359	2.53E-06	0.44787424	0.5	1.69755667	0.5
SAOUHSC_01104		0.08388521	4.73E-10	0.46332915	0.5	1.13199619	0.5
SAOUHSC_01154		0.44318182	2.97E-05	0.17248145	0.193108	0.19323961	0.076314
SAOUHSC_01175		0.17672601	0.000206	0.53098663	0.293714	0.37744002	0.293322
SAOUHSC_01186		0.08279221	0.006095	0.92558643	0.5	0.87366442	0.5
SAOUHSC_01228		0.0462963	5.63E-05	0.52002057	0.5	0.67507657	0.5
SAOUHSC_01239		0.07492975	0.004899	0.35389011	0.244185	0.52778073	0.5
SAOUHSC_01251		0.14912281	8.14E-05	*3.05027877	0.251381	0.39481066	0.400491
SAOUHSC_01265		0.02192982	1.65E-08	0.14848239	0.02722	0.31140387	0.5
SAOUHSC_01358		0.06545064	1.55E-11	0.18360432	2.83E-09	0.07800257	2.15E-13
SAOUHSC_01391		0.42081448	1	0.34325657	0.280899	0.18455858	0.048741
SAOUHSC_01416		0.05973025	9.07E-10	1.64136615	0.5	0.97211067	0.5
SAOUHSC_01418		0.05438402	1.65E-17	0.68165393	0.5	1.06010851	0.5
SAOUHSC_01491		0.06177606	0.002807	0.30823717	0.5	0.38244487	0.5

Table A5.2 (Continued):

		MR100		MR101			
		6.25µg/mL		12.5µg/mL		25µg/mL	
		Fold change	P-value	Fold change	P-value	Fold change	P-value
SAOUHSC_01587		0.14218645	0.02324	0.36483077	0.5	0.27287449	0.215668
SAOUHSC_01592		0.18181818	0.028886	0.60527632	0.5	0.61163838	0.5
SAOUHSC_01600		0.10628248	0.018182	0.38598226	0.380056	0.39769124	0.5
SAOUHSC_01652	PBP3	0.00774751	2.02E-24	0.14160998	4.87E-06	0.3768916	7.06E-07
SAOUHSC_01653		0.06592466	0.030236	0.50340163	0.5	0.45453146	0.5
SAOUHSC_01655		0.10182491	0.041294	0.26254831	0.170851	0.20778971	0.183326
SAOUHSC_01732		0.10084034	0.000135	0.69571568	0.5	*19.5858264	0.400491
SAOUHSC_01758	mreC	0.0128	1.41E-10	0.14985117	0.005695	0.16560876	0.026863
SAOUHSC_01759	mreD	0.02389791	2.12E-10	0.15606689	2.65E-05	0.22157593	0.001141
SAOUHSC_01818		0.06699752	7.22E-05	0.37406005	0.494791	0.41681249	0.5
SAOUHSC_01827	ezrA	0.01144492	3.03E-19	0.04484985	1.53E-05	0.19570467	0.024959
SAOUHSC_01859		0.07580175	0.006871	1.21653455	0.5	0.67019214	0.5
SAOUHSC_01863		0.04006969	0.004112	0.34086147	0.333051	0.2072293	0.127325
SAOUHSC_01882		0.17158035	0.020416	0.54716749	0.5	0.4330573	0.5
SAOUHSC_01902		0.02644836	0.000484	0.11240258	0.049177	0.18943017	0.232353
SAOUHSC_01908		0.00497512	4.25E-10	0.18100585	0.001024	0.27908478	0.051391
SAOUHSC_01910		0.19918699	2.24E-07	1.16449753	0.5	2.01961146	0.132688
SAOUHSC_01966		0.11226115	1.04E-05	0.3320912	0.002641	0.37757065	0.054323
SAOUHSC_01967		0.10561661	0.005494	0.3416649	0.280899	0.29689118	0.094564
SAOUHSC_01987		0.08691911	0.00266	0.28976841	0.012812	0.22594267	0.012977
SAOUHSC_02012	sgtB	0.02439024	2.63E-11	0.19541281	0.000355	0.15944868	0.002836
SAOUHSC_02121		0.03464444	1.49E-12	0.3145378	0.000315	0.20285742	5.89E-05
SAOUHSC_02269		0.16036977	0.006033	0.53081039	0.5	0.44470121	0.5
SAOUHSC_02298		0.1061993	0.000682	0.29302036	0.043118	0.25458	0.048741
SAOUHSC_02301		0.16393443	0.035018	0.33622999	0.055507	0.30973773	0.059553
SAOUHSC_02303		1.34736181	0.000404	0.18707565	0.014162	0.14769289	0.009075
SAOUHSC_02319	rodA	0.00774159	4.48E-15	0.1421893	1.58E-09	0.11187623	3.33E-09
SAOUHSC_02383		0.01346485	1.72E-19	0.10496037	5.53E-10	0.16049417	3.04E-05
SAOUHSC_02389		0.03884235	9.65E-14	0.13285381	4.01E-06	0.09738648	1.72E-05
SAOUHSC_02402		0.05204461	0.001765	0.32410944	0.5	0.3790519	0.5
SAOUHSC_02456		0.09458128	0.000818	0.48972449	0.5	0.5532154	0.5
SAOUHSC_02525		0.17607733	1.34E-06	0.24488186	6.19E-06	0.18892202	3.30E-08
SAOUHSC_02611		0.13278008	5.04E-07	0.4295226	0.494791	0.45528147	0.438087
SAOUHSC_02622		0.05529954	2.22E-10	0.3361789	0.023799	0.38005058	0.161978
SAOUHSC_02646		0.07359813	0.002807	0.17712605	0.021053	0.28828321	0.246176
SAOUHSC_02822		0.12121212	4.60E-07	0.27607935	0.5	0.74741266	0.267173
SAOUHSC_02869		0.05316607	1.82E-08	0.3024824	0.007546	0.3124141	0.053973
SAOUHSC_02885		0.16808609	0.000337	1.36030669	0.5	1.20298084	0.5
SAOUHSC_03052		0.09190372	1.75E-05	0.66562507	0.5	0.71455146	0.465664
SAOUHSC_A02450		0.09198113	0.035472	0.5753627	0.5	0.45780267	0.5

Figure A5.1: Inactivation insertion mutants in *mprF* raised to MR100: (A) A schematic of MprF showing that it is a transmembrane protein with 14 transmembrane helices. It consists of two separable domains, the synthase and the flippase (Continued) domain. The synthase domain synthesizes LPG from phosphatidylglycerol and lysyl-t-RNA. The six helices shown in light blue have been demonstrated to be sufficient for synthesis of LPG [20]. The flippase domain flips LPG to the correct orientation. The location of the insertions for each mutant are shown by red stars. Mutants were identified in both the synthase and the flippase domain. (B) The type of transposon construct inserted can be determined by sequencing the barcode that is a part of each donor construct [392]. The results of this mapping is shown and it is evident that each of these insertions are due to a different transposon construct, making them unique mutants. The amino acid each insertion interrupts is also shown.



Appendix 6: Transmission electron microscopy images of *ugtP-mprF* and *ItaA-mprF* double inactivation mutants

Figure A6.1: Transmission electron microscopy images of *ugtP mprF* and *ItaA*

***mprF* double inactivation mutants.** Cells were grown overnight in the presence of inducer and dilute 1:100 in fresh TSB with or without inducer. Cells were grown to 37°C until they reached an OD₆₀₀ of 0.3 to normalize for cell count. Samples were outgrown 2 hours or 4 hours after this point and then harvested. Normal WT cells (A) were compared with the mutant cells in the presence or absence of inducer (B-M). $\Delta mprF$ (B) and *tn::ItaA* (D) cells showed no defects in cell growth, but *tn::ugtP* cells (C) showed the presence of multiple septa (highlighted by red triangles). In the presence of inducer, *tn::ugtP* $\Delta mprF$ cells looked like WT at 4 hours (E) and at 2 hours (I). They did not show the presence of multiple septa that is characteristic of *ugtP* inactivation. In the absence of inducer, the double inactivation mutant showed significant lysis after 4 hours (F) and after 2 hours (J). After 2 hours, the cells clearly showed the presence of multiple septa that is characteristic of *ugtP* inactivation (highlighted by red triangles), but by 4 hours most of the cells were lysed as indicated by the ghost cells. In the presence of inducer, *tn::ItaA* $\Delta mprF$ cells showed no defects at 4 hours (G) and 2 hours (M), which is the phenotype observed for the single *ItaA* inactivation as well. At 4 hours, in the absence of inducer, these cells showed lysis as well (H), but at 2 hours, they showed the presence of multiple septa (K) and giant cells, which had clearly delayed cell division (L).

Figure A6.1 (Continued):

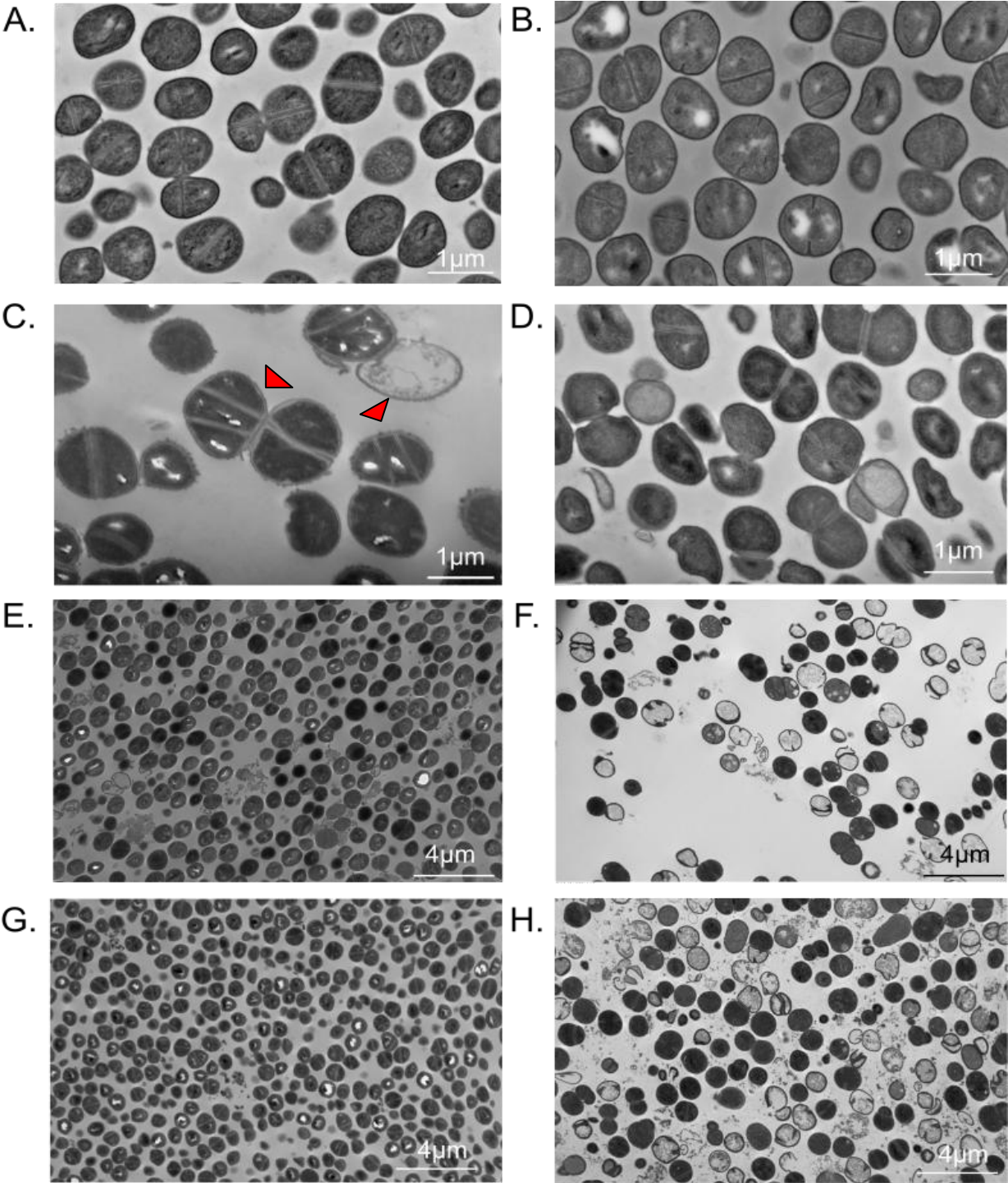
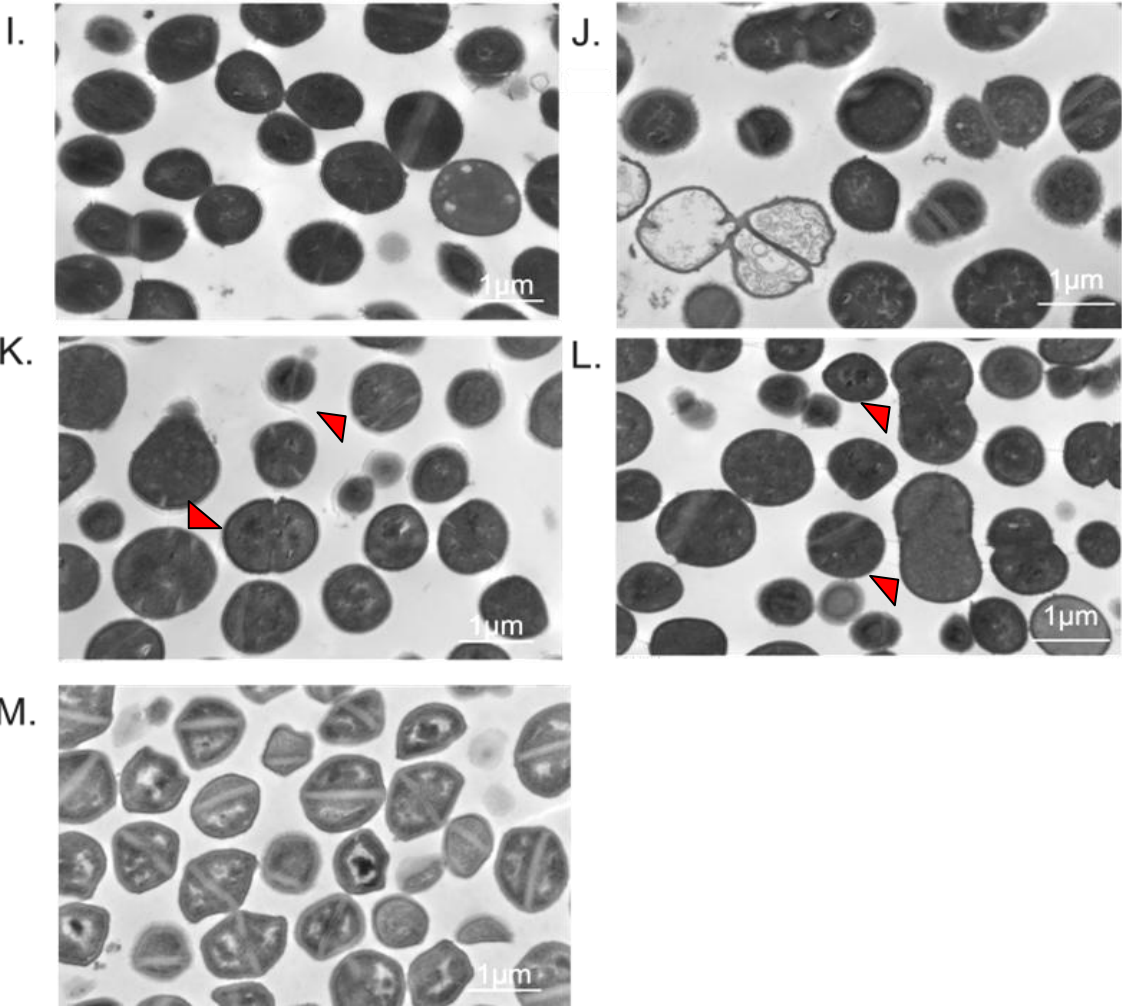


Figure A6.1 (Continued):



Appendix 7: Strains and primers used in this work

Table A7.1: List of strains used in this work		
Name	Genotype	Source if other than this work
Transposon library 1	Transposon library constructed in HG003	Gilmore Lab
Transposon library 2	~695000 mutant transposon library constructed in HG003 with six donor constructs (blunt, P _{pen} , P _{cap} , P _{erm} , P _{cap} , P _{pen} , P _{tuf} , P _{dual})	[392]
Transposon library 3	Transposon library constructed in HG003 with six donor constructs (blunt, P _{pen} , P _{cap} , P _{erm} , P _{cap} , P _{pen} , P _{tuf} , P _{dual})	Constructed by Dr. Tim Meredith
Transposon library 4	Transposon library constructed in HG003 with four donor constructs containing varying strengths of transcription terminators	Constructed by Dr. Tim Meredith
Transposon library 5	Transposon library constructed in HG003 Δ mprF with four donor constructs (blunt, P _{pen} , P _{cap} , P _{tuf})	
SHM062	HG003 Δ Φ 11::FRT with pWV01:CmR containing functional transposase	Constructed by Dr. Samir Moussa
SHM063	HG003 Δ Φ 11::FRT with pWV01:CmR containing truncated transposase	Constructed by Dr. Samir Moussa
MR031	HG003 Δ mprF:KanR	Constructed by Dr. Ting Pang
MR040	HG003 Δ Φ 11::FRT Δ mprF:KanR, with pWV01:CmR containing functional transposase	
MR041	HG003 Δ Φ 11::FRT Δ mprF:KanR, with pWV01:CmR containing truncated transposase	
MR100	<i>E. coli</i> Stellar with pTP63 containing an anhydrous tetracycline inducible copy of mprF: CarbR	
WL006	HG003 tn::ugtP:ErmR, with Nebraska library transposon mutant	Constructed by Dr. Wonsik Lee
WL009	HG003 tn::ltaA:ErmR, with Nebraska library transposon mutant	Constructed by Dr. Wonsik Lee
MR106	HG003 Δ mprF:KanR, tn::ltaA:ErmR, with pMR100:CamR	
MR107	HG003 Δ mprF:KanR, tn::ugtP:ErmR, with pMR100:CamR	
MR087	HG003 tn::SAOUHSC_00948:ErmR, transduced from Nebraska library	

	transposon mutant	
MR108	HG003 tn::SAOUHSC_00948:ErmR, Δ mprF:KanR	
WL078	RN4220 Δ ugtP:KanR	Constructed by Dr. Wonsik Lee
MR121	HG003 tn::SAOUHSC_00948:ErmR, Δ ugtP:KanR	
MR114	USA300 JE2 tn::SAOUHSC_01025: ErmR, transduction from Nebraska library transposon mutant	
MR118	USA300 JE2 tn::SAOUHSC_01050: ErmR, transduction from Nebraska library transposon mutant	
MR020	HG003 tn:: <i>mprF</i> :ErmR, (1) blunt transposon mutant interrupting amino acid 133, clean transduction	
MR025	HG003 tn:: <i>mprF</i> :ErmR, (2) strong TT rev ori transposon mutant interrupting amino acid 170, clean transduction	
MR024	HG003 tn:: <i>mprF</i> :ErmR, (3) P _{dual} transposon mutant interrupting amino acid 170, clean transduction	
MR022	HG003 tn:: <i>mprF</i> :ErmR, (4) OK TT transposon mutant interrupting amino acid 416, clean transduction	
MR023	HG003 tn:: <i>mprF</i> :ErmR, (5) strong TT rev ori transposon mutant interrupting amino acid 426, clean transduction	
MR021	HG003 tn:: <i>mprF</i> :ErmR, (6) Perm transposon mutant interrupting amino acid 495, clean transduction	
MR122	USA300:JE2 tn:: <i>fntA</i> , Nebraska library mutant	[443]
MR123	USA300:JE2 tn:: <i>ndh</i> Nebraska library mutant	[443]
MR124	USA300:JE2 tn:: <i>mprF</i> Nebraska library mutant	[443]
MR125	USA300: JE2 tn::SAOUHSC_01025, Nebraska library transposon mutant	[443]
MR126	USA300: JE2 tn::SAOUHSC_01050, Nebraska library transposon mutant	[443]
MR127	USA300: JE2 background strain for Nebraska library	[443]
MR012	Newman Δ <i>graR</i> :TetR	[204]
MR046	Newman Δ <i>dltA</i>	[204]
MR030	Newman Δ <i>mprF</i> :KanR	

MR015	Newman wildtype, MSSA	Acquired from John Santa Maria
MR004	USA400 (MW2) wildtype, community-acquired MRSA	Acquired from Dr. David Hooper
MR005	USA200 wildtype, hospital-acquired MRSA	Acquired from Dr. David Hooper
MR006	1784A wildtype, hospital-acquired MRSA	Acquired by Jonathan Swoboda from MRSA coreA facility
MR034	HG003 wildtype, MSSA	Acquired from John Santa Maria
JGS0404	B5340A wildtype, clinical isolate	Acquired by Jonathan Swoboda from MRSA coreA facility

Table A7.2: List of primers used in this work	
Primer Name	Sequence
For mapping of transposon mutants:	
HGTnInvPCRoutF	5' CCACGCGTGCCATAAC 3'
HGTnInvPCRoutR	5' TCGTATGCCGTGTTCTG 3'
HGTnInvPCRseqF	5' CGGGGACTTATCATCCAACC 3'
TM168	5' CATCAAGCAATGAAACACGCC 3'
For confirmation of deletion or inactivation mutants:	
MprFdccfwd2	5' CTTAGTATTAGCTAGTATTGCGGC 3'
MprFdccrev2	5' CAACAATCAGAAGAATGATAGG 3'
948 TnF	5' CTG GTG CTG TTTGATCCAATTGC 3'
948 TnR	5' GTAGATAGCGGATTCCACGC 3'
UgtP orf F	5' ATGGTTACTCAAATAAAAAGATATTGATTA 3'
UgtP orf R	5' TTAGCTTTTTCTCTATTTACTATAAAGT 3'
UgtP CA	5' TCGATTAATTTGTTCCATACCAT 3'
UgtP CB	5' ACAAAGCTTCTAGCTTCAAACC 3'
LtaA orfF	5' ATGGTTACTCAAATAAAAAGATATTGATTA 3'
LtaA orfR	5' TTAGCTTTTTCTCTATTTACTATAAAGT 3'
For inducible mprF complementation constructs	
i-mprF pTP63 F	5' AATCACAGGT <u>ACCCAGAAATAATTAG</u> AATTGATGTGAAAA 3'
mprF-B-pTP63R	5' CATAAC <u>GCTCAGCGG</u> CGACTTAACTTTAGCTC 3'
Cm to HindIII	5' CTCTCCGTCGCTATTGTAACC 3'
* Bold indicates putative ribosome binding sites, underlined indicates restriction sites	

References Cited

1. Rajagopal, M. and S. Walker, *Envelope Structures of Gram-Positive Bacteria*. Curr Top Microbiol Immunol, 2016.
2. Silhavy, T.J., D. Kahne, and S. Walker, *The bacterial cell envelope*. Cold Spring Harb Perspect Biol, 2010. **2**(5): p. a000414.
3. Vollmer, W., D. Blanot, and M.A. de Pedro, *Peptidoglycan structure and architecture*. FEMS Microbiol Rev, 2008. **32**(2): p. 149-67.
4. Brown, S., J.P. Santa Maria, Jr., and S. Walker, *Wall teichoic acids of gram-positive bacteria*. Annu Rev Microbiol, 2013. **67**: p. 313-36.
5. Percy, M.G. and A. Grundling, *Lipoteichoic acid synthesis and function in gram-positive bacteria*. Annu Rev Microbiol, 2014. **68**: p. 81-100.
6. Schneewind, O. and D. Missiakas, *Lipoteichoic acids, phosphate-containing polymers in the envelope of gram-positive bacteria*. J Bacteriol, 2014. **196**(6): p. 1133-42.
7. Buist, G., et al., *LysM, a widely distributed protein motif for binding to (peptidoglycans*. Mol Microbiol, 2008. **68**(4): p. 838-47.
8. Kovacs-Simon, A., R.W. Titball, and S.L. Michell, *Lipoproteins of bacterial pathogens*. Infect Immun, 2011. **79**(2): p. 548-61.
9. Navarre, W.W. and O. Schneewind, *Surface proteins of gram-positive bacteria and mechanisms of their targeting to the cell wall envelope*. Microbiol Mol Biol Rev, 1999. **63**(1): p. 174-229.
10. Stock, A.M., V.L. Robinson, and P.N. Goudreau, *Two-component signal transduction*. Annu Rev Biochem, 2000. **69**: p. 183-215.
11. Zhen, M., Jacobsen, F.E., Giedroc, D.P., *Metal transporters and metal sensors: how coordination chemistry controls bacterial metal homeostasis*. Chem Rev, 2009. **109**(10): p. 4644-4681.
12. Arciola, C.R., et al., *Polysaccharide intercellular adhesin in biofilm: structural and regulatory aspects*. Front Cell Infect Microbiol, 2015. **5**: p. 7.
13. Yother, J., *Capsules of Streptococcus pneumoniae and other bacteria: paradigms for polysaccharide biosynthesis and regulation*. Annu Rev Microbiol, 2011. **65**: p. 563-81.
14. Walsh, C., *Antibiotics that act on cell wall biosynthesis*, in *Antibiotics: actions, origins, resistance*. 2003, ASM Press: Washington D.C.

15. Clejan, S., et al., *Membrane lipid composition of obligately and facultatively alkalophilic strains of Bacillus spp.* J Bacteriol, 1986. **168**(1): p. 334-40.
16. Haque, M.A. and N.J. Russell, *Strains of Bacillus cereus vary in the phenotypic adaptation of their membrane lipid composition in response to low water activity, reduced temperature and growth in rice starch.* Microbiology, 2004. **150**(Pt 5): p. 1397-404.
17. Minnikin, D.E. and H. Abdolrahimzadeh, *Effect of pH on the proportions of polar lipids, in chemostat cultures of Bacillus subtilis.* J Bacteriol, 1974. **120**(3): p. 999-1003.
18. Epanand, R.F., P.B. Savage, and R.M. Epanand, *Bacterial lipid composition and the antimicrobial efficacy of cationic steroid compounds (Ceragenins).* Biochim Biophys Acta, 2007. **1768**(10): p. 2500-9.
19. Parsons, J.B., Rock, C.O., *Bacterial lipids: metabolism and membrane homeostasis.* Prog Lipid Res, 2014. **52**(3): p. 249-276.
20. Ernst, C.M., et al., *The bacterial defensin resistance protein MprF consists of separable domains for lipid lysinylation and antimicrobial peptide repulsion.* PLoS Pathog, 2009. **5**(11): p. e1000660.
21. Kristian, S.A., et al., *MprF-mediated lysinylation of phospholipids in Staphylococcus aureus leads to protection against oxygen-independent neutrophil killing.* Infect Immun, 2003. **71**(1): p. 546-9.
22. Peschel, A., et al., *Staphylococcus aureus resistance to human defensins and evasion of neutrophil killing via the novel virulence factor MprF is based on modification of membrane lipids with L-lysine.* J Exp Med, 2001. **193**(9): p. 1067-76.
23. Nishi, H., et al., *Reduced content of lysyl-phosphatidylglycerol in the cytoplasmic membrane affects susceptibility to moenomycin, as well as vancomycin, gentamicin, and antimicrobial peptides, in Staphylococcus aureus.* Antimicrob Agents Chemother, 2004. **48**(12): p. 4800-7.
24. Komatsuzawa, H., et al., *Cloning and sequencing of the gene, fmtC, which affects oxacillin resistance in methicillin-resistant Staphylococcus aureus.* FEMS Microbiol Lett, 2001. **203**(1): p. 49-54.
25. Friedman, L., J.D. Alder, and J.A. Silverman, *Genetic changes that correlate with reduced susceptibility to daptomycin in Staphylococcus aureus.* Antimicrob Agents Chemother, 2006. **50**(6): p. 2137-45.
26. Jones, T., et al., *Failures in clinical treatment of Staphylococcus aureus Infection with daptomycin are associated with alterations in surface charge, membrane*

- phospholipid asymmetry, and drug binding*. Antimicrob Agents Chemother, 2008. **52**(1): p. 269-78.
27. Julian, K., et al., *Characterization of a daptomycin-nonsusceptible vancomycin-intermediate Staphylococcus aureus strain in a patient with endocarditis*. Antimicrob Agents Chemother, 2007. **51**(9): p. 3445-8.
 28. Yang, S.J., et al., *Regulation of mprF in daptomycin-nonsusceptible Staphylococcus aureus strains*. Antimicrob Agents Chemother, 2009. **53**(6): p. 2636-7.
 29. Ernst, C.M. and A. Peschel, *Broad-spectrum antimicrobial peptide resistance by MprF-mediated aminoacylation and flipping of phospholipids*. Mol Microbiol, 2011. **80**(2): p. 290-9.
 30. Zhang, Y.M. and C.O. Rock, *Membrane lipid homeostasis in bacteria*. Nat Rev Microbiol, 2008. **6**(3): p. 222-33.
 31. de Mendoza, D., *Temperature sensing by membranes*. Annu Rev Microbiol, 2014. **68**: p. 101-16.
 32. Falord, M., et al., *Investigation of the Staphylococcus aureus GraSR regulon reveals novel links to virulence, stress response and cell wall signal transduction pathways*. PLoS One, 2011. **6**(7): p. e21323.
 33. Li, M., et al., *The antimicrobial peptide-sensing system aps of Staphylococcus aureus*. Mol Microbiol, 2007. **66**(5): p. 1136-47.
 34. Li, M., et al., *Gram-positive three-component antimicrobial peptide-sensing system*. Proc Natl Acad Sci U S A, 2007. **104**(22): p. 9469-74.
 35. Yang, S.J., et al., *The Staphylococcus aureus two-component regulatory system, GraRS, senses and confers resistance to selected cationic antimicrobial peptides*. Infect Immun, 2012. **80**(1): p. 74-81.
 36. Bayer, A.S., T. Schneider, and H.G. Sahl, *Mechanisms of daptomycin resistance in Staphylococcus aureus: role of the cell membrane and cell wall*. Ann N Y Acad Sci, 2013. **1277**: p. 139-58.
 37. Revilla-Guarinos, A., et al., *Defence against antimicrobial peptides: different strategies in Firmicutes*. Environ Microbiol, 2014. **16**(5): p. 1225-37.
 38. Schneewind, O. and D.M. Missiakas, *Protein secretion and surface display in Gram-positive bacteria*. Philos Trans R Soc Lond B Biol Sci, 2012. **367**(1592): p. 1123-39.
 39. Mitchell, P., Moyle J, *Osmotic structure and function in bacteria*. Sym Soc Gen Microbiol, 1956. **6**: p. 150-180.

40. Norris, V., Sweeney, S., *Deformations in the cytoplasmic membrane of Escherichia coli direct the repair of peptidoglycan*, in *Bacterial growth and lysis: metabolism and structure of the bacterial sacculus*, M.A. de Pedro, Holtje, J.V., Löffelhardt, W., Editor. 1993, Springer: US. p. 375-385.
41. Schleifer, K.H. and O. Kandler, *Peptidoglycan types of bacterial cell walls and their taxonomic implications*. *Bacteriol Rev*, 1972. **36**(4): p. 407-77.
42. Boneca, I.G., et al., *Characterization of Staphylococcus aureus cell wall glycan strands, evidence for a new beta-N-acetylglucosaminidase activity*. *J Biol Chem*, 2000. **275**(14): p. 9910-8.
43. Ward, J.B., *The chain length of the glycans in bacterial cell walls*. *Biochem J*, 1973. **133**(2): p. 395-8.
44. Hayhurst, E.J., et al., *Cell wall peptidoglycan architecture in Bacillus subtilis*. *Proc Natl Acad Sci U S A*, 2008. **105**(38): p. 14603-8.
45. de Jonge, B.L., et al., *Altered muropeptide composition in Staphylococcus aureus strains with an inactivated femA locus*. *J Bacteriol*, 1993. **175**(9): p. 2779-82.
46. de Jonge, B.L., S. Handwerger, and D. Gage, *Altered peptidoglycan composition in vancomycin-resistant Enterococcus faecalis*. *Antimicrob Agents Chemother*, 1996. **40**(4): p. 863-9.
47. Severin, A. and A. Tomasz, *Naturally occurring peptidoglycan variants of Streptococcus pneumoniae*. *J Bacteriol*, 1996. **178**(1): p. 168-74.
48. Garcia-Bustos, J.F., B.T. Chait, and A. Tomasz, *Structure of the peptide network of pneumococcal peptidoglycan*. *J Biol Chem*, 1987. **262**(32): p. 15400-5.
49. Patti, G.J., et al., *Characterization of structural variations in the peptidoglycan of vancomycin-susceptible Enterococcus faecium: understanding glycopeptide-antibiotic binding sites using mass spectrometry*. *J Am Soc Mass Spectrom*, 2008. **19**(10): p. 1467-75.
50. Lavollay, M., et al., *The peptidoglycan of Mycobacterium abscessus is predominantly cross-linked by L,D-transpeptidases*. *J Bacteriol*, 2011. **193**(3): p. 778-82.
51. Lavollay, M., et al., *The peptidoglycan of stationary-phase Mycobacterium tuberculosis predominantly contains cross-links generated by L,D-transpeptidation*. *J Bacteriol*, 2008. **190**(12): p. 4360-6.
52. Mainardi, J.L., et al., *Novel mechanism of beta-lactam resistance due to bypass of DD-transpeptidation in Enterococcus faecium*. *J Biol Chem*, 2000. **275**(22): p. 16490-6.

53. Marquardt, J.L., et al., *Cloning and sequencing of Escherichia coli murZ and purification of its product, a UDP-N-acetylglucosamine enolpyruvyl transferase*. J Bacteriol, 1992. **174**(17): p. 5748-52.
54. Blake, K.L., et al., *The nature of Staphylococcus aureus MurA and MurZ and approaches for detection of peptidoglycan biosynthesis inhibitors*. Mol Microbiol, 2009. **72**(2): p. 335-43.
55. Du, W., et al., *Two active forms of UDP-N-acetylglucosamine enolpyruvyl transferase in gram-positive bacteria*. J Bacteriol, 2000. **182**(15): p. 4146-52.
56. Kock, H., U. Gerth, and M. Hecker, *MurAA, catalysing the first committed step in peptidoglycan biosynthesis, is a target of Clp-dependent proteolysis in Bacillus subtilis*. Mol Microbiol, 2004. **51**(4): p. 1087-102.
57. Benson, T.E., et al., *Overexpression, purification, and mechanistic study of UDP-N-acetylenolpyruvylglucosamine reductase*. Biochemistry, 1993. **32**(8): p. 2024-30.
58. Bouhss, A., et al., *Invariant amino acids in the Mur peptide synthetases of bacterial peptidoglycan synthesis and their modification by site-directed mutagenesis in the UDP-MurNAc:L-alanine ligase from Escherichia coli*. Biochemistry, 1997. **36**(39): p. 11556-63.
59. Patin, D., et al., *Purification and biochemical characterization of Mur ligases from Staphylococcus aureus*. Biochimie, 2010. **92**(12): p. 1793-800.
60. Walsh, C.T., *Enzymes in the D-alanine branch of bacterial cell wall peptidoglycan assembly*. J Biol Chem, 1989. **264**(5): p. 2393-6.
61. Mahapatra, S., et al., *Mycobacterial lipid II is composed of a complex mixture of modified muramyl and peptide moieties linked to decaprenyl phosphate*. J Bacteriol, 2005. **187**(8): p. 2747-57.
62. Bouhss, A., et al., *Purification and characterization of the bacterial MraY translocase catalyzing the first membrane step of peptidoglycan biosynthesis*. J Biol Chem, 2004. **279**(29): p. 29974-80.
63. Chung, B.C., et al., *Crystal structure of MraY, an essential membrane enzyme for bacterial cell wall synthesis*. Science, 2013. **341**(6149): p. 1012-6.
64. Pless, D.D. and F.C. Neuhaus, *Initial membrane reaction in peptidoglycan synthesis. Lipid dependence of phospho-n-acetylmuramyl-pentapeptide translocase (exchange reaction)*. J Biol Chem, 1973. **248**(5): p. 1568-76.
65. Hu, Y., et al., *Crystal structure of the MurG:UDP-GlcNAc complex reveals common structural principles of a superfamily of glycosyltransferases*. Proc Natl Acad Sci U S A, 2003. **100**(3): p. 845-9.

66. Helm, J.S., et al., *Identification of active-site inhibitors of MurG using a generalizable, high-throughput glycosyltransferase screen*. J Am Chem Soc, 2003. **125**(37): p. 11168-9.
67. Mengin-Lecreulx, D., et al., *The murG gene of Escherichia coli codes for the UDP-N-acetylglucosamine: N-acetylmuramyl-(pentapeptide) pyrophosphoryl-undecaprenol N-acetylglucosamine transferase involved in the membrane steps of peptidoglycan synthesis*. J Bacteriol, 1991. **173**(15): p. 4625-36.
68. Figueiredo, T.A., et al., *Identification of genetic determinants and enzymes involved with the amidation of glutamic acid residues in the peptidoglycan of Staphylococcus aureus*. PLoS Pathog, 2012. **8**(1): p. e1002508.
69. Munch, D., et al., *Identification and in vitro analysis of the GatD/MurT enzyme-complex catalyzing lipid II amidation in Staphylococcus aureus*. PLoS Pathog, 2012. **8**(1): p. e1002509.
70. Rogers, H.J., Perkins, H.R., Ward, J.B., *Biosynthesis of peptidoglycan*, in *Microbial cell walls and cell membranes*. 1980, Chapman and Hall: London. p. 239-290.
71. Henze, U., et al., *Influence of femB on methicillin resistance and peptidoglycan metabolism in Staphylococcus aureus*. J Bacteriol, 1993. **175**(6): p. 1612-20.
72. Maidhof, H., et al., *femA, which encodes a factor essential for expression of methicillin resistance, affects glycine content of peptidoglycan in methicillin-resistant and methicillin-susceptible Staphylococcus aureus strains*. J Bacteriol, 1991. **173**(11): p. 3507-13.
73. Rohrer, S., et al., *The essential Staphylococcus aureus gene fmhB is involved in the first step of peptidoglycan pentaglycine interpeptide formation*. Proc Natl Acad Sci U S A, 1999. **96**(16): p. 9351-6.
74. Schneider, T., et al., *In vitro assembly of a complete, pentaglycine interpeptide bridge containing cell wall precursor (lipid II-Gly5) of Staphylococcus aureus*. Mol Microbiol, 2004. **53**(2): p. 675-85.
75. Thumm, G. and F. Gotz, *Studies on polysostaphin processing and characterization of the lysostaphin immunity factor (Lif) of Staphylococcus simulans biovar staphylolyticus*. Mol Microbiol, 1997. **23**(6): p. 1251-65.
76. Tschierske, M., et al., *Lif, the lysostaphin immunity factor, complements FemB in staphylococcal peptidoglycan interpeptide bridge formation*. FEMS Microbiol Lett, 1997. **153**(2): p. 261-4.
77. Bouhss, A., et al., *Synthesis of the L-alanyl-L-alanine cross-bridge of Enterococcus faecalis peptidoglycan*. J Biol Chem, 2002. **277**(48): p. 45935-41.

78. Filipe, S.R., M.G. Pinho, and A. Tomasz, *Characterization of the murMN operon involved in the synthesis of branched peptidoglycan peptides in Streptococcus pneumoniae*. J Biol Chem, 2000. **275**(36): p. 27768-74.
79. Kresge, N., Simoni, R.D., Hill, R.L. , *t-RNA involvement in peptidoglycan synthesis: the work of Dieter Soll*. J Biol Chem, 2007. **282**(26): p. e20-e21.
80. Mohammadi, T., et al., *Identification of FtsW as a transporter of lipid-linked cell wall precursors across the membrane*. EMBO J, 2011. **30**(8): p. 1425-32.
81. Ruiz, N., *Bioinformatics identification of MurJ (MviN) as the peptidoglycan lipid II flippase in Escherichia coli*. Proc Natl Acad Sci U S A, 2008. **105**(40): p. 15553-7.
82. Ruiz, N., *Streptococcus pyogenes YtgP (Spy_0390) complements Escherichia coli strains depleted of the putative peptidoglycan flippase MurJ*. Antimicrob Agents Chemother, 2009. **53**(8): p. 3604-5.
83. Sham, L.T., et al., *Bacterial cell wall. MurJ is the flippase of lipid-linked precursors for peptidoglycan biogenesis*. Science, 2014. **345**(6193): p. 220-2.
84. Meeske, A.J., et al., *MurJ and a novel lipid II flippase are required for cell wall biogenesis in Bacillus subtilis*. Proc Natl Acad Sci U S A, 2015. **112**(20): p. 6437-42.
85. Blumberg, P.M. and J.L. Strominger, *Interaction of penicillin with the bacterial cell: penicillin-binding proteins and penicillin-sensitive enzymes*. Bacteriol Rev, 1974. **38**(3): p. 291-335.
86. Ghuysen, J.M., *Serine beta-lactamases and penicillin-binding proteins*. Annu Rev Microbiol, 1991. **45**: p. 37-67.
87. Sauvage, E., et al., *The penicillin-binding proteins: structure and role in peptidoglycan biosynthesis*. FEMS Microbiol Rev, 2008. **32**(2): p. 234-58.
88. Waxman, D.J. and J.L. Strominger, *Penicillin-binding proteins and the mechanism of action of beta-lactam antibiotics*. Annu Rev Biochem, 1983. **52**: p. 825-69.
89. Pinho, M.G., H. de Lencastre, and A. Tomasz, *Cloning, characterization, and inactivation of the gene pbpC, encoding penicillin-binding protein 3 of Staphylococcus aureus*. J Bacteriol, 2000. **182**(4): p. 1074-9.
90. Wada, A. and H. Watanabe, *Penicillin-binding protein 1 of Staphylococcus aureus is essential for growth*. J Bacteriol, 1998. **180**(10): p. 2759-65.
91. Pinho, M.G., H. de Lencastre, and A. Tomasz, *An acquired and a native penicillin-binding protein cooperate in building the cell wall of drug-resistant staphylococci*. Proc Natl Acad Sci U S A, 2001. **98**(19): p. 10886-91.

92. Kozarich, J.W. and J.L. Strominger, *A membrane enzyme from Staphylococcus aureus which catalyzes transpeptidase, carboxypeptidase, and penicillinase activities*. J Biol Chem, 1978. **253**(4): p. 1272-8.
93. Qiao, Y., et al., *Detection of lipid-linked peptidoglycan precursors by exploiting an unexpected transpeptidase reaction*. J Am Chem Soc, 2014. **136**(42): p. 14678-81.
94. Wyke, A.W., et al., *A role in vivo for penicillin-binding protein-4 of Staphylococcus aureus*. Eur J Biochem, 1981. **119**(2): p. 389-93.
95. Hartman, B.J. and A. Tomasz, *Low-affinity penicillin-binding protein associated with beta-lactam resistance in Staphylococcus aureus*. J Bacteriol, 1984. **158**(2): p. 513-6.
96. Lim, D. and N.C. Strynadka, *Structural basis for the beta lactam resistance of PBP2a from methicillin-resistant Staphylococcus aureus*. Nat Struct Biol, 2002. **9**(11): p. 870-6.
97. Reed, P., et al., *Monofunctional transglycosylases are not essential for Staphylococcus aureus cell wall synthesis*. J Bacteriol, 2011. **193**(10): p. 2549-56.
98. Heaslet, H., et al., *Characterization of the active site of S. aureus monofunctional glycosyltransferase (Mtg) by site-directed mutation and structural analysis of the protein complexed with moenomycin*. J Struct Biol, 2009. **167**(2): p. 129-35.
99. Terrak, M. and M. Nguyen-Disteche, *Kinetic characterization of the monofunctional glycosyltransferase from Staphylococcus aureus*. J Bacteriol, 2006. **188**(7): p. 2528-32.
100. Pinho, M.G., et al., *Complementation of the essential peptidoglycan transpeptidase function of penicillin-binding protein 2 (PBP2) by the drug resistance protein PBP2A in Staphylococcus aureus*. J Bacteriol, 2001. **183**(22): p. 6525-31.
101. Reed, P., et al., *Staphylococcus aureus Survives with a Minimal Peptidoglycan Synthesis Machine but Sacrifices Virulence and Antibiotic Resistance*. PLoS Pathog, 2015. **11**(5): p. e1004891.
102. Zapun, A., T. Vernet, and M.G. Pinho, *The different shapes of cocci*. FEMS Microbiol Rev, 2008. **32**(2): p. 345-60.
103. Claessen, D., et al., *Control of the cell elongation-division cycle by shuttling of PBP1 protein in Bacillus subtilis*. Mol Microbiol, 2008. **68**(4): p. 1029-46.

104. Daniel, R.A., E.J. Harry, and J. Errington, *Role of penicillin-binding protein PBP 2B in assembly and functioning of the division machinery of Bacillus subtilis*. Mol Microbiol, 2000. **35**(2): p. 299-311.
105. Spratt, B.G., *Distinct penicillin binding proteins involved in the division, elongation, and shape of Escherichia coli K12*. Proc Natl Acad Sci U S A, 1975. **72**(8): p. 2999-3003.
106. Scheffers, D.J. and M.G. Pinho, *Bacterial cell wall synthesis: new insights from localization studies*. Microbiol Mol Biol Rev, 2005. **69**(4): p. 585-607.
107. Bouhss, A., et al., *The biosynthesis of peptidoglycan lipid-linked intermediates*. FEMS Microbiol Rev, 2008. **32**(2): p. 208-33.
108. El Ghachi, M., et al., *Identification of multiple genes encoding membrane proteins with undecaprenyl pyrophosphate phosphatase (UppP) activity in Escherichia coli*. J Biol Chem, 2005. **280**(19): p. 18689-95.
109. El Ghachi, M., et al., *The bacA gene of Escherichia coli encodes an undecaprenyl pyrophosphate phosphatase activity*. J Biol Chem, 2004. **279**(29): p. 30106-13.
110. Moynihan, P.J., D. Sychantha, and A.J. Clarke, *Chemical biology of peptidoglycan acetylation and deacetylation*. Bioorg Chem, 2014. **54**: p. 44-50.
111. Davis, K.M. and J.N. Weiser, *Modifications to the peptidoglycan backbone help bacteria to establish infection*. Infect Immun, 2011. **79**(2): p. 562-70.
112. Ohno, N., T. Yadomae, and T. Miyazaki, *Identification of 2-amino-2-deoxyglucose residues in the peptidoglycan of Streptococcus pneumoniae*. Carbohydr Res, 1982. **107**(1): p. 152-5.
113. Hayashi, H., Y. Araki, and E. Ito, *Occurrence of glucosamine residues with free amino groups in cell wall peptidoglycan from bacilli as a factor responsible for resistance to lysozyme*. J Bacteriol, 1973. **113**(2): p. 592-8.
114. Vollmer, W. and A. Tomasz, *The pgdA gene encodes for a peptidoglycan N-acetylglucosamine deacetylase in Streptococcus pneumoniae*. J Biol Chem, 2000. **275**(27): p. 20496-501.
115. Zipperle, G.F., Jr., J.W. Ezzell, Jr., and R.J. Doyle, *Glucosamine substitution and muramidase susceptibility in Bacillus anthracis*. Can J Microbiol, 1984. **30**(5): p. 553-9.
116. Fukushima, T., T. Kitajima, and J. Sekiguchi, *A polysaccharide deacetylase homologue, PdaA, in Bacillus subtilis acts as an N-acetylmuramic acid deacetylase in vitro*. J Bacteriol, 2005. **187**(4): p. 1287-92.

117. Kobayashi, K., et al., *Identification and characterization of a novel polysaccharide deacetylase C (PdaC) from Bacillus subtilis*. J Biol Chem, 2012. **287**(13): p. 9765-76.
118. Fukushima, T., et al., *A polysaccharide deacetylase gene (pdaA) is required for germination and for production of muramic delta-lactam residues in the spore cortex of Bacillus subtilis*. J Bacteriol, 2002. **184**(21): p. 6007-15.
119. Clarke, A.J. and C. Dupont, *O-acetylated peptidoglycan: its occurrence, pathobiological significance, and biosynthesis*. Can J Microbiol, 1992. **38**(2): p. 85-91.
120. Bera, A., et al., *Why are pathogenic staphylococci so lysozyme resistant? The peptidoglycan O-acetyltransferase OatA is the major determinant for lysozyme resistance of Staphylococcus aureus*. Mol Microbiol, 2005. **55**(3): p. 778-87.
121. Crisostomo, M.I., et al., *Attenuation of penicillin resistance in a peptidoglycan O-acetyl transferase mutant of Streptococcus pneumoniae*. Mol Microbiol, 2006. **61**(6): p. 1497-509.
122. Hebert, L., et al., *Enterococcus faecalis constitutes an unusual bacterial model in lysozyme resistance*. Infect Immun, 2007. **75**(11): p. 5390-8.
123. Laaberki, M.H., et al., *O-Acetylation of peptidoglycan is required for proper cell separation and S-layer anchoring in Bacillus anthracis*. J Biol Chem, 2011. **286**(7): p. 5278-88.
124. Lunderberg, J.M., et al., *Bacillus anthracis acetyltransferases PatA1 and PatA2 modify the secondary cell wall polysaccharide and affect the assembly of S-layer proteins*. J Bacteriol, 2013. **195**(5): p. 977-89.
125. Aubry, C., et al., *OatA, a peptidoglycan O-acetyltransferase involved in Listeria monocytogenes immune escape, is critical for virulence*. J Infect Dis, 2011. **204**(5): p. 731-40.
126. Bera, A., et al., *The presence of peptidoglycan O-acetyltransferase in various staphylococcal species correlates with lysozyme resistance and pathogenicity*. Infect Immun, 2006. **74**(8): p. 4598-604.
127. Shimada, T., et al., *Staphylococcus aureus evades lysozyme-based peptidoglycan digestion that links phagocytosis, inflammasome activation, and IL-1beta secretion*. Cell Host Microbe, 2010. **7**(1): p. 38-49.
128. Bernard, E., et al., *Characterization of O-acetylation of N-acetylglucosamine: a novel structural variation of bacterial peptidoglycan*. J Biol Chem, 2011. **286**(27): p. 23950-8.

129. Perry, A.M., et al., *Anchoring of surface proteins to the cell wall of Staphylococcus aureus. III. Lipid II is an in vivo peptidoglycan substrate for sortase-catalyzed surface protein anchoring.* J Biol Chem, 2002. **277**(18): p. 16241-8.
130. Ruzin, A., et al., *Further evidence that a cell wall precursor [C(55)-MurNAc-(peptide)-GlcNAc] serves as an acceptor in a sorting reaction.* J Bacteriol, 2002. **184**(8): p. 2141-7.
131. Powell, D.A., M. Duckworth, and J. Baddiley, *A membrane-associated lipomannan in micrococci.* Biochem J, 1975. **151**(2): p. 387-97.
132. Neuhaus, F.C. and J. Baddiley, *A continuum of anionic charge: structures and functions of D-alanyl-teichoic acids in gram-positive bacteria.* Microbiol Mol Biol Rev, 2003. **67**(4): p. 686-723.
133. Tempest, D.W., J.W. Dicks, and D.C. Ellwood, *Influence of growth condition on the concentration of potassium in Bacillus subtilis var. niger and its possible relationship to cellular ribonucleic acid, teichoic acid and teichuronic acid.* Biochem J, 1968. **106**(1): p. 237-43.
134. Bhavsar, A.P., et al., *Teichoic acid is an essential polymer in Bacillus subtilis that is functionally distinct from teichuronic acid.* J Bacteriol, 2004. **186**(23): p. 7865-73.
135. Taylor, V.L., S.M. Huszczyński, and J.S. Lam, *Membrane Translocation and Assembly of Sugar Polymer Precursors.* Curr Top Microbiol Immunol, 2016.
136. Hancock, I.C., *Bacterial cell surface carbohydrates: structure and assembly.* Biochem Soc Trans, 1997. **25**(1): p. 183-7.
137. Armstrong, J.J., J. Baddiley, and J.G. Buchanan, *Structure of the ribitol teichoic acid from the walls of Bacillus subtilis.* Biochem J, 1960. **76**: p. 610-21.
138. Kojima, N., Y. Araki, and E. Ito, *Structure of the linkage units between ribitol teichoic acids and peptidoglycan.* J Bacteriol, 1985. **161**(1): p. 299-306.
139. Denapaite, D., et al., *Biosynthesis of teichoic acids in Streptococcus pneumoniae and closely related species: lessons from genomes.* Microb Drug Resist, 2012. **18**(3): p. 344-58.
140. Fischer, W., et al., *Teichoic acid and lipoteichoic acid of Streptococcus pneumoniae possess identical chain structures. A reinvestigation of teichoid acid (C polysaccharide).* Eur J Biochem, 1993. **215**(3): p. 851-7.
141. Theilacker, C., et al., *The structure of the wall teichoic acid isolated from Enterococcus faecalis strain 12030.* Carbohydr Res, 2012. **354**: p. 106-9.

142. Bychowska, A., et al., *Chemical structure of wall teichoic acid isolated from Enterococcus faecium strain U0317*. Carbohydr Res, 2011. **346**(17): p. 2816-9.
143. Brown, S., et al., *Staphylococcus aureus and Bacillus subtilis W23 make polyribitol wall teichoic acids using different enzymatic pathways*. Chem Biol, 2010. **17**(10): p. 1101-10.
144. Brown, S., Y.H. Zhang, and S. Walker, *A revised pathway proposed for Staphylococcus aureus wall teichoic acid biosynthesis based on in vitro reconstitution of the intracellular steps*. Chem Biol, 2008. **15**(1): p. 12-21.
145. Lazarevic, V., et al., *Comparison of ribitol and glycerol teichoic acid genes in Bacillus subtilis W23 and 168: identical function, similar divergent organization, but different regulation*. Microbiology, 2002. **148**(Pt 3): p. 815-24.
146. Mael, C., M. Young, and D. Karamata, *Genes concerned with synthesis of poly(glycerol phosphate), the essential teichoic acid in Bacillus subtilis strain 168, are organized in two divergent transcription units*. J Gen Microbiol, 1991. **137**(4): p. 929-41.
147. Soldo, B., V. Lazarevic, and D. Karamata, *tagO is involved in the synthesis of all anionic cell-wall polymers in Bacillus subtilis 168*. Microbiology, 2002. **148**(Pt 7): p. 2079-87.
148. Ginsberg, C., et al., *In vitro reconstitution of two essential steps in wall teichoic acid biosynthesis*. ACS Chem Biol, 2006. **1**(1): p. 25-8.
149. D'Elia, M.A., et al., *The N-acetylmannosamine transferase catalyzes the first committed step of teichoic acid assembly in Bacillus subtilis and Staphylococcus aureus*. J Bacteriol, 2009. **191**(12): p. 4030-4.
150. Bhavsar, A.P., R. Truant, and E.D. Brown, *The TagB protein in Bacillus subtilis 168 is an intracellular peripheral membrane protein that can incorporate glycerol phosphate onto a membrane-bound acceptor in vitro*. J Biol Chem, 2005. **280**(44): p. 36691-700.
151. Pereira, M.P., et al., *The wall teichoic acid polymerase TagF efficiently synthesizes poly(glycerol phosphate) on the TagB product lipid III*. ChemBiochem, 2008. **9**(9): p. 1385-90.
152. Meredith, T.C., J.G. Swoboda, and S. Walker, *Late-stage polyribitol phosphate wall teichoic acid biosynthesis in Staphylococcus aureus*. J Bacteriol, 2008. **190**(8): p. 3046-56.
153. Lazarevic, V. and D. Karamata, *The tagGH operon of Bacillus subtilis 168 encodes a two-component ABC transporter involved in the metabolism of two wall teichoic acids*. Mol Microbiol, 1995. **16**(2): p. 345-55.

154. Chaudhuri, R.R., et al., *Comprehensive identification of essential Staphylococcus aureus genes using Transposon-Mediated Differential Hybridisation (TMDH)*. BMC Genomics, 2009. **10**: p. 291.
155. Kobayashi, K., et al., *Essential Bacillus subtilis genes*. Proc Natl Acad Sci U S A, 2003. **100**(8): p. 4678-83.
156. D'Elia, M.A., et al., *Lesions in teichoic acid biosynthesis in Staphylococcus aureus lead to a lethal gain of function in the otherwise dispensable pathway*. J Bacteriol, 2006. **188**(12): p. 4183-9.
157. D'Elia, M.A., et al., *Probing teichoic acid genetics with bioactive molecules reveals new interactions among diverse processes in bacterial cell wall biogenesis*. Chem Biol, 2009. **16**(5): p. 548-56.
158. Xayarath, B. and J. Yother, *Mutations blocking side chain assembly, polymerization, or transport of a Wzy-dependent Streptococcus pneumoniae capsule are lethal in the absence of suppressor mutations and can affect polymer transfer to the cell wall*. J Bacteriol, 2007. **189**(9): p. 3369-81.
159. Kawai, Y., et al., *A widespread family of bacterial cell wall assembly proteins*. EMBO J, 2011. **30**(24): p. 4931-41.
160. Over, B., et al., *LytR-CpsA-Psr proteins in Staphylococcus aureus display partial functional redundancy and the deletion of all three severely impairs septum placement and cell separation*. FEMS Microbiol Lett, 2011. **320**(2): p. 142-51.
161. Dengler, V., et al., *Deletion of hypothetical wall teichoic acid ligases in Staphylococcus aureus activates the cell wall stress response*. FEMS Microbiol Lett, 2012. **333**(2): p. 109-20.
162. Chan, Y.G., et al., *The capsular polysaccharide of Staphylococcus aureus is attached to peptidoglycan by the LytR-CpsA-Psr (LCP) family of enzymes*. J Biol Chem, 2014. **289**(22): p. 15680-90.
163. Chan, Y.G., et al., *Staphylococcus aureus mutants lacking the LytR-CpsA-Psr family of enzymes release cell wall teichoic acids into the extracellular medium*. J Bacteriol, 2013. **195**(20): p. 4650-9.
164. Schaefer, K., Matano, L.M., Qiao, Y., Kahne, D., Walker, S., *A reconstitution of cell wall glycopolymers reveals attachment to pre-formed peptidoglycan*. Submitted, 2016.
165. Fischer, W., *Physiology of lipoteichoic acids in bacteria*. Adv Microb Physiol, 1988. **29**: p. 233-302.

166. Kiriukhin, M.Y., et al., *Biosynthesis of the glycolipid anchor in lipoteichoic acid of Staphylococcus aureus RN4220: role of YpfP, the diglucoxyldiacylglycerol synthase*. J Bacteriol, 2001. **183**(11): p. 3506-14.
167. Jorasch, P., et al., *A UDP glucosyltransferase from Bacillus subtilis successively transfers up to four glucose residues to 1,2-diacylglycerol: expression of ypfP in Escherichia coli and structural analysis of its reaction products*. Mol Microbiol, 1998. **29**(2): p. 419-30.
168. Grundling, A. and O. Schneewind, *Genes required for glycolipid synthesis and lipoteichoic acid anchoring in Staphylococcus aureus*. J Bacteriol, 2007. **189**(6): p. 2521-30.
169. Grundling, A. and O. Schneewind, *Synthesis of glycerol phosphate lipoteichoic acid in Staphylococcus aureus*. Proc Natl Acad Sci U S A, 2007. **104**(20): p. 8478-83.
170. Lu, D., et al., *Structure-based mechanism of lipoteichoic acid synthesis by Staphylococcus aureus LtaS*. Proc Natl Acad Sci U S A, 2009. **106**(5): p. 1584-9.
171. Schirner, K., et al., *Distinct and essential morphogenic functions for wall- and lipo-teichoic acids in Bacillus subtilis*. EMBO J, 2009. **28**(7): p. 830-42.
172. Webb, A.J., M. Karatsa-Dodgson, and A. Grundling, *Two-enzyme systems for glycolipid and polyglycerolphosphate lipoteichoic acid synthesis in Listeria monocytogenes*. Mol Microbiol, 2009. **74**(2): p. 299-314.
173. Campeotto, I., et al., *Structural and mechanistic insight into the Listeria monocytogenes two-enzyme lipoteichoic acid synthesis system*. J Biol Chem, 2014. **289**(41): p. 28054-69.
174. Karatsa-Dodgson, M., M.E. Wormann, and A. Grundling, *In vitro analysis of the Staphylococcus aureus lipoteichoic acid synthase enzyme using fluorescently labeled lipids*. J Bacteriol, 2010. **192**(20): p. 5341-9.
175. Jerga, A., et al., *Identification of a soluble diacylglycerol kinase required for lipoteichoic acid production in Bacillus subtilis*. J Biol Chem, 2007. **282**(30): p. 21738-45.
176. Wormann, M.E., et al., *Enzymatic activities and functional interdependencies of Bacillus subtilis lipoteichoic acid synthesis enzymes*. Mol Microbiol, 2011. **79**(3): p. 566-83.
177. Jervis, A.J., et al., *SigM-responsive genes of Bacillus subtilis and their promoters*. J Bacteriol, 2007. **189**(12): p. 4534-8.
178. Corrigan, R.M., et al., *Systematic identification of conserved bacterial c-di-AMP receptor proteins*. Proc Natl Acad Sci U S A, 2013. **110**(22): p. 9084-9.

179. Corrigan, R.M., et al., *c-di-AMP is a new second messenger in Staphylococcus aureus with a role in controlling cell size and envelope stress*. PLoS Pathog, 2011. **7**(9): p. e1002217.
180. Oku, Y., et al., *Pleiotropic roles of polyglycerolphosphate synthase of lipoteichoic acid in growth of Staphylococcus aureus cells*. J Bacteriol, 2009. **191**(1): p. 141-51.
181. Heaton, M.P. and F.C. Neuhaus, *Biosynthesis of D-alanyl-lipoteichoic acid: cloning, nucleotide sequence, and expression of the Lactobacillus casei gene for the D-alanine-activating enzyme*. J Bacteriol, 1992. **174**(14): p. 4707-17.
182. Heaton, M.P. and F.C. Neuhaus, *Role of the D-alanyl carrier protein in the biosynthesis of D-alanyl-lipoteichoic acid*. J Bacteriol, 1994. **176**(3): p. 681-90.
183. Perego, M., et al., *Incorporation of D-alanine into lipoteichoic acid and wall teichoic acid in Bacillus subtilis. Identification of genes and regulation*. J Biol Chem, 1995. **270**(26): p. 15598-606.
184. Volkman, B.F., et al., *Biosynthesis of D-alanyl-lipoteichoic acid: the tertiary structure of apo-D-alanyl carrier protein*. Biochemistry, 2001. **40**(27): p. 7964-72.
185. Yonus, H., et al., *Crystal structure of DltA. Implications for the reaction mechanism of non-ribosomal peptide synthetase adenylation domains*. J Biol Chem, 2008. **283**(47): p. 32484-91.
186. Hofmann, K., *A superfamily of membrane-bound O-acyltransferases with implications for wnt signaling*. Trends Biochem Sci, 2000. **25**(3): p. 111-2.
187. Reichmann, N.T., C.P. Cassona, and A. Grundling, *Revised mechanism of D-alanine incorporation into cell wall polymers in Gram-positive bacteria*. Microbiology, 2013. **159**(Pt 9): p. 1868-77.
188. Koch, H.U., R. Doker, and W. Fischer, *Maintenance of D-alanine ester substitution of lipoteichoic acid by reesterification in Staphylococcus aureus*. J Bacteriol, 1985. **164**(3): p. 1211-7.
189. Haas, R., Koch, H.U., Fischer, W., *Alanyl turnover from lipoteichoic acid to teichoic acid in Staphylococcus aureus*. FEMS Microbiol Lett, 1984. **21**(1): p. 27-31.
190. Draing, C., et al., *Comparison of lipoteichoic acid from different serotypes of Streptococcus pneumoniae*. J Biol Chem, 2006. **281**(45): p. 33849-59.
191. Allison, S.E., et al., *Studies of the genetics, function, and kinetic mechanism of TagE, the wall teichoic acid glycosyltransferase in Bacillus subtilis 168*. J Biol Chem, 2011. **286**(27): p. 23708-16.

192. Brown, S., et al., *Methicillin resistance in Staphylococcus aureus requires glycosylated wall teichoic acids*. Proc Natl Acad Sci U S A, 2012. **109**(46): p. 18909-14.
193. Sobhanifar, S., et al., *Structure and mechanism of Staphylococcus aureus TarM, the wall teichoic acid alpha-glycosyltransferase*. Proc Natl Acad Sci U S A, 2015. **112**(6): p. E576-85.
194. Xia, G., et al., *Glycosylation of wall teichoic acid in Staphylococcus aureus by TarM*. J Biol Chem, 2010. **285**(18): p. 13405-15.
195. Boylan, R.J., et al., *Regulation of the bacterial cell wall: analysis of a mutant of Bacillus subtilis defective in biosynthesis of teichoic acid*. J Bacteriol, 1972. **110**(1): p. 281-90.
196. Pollack, J.H. and F.C. Neuhaus, *Changes in wall teichoic acid during the rod-sphere transition of Bacillus subtilis 168*. J Bacteriol, 1994. **176**(23): p. 7252-9.
197. Schirner, K., et al., *Lipid-linked cell wall precursors regulate membrane association of bacterial actin MreB*. Nat Chem Biol, 2015. **11**(1): p. 38-45.
198. Matsuoka, S., et al., *Abnormal morphology of Bacillus subtilis ugtP mutant cells lacking glucolipids*. Genes Genet Syst, 2011. **86**(5): p. 295-304.
199. Weart, R.B., et al., *A metabolic sensor governing cell size in bacteria*. Cell, 2007. **130**(2): p. 335-47.
200. Campbell, J., et al., *Synthetic lethal compound combinations reveal a fundamental connection between wall teichoic acid and peptidoglycan biosyntheses in Staphylococcus aureus*. ACS Chem Biol, 2011. **6**(1): p. 106-16.
201. Valentino, M.D., et al., *Genes contributing to Staphylococcus aureus fitness in abscess- and infection-related ecologies*. MBio, 2014. **5**(5): p. e01729-14.
202. Wang, H., et al., *Discovery of wall teichoic acid inhibitors as potential anti-MRSA beta-lactam combination agents*. Chem Biol, 2013. **20**(2): p. 272-84.
203. Weidenmaier, C., et al., *Lack of wall teichoic acids in Staphylococcus aureus leads to reduced interactions with endothelial cells and to attenuated virulence in a rabbit model of endocarditis*. J Infect Dis, 2005. **191**(10): p. 1771-7.
204. Santa Maria, J.P., Jr., et al., *Compound-gene interaction mapping reveals distinct roles for Staphylococcus aureus teichoic acids*. Proc Natl Acad Sci U S A, 2014. **111**(34): p. 12510-5.
205. Archibald, A.R., J. Baddiley, and S. Heptinstall, *The alanine ester content and magnesium binding capacity of walls of Staphylococcus aureus H grown at different pH values*. Biochim Biophys Acta, 1973. **291**(3): p. 629-34.

206. Chatterjee, A.N., *Use of bacteriophage-resistant mutants to study the nature of the bacteriophage receptor site of Staphylococcus aureus*. J Bacteriol, 1969. **98**(2): p. 519-27.
207. Young, F.E., *Requirement of glucosylated teichoic acid for adsorption of phage in Bacillus subtilis 168*. Proc Natl Acad Sci U S A, 1967. **58**(6): p. 2377-84.
208. Qamar, A. and D. Golemi-Kotra, *Dual roles of FmtA in Staphylococcus aureus cell wall biosynthesis and autolysis*. Antimicrob Agents Chemother, 2012. **56**(7): p. 3797-805.
209. Fischer, W., *Phosphocholine of pneumococcal teichoic acids: role in bacterial physiology and pneumococcal infection*. Res Microbiol, 2000. **151**(6): p. 421-7.
210. Giudicelli, S. and A. Tomasz, *Attachment of pneumococcal autolysin to wall teichoic acids, an essential step in enzymatic wall degradation*. J Bacteriol, 1984. **158**(3): p. 1188-90.
211. Gosink, K.K., et al., *Role of novel choline binding proteins in virulence of Streptococcus pneumoniae*. Infect Immun, 2000. **68**(10): p. 5690-5.
212. Hakenbeck, R., et al., *Versatility of choline metabolism and choline-binding proteins in Streptococcus pneumoniae and commensal streptococci*. FEMS Microbiol Rev, 2009. **33**(3): p. 572-86.
213. Rosenow, C., et al., *Contribution of novel choline-binding proteins to adherence, colonization and immunogenicity of Streptococcus pneumoniae*. Mol Microbiol, 1997. **25**(5): p. 819-29.
214. Jonquieres, R., et al., *Interaction between the protein InlB of Listeria monocytogenes and lipoteichoic acid: a novel mechanism of protein association at the surface of gram-positive bacteria*. Mol Microbiol, 1999. **34**(5): p. 902-14.
215. Cabanes, D., et al., *Surface proteins and the pathogenic potential of Listeria monocytogenes*. Trends Microbiol, 2002. **10**(5): p. 238-45.
216. Schlag, M., et al., *Role of staphylococcal wall teichoic acid in targeting the major autolysin Atl*. Mol Microbiol, 2010. **75**(4): p. 864-73.
217. Peschel, A., et al., *The D-alanine residues of Staphylococcus aureus teichoic acids alter the susceptibility to vancomycin and the activity of autolytic enzymes*. Antimicrob Agents Chemother, 2000. **44**(10): p. 2845-7.
218. Atilano, M.L., et al., *Teichoic acids are temporal and spatial regulators of peptidoglycan cross-linking in Staphylococcus aureus*. Proc Natl Acad Sci U S A, 2010. **107**(44): p. 18991-6.

219. Kohler, T., C. Weidenmaier, and A. Peschel, *Wall teichoic acid protects Staphylococcus aureus against antimicrobial fatty acids from human skin*. J Bacteriol, 2009. **191**(13): p. 4482-4.
220. Collins, L.V., et al., *Staphylococcus aureus strains lacking D-alanine modifications of teichoic acids are highly susceptible to human neutrophil killing and are virulence attenuated in mice*. J Infect Dis, 2002. **186**(2): p. 214-9.
221. Kristian, S.A., et al., *D-alanylation of teichoic acids promotes group a streptococcus antimicrobial peptide resistance, neutrophil survival, and epithelial cell invasion*. J Bacteriol, 2005. **187**(19): p. 6719-25.
222. Peschel, A., et al., *Inactivation of the dlt operon in Staphylococcus aureus confers sensitivity to defensins, protegrins, and other antimicrobial peptides*. J Biol Chem, 1999. **274**(13): p. 8405-10.
223. Kovacs, M., et al., *A functional dlt operon, encoding proteins required for incorporation of d-alanine in teichoic acids in gram-positive bacteria, confers resistance to cationic antimicrobial peptides in Streptococcus pneumoniae*. J Bacteriol, 2006. **188**(16): p. 5797-805.
224. Fabretti, F., et al., *Alanine esters of enterococcal lipoteichoic acid play a role in biofilm formation and resistance to antimicrobial peptides*. Infect Immun, 2006. **74**(7): p. 4164-71.
225. Yang, S.J., et al., *Enhanced expression of dltABCD is associated with the development of daptomycin nonsusceptibility in a clinical endocarditis isolate of Staphylococcus aureus*. J Infect Dis, 2009. **200**(12): p. 1916-20.
226. Mishra, N.N., et al., *Phenotypic and genotypic characterization of daptomycin-resistant methicillin-resistant Staphylococcus aureus strains: relative roles of mprF and dlt operons*. PLoS One, 2014. **9**(9): p. e107426.
227. Saar-Dover, R., et al., *D-alanylation of lipoteichoic acids confers resistance to cationic peptides in group B streptococcus by increasing the cell wall density*. PLoS Pathog, 2012. **8**(9): p. e1002891.
228. Gross, M., et al., *Key role of teichoic acid net charge in Staphylococcus aureus colonization of artificial surfaces*. Infect Immun, 2001. **69**(5): p. 3423-6.
229. Jett, B.D., M.M. Huycke, and M.S. Gilmore, *Virulence of enterococci*. Clin Microbiol Rev, 1994. **7**(4): p. 462-78.
230. Hall-Stoodley, L., J.W. Costerton, and P. Stoodley, *Bacterial biofilms: from the natural environment to infectious diseases*. Nat Rev Microbiol, 2004. **2**(2): p. 95-108.

231. Sutherland, I., *Biofilm exopolysaccharides: a strong and sticky framework*. Microbiology, 2001. **147**(Pt 1): p. 3-9.
232. Abee, T., et al., *Biofilm formation and dispersal in Gram-positive bacteria*. Curr Opin Biotechnol, 2011. **22**(2): p. 172-9.
233. Aly, R., et al., *Role of teichoic acid in the binding of Staphylococcus aureus to nasal epithelial cells*. J Infect Dis, 1980. **141**(4): p. 463-5.
234. Baur, S., et al., *A nasal epithelial receptor for Staphylococcus aureus WTA governs adhesion to epithelial cells and modulates nasal colonization*. PLoS Pathog, 2014. **10**(5): p. e1004089.
235. Weidenmaier, C., et al., *Role of teichoic acids in Staphylococcus aureus nasal colonization, a major risk factor in nosocomial infections*. Nat Med, 2004. **10**(3): p. 243-5.
236. Winstel, V., et al., *Wall Teichoic Acid Glycosylation Governs Staphylococcus aureus Nasal Colonization*. MBio, 2015. **6**(4): p. e00632.
237. Abachin, E., et al., *Formation of D-alanyl-lipoteichoic acid is required for adhesion and virulence of Listeria monocytogenes*. Mol Microbiol, 2002. **43**(1): p. 1-14.
238. Fittipaldi, N., et al., *D-alanylation of lipoteichoic acid contributes to the virulence of Streptococcus suis*. Infect Immun, 2008. **76**(8): p. 3587-94.
239. Suzuki, T., et al., *Role of wall teichoic acids in Staphylococcus aureus endophthalmitis*. Invest Ophthalmol Vis Sci, 2011. **52**(6): p. 3187-92.
240. Xu, H., et al., *Pneumococcal wall teichoic acid is required for the pathogenesis of Streptococcus pneumoniae in murine models*. J Microbiol, 2015. **53**(2): p. 147-54.
241. Kharat, A.S. and A. Tomasz, *Drastic reduction in the virulence of Streptococcus pneumoniae expressing type 2 capsular polysaccharide but lacking choline residues in the cell wall*. Mol Microbiol, 2006. **60**(1): p. 93-107.
242. Ginsburg, I., *Role of lipoteichoic acid in infection and inflammation*. Lancet Infect Dis, 2002. **2**(3): p. 171-9.
243. Hashimoto, M., et al., *Lipoprotein is a predominant Toll-like receptor 2 ligand in Staphylococcus aureus cell wall components*. Int Immunol, 2006. **18**(2): p. 355-62.
244. Hashimoto, M., et al., *Not lipoteichoic acid but lipoproteins appear to be the dominant immunobiologically active compounds in Staphylococcus aureus*. J Immunol, 2006. **177**(5): p. 3162-9.

245. Bunk, S., et al., *Internalization and coreceptor expression are critical for TLR2-mediated recognition of lipoteichoic acid in human peripheral blood*. J Immunol, 2010. **185**(6): p. 3708-17.
246. Mohamadzadeh, M., et al., *Regulation of induced colonic inflammation by Lactobacillus acidophilus deficient in lipoteichoic acid*. Proc Natl Acad Sci U S A, 2011. **108 Suppl 1**: p. 4623-30.
247. von Aulock, S., T. Hartung, and C. Hermann, *Comment on "Not lipoteichoic acid but lipoproteins appear to be the dominant immunobiologically active compounds in Staphylococcus aureus"*. J Immunol, 2007. **178**(5): p. 2610; author reply 2610-1.
248. Bhakdi, S., et al., *Stimulation of monokine production by lipoteichoic acids*. Infect Immun, 1991. **59**(12): p. 4614-20.
249. Draing, C., et al., *Cytokine induction by Gram-positive bacteria*. Immunobiology, 2008. **213**(3-4): p. 285-96.
250. Ray, A., et al., *Bacterial cell wall macroamphiphiles: pathogen-/microbe-associated molecular patterns detected by mammalian innate immune system*. Biochimie, 2013. **95**(1): p. 33-42.
251. Ryu, Y.H., et al., *Differential immunostimulatory effects of Gram-positive bacteria due to their lipoteichoic acids*. Int Immunopharmacol, 2009. **9**(1): p. 127-33.
252. Schroder, N.W., et al., *Lipoteichoic acid (LTA) of Streptococcus pneumoniae and Staphylococcus aureus activates immune cells via Toll-like receptor (TLR)-2, lipopolysaccharide-binding protein (LBP), and CD14, whereas TLR-4 and MD-2 are not involved*. J Biol Chem, 2003. **278**(18): p. 15587-94.
253. Fiedel, B.A. and R.W. Jackson, *Activation of the alternative complement pathway by a streptococcal lipoteichoic acid*. Infect Immun, 1978. **22**(1): p. 286-7.
254. Loos, M., F. Clas, and W. Fischer, *Interaction of purified lipoteichoic acid with the classical complement pathway*. Infect Immun, 1986. **53**(3): p. 595-9.
255. Keller, R., et al., *Macrophage response to bacteria: induction of marked secretory and cellular activities by lipoteichoic acids*. Infect Immun, 1992. **60**(9): p. 3664-72.
256. Theilacker, C., et al., *Opsonic antibodies to Enterococcus faecalis strain 12030 are directed against lipoteichoic acid*. Infect Immun, 2006. **74**(10): p. 5703-12.
257. Jedrzejewski, M.J., *Pneumococcal virulence factors: structure and function*. Microbiol Mol Biol Rev, 2001. **65**(2): p. 187-207 ; first page, table of contents.

258. Sorensen, U.B., et al., *Covalent linkage between the capsular polysaccharide and the cell wall peptidoglycan of Streptococcus pneumoniae revealed by immunochemical methods*. Microb Pathog, 1990. **8**(5): p. 325-34.
259. O'Riordan, K. and J.C. Lee, *Staphylococcus aureus capsular polysaccharides*. Clin Microbiol Rev, 2004. **17**(1): p. 218-34.
260. Roberts, I.S., *The biochemistry and genetics of capsular polysaccharide production in bacteria*. Annu Rev Microbiol, 1996. **50**: p. 285-315.
261. Kalin, M., *Pneumococcal serotypes and their clinical relevance*. Thorax, 1998. **53**(3): p. 159-62.
262. Coffey, T.J., et al., *Recombinational exchanges at the capsular polysaccharide biosynthetic locus lead to frequent serotype changes among natural isolates of Streptococcus pneumoniae*. Mol Microbiol, 1998. **27**(1): p. 73-83.
263. Calix, J.J., et al., *Spectrum of pneumococcal serotype 11A variants results from incomplete loss of capsule O-acetylation*. J Clin Microbiol, 2014. **52**(3): p. 758-65.
264. Calix, J.J. and M.H. Nahm, *A new pneumococcal serotype, 11E, has a variably inactivated wcjE gene*. J Infect Dis, 2010. **202**(1): p. 29-38.
265. van Selm, S., et al., *Genetic basis for the structural difference between Streptococcus pneumoniae serotype 15B and 15C capsular polysaccharides*. Infect Immun, 2003. **71**(11): p. 6192-8.
266. Venkateswaran, P.S., N. Stanton, and R. Austrian, *Type variation of strains of Streptococcus pneumoniae in capsular serogroup 15*. J Infect Dis, 1983. **147**(6): p. 1041-54.
267. Kenne, L., B. Lindberg, and S. Svensson, *The structure of capsular polysaccharide of the Pneumococcus type II*. Carbohydr Res, 1975. **40**(1): p. 69-75.
268. Oliver, M.B., et al., *Streptococcus pneumoniae serotype 11D has a bispecific glycosyltransferase and expresses two different capsular polysaccharide repeating units*. J Biol Chem, 2013. **288**(30): p. 21945-54.
269. Oliver, M.B., et al., *Discovery of Streptococcus pneumoniae serotype 6 variants with glycosyltransferases synthesizing two differing repeating units*. J Biol Chem, 2013. **288**(36): p. 25976-85.
270. Wilkinson, B.J. and K.M. Holmes, *Staphylococcus aureus cell surface: capsule as a barrier to bacteriophage adsorption*. Infect Immun, 1979. **23**(2): p. 549-52.

271. Tzianabos, A.O., J.Y. Wang, and J.C. Lee, *Structural rationale for the modulation of abscess formation by Staphylococcus aureus capsular polysaccharides*. Proc Natl Acad Sci U S A, 2001. **98**(16): p. 9365-70.
272. Cunnion, K.M., H.M. Zhang, and M.M. Frank, *Availability of complement bound to Staphylococcus aureus to interact with membrane complement receptors influences efficiency of phagocytosis*. Infect Immun, 2003. **71**(2): p. 656-62.
273. Peterson, P.K., et al., *Influence of encapsulation on staphylococcal opsonization and phagocytosis by human polymorphonuclear leukocytes*. Infect Immun, 1978. **19**(3): p. 943-9.
274. Thurlow, L.R., et al., *Enterococcus faecalis capsular polysaccharide serotypes C and D and their contributions to host innate immune evasion*. Infect Immun, 2009. **77**(12): p. 5551-7.
275. Carlin, A.F., et al., *Group B streptococcal capsular sialic acids interact with siglecs (immunoglobulin-like lectins) on human leukocytes*. J Bacteriol, 2007. **189**(4): p. 1231-7.
276. Carlin, A.F., et al., *Molecular mimicry of host sialylated glycans allows a bacterial pathogen to engage neutrophil Siglec-9 and dampen the innate immune response*. Blood, 2009. **113**(14): p. 3333-6.
277. Macleod, C.M., et al., *Prevention of Pneumococcal Pneumonia by Immunization with Specific Capsular Polysaccharides*. J Exp Med, 1945. **82**(6): p. 445-65.
278. Shapiro, E.D., et al., *The protective efficacy of polyvalent pneumococcal polysaccharide vaccine*. N Engl J Med, 1991. **325**(21): p. 1453-60.
279. de Velasco, E.A., et al., *Synthetic peptides representing T-cell epitopes act as carriers in pneumococcal polysaccharide conjugate vaccines*. Infect Immun, 1995. **63**(3): p. 961-8.
280. Bogaert, D., et al., *Pneumococcal vaccines: an update on current strategies*. Vaccine, 2004. **22**(17-18): p. 2209-20.
281. Pilishvili, T. and N.M. Bennett, *Pneumococcal disease prevention among adults: Strategies for the use of pneumococcal vaccines*. Vaccine, 2015. **33 Suppl 4**: p. D60-5.
282. Steens, A., et al., *A review of the evidence to inform pneumococcal vaccine recommendations for risk groups aged 2 years and older*. Epidemiol Infect, 2014. **142**(12): p. 2471-82.
283. Dagan, R., J. Poolman, and C.A. Siegrist, *Glycoconjugate vaccines and immune interference: A review*. Vaccine, 2010. **28**(34): p. 5513-23.

284. Pobre, K., et al., *Carrier priming or suppression: understanding carrier priming enhancement of anti-polysaccharide antibody response to conjugate vaccines*. *Vaccine*, 2014. **32**(13): p. 1423-30.
285. Pelton, S.I., A.M. Loughlin, and C.D. Marchant, *Seven valent pneumococcal conjugate vaccine immunization in two Boston communities: changes in serotypes and antimicrobial susceptibility among *Streptococcus pneumoniae* isolates*. *Pediatr Infect Dis J*, 2004. **23**(11): p. 1015-22.
286. Jefferies, J.M., et al., *Risk of red queen dynamics in pneumococcal vaccine strategy*. *Trends Microbiol*, 2011. **19**(8): p. 377-81.
287. Nurhonen, M. and K. Auranen, *Optimal serotype compositions for Pneumococcal conjugate vaccination under serotype replacement*. *PLoS Comput Biol*, 2014. **10**(2): p. e1003477.
288. Creech, C.B., 2nd, et al., *Vaccination as infection control: a pilot study to determine the impact of *Staphylococcus aureus* vaccination on nasal carriage*. *Vaccine*, 2009. **28**(1): p. 256-60.
289. Fattom, A.I., et al., *Development of StaphVAX, a polysaccharide conjugate vaccine against *S. aureus* infection: from the lab bench to phase III clinical trials*. *Vaccine*, 2004. **22**(7): p. 880-7.
290. Robbins, J.B., et al., **Staphylococcus aureus* types 5 and 8 capsular polysaccharide-protein conjugate vaccines*. *Am Heart J*, 2004. **147**(4): p. 593-8.
291. Bagnoli, F., S. Bertholet, and G. Grandi, *Inferring reasons for the failure of *Staphylococcus aureus* vaccines in clinical trials*. *Front Cell Infect Microbiol*, 2012. **2**: p. 16.
292. Cook, J., et al., **Staphylococcus aureus* capsule type 8 antibodies provide inconsistent efficacy in murine models of staphylococcal infection*. *Hum Vaccin*, 2009. **5**(4): p. 254-63.
293. Skurnik, D., et al., *Natural antibodies in normal human serum inhibit *Staphylococcus aureus* capsular polysaccharide vaccine efficacy*. *Clin Infect Dis*, 2012. **55**(9): p. 1188-97.
294. Otto, M., *Staphylococcal biofilms*. *Curr Top Microbiol Immunol*, 2008. **322**: p. 207-28.
295. Vlamakis, H., et al., *Sticking together: building a biofilm the *Bacillus subtilis* way*. *Nat Rev Microbiol*, 2013. **11**(3): p. 157-68.
296. Mack, D., et al., *The intercellular adhesin involved in biofilm accumulation of *Staphylococcus epidermidis* is a linear beta-1,6-linked glucosaminoglycan: purification and structural analysis*. *J Bacteriol*, 1996. **178**(1): p. 175-83.

297. Itoh, Y., et al., *Depolymerization of beta-1,6-N-acetyl-D-glucosamine disrupts the integrity of diverse bacterial biofilms*. J Bacteriol, 2005. **187**(1): p. 382-7.
298. Vuong, C., et al., *A crucial role for exopolysaccharide modification in bacterial biofilm formation, immune evasion, and virulence*. J Biol Chem, 2004. **279**(52): p. 54881-6.
299. Gerke, C., et al., *Characterization of the N-acetylglucosaminyltransferase activity involved in the biosynthesis of the Staphylococcus epidermidis polysaccharide intercellular adhesin*. J Biol Chem, 1998. **273**(29): p. 18586-93.
300. Heilmann, C., et al., *Molecular basis of intercellular adhesion in the biofilm-forming Staphylococcus epidermidis*. Mol Microbiol, 1996. **20**(5): p. 1083-91.
301. Rohde, H., et al., *Structure, function and contribution of polysaccharide intercellular adhesin (PIA) to Staphylococcus epidermidis biofilm formation and pathogenesis of biomaterial-associated infections*. Eur J Cell Biol, 2010. **89**(1): p. 103-11.
302. Maira-Litran, T., et al., *Synthesis and evaluation of a conjugate vaccine composed of Staphylococcus aureus poly-N-acetyl-glucosamine and clumping factor A*. PLoS One, 2012. **7**(9): p. e43813.
303. O'Gara, J.P., *ica and beyond: biofilm mechanisms and regulation in Staphylococcus epidermidis and Staphylococcus aureus*. FEMS Microbiol Lett, 2007. **270**(2): p. 179-88.
304. Kahan, F.M., et al., *The mechanism of action of fosfomycin (phosphonomycin)*. Ann N Y Acad Sci, 1974. **235**(0): p. 364-86.
305. Anderson, J.S., et al., *Biosynthesis of the peptidoglycan of bacterial cell walls. II. Phospholipid carriers in the reaction sequence*. J Biol Chem, 1967. **242**(13): p. 3180-90.
306. Perkins, H.R. and M. Nieto, *The chemical basis for the action of the vancomycin group of antibiotics*. Ann N Y Acad Sci, 1974. **235**(0): p. 348-63.
307. Perkins, H.R., *Specificity of combination between mucopeptide precursors and vancomycin or ristocetin*. Biochem J, 1969. **111**(2): p. 195-205.
308. Reynolds, P.E., *Structure, biochemistry and mechanism of action of glycopeptide antibiotics*. Eur J Clin Microbiol Infect Dis, 1989. **8**(11): p. 943-50.
309. Lo, M., Men, H., Branstrom, A., Helm, J., Yao, N., Golman, R., Walker, S., *A new mechanism of action proposed for ramoplanin*. J Am Chem Soc, 2000. **122**(14): p. 3540-3541.

310. Hu, Y., et al., *Ramoplanin inhibits bacterial transglycosylases by binding as a dimer to lipid II*. J Am Chem Soc, 2003. **125**(29): p. 8736-7.
311. Brotz, H., et al., *Role of lipid-bound peptidoglycan precursors in the formation of pores by nisin, epidermin and other lantibiotics*. Mol Microbiol, 1998. **30**(2): p. 317-27.
312. Hsu, S.T., et al., *The nisin-lipid II complex reveals a pyrophosphate cage that provides a blueprint for novel antibiotics*. Nat Struct Mol Biol, 2004. **11**(10): p. 963-7.
313. Oman, T.J., et al., *Haloduracin alpha binds the peptidoglycan precursor lipid II with 2:1 stoichiometry*. J Am Chem Soc, 2011. **133**(44): p. 17544-7.
314. Patton, G.C. and W.A. van der Donk, *New developments in lantibiotic biosynthesis and mode of action*. Curr Opin Microbiol, 2005. **8**(5): p. 543-51.
315. Ling, L.L., et al., *A new antibiotic kills pathogens without detectable resistance*. Nature, 2015. **517**(7535): p. 455-9.
316. Schneider, T., et al., *Plectasin, a fungal defensin, targets the bacterial cell wall precursor Lipid II*. Science, 2010. **328**(5982): p. 1168-72.
317. Sass, V., et al., *Human beta-defensin 3 inhibits cell wall biosynthesis in Staphylococci*. Infect Immun, 2010. **78**(6): p. 2793-800.
318. de Leeuw, E., et al., *Functional interaction of human neutrophil peptide-1 with the cell wall precursor lipid II*. FEBS Lett, 2010. **584**(8): p. 1543-8.
319. Wright, G.D., *Molecular mechanisms of antibiotic resistance*. Chem Commun (Camb), 2011. **47**(14): p. 4055-61.
320. Gardete, S. and A. Tomasz, *Mechanisms of vancomycin resistance in Staphylococcus aureus*. J Clin Invest, 2014. **124**(7): p. 2836-40.
321. Walsh, T.R. and R.A. Howe, *The prevalence and mechanisms of vancomycin resistance in Staphylococcus aureus*. Annu Rev Microbiol, 2002. **56**: p. 657-75.
322. Healy, V.L., et al., *Vancomycin resistance in enterococci: reprogramming of the D-ala-D-Ala ligases in bacterial peptidoglycan biosynthesis*. Chem Biol, 2000. **7**(5): p. R109-19.
323. Arthur, M. and P. Courvalin, *Genetics and mechanisms of glycopeptide resistance in enterococci*. Antimicrob Agents Chemother, 1993. **37**(8): p. 1563-71.

324. Palmer, K.L., V.N. Kos, and M.S. Gilmore, *Horizontal gene transfer and the genomics of enterococcal antibiotic resistance*. *Curr Opin Microbiol*, 2010. **13**(5): p. 632-9.
325. Marshall, C.G., et al., *Glycopeptide antibiotic resistance genes in glycopeptide-producing organisms*. *Antimicrob Agents Chemother*, 1998. **42**(9): p. 2215-20.
326. Handwerger, S., et al., *The cytoplasmic peptidoglycan precursor of vancomycin-resistant *Enterococcus faecalis* terminates in lactate*. *J Bacteriol*, 1992. **174**(18): p. 5982-4.
327. Bugg, T.D., et al., *Molecular basis for vancomycin resistance in *Enterococcus faecium* BM4147: biosynthesis of a depsipeptide peptidoglycan precursor by vancomycin resistance proteins VanH and VanA*. *Biochemistry*, 1991. **30**(43): p. 10408-15.
328. Depardieu, F., et al., *Modes and modulations of antibiotic resistance gene expression*. *Clin Microbiol Rev*, 2007. **20**(1): p. 79-114.
329. Lebreton, F., et al., *D-Ala-d-Ser VanN-type transferable vancomycin resistance in *Enterococcus faecium**. *Antimicrob Agents Chemother*, 2011. **55**(10): p. 4606-12.
330. Perichon, B. and P. Courvalin, *VanA-type vancomycin-resistant *Staphylococcus aureus**. *Antimicrob Agents Chemother*, 2009. **53**(11): p. 4580-7.
331. Weigel, L.M., et al., *Genetic analysis of a high-level vancomycin-resistant isolate of *Staphylococcus aureus**. *Science*, 2003. **302**(5650): p. 1569-71.
332. Zhu, W., et al., *Vancomycin-resistant *Staphylococcus aureus* isolates associated with Inc18-like vanA plasmids in Michigan*. *Antimicrob Agents Chemother*, 2008. **52**(2): p. 452-7.
333. Sievert, D.M., et al., *Vancomycin-resistant *Staphylococcus aureus* in the United States, 2002-2006*. *Clin Infect Dis*, 2008. **46**(5): p. 668-74.
334. Chang, S., et al., *Infection with vancomycin-resistant *Staphylococcus aureus* containing the vanA resistance gene*. *N Engl J Med*, 2003. **348**(14): p. 1342-7.
335. Whitener, C.J., et al., *Vancomycin-resistant *Staphylococcus aureus* in the absence of vancomycin exposure*. *Clin Infect Dis*, 2004. **38**(8): p. 1049-55.
336. Paknikar, S.S. and S. Narayana, *Newer antibacterials in therapy and clinical trials*. *N Am J Med Sci*, 2012. **4**(11): p. 537-47.
337. Schmidt, J.W., et al., *Generation of ramoplanin-resistant *Staphylococcus aureus**. *FEMS Microbiol Lett*, 2010. **310**(2): p. 104-11.

338. Yocum, R.R., J.R. Rasmussen, and J.L. Strominger, *The mechanism of action of penicillin. Penicillin acylates the active site of Bacillus stearothermophilus D-alanine carboxypeptidase.* J Biol Chem, 1980. **255**(9): p. 3977-86.
339. Yocum, R.R., et al., *Mechanism of penicillin action: penicillin and substrate bind covalently to the same active site serine in two bacterial D-alanine carboxypeptidases.* Proc Natl Acad Sci U S A, 1979. **76**(6): p. 2730-4.
340. Gutkind, G.O., et al., *beta-lactamase-mediated resistance: a biochemical, epidemiological and genetic overview.* Curr Pharm Des, 2013. **19**(2): p. 164-208.
341. Drawz, S.M., K.M. Papp-Wallace, and R.A. Bonomo, *New beta-lactamase inhibitors: a therapeutic renaissance in an MDR world.* Antimicrob Agents Chemother, 2014. **58**(4): p. 1835-46.
342. Reading, C. and M. Cole, *Clavulanic acid: a beta-lactamase-inhibiting beta-lactam from Streptomyces clavuligerus.* Antimicrob Agents Chemother, 1977. **11**(5): p. 852-7.
343. White, A.R., et al., *Augmentin (amoxicillin/clavulanate) in the treatment of community-acquired respiratory tract infection: a review of the continuing development of an innovative antimicrobial agent.* J Antimicrob Chemother, 2004. **53 Suppl 1**: p. i3-20.
344. Hong, D.J., et al., *Epidemiology and Characteristics of Metallo-beta-Lactamase-Producing Pseudomonas aeruginosa.* Infect Chemother, 2015. **47**(2): p. 81-97.
345. Pitout, J.D., P. Nordmann, and L. Poirel, *Carbapenemase-Producing Klebsiella pneumoniae, a Key Pathogen Set for Global Nosocomial Dominance.* Antimicrob Agents Chemother, 2015. **59**(10): p. 5873-84.
346. Fuda, C., et al., *The basis for resistance to beta-lactam antibiotics by penicillin-binding protein 2a of methicillin-resistant Staphylococcus aureus.* J Biol Chem, 2004. **279**(39): p. 40802-6.
347. Davies, T.A., et al., *Binding of ceftobiprole and comparators to the penicillin-binding proteins of Escherichia coli, Pseudomonas aeruginosa, Staphylococcus aureus, and Streptococcus pneumoniae.* Antimicrob Agents Chemother, 2007. **51**(7): p. 2621-4.
348. Moisan, H., M. Pruneau, and F. Malouin, *Binding of ceftaroline to penicillin-binding proteins of Staphylococcus aureus and Streptococcus pneumoniae.* J Antimicrob Chemother, 2010. **65**(4): p. 713-6.
349. Hall, R.G., 2nd and H.N. Michaels, *Profile of tedizolid phosphate and its potential in the treatment of acute bacterial skin and skin structure infections.* Infect Drug Resist, 2015. **8**: p. 75-82.

350. Holmes, N.E. and B.P. Howden, *What's new in the treatment of serious MRSA infection?* *Curr Opin Infect Dis*, 2014. **27**(6): p. 471-8.
351. McDanel, P.M., et al., *Use of daptomycin to treat infections with methicillin-resistant Staphylococcus aureus isolates having vancomycin minimum inhibitory concentrations of 1.5 to 2 mug/mL.* *Ann Pharmacother*, 2013. **47**(12): p. 1654-65.
352. Mitra, S., et al., *Profile of oritavancin and its potential in the treatment of acute bacterial skin structure infections.* *Infect Drug Resist*, 2015. **8**: p. 189-97.
353. Huber, J., et al., *Chemical genetic identification of peptidoglycan inhibitors potentiating carbapenem activity against methicillin-resistant Staphylococcus aureus.* *Chem Biol*, 2009. **16**(8): p. 837-48.
354. Berger-Bachi, B. and S. Rohrer, *Factors influencing methicillin resistance in staphylococci.* *Arch Microbiol*, 2002. **178**(3): p. 165-71.
355. Ludovice, A.M., S.W. Wu, and H. de Lencastre, *Molecular cloning and DNA sequencing of the Staphylococcus aureus UDP-N-acetylmuramyl tripeptide synthetase (murE) gene, essential for the optimal expression of methicillin resistance.* *Microb Drug Resist*, 1998. **4**(2): p. 85-90.
356. Weber, B., et al., *The fib locus in Streptococcus pneumoniae is required for peptidoglycan crosslinking and PBP-mediated beta-lactam resistance.* *FEMS Microbiol Lett*, 2000. **188**(1): p. 81-5.
357. Memmi, G., et al., *Staphylococcus aureus PBP4 is essential for beta-lactam resistance in community-acquired methicillin-resistant strains.* *Antimicrob Agents Chemother*, 2008. **52**(11): p. 3955-66.
358. Komatsuzawa, H., et al., *Cloning and characterization of the fmt gene which affects the methicillin resistance level and autolysis in the presence of triton X-100 in methicillin-resistant Staphylococcus aureus.* *Antimicrob Agents Chemother*, 1997. **41**(11): p. 2355-61.
359. Hancock, I.C., G. Wiseman, and J. Baddiley, *Biosynthesis of the unit that links teichoic acid to the bacterial wall: inhibition by tunicamycin.* *FEBS Lett*, 1976. **69**(1): p. 75-80.
360. Farha, M.A., et al., *Designing analogs of ticlopidine, a wall teichoic acid inhibitor, to avoid formation of its oxidative metabolites.* *Bioorg Med Chem Lett*, 2014. **24**(3): p. 905-10.
361. Swoboda, J.G., et al., *Discovery of a small molecule that blocks wall teichoic acid biosynthesis in Staphylococcus aureus.* *ACS Chem Biol*, 2009. **4**(10): p. 875-83.

362. Lee, K., et al., *Development of improved inhibitors of wall teichoic acid biosynthesis with potent activity against Staphylococcus aureus*. Bioorg Med Chem Lett, 2010. **20**(5): p. 1767-70.
363. Campbell, J., et al., *An antibiotic that inhibits a late step in wall teichoic acid biosynthesis induces the cell wall stress stimulon in Staphylococcus aureus*. Antimicrob Agents Chemother, 2012. **56**(4): p. 1810-20.
364. Suzuki, T., et al., *In vitro antimicrobial activity of wall teichoic acid biosynthesis inhibitors against Staphylococcus aureus isolates*. Antimicrob Agents Chemother, 2011. **55**(2): p. 767-74.
365. Richter, S.G., et al., *Small molecule inhibitor of lipoteichoic acid synthesis is an antibiotic for Gram-positive bacteria*. Proc Natl Acad Sci U S A, 2013. **110**(9): p. 3531-6.
366. May, J.J., et al., *Inhibition of the D-alanine:D-alanyl carrier protein ligase from Bacillus subtilis increases the bacterium's susceptibility to antibiotics that target the cell wall*. FEBS J, 2005. **272**(12): p. 2993-3003.
367. Pasquina, L., et al., *A synthetic lethal approach for compound and target identification in Staphylococcus aureus*. Nat Chem Biol, 2016. **12**(1): p. 40-5.
368. Chen, M., Q. Yu, and H. Sun, *Novel strategies for the prevention and treatment of biofilm related infections*. Int J Mol Sci, 2013. **14**(9): p. 18488-501.
369. Silver, L.L., *Viable screening targets related to the bacterial cell wall*. Ann N Y Acad Sci, 2013. **1277**: p. 29-53.
370. Rajagopal, M.*, Martin, M.J.*, Santiago, M.*, Lee, W., Kos, V.N., Meredith, T., Gilmore, M.S., Walker, S. (*Co-authors), *Multi-drug resistance factors in Staphylococcus aureus identified by profiling fitness within high diversity transposon libraries*. Submitted, 2016.
371. Davies, J., *Where have All the Antibiotics Gone?* Can J Infect Dis Med Microbiol, 2006. **17**(5): p. 287-90.
372. Clatworthy, A.E., E. Pierson, and D.T. Hung, *Targeting virulence: a new paradigm for antimicrobial therapy*. Nat Chem Biol, 2007. **3**(9): p. 541-8.
373. Levy, S.B. and B. Marshall, *Antibacterial resistance worldwide: causes, challenges and responses*. Nat Med, 2004. **10**(12 Suppl): p. S122-9.
374. Chambers, H.F., *The changing epidemiology of Staphylococcus aureus?* Emerg Infect Dis, 2001. **7**(2): p. 178-82.
375. Jevons, M.P., *"Celbenin"-resistant staphylococci*. British Medical Journal, 1961. **1**: p. 124-125.

376. Montgomery, D., *Clinical trial of BRL 1241 (Celbenin)*. Ir J Med Sci, 1962. **437**: p. 221-3.
377. Deresinski, S., *Methicillin-resistant Staphylococcus aureus: an evolutionary, epidemiologic, and therapeutic odyssey*. Clin Infect Dis, 2005. **40**(4): p. 562-73.
378. CDC, *Antibiotic resistance threats in the United States*. 2013.
379. Fischbach, M.A. and C.T. Walsh, *Antibiotics for emerging pathogens*. Science, 2009. **325**(5944): p. 1089-93.
380. Delcour, A.H., *Outer membrane permeability and antibiotic resistance*. Biochim Biophys Acta, 2009. **1794**(5): p. 808-16.
381. Li, X.Z., P. Plesiat, and H. Nikaido, *The challenge of efflux-mediated antibiotic resistance in Gram-negative bacteria*. Clin Microbiol Rev, 2015. **28**(2): p. 337-418.
382. Olaitan, A.O., S. Morand, and J.M. Rolain, *Mechanisms of polymyxin resistance: acquired and intrinsic resistance in bacteria*. Front Microbiol, 2014. **5**: p. 643.
383. Grossman, T.H., *Tetracycline Antibiotics and Resistance*. Cold Spring Harb Perspect Med, 2016. **6**(4).
384. Craig, N.L., *Target site selection in transposition*. Annu Rev Biochem, 1997. **66**: p. 437-74.
385. Pray, L., Zhaurova, K., *Barbara McClintock and the discovery of jumping genes (transposons)*. Nature Education, 2008. **1**(1): p. 169.
386. Kleckner, N., J. Roth, and D. Botstein, *Genetic engineering in vivo using translocatable drug-resistance elements. New methods in bacterial genetics*. J Mol Biol, 1977. **116**(1): p. 125-59.
387. Hayes, F., *Transposon-based strategies for microbial functional genomics and proteomics*. Annu Rev Genet, 2003. **37**: p. 3-29.
388. van Opijnen, T. and A. Camilli, *Transposon insertion sequencing: a new tool for systems-level analysis of microorganisms*. Nat Rev Microbiol, 2013. **11**(7): p. 435-42.
389. Maki, H., T. Yamaguchi, and K. Murakami, *Cloning and characterization of a gene affecting the methicillin resistance level and the autolysis rate in Staphylococcus aureus*. J Bacteriol, 1994. **176**(16): p. 4993-5000.
390. Picardeau, M., *Transposition of fly mariner elements into bacteria as a genetic tool for mutagenesis*. Genetica, 2010. **138**(5): p. 551-8.

391. Lampe, D.J., M.E. Churchill, and H.M. Robertson, *A purified mariner transposase is sufficient to mediate transposition in vitro*. EMBO J, 1996. **15**(19): p. 5470-9.
392. Santiago, M., et al., *A new platform for ultra-high density Staphylococcus aureus transposon libraries*. BMC Genomics, 2015. **16**: p. 252.
393. van Opijnen, T., K.L. Bodi, and A. Camilli, *Tn-seq: high-throughput parallel sequencing for fitness and genetic interaction studies in microorganisms*. Nat Methods, 2009. **6**(10): p. 767-72.
394. Klein, B.A., et al., *Identification of essential genes of the periodontal pathogen Porphyromonas gingivalis*. BMC Genomics, 2012. **13**: p. 578.
395. Langridge, G.C., et al., *Simultaneous assay of every Salmonella Typhi gene using one million transposon mutants*. Genome Res, 2009. **19**(12): p. 2308-16.
396. Chao, M.C., et al., *High-resolution definition of the Vibrio cholerae essential gene set with hidden Markov model-based analyses of transposon-insertion sequencing data*. Nucleic Acids Res, 2013. **41**(19): p. 9033-48.
397. Zhang, Y.J., et al., *Global assessment of genomic regions required for growth in Mycobacterium tuberculosis*. PLoS Pathog, 2012. **8**(9): p. e1002946.
398. Gawronski, J.D., et al., *Tracking insertion mutants within libraries by deep sequencing and a genome-wide screen for Haemophilus genes required in the lung*. Proc Natl Acad Sci U S A, 2009. **106**(38): p. 16422-7.
399. Skurnik, D., et al., *A comprehensive analysis of in vitro and in vivo genetic fitness of Pseudomonas aeruginosa using high-throughput sequencing of transposon libraries*. PLoS Pathog, 2013. **9**(9): p. e1003582.
400. Subashchandrabose, S., et al., *Genome-wide detection of fitness genes in uropathogenic Escherichia coli during systemic infection*. PLoS Pathog, 2013. **9**(12): p. e1003788.
401. Turner, K.H., et al., *Essential genome of Pseudomonas aeruginosa in cystic fibrosis sputum*. Proc Natl Acad Sci U S A, 2015. **112**(13): p. 4110-5.
402. Gallagher, L.A., J. Shendure, and C. Manoil, *Genome-scale identification of resistance functions in Pseudomonas aeruginosa using Tn-seq*. MBio, 2011. **2**(1): p. e00315-10.
403. Murray, J.L., et al., *Intrinsic Antimicrobial Resistance Determinants in the Superbug Pseudomonas aeruginosa*. MBio, 2015. **6**(6): p. e01603-15.
404. Christiansen, M.T., et al., *Genome-wide high-throughput screening to investigate essential genes involved in methicillin-resistant Staphylococcus aureus Sequence Type 398 survival*. PLoS One, 2014. **9**(2): p. e89018.

405. Bae, T., et al., *Staphylococcus aureus* virulence genes identified by bursa aurealis mutagenesis and nematode killing. Proc Natl Acad Sci U S A, 2004. **101**(33): p. 12312-7.
406. Wilde, A.D., et al., *Bacterial Hypoxic Responses Revealed as Critical Determinants of the Host-Pathogen Outcome by TnSeq Analysis of Staphylococcus aureus Invasive Infection*. PLoS Pathog, 2015. **11**(12): p. e1005341.
407. Meredith, T.C., et al., *Harnessing the power of transposon mutagenesis for antibacterial target identification and evaluation*. Mob Genet Elements, 2012. **2**(4): p. 171-178.
408. Wang, H., et al., *High-frequency transposition for determining antibacterial mode of action*. Nat Chem Biol, 2011. **7**(10): p. 720-9.
409. Silverman, J.A., N.G. Perlmutter, and H.M. Shapiro, *Correlation of daptomycin bactericidal activity and membrane depolarization in Staphylococcus aureus*. Antimicrob Agents Chemother, 2003. **47**(8): p. 2538-44.
410. Pogliano, J., N. Pogliano, and J.A. Silverman, *Daptomycin-mediated reorganization of membrane architecture causes mislocalization of essential cell division proteins*. J Bacteriol, 2012. **194**(17): p. 4494-504.
411. Drlica, K., *Mechanism of fluoroquinolone action*. Curr Opin Microbiol, 1999. **2**(5): p. 504-8.
412. Barna, J.C. and D.H. Williams, *The structure and mode of action of glycopeptide antibiotics of the vancomycin group*. Annu Rev Microbiol, 1984. **38**: p. 339-57.
413. Frere, J.M., *Mechanism of action of beta-lactam antibiotics at the molecular level*. Biochem Pharmacol, 1977. **26**(23): p. 2203-10.
414. Kotra, L.P., J. Haddad, and S. Mobashery, *Aminoglycosides: perspectives on mechanisms of action and resistance and strategies to counter resistance*. Antimicrob Agents Chemother, 2000. **44**(12): p. 3249-56.
415. Shinabarger, D., *Mechanism of action of the oxazolidinone antibacterial agents*. Expert Opin Investig Drugs, 1999. **8**(8): p. 1195-202.
416. Goecks, J., et al., *Galaxy: a comprehensive approach for supporting accessible, reproducible, and transparent computational research in the life sciences*. Genome Biol, 2010. **11**(8): p. R86.
417. Giardine, B., et al., *Galaxy: a platform for interactive large-scale genome analysis*. Genome Res, 2005. **15**(10): p. 1451-5.

418. Blankenberg, D., et al., *Galaxy: a web-based genome analysis tool for experimentalists*. Curr Protoc Mol Biol, 2010. **Chapter 19**: p. Unit 19 10 1-21.
419. DeJesus, M.A., et al., *Bayesian analysis of gene essentiality based on sequencing of transposon insertion libraries*. Bioinformatics, 2013. **29(6)**: p. 695-703.
420. DeJesus, M.A. and T.R. Ioerger, *A Hidden Markov Model for identifying essential and growth-defect regions in bacterial genomes from transposon insertion sequencing data*. BMC Bioinformatics, 2013. **14**: p. 303.
421. DeJesus, M.A., et al., *TRANSIT--A Software Tool for Himar1 TnSeq Analysis*. PLoS Comput Biol, 2015. **11(10)**: p. e1004401.
422. Solaimanpour, S., F. Sarmiento, and J. Mrazek, *Tn-seq explorer: a tool for analysis of high-throughput sequencing data of transposon mutant libraries*. PLoS One, 2015. **10(5)**: p. e0126070.
423. Pritchard, J.R., et al., *ARTIST: high-resolution genome-wide assessment of fitness using transposon-insertion sequencing*. PLoS Genet, 2014. **10(11)**: p. e1004782.
424. Mates, S.M., et al., *Membrane potential and gentamicin uptake in Staphylococcus aureus*. Proc Natl Acad Sci U S A, 1982. **79(21)**: p. 6693-7.
425. Bryan, L.E. and H.M. Van Den Elzen, *Effects of membrane-energy mutations and cations on streptomycin and gentamicin accumulation by bacteria: a model for entry of streptomycin and gentamicin in susceptible and resistant bacteria*. Antimicrob Agents Chemother, 1977. **12(2)**: p. 163-77.
426. Morikawa, K., et al., *Overexpression of sigma factor, sigma(B), urges Staphylococcus aureus to thicken the cell wall and to resist beta-lactams*. Biochem Biophys Res Commun, 2001. **288(2)**: p. 385-9.
427. Kuroda, M., et al., *Two-component system VraSR positively modulates the regulation of cell-wall biosynthesis pathway in Staphylococcus aureus*. Mol Microbiol, 2003. **49(3)**: p. 807-21.
428. Qureshi, N.K., S. Yin, and S. Boyle-Vavra, *The role of the Staphylococcal VraTSR regulatory system on vancomycin resistance and vanA operon expression in vancomycin-resistant Staphylococcus aureus*. PLoS One, 2014. **9(1)**: p. e85873.
429. Gardete, S., et al., *Role of VraSR in antibiotic resistance and antibiotic-induced stress response in Staphylococcus aureus*. Antimicrob Agents Chemother, 2006. **50(10)**: p. 3424-34.

430. Yin, S., R.S. Daum, and S. Boyle-Vavra, *VraSR two-component regulatory system and its role in induction of pbp2 and vraSR expression by cell wall antimicrobials in Staphylococcus aureus*. *Antimicrob Agents Chemother*, 2006. **50**(1): p. 336-43.
431. Leski, T.A. and A. Tomasz, *Role of penicillin-binding protein 2 (PBP2) in the antibiotic susceptibility and cell wall cross-linking of Staphylococcus aureus: evidence for the cooperative functioning of PBP2, PBP4, and PBP2A*. *J Bacteriol*, 2005. **187**(5): p. 1815-24.
432. Ubukata, K., N. Itoh-Yamashita, and M. Konno, *Cloning and expression of the norA gene for fluoroquinolone resistance in Staphylococcus aureus*. *Antimicrob Agents Chemother*, 1989. **33**(9): p. 1535-9.
433. Neyfakh, A.A., C.M. Borsch, and G.W. Kaatz, *Fluoroquinolone resistance protein NorA of Staphylococcus aureus is a multidrug efflux transporter*. *Antimicrob Agents Chemother*, 1993. **37**(1): p. 128-9.
434. Schurig-Briccio, L.A., et al., *Characterization of the type 2 NADH:menaquinone oxidoreductases from Staphylococcus aureus and the bactericidal action of phenothiazines*. *Biochim Biophys Acta*, 2014. **1837**(7): p. 954-63.
435. Proctor, R.A., et al., *Small colony variants: a pathogenic form of bacteria that facilitates persistent and recurrent infections*. *Nat Rev Microbiol*, 2006. **4**(4): p. 295-305.
436. Proctor, R.A., et al., *Staphylococcal small colony variants have novel mechanisms for antibiotic resistance*. *Clin Infect Dis*, 1998. **27 Suppl 1**: p. S68-74.
437. Bulger, R.J., *In vitro studies on highly resistant small colony variants of Staphylococcus aureus resistant to methicillin*. *J Infect Dis*, 1969. **120**(4): p. 491-4.
438. Schnitzer, R.J., L.J. Camagni, and M. Buck, *Resistance of small colony variants (G Forms) of a staphylococcus towards the bacteriostatic activity of penicillin*. *Proceedings of the Society for Experimental Biology and Medicine*, 1943. **53**(1): p. 75-78.
439. Chuard, C., et al., *Decreased susceptibility to antibiotic killing of a stable small colony variant of Staphylococcus aureus in fluid phase and on fibronectin-coated surfaces*. *J Antimicrob Chemother*, 1997. **39**(5): p. 603-8.
440. Rahman, M.M., et al., *The Staphylococcus aureus Methicillin Resistance Factor FmtA Is a d-Amino Esterase That Acts on Teichoic Acids*. *MBio*, 2015. **7**(1).

441. Komatsuzawa, H., et al., *Characterization of *fmtA*, a gene that modulates the expression of methicillin resistance in *Staphylococcus aureus**. *Antimicrob Agents Chemother*, 1999. **43**(9): p. 2121-5.
442. Oku, Y., et al., *Characterization of the *Staphylococcus aureus* *mprF* gene, involved in lysinylation of phosphatidylglycerol*. *Microbiology*, 2004. **150**(Pt 1): p. 45-51.
443. Fey, P.D., et al., *A genetic resource for rapid and comprehensive phenotype screening of nonessential *Staphylococcus aureus* genes*. *MBio*, 2013. **4**(1): p. e00537-12.
444. Mishra, N.N., et al., *Analysis of cell membrane characteristics of in vitro-selected daptomycin-resistant strains of methicillin-resistant *Staphylococcus aureus**. *Antimicrob Agents Chemother*, 2009. **53**(6): p. 2312-8.
445. Arvidson, S. and K. Tegmark, *Regulation of virulence determinants in *Staphylococcus aureus**. *Int J Med Microbiol*, 2001. **291**(2): p. 159-70.
446. George, E.A. and T.W. Muir, *Molecular mechanisms of *agr* quorum sensing in virulent staphylococci*. *Chembiochem*, 2007. **8**(8): p. 847-55.
447. Singh, V.K., M.R. Carlos, and K. Singh, *Physiological significance of the peptidoglycan hydrolase, *LytM*, in *Staphylococcus aureus**. *FEMS Microbiol Lett*, 2010. **311**(2): p. 167-75.
448. Cheung, A.L., et al., *Regulation of exoprotein expression in *Staphylococcus aureus* by a locus (*sar*) distinct from *agr**. *Proc Natl Acad Sci U S A*, 1992. **89**(14): p. 6462-6.
449. Yarwood, J.M. and P.M. Schlievert, *Quorum sensing in *Staphylococcus* infections*. *J Clin Invest*, 2003. **112**(11): p. 1620-5.
450. Lioliou, E., et al., *Various checkpoints prevent the synthesis of *Staphylococcus aureus* peptidoglycan hydrolase *LytM* in the stationary growth phase*. *RNA Biol*, 2016: p. 0.
451. Piriz Duran, S., F.H. Kayser, and B. Berger-Bachi, *Impact of *sar* and *agr* on methicillin resistance in *Staphylococcus aureus**. *FEMS Microbiol Lett*, 1996. **141**(2-3): p. 255-60.
452. Zhang, L., et al., *Transmembrane topology of *AgrB*, the protein involved in the post-translational modification of *AgrD* in *Staphylococcus aureus**. *J Biol Chem*, 2002. **277**(38): p. 34736-42.
453. Lina, G., et al., *Transmembrane topology and histidine protein kinase activity of *AgrC*, the *agr* signal receptor in *Staphylococcus aureus**. *Mol Microbiol*, 1998. **28**(3): p. 655-62.

454. Sakoulas, G., *The accessory gene regulator (agr) in methicillin-resistant Staphylococcus aureus: role in virulence and reduced susceptibility to glycopeptide antibiotics*. Drug Discovery Today: Disease Mechanisms, 2006. **3**(2): p. 287-294.
455. Kotera, Y., et al., *Factors influencing the uptake of norfloxacin by Escherichia coli*. J Antimicrob Chemother, 1991. **27**(6): p. 733-9.
456. Ham, J.S., et al., *Powerful usage of phylogenetically diverse Staphylococcus aureus control strains for detecting multidrug resistance genes in transcriptomics studies*. Mol Cells, 2010. **30**(1): p. 71-6.
457. Branger, C., et al., *Genetic relationship between methicillin-sensitive and methicillin-resistant Staphylococcus aureus strains from France and from international sources: delineation of genomic groups*. J Clin Microbiol, 2003. **41**(7): p. 2946-51.
458. Jones, M.B., et al., *Genomic and transcriptomic differences in community acquired methicillin resistant Staphylococcus aureus USA300 and USA400 strains*. BMC Genomics, 2014. **15**: p. 1145.
459. Lindsay, J.A. and M.T. Holden, *Staphylococcus aureus: superbug, super genome?* Trends Microbiol, 2004. **12**(8): p. 378-85.
460. El Garch, F., et al., *StaphVar-DNA microarray analysis of accessory genome elements of community-acquired methicillin-resistant Staphylococcus aureus*. J Antimicrob Chemother, 2009. **63**(5): p. 877-85.
461. Memmi, G., D.R. Nair, and A. Cheung, *Role of ArlRS in autolysis in methicillin-sensitive and methicillin-resistant Staphylococcus aureus strains*. J Bacteriol, 2012. **194**(4): p. 759-67.
462. Rebets, Y., et al., *Moenomycin resistance mutations in Staphylococcus aureus reduce peptidoglycan chain length and cause aberrant cell division*. ACS Chem Biol, 2014. **9**(2): p. 459-67.
463. Wallhausser, K.H., et al., *Moenomycin, a new antibiotic. I. Fermentation and isolation*. Antimicrob Agents Chemother (Bethesda), 1965. **5**: p. 734-6.
464. Walker, S., et al., *Chemistry and biology of ramoplanin: a lipoglycopeptide with potent antibiotic activity*. Chem Rev, 2005. **105**(2): p. 449-76.
465. Cudic, P., et al., *Complexation of peptidoglycan intermediates by the lipoglycopeptide antibiotic ramoplanin: minimal structural requirements for intermolecular complexation and fibril formation*. Proc Natl Acad Sci U S A, 2002. **99**(11): p. 7384-9.

466. Fang, X., et al., *The mechanism of action of ramoplanin and enduracidin*. Mol Biosyst, 2006. **2**(1): p. 69-76.
467. Lee, W., et al., *The Mechanism of Action of Lysobactin*. J Am Chem Soc, 2016. **138**(1): p. 100-3.
468. Stone, K.J. and J.L. Strominger, *Mechanism of action of bacitracin: complexation with metal ion and C 55 -isoprenyl pyrophosphate*. Proc Natl Acad Sci U S A, 1971. **68**(12): p. 3223-7.
469. Villet, R.A., et al., *Regulation of expression of abcA and its response to environmental conditions*. J Bacteriol, 2014. **196**(8): p. 1532-9.
470. Cain, B.D., et al., *Amplification of the bacA gene confers bacitracin resistance to Escherichia coli*. J Bacteriol, 1993. **175**(12): p. 3784-9.
471. Komatsuzawa, H., et al., *Subcellular localization of the major autolysin, ATL and its processed proteins in Staphylococcus aureus*. Microbiol Immunol, 1997. **41**(6): p. 469-79.
472. Takahashi, J., et al., *Molecular characterization of an atl null mutant of Staphylococcus aureus*. Microbiol Immunol, 2002. **46**(9): p. 601-12.
473. Mann, P.A., et al., *Chemical Genetic Analysis and Functional Characterization of Staphylococcal Wall Teichoic Acid 2-Epimerases Reveals Unconventional Antibiotic Drug Targets*. PLoS Pathog, 2016. **12**(5): p. e1005585.
474. Xu, Q., et al., *Bacterial pleckstrin homology domains: a prokaryotic origin for the PH domain*. J Mol Biol, 2010. **396**(1): p. 31-46.
475. Lemmon, M.A., *Pleckstrin homology (PH) domains and phosphoinositides*. Biochem Soc Symp, 2007(74): p. 81-93.
476. Wang, X., et al., *Calmodulin and PI(3,4,5)P(3) cooperatively bind to the ltk pleckstrin homology domain to promote efficient calcium signaling and IL-17A production*. Sci Signal, 2014. **7**(337): p. ra74.
477. Eliopoulos, G.M., et al., *In vitro and in vivo activity of LY 146032, a new cyclic lipopeptide antibiotic*. Antimicrob Agents Chemother, 1986. **30**(4): p. 532-5.
478. Jung, D., et al., *Structural transitions as determinants of the action of the calcium-dependent antibiotic daptomycin*. Chem Biol, 2004. **11**(7): p. 949-57.
479. Hughes, J. and G. Mellows, *Inhibition of isoleucyl-transfer ribonucleic acid synthetase in Escherichia coli by pseudomonic acid*. Biochem J, 1978. **176**(1): p. 305-18.

480. Hartmann, G., et al., *The specific inhibition of the DNA-directed RNA synthesis by rifamycin*. Biochim Biophys Acta, 1967. **145**(3): p. 843-4.
481. Campbell, E.A., et al., *Structural mechanism for rifampicin inhibition of bacterial rna polymerase*. Cell, 2001. **104**(6): p. 901-12.
482. Pedregosa, F., et al., *Scikit-learn: Machine Learning in Python*. Journal of Machine Learning Research, 2011. **12**: p. 2825-2830.
483. Ikuo, M., C. Kaito, and K. Sekimizu, *The cvfC operon of Staphylococcus aureus contributes to virulence via expression of the thyA gene*. Microb Pathog, 2010. **49**(1-2): p. 1-7.
484. Kaito, C., et al., *Silkworm pathogenic bacteria infection model for identification of novel virulence genes*. Mol Microbiol, 2005. **56**(4): p. 934-44.
485. Tsompanidou, E., et al., *Requirement of the agr locus for colony spreading of Staphylococcus aureus*. J Bacteriol, 2011. **193**(5): p. 1267-72.
486. Chambers, H.F. and M. Sachdeva, *Binding of beta-lactam antibiotics to penicillin-binding proteins in methicillin-resistant Staphylococcus aureus*. J Infect Dis, 1990. **161**(6): p. 1170-6.
487. Chambers, H.F. and C. Miick, *Characterization of penicillin-binding protein 2 of Staphylococcus aureus: deacylation reaction and identification of two penicillin-binding peptides*. Antimicrob Agents Chemother, 1992. **36**(3): p. 656-61.
488. Neuhaus, F.C. and J.L. Lynch, *The Enzymatic Synthesis of D-Alanyl-D-Alanine. 3. On the Inhibition of D-Alanyl-D-Alanine Synthetase by the Antibiotic D-Cycloserine*. Biochemistry, 1964. **3**: p. 471-80.
489. Lynch, J.L. and F.C. Neuhaus, *On the mechanism of action of the antibiotic O-carbamyl-D-serine in Streptococcus faecalis*. J Bacteriol, 1966. **91**(1): p. 449-60.
490. Strominger, J.L., Ito, E., Threnn, R.H., *Competitive inhibition of enzymatic reactions by oxamycin*. J Am Chem Soc, 1960. **82**: p. 998-999.
491. Yu, Z., et al., *Antibacterial mechanisms of polymyxin and bacterial resistance*. Biomed Res Int, 2015. **2015**: p. 679109.
492. Storm, D.R., K.S. Rosenthal, and P.E. Swanson, *Polymyxin and related peptide antibiotics*. Annu Rev Biochem, 1977. **46**: p. 723-63.
493. Mogi, T., et al., *Polymyxin B identified as an inhibitor of alternative NADH dehydrogenase and malate: quinone oxidoreductase from the Gram-positive bacterium Mycobacterium smegmatis*. J Biochem, 2009. **146**(4): p. 491-9.

494. Chen, Y.F., et al., *Interaction of daptomycin with lipid bilayers: a lipid extracting effect*. *Biochemistry*, 2014. **53**(33): p. 5384-92.
495. Wisseman, C.L., Jr., et al., *Mode of action of chloramphenicol. I. Action of chloramphenicol on assimilation of ammonia and on synthesis of proteins and nucleic acids in Escherichia coli*. *J Bacteriol*, 1954. **67**(6): p. 662-73.
496. Wilson, D.N., *Ribosome-targeting antibiotics and mechanisms of bacterial resistance*. *Nat Rev Microbiol*, 2014. **12**(1): p. 35-48.
497. Chopra, I. and M. Roberts, *Tetracycline antibiotics: mode of action, applications, molecular biology, and epidemiology of bacterial resistance*. *Microbiol Mol Biol Rev*, 2001. **65**(2): p. 232-60 ; second page, table of contents.
498. Chopra, I., P.M. Hawkey, and M. Hinton, *Tetracyclines, molecular and clinical aspects*. *J Antimicrob Chemother*, 1992. **29**(3): p. 245-77.
499. Ng, E.Y., M. Trucksis, and D.C. Hooper, *Quinolone resistance mutations in topoisomerase IV: relationship to the flqA locus and genetic evidence that topoisomerase IV is the primary target and DNA gyrase is the secondary target of fluoroquinolones in Staphylococcus aureus*. *Antimicrob Agents Chemother*, 1996. **40**(8): p. 1881-8.
500. Fujimoto-Nakamura, M., et al., *Accumulation of mutations in both gyrB and parE genes is associated with high-level resistance to novobiocin in Staphylococcus aureus*. *Antimicrob Agents Chemother*, 2005. **49**(9): p. 3810-5.
501. Drlica, K. and X. Zhao, *DNA gyrase, topoisomerase IV, and the 4-quinolones*. *Microbiol Mol Biol Rev*, 1997. **61**(3): p. 377-92.
502. Fournier, B., et al., *Selective targeting of topoisomerase IV and DNA gyrase in Staphylococcus aureus: different patterns of quinolone-induced inhibition of DNA synthesis*. *Antimicrob Agents Chemother*, 2000. **44**(8): p. 2160-5.
503. Collin, F., S. Karkare, and A. Maxwell, *Exploiting bacterial DNA gyrase as a drug target: current state and perspectives*. *Appl Microbiol Biotechnol*, 2011. **92**(3): p. 479-97.
504. Roland, S., et al., *The characteristics and significance of sulfonamides as substrates for Escherichia coli dihydropteroate synthase*. *J Biol Chem*, 1979. **254**(20): p. 10337-45.
505. Achari, A., et al., *Crystal structure of the anti-bacterial sulfonamide drug target dihydropteroate synthase*. *Nat Struct Biol*, 1997. **4**(6): p. 490-7.
506. Brown, G.M., *The biosynthesis of folic acid. II. Inhibition by sulfonamides*. *J Biol Chem*, 1962. **237**: p. 536-40.

507. Hitchings, G.H., Jr., *Nobel lecture in physiology or medicine--1988. Selective inhibitors of dihydrofolate reductase*. In *Vitro Cell Dev Biol*, 1989. **25**(4): p. 303-10.
508. Quinlivan, E.P., et al., *Mechanism of the antimicrobial drug trimethoprim revisited*. *FASEB J*, 2000. **14**(15): p. 2519-24.
509. Champness, J.N., D.K. Stammers, and C.R. Beddell, *Crystallographic investigation of the cooperative interaction between trimethoprim, reduced cofactor and dihydrofolate reductase*. *FEBS Lett*, 1986. **199**(1): p. 61-7.
510. Trepalin, S.V., Yarkov, A.V., *Hierarchical clustering of large databases and classification of antibiotics at high noise levels*. *Algorithms*, 2008. **1**(2): p. 183-200.
511. Rubin, V., Willet, P., *A comparison of some hierarchical monothetic divisive clustering algorithms for structure-property correlation*. *Analytica Chimica Acta*, 1983. **151**: p. 161-166.
512. Wildenhain, J., Spitzer, M., Dolma, S., Jarvik, N., White, R., Roy, M., Griffiths, E., Bellows, D.S., Wright, G.D., Tyers, M., *Prediction of synergism from chemical-genetic interactions by machine learning*. *Cell Systems*, 2015. **1**: p. 383-395.
513. Kato, A., et al., *A new anti-MRSA antibiotic complex, WAP-8294A. I. Taxonomy, isolation and biological activities*. *J Antibiot (Tokyo)*, 1998. **51**(10): p. 929-35.
514. Kato, A., et al., *A new anti-MRSA antibiotic complex, WAP-8294A II. Structure characterization of minor components by ESI LCMS and MS/MS*. *J Antibiot (Tokyo)*, 2011. **64**(5): p. 373-9.
515. Zhang, W., et al., *Identification and characterization of the anti-methicillin-resistant Staphylococcus aureus WAP-8294A2 biosynthetic gene cluster from Lysobacter enzymogenes OH11*. *Antimicrob Agents Chemother*, 2011. **55**(12): p. 5581-9.
516. Qiao, Y., *Reconstitution of the final step in Staphylococcus aureus peptidoglycan assembly*, in *The committee on higher degrees in chemical biology*. 2016, Harvard University.
517. Ruzin, A., et al., *Inactivation of mprF affects vancomycin susceptibility in Staphylococcus aureus*. *Biochim Biophys Acta*, 2003. **1621**(2): p. 117-21.
518. Fernebro, J., *Fighting bacterial infections-future treatment options*. *Drug Resist Updat*, 2011. **14**(2): p. 125-39.
519. Hernick, M., *Mycothioli: a target for potentiation of rifampin and other antibiotics against Mycobacterium tuberculosis*. *Expert Rev Anti Infect Ther*, 2013. **11**(1): p. 49-67.

520. Wolff, K.A. and L. Nguyen, *Strategies for potentiation of ethionamide and folate antagonists against Mycobacterium tuberculosis*. *Expert Rev Anti Infect Ther*, 2012. **10**(9): p. 971-81.
521. Stapleton, P.D. and P.W. Taylor, *Methicillin resistance in Staphylococcus aureus: mechanisms and modulation*. *Sci Prog*, 2002. **85**(Pt 1): p. 57-72.
522. Roemer, T., T. Schneider, and M.G. Pinho, *Auxiliary factors: a chink in the armor of MRSA resistance to beta-lactam antibiotics*. *Curr Opin Microbiol*, 2013. **16**(5): p. 538-48.
523. Furlani, R.E., A.A. Yeagley, and C. Melander, *A flexible approach to 1,4-disubstituted 2-aminoimidazoles that inhibit and disperse biofilms and potentiate the effects of beta-lactams against multi-drug resistant bacteria*. *Eur J Med Chem*, 2013. **62**: p. 59-70.
524. Lee, S.H., et al., *Antagonism of chemical genetic interaction networks resensitize MRSA to beta-lactam antibiotics*. *Chem Biol*, 2011. **18**(11): p. 1379-89.
525. Shlaes, D.M., *New beta-lactam-beta-lactamase inhibitor combinations in clinical development*. *Ann N Y Acad Sci*, 2013. **1277**: p. 105-14.
526. Buynak, J.D., *beta-Lactamase inhibitors: a review of the patent literature (2010 - 2013)*. *Expert Opin Ther Pat*, 2013. **23**(11): p. 1469-81.
527. Harris, P.N., P.A. Tambyah, and D.L. Paterson, *beta-lactam and beta-lactamase inhibitor combinations in the treatment of extended-spectrum beta-lactamase producing Enterobacteriaceae: time for a reappraisal in the era of few antibiotic options?* *Lancet Infect Dis*, 2015. **15**(4): p. 475-85.
528. Toussaint, K.A. and J.C. Gallagher, *beta-lactam/beta-lactamase inhibitor combinations: from then to now*. *Ann Pharmacother*, 2015. **49**(1): p. 86-98.
529. Bush, K., *A resurgence of beta-lactamase inhibitor combinations effective against multidrug-resistant Gram-negative pathogens*. *Int J Antimicrob Agents*, 2015. **46**(5): p. 483-93.
530. Farha, M.A., et al., *Inhibition of WTA synthesis blocks the cooperative action of PBPs and sensitizes MRSA to beta-lactams*. *ACS Chem Biol*, 2013. **8**(1): p. 226-33.
531. Lee, S.H., et al., *TarO-specific inhibitors of wall teichoic acid biosynthesis restore beta-lactam efficacy against methicillin-resistant staphylococci*. *Sci Transl Med*, 2016. **8**(329): p. 329ra32.
532. Chan, F.Y., et al., *Antimicrobial activity of a quinuclidine-based FtsZ inhibitor and its synergistic potential with beta-lactam antibiotics*. *J Antibiot (Tokyo)*, 2015. **68**(4): p. 253-8.

533. Tan, C.M., et al., *Restoring methicillin-resistant Staphylococcus aureus susceptibility to beta-lactam antibiotics*. *Sci Transl Med*, 2012. **4**(126): p. 126ra35.
534. Koyama, N., et al., *The nonantibiotic small molecule cyclabdan enhances the potency of beta-lactams against MRSA by inhibiting pentaglycine interpeptide bridge synthesis*. *PLoS One*, 2012. **7**(11): p. e48981.
535. Strandén, A.M., et al., *Cell wall monoglycine cross-bridges and methicillin hypersusceptibility in a femAB null mutant of methicillin-resistant Staphylococcus aureus*. *J Bacteriol*, 1997. **179**(1): p. 9-16.
536. Stapleton, P.D., et al., *Modulation of beta-lactam resistance in Staphylococcus aureus by catechins and gallates*. *Int J Antimicrob Agents*, 2004. **23**(5): p. 462-7.
537. Hu, Z.Q., et al., *Epigallocatechin gallate synergistically enhances the activity of carbapenems against methicillin-resistant Staphylococcus aureus*. *Antimicrob Agents Chemother*, 2002. **46**(2): p. 558-60.
538. Matsumoto, Y., et al., *Antibacterial and antifungal activities of new acylated derivatives of epigallocatechin gallate*. *Front Microbiol*, 2012. **3**: p. 53.
539. Liu, I.X., D.G. Durham, and R.M. Richards, *Baicalin synergy with beta-lactam antibiotics against methicillin-resistant Staphylococcus aureus and other beta-lactam-resistant strains of S. aureus*. *J Pharm Pharmacol*, 2000. **52**(3): p. 361-6.
540. Shah, S., P.D. Stapleton, and P.W. Taylor, *The polyphenol (-)-epicatechin gallate disrupts the secretion of virulence-related proteins by Staphylococcus aureus*. *Lett Appl Microbiol*, 2008. **46**(2): p. 181-5.
541. Stapleton, P.D., et al., *The beta-lactam-resistance modifier (-)-epicatechin gallate alters the architecture of the cell wall of Staphylococcus aureus*. *Microbiology*, 2007. **153**(Pt 7): p. 2093-103.
542. Bernal, P., et al., *Insertion of epicatechin gallate into the cytoplasmic membrane of methicillin-resistant Staphylococcus aureus disrupts penicillin-binding protein (PBP) 2a-mediated beta-lactam resistance by delocalizing PBP2*. *J Biol Chem*, 2010. **285**(31): p. 24055-65.
543. Campbell, J., *High-throughput assessment of bacterial growth inhibition by optical density measurements*. *Curr Protoc Chem Biol*, 2011. **3**(3).
544. Truesdell, S.E., G.E. Zurenko, and A.L. Laborde, *Interaction of cephalosporins with penicillin-binding proteins of methicillin-resistant Staphylococcus aureus*. *J Antimicrob Chemother*, 1989. **23 Suppl D**: p. 13-9.

545. Hayes, M.V. and D.C. Orr, *Mode of action of ceftazidime: affinity for the penicillin-binding proteins of Escherichia coli K12, Pseudomonas aeruginosa and Staphylococcus aureus*. J Antimicrob Chemother, 1983. **12**(2): p. 119-26.
546. Siewert, G. and J.L. Strominger, *Bacitracin: an inhibitor of the dephosphorylation of lipid pyrophosphate, an intermediate in the biosynthesis of the peptidoglycan of bacterial cell walls*. Proc Natl Acad Sci U S A, 1967. **57**(3): p. 767-73.
547. Bayer, A.S., et al., *Heterogeneity of mprF Sequences in Methicillin-Resistant Staphylococcus aureus Clinical Isolates: Role in Cross-Resistance between Daptomycin and Host Defense Antimicrobial Peptides*. Antimicrob Agents Chemother, 2014.
548. Yang, S.J., et al., *Causal role of single nucleotide polymorphisms within the mprF gene of Staphylococcus aureus in daptomycin resistance*. Antimicrob Agents Chemother, 2013. **57**(11): p. 5658-64.
549. Bae, T., et al., *Generating a collection of insertion mutations in the Staphylococcus aureus genome using bursa aurealis*. Methods Mol Biol, 2008. **416**: p. 103-16.